UNIVERSIDAD COMPLUTENSE DE MADRID

FACULTAD DE CIENCIAS FÍSICAS

PROGRAMA DE DOCTORADO EN FÍSICA

TESIS DOCTORAL

SimVis Simulations for Contact Lens Practice:
Technological Developments,
Optical Replication of Multifocal Contact Lenses,
Clinical Validation and Perceptual Aspects

Simulaciones SimVis para Contactología:
Desarrollos Tecnológicos,
Replicación Óptica de Lentes de Contacto Multifocales,
Validación Clínica y Aspectos Perceptuales

MEMORIA PARA OPTAR AL GRADO DE DOCTOR

PRESENTADA POR

EDUARDO ESTEBAN IBÁÑEZ

DIRECTORES

ENRIQUE GAMBRA URRALBURU

CARLOS DORRONSORO DIAZ

VioBio Lab.
Instituto de Óptica
CSIC

2EyesVision S.L.
Madrid

Departamento de Óptica
Facultad de Ciencias Físicas
UCM

UNIVERSIDAD COMPLUTENSE DE MADRID

FACULTAD DE CIENCIAS FÍSICAS

PROGRAMA DE DOCTORADO EN FÍSICA

TESIS DOCTORAL

SimVis Simulations for Contact Lens Practice:
Technological Developments,
Optical Replication of Multifocal Contact Lenses,
Clinical Validation and Perceptual Aspects

Simulaciones SimVis para Contactología:
Desarrollos Tecnológicos,
Replicación Óptica de Lentes de Contacto Multifocales,
Validación Clínica y Aspectos Perceptuales

MEMORIA PARA OPTAR AL GRADO DE DOCTOR

PRESENTADA POR

EDUARDO ESTEBAN IBÁÑEZ

DIRECTORES

ENRIQUE GAMBRA URRALBURU

CARLOS DORRONSORO DÍAZ

UNIVERSIDAD COMPLUTENSE MADRID

DECLARACIÓN DE AUTORÍA Y ORIGINALIDAD DE LA TESIS PRESENTADA PARA OBTENER EL TÍTULO DE DOCTOR

D./Dña. **Eduardo Esteban Ibáñez**, estudiante en el Programa de Doctorado en Física, de la Facultad de Ciencias Físicas de la Universidad Complutense de Madrid, como autor/a de la tesis presentada para la obtención del título de Doctor y titulada:

Simulaciones SimVis para Contactología:
Desarrollos Tecnológicos,
Replicación Óptica de Lentes de Contacto Multifocales,
Validación Clínica y Aspectos Perceptuales

Y dirigida por: Dr. **Enrique Gambra** y Dr. **Carlos Dorronsoro**.

DECLARO QUE:

La tesis es una obra original que no infringe los derechos de propiedad intelectual ni los derechos de propiedad industrial u otros, de acuerdo con el ordenamiento jurídico vigente, en particular, la Ley de Propiedad Intelectual (R.D. legislativo 1/1996, de 12 de abril, por el que se aprueba el texto refundido de la Ley de Propiedad Intelectual, modificado por la Ley 2/2019, de 1 de marzo, regularizando, aclarando y armonizando las disposiciones legales vigentes sobre la materia), en particular, las disposiciones referidas al derecho de cita.

Del mismo modo, asumo frente a la Universidad cualquier responsabilidad que pudiera derivarse de la autoría o falta de originalidad del contenido de la tesis presentada de conformidad con el ordenamiento jurídico vigente.

En Madrid, a 20 de mayo de 2024

ESTEBAN IBAÑEZ EDUARDO - 77215103D

Firmado digitalmente por ESTEBAN IBAÑEZ EDUARDO - 77215103D
Fecha: 2024.05.20 03:29:08 +02'00'

Fdo.

Esta DECLARACIÓN DE AUTORÍA Y ORIGINALIDAD debe ser insertada en la primera página de la tesis presentada para la obtención del título de Doctor.

A los que ya no están y no pueden celebrar el fin de esta etapa conmigo,

A Álvaro y Ángel, por vivir parte del camino

A Pablo, por no poderlo ver empezar

"*Everything is impossible until somebody does it.*"

Decía una galleta de la suerte en algún restaurante de Rochester,

que guarde hasta hoy en la funda de mi móvil.

"*We did it because we didn't know it was impossible.*"

Ponía en una nota que alguien dejo también dentro de la funda del móvil.

A modo de contestación, después habérmelo olvidado en una sala de reunión.

El C-A-M-I-N-O de la Tesis

Agradecimientos

Y por fin llegamos al paso 8 de este Camino, por lo que es momento de mirar a atrás y sonreír. Todo el mundo dice que se hace corto y largo al mismo tiempo, así que no voy a ser yo quien lo discuta. Pero hay que ver la cantidad de cosas buenas y malas que han pasado en estos 3 años de superación, de aprendizaje científico y también vital, del que no me arrepiento haber elegido.

Y como no podía ser de otra forma, también toca agradecer a todo el mundo que ha formado parte de este camino. Porque la ciencia trata de eso, de un constante trabajo colaborativo, y en esta tesis ha habido un montón de ello.

En primer lugar, me gustaría agradecer a mis directores. Enrique, creo que no caben en este texto suficientes palabras para agradecerte todo lo que has hecho por mi durante esta tesis. No solo por tus consejos y orientación científica, que obviamente también han sido fundamentales en esta tesis, si no por entenderme como persona y guiarme en los momentos en los que estaba desbordado. Tienes esa habilidad de quitarle importancia a los problemas. Sobre todo, quiero agradecer tu implicación en los últimos meses, sacando tiempo de donde no tenías. Carlos, porque todo este camino empezó por un contrato de técnico en el CSIC (que pillo con un confinamiento y una pandemia de por medio) y enseguida me ofreciste hacer la tesis entre el CSIC y 2Eyesvision. No sé qué viste en mí, pero gracias por esta oportunidad. Muchas gracias también por todas las discusiones científicas, las ideas locas que con el tiempo dejan de serlo tanto, y por la pasión que transmites por la ciencia. Sin tu esfuerzo estos últimos meses de llamadas fuera del horario laboral, correcciones y consejos, no hubiera sido posible.

A Susana, que me abrió las puertas de VioBio Lab, pero también las de MarcosLab para hacer la estancia en la Universidad de Rochester. Gracias por darme la oportunidad, por hacer que me sintiera en casa a tantos kms de distancia y por todo el tiempo que me dedicaste en las discusiones y diseño de estudios.

A Víctor, también llamado VRL, que ha sido parte fundamental de esta tesis. A pesar de no haber participado de una manera muy directa, tus enseñanzas de Matlab, psicofísica y ciencia en general han sido determinantes para poder “volar” solo y poder afrontar todos los retos de esta tesis. Por estar siempre dispuesto a contestar preguntas, pero también por hacer que me diera cuenta de las cosas por mí mismo. GRACIAS.

A Xoa, por ser mi primera amiga en Madrid y organizar distintos planes para conocer más gente en tiempos de pandemia. Por todo lo que he aprendido de ti y ser pionera en tantas cosas que se han hecho en la empresa, eres todo un referente y un modelo a seguir. Que no se te olvide lo gran profesional que eres y todo lo que vales.

A Pilar (que no María Pilar) por todos los momentos vividos, planes organizados y estar siempre disponible para quedar el primer año viviendo en Madrid. Muchas gracias también

por tu generosidad, siempre dispuesta a ayudar en los temas administrativos de la tesis y también en los temas científicos.

A Sara, que ya eras amiga, pero durante la estancia en Rochester pude conocerte mejor y darme cuenta de lo gran científica y mejor persona que eres. Todas nuestras comidas y cenas semanales en cada uno de los restaurantes de College Town y los viajes a la cafetería de los Finger Lakes, fueron de los mejores momentos de la estancia sin duda.

A mi familia de Tres Cantos, 2EyesVision. Que, aunque al principio no nos veíamos mucho, habéis sido fundamentales en todo el proceso. A Yassine, que tanto me ha ayudado en la tesis y tantas preguntas me ha resuelto cuando iba a preguntarle con un ¿qué tal estas? con doble intención. Por todas las conversaciones de vuelta en cercanías, que hacía más ameno el viaje, y que se echan en falta ahora. A Carmen, con la que coincidí menos tiempo del que me hubiera gustado, pero que cundió bastante tanto en el despacho como en IOSA/IOPTICA. Como dijo el niño amante de los dinosaurios en Calviá: ¡Lo ha hecho! A Lucie, por todos los trayectos a Tres Cantos discutiendo cosas científicas y por haberme enseñado tanto en el tiempo en el que coincidimos. Tu ayuda también fue imprescindible en esta tesis. A JR, porque las horas de tortura en los distintos experimentos han tenido su fruto. Gracias también por tu forma de ser, y tener siempre tiempo para preguntar cómo va la vida. A Irene, por compartir ciudad y palabras que solo se usan en Zaragoza, por lo que me has enseñado dentro del área clínica y por haber tenido paciencia conmigo mientras terminaba la tesis.

Al resto de gente que ha formado parte del equipo durante este tiempo: Diana, Joshua, Álvaro, Cris, Cándido, Juan, Gonzalo, Petros, Lucía, Teresa, Marina, Ricardo, Xavi, Edu y Alejandra.

A mi otra familia del CSIC. Alberto, por siempre tener la puerta del despacho abierta, y no tener nunca ningún problema en explicar cualquier duda que tuviera. También por acompañarme y ser mi “padrino” en mi primer congreso internacional (VPO). Rocío, por todas las conversaciones viniendo a mi despacho para charlar, la ayuda proporcionada con temas de divulgación y por siempre responder a mis buenos días. Edu Senior, por poder conocerte un poco más en el Fall Vision y darme cuenta de lo único que eres. Ojalá haberte podido disfrutar un poco más día a día, porque eres genial. Fernando, que fuiste vecino y pude compartir muchas cervezas y conversaciones profundas contigo en nuestra calle Ponzano. Al equipo café (Dani, Álvaro y Paulina) por acudir siempre puntuales a la cita de las 11:00h, las conversaciones random, historietas etc… que siempre se traducían en buenos ratos. Elena, que siempre estabas ahí para resolver cualquier duda o problema administrativo, pero también para escuchar nuestros problemas. Lupe, por ir siempre corriendo por los pasillos por tener prisa, pero tener tiempo para preguntar como estas y que tal llevas la tesis. Clara, que por desgracia no pude coincidir mucho contigo en VioBio, pero he podido conocerte mejor fuera, he incluso estar en la presentación de tu primer libro.

También al resto de gente de VioBio: Ana, James, Amal, Andrés, Judith, Nohelia, Lekha, Celia, Mar, María, Paula, Pablo… y de otros grupos: Sergio, Javier etc…

No podían faltar tampoco mis agradecimientos a la gente que formo IOSA/IOPTICA durante todos mis años haciendo actividades de divulgación. Especialmente a Raquel y Pablo, que me ayudaron durante mi año de presidente y estuvieron dispuestos a echar una mano en todo. Ojalá que el grupo siga activo durante mucho tiempo, porque la divulgación es super necesaria.

Especial agradecimiento a todos los grupos e instituciones que han colaborado conmigo en esta tesis que me hace sentir tan afortunado: Walter y Diego de la Universidad de Valencia; David, Ainhoa y Elena de la Universidad de Alicante; y Manu y Joaquín de Qvision.

También quiero recordar a los integrantes de Marcos Lab de la Universidad de Rochester. Gracias a David, por todas las comidas en el comedor, los cafés que preparabas con tanto esmero (espuma incluida) y los partidos de Champions. Tianlun, for the car trips, for teaching me how to eat with chopsticks and for that invitation to climb that could not be. También a Aldo y Jiaxi por los momentos compartidos.

A Alvaro Fanlo, aunque ya no nos podemos ver tanto como nos gustaría, también quiero agradecerte todo lo vivido en esos años de universidad, tardes/ noches estudiando, los momentos épicos con In Waves, las celebraciones con Voll-damn por cada examen aprobado y un largo etc…

A Marta, que siempre consigue sacar algo de tiempo en su ajetreada vida compuesta por mil actividades para quedar. Los cafés hablando de todo y de nada contigo son reparadores. Ojalá no falten nunca.

A Ana, que estuviste en los momentos más duros del doctorado y de estos años viviendo en Madrid, siempre dispuesta a sacarme de casa y ofrecerme planes de distinto tipo. Mil gracias por todo.

A Salim, por ser un compañero de piso excepcional y convertirte también en amigo. Por seguir quedando para tomar algo, dar paseos y hacer lo que más nos gusta: comer pizzas del Amici di Napoli.

A mis excompañeros del hospital infantil de Zaragoza, de los que tanto aprendí en mis primeros pasos en investigación y que siempre agradecían tanto las visitas. En especial a Victoria Pueyo, por darme la oportunidad, pero también por animarme y entender mi decisión de irme a Madrid.

A mi grupo de ópticos, que siempre intento ver cuando estoy de vuelta por Zaragoza: Raquel, Silvia, Jorge, Sara y David. Porque también proporcionasteis lentes de contacto que han sido medidas en esta tesis.

A mis amigos de patines, esa afición que me ayudo a desconectar durante esta etapa, y que siempre han estado ahí para dar una vuelta: Paula, Lorenzo, Adriana, Mel, Sara y Eugenio.

María, que entro en mi vida de manera inesperada gracias a esta tesis por coincidir en un congreso en Aveiro. Muchas gracias por tu apoyo incondicional en cada momento de

desesperación, estrés y dudas que he tenido durante este proceso y han hecho que no estuviera ahí de la forma en la que me hubiera gustado. Por creer en mí, muchas veces, más de lo que yo lo hago. En definitiva, por quererme de la forma en la que lo haces, siempre tan bonita.

A mi OHANA, porque familia se queda corto con vosotros. No solo en los momentos buenos, también en los malos... Sin vosotros esto no podría haber sido posible. Mil gracias a cada un@ de vosotros: Álvaro, Carlos, Dani, Edgar, Fercho, Lore, Maca, Robert y Vir. También a Miguel, que para mí forma también parte de esta familia y siempre está ahí.

Y, por último, a la familia de sangre. Gracias Papá y Mamá por darme la educación necesaria para ser una buena persona y tener los valores de humildad, superación y esfuerzo. Gracias a mi padre por apoyarme siempre en esta aventura, a pesar de que suponía estar lejos durante una situación complicada. Se que estas muy orgulloso de mi. Mama, también a ti te tengo que dar las gracias. Por tu amor incondicional, siempre preocupándote por mí, a pesar de estar lejos estos años, siempre te he sentido a mi lado. No me olvido de mi hermano Roberto, mi cuñada María y mi sobrina Ixeia, que me han hecho varias visitas a Madrid este tiempo y siempre me apoyan desde la lejanía. También quiero agradecer al resto de familia: ti@s, prim@s etc…

A todos los que me he podido haber olvidado, y que seguro han formado parte también de esta tesis. GRACIAS.

Funding

The research developed during this thesis would have not been possible without the funding received from the following institutions:

- Madrid Regional Government (CAM): Industrial PhD Grant IND2020/BMD-17262 to Eduardo Esteban Ibáñez.

- Ayuda de Movilidad C (Estancia) de la convocatoria de ayudas para la participación en Congresos y Movilidad de los estudiantes de doctorado de la UCM, curso 2022-2023 to Eduardo Esteban Ibáñez. Research Stay: Marcos Lab, Center for Visual Science – University of Rochester, Rochester (USA).

- Marcos Lab – University of Rochester, Rochester (USA), which funded part of the research stay.

- Ministerio de Ciencia e Innovación (Spain): (1) Ayudas a proyectos de colaboración público-privada (CPP2021-008388) to Carlos Dorronsoro, Enrique Gambra and Alberto de Castro. (2) Torres Quevedo Grant (PTQ2021-011963) to Irene Sisó-Fuertes. (3) Spanish Government grant (PID2020-115191RB-I00) to Alberto de Castro and Susana Marcos.

Abstract

SimVis Simulations for Contact Lens Practice: Technological Developments, Optical Replication of Multifocal Contact Lenses, Clinical Validation and Perceptual Aspects

The development of new corrections and designs for presbyopia has increased the number of options available for patients that would potentially satisfy their specific requirements. However, monofocal or progressive spectacles lenses and the implantation of premium intraocular lenses remain the most popular choices, while multifocal contact lenses (MCLs) have a lower adoption probably due to the difficulty of selecting an appropriate lens for each patient.

This thesis focuses on overcoming these challenges through the development, evaluation and validation of new functionalities for SimVis Gekko, the first wearable and binocular visual simulator of presbyopic corrections, oriented towards the simulation of MCLs.

First, a new method was developed to obtain simulations of any MCL design, from in-vitro measurements provided by a commercial metrology device (NIMO TR1504) and through computational characterization. The simulations of 11 daily soft MCLs from 4 manufacturers were obtained using this procedure and were clinically validated in presbyopic subjects, obtaining results comparable to those provided by real MCLs in the same group of subjects.

All the combinations corresponding to the different steps of the MCL fitting guides were implemented in SimVis Gekko. This allows for the complete replication and simulation of the fitting guides, with the goal of reducing and potentially eliminating the use of trial MCLs and decreasing the number of fitted lenses until the optimal combination is achieved in a single visit. To validate the approach, several steps of the fitting guides were simulated using SimVis Gekko in a group of subjects with the aim of validating a novel metric based on visual acuities at different distances (3D-VA) that allowed to detect for each fitting guide step, if there was an alternative with better visual performance, which were later verified with the corresponding real MCLs.

The second part of this thesis focused on the development and implementation of two new functionalities of SimVis Gekko. These enhancements transform it into a device capable of performing visual function tests in an optimized manner, thereby enabling the evaluation of the visual performance of the MCL simulations and saving chair-time. Specifically, these improvements included: 1) the utilization of SimVis Gekko as a method of introducing spherical optical power to perform defocus curves of Visual Acuity and Contrast Sensitivity with the synchronization of an app that uses adaptive methods, and 2) the introduction of astigmatism in an automated, accurate, and fast manner through the development of assemblies based on Stokes lenses for implementation in SimVis Gekko, allowing the eventual simulation of toric MCL designs.

Lastly, the component of neural adaptation in corrections based on simultaneous vision (SV) was examined in two different studies: 1) The evaluation of visual perception obtained through bifocal simulations with different energy balances (between far and near) and additions introduced using different adaptation conditions. The results demonstrate that these parameters significantly influence perceptual vision, but the outcomes may vary depending on the previous adaptation state, type of transition and the transition time. 2) The short-term adaptation aftereffects of both generic bifocal designs and commercial lenses simulated with SimVis Gekko were measured. All of them produce an adaptation compared to monofocal lens, with the largest effect produced by lenses with small additions, high energy percentage at near, and the equivalent design of commercial lenses.

In conclusion, this thesis has achieved accurate simulations of MCLs, which have been validated within a presbyopic group. These simulations have been used to replicate and improve their fitting guides in a clinical setting, using an innovative metric based on SimVis Gekko measurements. The capability to perform visual function tests in a faster and optimized way to evaluate visual performance through MCLs has been developed, including astigmatism correction to simulate toric designs. Finally, the main factors involved in adaptation, including time, type of transition, previous adaptation state and different parameters of SV designs, such as energy balance and addition for generic and commercial corrections, have been thoroughly analyzed.

Resumen de la tesis

Simulaciones SimVis para Contactología: Desarrollos Tecnológicos, Replicación Óptica de Lentes de Contacto Multifocales, Validación Clínica y Aspectos Perceptuales.

El desarrollo de nuevas correcciones y diseños para la presbicia ha aumentado el número de opciones disponibles para los pacientes que podrían satisfacer sus necesidades específicas. A pesar de ello, las lentes monofocales o progresivas en gafa y la implantación de lentes intraoculares premium siguen siendo las elecciones más populares, mientras que las lentes de contacto multifocales (LCMs) tienen una menor adopción, probablemente por la dificultad de seleccionar una lente apropiada para cada paciente.

Esta tesis se centra en superar estos desafíos mediante la adaptación y evaluación de nuevas funcionalidades del simulador visual SimVis Gekko, el primer simulador visual binocular y llevable de correcciones para présbita, orientado a la simulación de LCMs.

En primer lugar, se desarrolló un nuevo método para obtener simulaciones de cualquier diseño de LCM a través de su caracterización computacional, obtenida utilizando medidas *in-vitro* proporcionadas por un dispositivo comercial (NIMO TR1504). Las simulaciones de 11 LCMs blandas diarias de 4 fabricantes fueron obtenidas utilizando este proceso y se validaron clínicamente en sujetos présbitas, obteniendo resultados comparables con las LCMs reales en el mismo grupo de sujetos.

Se implementaron todas las combinaciones correspondientes a los pasos de las guías de adaptación de las LCMs en SimVis Gekko. Esto permitió replicar y simular las guías de adaptación en su totalidad, con el objetivo de reducir y potencialmente eliminar el uso de LCMs de prueba, y disminuir el número de lentes adaptadas hasta encontrar la combinación optima en una única sesión. Para validar el proceso, varios pasos de las guías de adaptación fueron simulados usando SimVis Gekko en un grupo de sujetos con el objetivo de validar una nueva métrica basada en las agudezas visuales a distintas distancias (3D-VA) que permitió detectar para cada paso de la guía de adaptación, si había alguna alternativa con mejor rendimiento visual, que posteriormente se comprobaron con las correspondientes LCMs reales.

La segunda parte de esta tesis se centró en el desarrollo e implementación de nuevas funcionalidades de SimVis Gekko. Estas mejoras lo convierten en un dispositivo capaz de realizar tests de función visual de manera optimizada para poder evaluar el rendimiento visual de las simulaciones de LCMs ahorrando tiempo de evaluación. Específicamente, esas mejoras incluyeron: 1) La utilización de SimVis Gekko como método de introducción de potencia óptica esférica para realizar curvas de desenfoque de Agudeza Visual y Sensibilidad al Contraste con la sincronización de una app que utiliza métodos adaptativos, y 2) la introducción de astigmatismo manera automática, precisa y rápida a través del desarrollo de unos montajes

basados en las lentes de Stokes para ser implementados en SimVis Gekko, permitiendo la simulación eventual de diseños tóricos de LCMs.

Finalmente, el componente de adaptación neural en las correcciones basadas en visión simultánea (VS) fue evaluada en dos estudios diferentes: 1) la evaluación de la percepción visual obtenida a través de simulaciones bifocales con distinto balance energético (entre lejos y cerca) y adición, introducidas utilizando distintas condiciones de adaptación. Los resultados demostraron que esos parámetros influyeron significativamente en la percepción visual, pero pueden variar en función del estado de adaptación previo, el tipo de transición o el tiempo de transición. 2) Los efectos posteriores a adaptación a corto plazo tanto de diseños bifocales genéricos como lentes comerciales simuladas con SimVis Gekko fueron analizados, produciendo todos ellos una adaptación en comparación con lente monofocal, con el mayor efecto producido por las lentes con adición pequeña, alto porcentaje de energía en cerca y los diseños equivalentes en lentes comerciales.

En conclusión, en esta tesis se ha logrado obtener simulaciones precisas de LCMs, las cuales han sido validadas en un grupo de sujetos présbitas. Estas simulaciones han sido utilizadas para replicar y mejorar sus guías de adaptación en un entorno clínico, usando una nueva métrica basada en medidas con SimVis Gekko. Se ha desarrollado la capacidad de realizar tests de función visual de manera más rápida y optimizada para evaluar el rendimiento visual a través de LCMs, incluyendo corrección de astigmatismo para simular diseños tóricos. Por último, se han analizado los principales factores que intervienen en la adaptación a los distintos diseños de VS, incluyendo el tiempo, tipo de transición, estado de adaptación previo y distintos parámetros de los diseños de SV, como la distribución de energía y adición en correcciones genéricas y comerciales.

Keywords


visualadaptation
additionlenses
lens
multifocal
perceptual
high
astigmatism
corrections
gekko
optical
low
near
mcls
conditions
measurements
designs
evaluated
performance
test
system
study
power
eye
far
ophthalmol
short-term
fitting
monofocal
bifocal
vision
energy
distances
stokes
image
refractive
transition
simulations
blur
clinical
curves
simulation
presbyopia
correction
experiment
balance
pupil
contact
values
represents
contrast
introduction
manufacturer
intermediate
sharp
statistical
comparison
additions
combination
higher
validation
thesis
conducted
color
only
process
represented
respectively
steps
group
focus
considering
scores
patients
dorronsoro
defocus
commercial
standard
described
adaptive
metric
aftereffects
measurement
step
among
better
state
fig
without
same
deg

List of most used abbreviations

A
AFC: Alternative Forced Choice
AO: Adaptive optics
B
BC: Base Curve
C
C: Cylinder
CL: Contact lens
CS: Contrast Sensitivity
CSF: Contrast Sensitivity Function
D
D: Diopters
DCNVA: Distance Corrected Near Visual Acuity
DED: Dry Eye Disease
E
ECP: Eye Care professional
EDOF: Extended Depth of Focus
F
F: Far
FA: Final axis
FG: Fitting Guide
FoV: Field of view
G
H
HOA: Higher Order Aberrations
Hz: Hertz
I
IOL: Intraocular lens
J
K
L
M
MCL: Multifocal Contact Lens
M-IOL: Multifocal intraocular lens
MLA: Multifocal Lens Analyzer
MTF: Modulation transfer function

N
N: Near
NPF: Natural Perceived Focus
NVAQ: Near Vision Activities Questionnaire
O
O: Other
OQB: Optical Quality Bench
OTL: Optotunable lens
P
PAL: Progressive addition lens
PRK: Photorefractive keratectomy
PS: Perceptual Score
PSM: Perceptual Satisfaction Module
PWM: Pulse width modulation
PIQT: Perceived Image Quality Threshold
PDT: Perceived Degradation Thresholds
Q
QUEST: Quick Estimation by Sequential Testing
R
RGP: Rigid gas permeable
RMSE: Root mean square error
S
S: Sphere
SA: Spherical Aberration
Si-Hy: Silicone Hydrogel
SPDT: Shift in the perceived degradation threshold
SV: Simultaneous Vision; SimVis
T
TF-VA: Through focus visual acuity
TF-VS: Through focus Visual Strehl
U
UDVA: Uncorrected distance visual acuity
UNVA: Uncorrected near visual acuity
V
VA: Visual Acuity
VS: Visual Strehl
W
X
Y
Z

Table of contents

Chapter 1

Introduction

1.1 – Eye Ageing

1.1.1 – Presbyopia

Presbyopia is commonly defined as a progressive, age-related condition in which the eye gradually loses its ability to focus at near distances. The origin of this presbyopia is the hardening (sclerosis) of the crystalline lens, affecting the accommodation mechanism (Figure 1.1), The first symptoms typically occur around the age of 45 and progresses with age to the point of completely losing the ability to focus a few years later. This condition has been explained by several authors as a loss of elasticity in the crystalline lens [1–3]. In addition, the development of cataracts is also associated with the aging of the eye, resulting in clouding and optical deterioration of the lens [4,5].

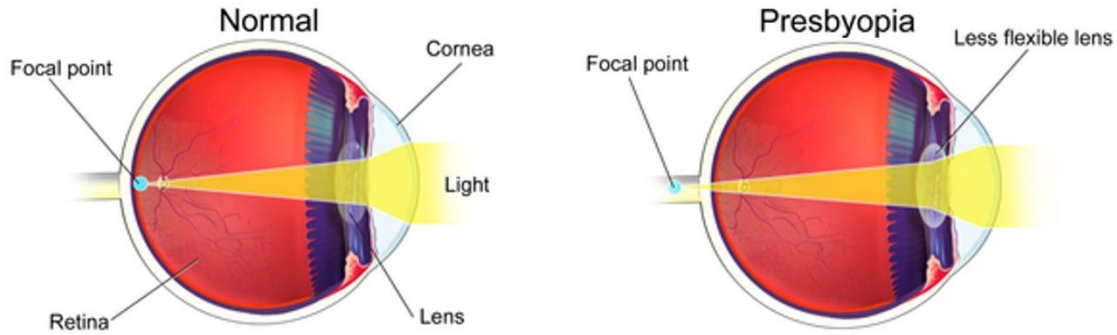

***Figure 1.1*. Normal eye with accommodation (left) vs. presbyopic eye with reduced flexibility (right), struggling to focus on the retina**. *Source: Wikipedia*

Due to the age increase in the global population, the number of people affected by presbyopia is constantly growing, expecting to reach 2.1 billion worldwide in 2030 [6], posing a significant future challenge. These circumstances are anticipated to give rise to various economic and productivity issues, the extent of which may vary based on local or global analysis [7].

The primary symptoms in individuals with presbyopia are considered to be the inability to maintain sharp focus on close objects for extended periods, eye pain, neck pain, eye strain and asthenopia following near activities [8,9].

The most common treatment for this condition, despite the development of new strategies and types of corrections, remains the use of reading spectacles [10], which creates a dependency on this optical aid. Other solutions also have drawbacks, such as peripheral blur

(when using progressive lenses), compromised visual performance between the different correction distances (for various multifocal solutions) and/or the need for surgery in different types of treatment (See 1.2).

In addition to these, it's worth noting that presbyopia can also lead to changes in lifestyle and work productivity impacting patients' quality of life, as individuals may find it more challenging to perform tasks that require sharp near vision. Furthermore, the psychological impact of presbyopia should not be underestimated, as the condition is often associated with aging and can lead to emotional impact [11]: anger, fear and sadness [12].

1.1.2 – Dry eye disease and tear film issues related to aging

The Lacrimal Functional Unit (LFU), comprising the lacrimal glands, meibomian glands, ocular surface (cornea and conjunctiva), and the nerves that interconnect them, plays a crucial role in maintaining the tear film's homeostatic balance with a correct osmolarity. This balance ensures stability and local immunity.

The tear film structure (shown in Figure 1.2) includes an aqueous-mucin layer, which is composed of fluid and soluble factors from the lacrimal glands and mucin secreted by goblet cells [13]. This layer is covered by a lipid layer that prevents evaporation.

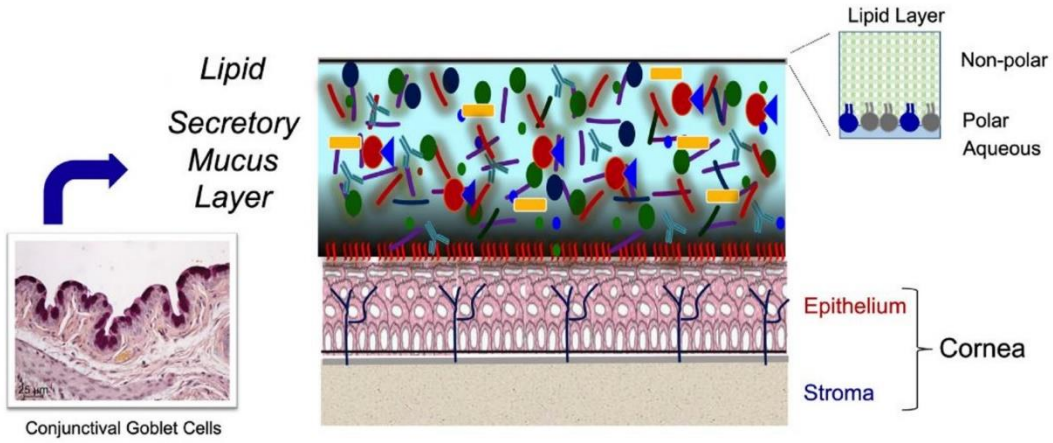

Figure 1.2. Tear film structure. *Secretory mucus layer with mucin secreted by conjunctival goblet cells, aqueous fluid and electrolytes and proteins secreted by lacrimal glands. A covering lipid layer avoids evaporation. Adapted from Pflugfelder et al [13].*

Aging significantly impacts the LFU, leading to alterations in the tear film components, generating the multifactorial Dry Eye Disease (DED) [14]. The prevalence of DED reaches its peak in the age group of 50-74 for women and in the age group of ≥ 75 for men, reaching a maximum of 70 % and 40 %, respectively. This suggests that the prevalence of DED in women is nearly twice that in men [15]. This age-related effect particularly influences the diminution of lacrimal secretion [16], affecting its composition and contributing to tear film instability.

Presbyopic eyes undergoing surgical procedures are at an increased risk of dry eye [17]. The degree of impact is linked to the invasiveness of the procedure and the extent of nerves

involvement in the corneal stroma. These surgical interventions can exacerbate dry eye symptoms, especially in presbyopic individuals.

DED, exacerbated by aging, poses a significant barrier to successful contact lens use in presbyopic individuals due mainly to the precorneal tear film instability which generates ocular discomfort [18]. However, advancements in contact lens materials, and innovative approaches like scleral lenses, show promise in mitigating these challenges [17,19,20].

The relationship between DED, digital eye strain, and presbyopia is complex. Signs and symptoms can be challenging to distinguish. The visual difficulties associated with presbyopia and DED may overlap with the impact of prolonged screen time in the current lifestyle, representing a challenge to elucidate the main reason for the symptoms and determining the most precise treatment.

1.2 – Types of corrections for presbyopia

Nowadays, a multitude of options exists to address presbyopia or alleviate its symptoms. In this section, we adhere to the classification proposed by Wolffsohn et al. [21], organizing these solutions based on the utilized platform, such as optical elements, pharmaceutical treatments etc... These correction methods or platforms can be further categorized based on whether they require surgical intervention. It is crucial to emphasize that within each platform, various correction strategies exist, and these will be explained in detail in the subsequent section (Section 1.3).

Table 1.1: Summary of correction types, categorized by surgical intervention, platform used, and strategies implemented.

Method	Platform	Strategy
Non-surgical corrections: External optical treatments	Spectacles	Monofocal Alternating Vision
	Contact lenses (CLs)	Monofocal Multifocal Extended Depth of Focus (EDOF) Monovision Enhanced monovision
Non-surgical corrections: Pharmacological treatments	Miotic drugs Lens Softening drugs	-
Surgical Corrections	Intraocular lenses (IOL)	Monofocal Multifocal EDOF Monovision Mix and Match Modified monovision

		Accommodative IOLs
	Ablation patterns	Monofocal Multifocal Monovision Blended Vision
	Corneal Inlays	EDOF Multifocal Monovision Modified Monovision
	Scleral Treatments	-

1.2.1 – Non-surgical corrections

External optical treatments:

Spectacles and Contact Lenses (CLs) serve as external optical elements to address presbyopia. Monofocal spectacles have a longstanding history, used as reading glasses to provide sharp vision at a fixed distance based on user preferences. Nevertheless, adapting to the contemporary lifestyle, which involves frequent use of electronic devices at varying distances like computers, smartphones and screens, has led to the emergence of new lens designs.

Progressive Addition Lenses (PALs) offer distinct optical powers across the surface of the ophthalmic lens along the central corridor, spanning the range from distance to near vision. This design allows the users to seamlessly shift their gaze across the lens for efficient vision at different distances. The progressive change in addition powers generate peripheral aberrations that blur vision if the user does not see through the central area [22].

Occupational lenses represent a specific type of PAL designed for computer users and office workers. These lenses feature a smooth transition between intermediate and near distances, minimizing peripheral blur compared to generic PALs. Several studies have demonstrated improved comfort and reduction in Computer Vision Syndrome with occupational lenses compared to traditional PALs [23,24], making it a good choice specially for people who work many hours at intermediate distance (e.g. with a computer).

Regarding CLs, despite the emergence of different alternatives to treat presbyopia through the use of different type of material (rigid gas permeable (RGP), soft or hybrid materials) and optical design (spherical, bifocal or multifocal), their market penetration is low compared to that of spectacles (with only 5.8 % users according to a survey [25]), considering the advantages that CLs offer in terms of aesthetics and independence from glasses [26]. New designs of multifocal contact lenses (MCLs), based on increase of depth of focus, are

constantly being developed to revert this trend, although these type of CLs remains being only between 25 and 29 % of presbyopic CL users [27,28]. Smart lenses based on artificial irises are emerging [29], adapting to light conditions and potentially enhancing the depth of focus for presbyopic users, even though they are still in the development phase.

Pharmaceutical treatments:

The use of pharmaceutical agents as method to compensate the presbyopia effects involves the investigation of two distinct mechanisms through instillation eyedrops [30]: (1) inducing pupil miosis and (2) facilitating lens softening. Ongoing research primarily through various clinical trials, is exploring the effectiveness of both approaches.

The pupil miosis strategy aims to strategically modify pupil size, effectively extending the depth of focus with a pinhole effect and myopic shift. This pathway predominantly involves the use of pilocarpine or other muscarinic agonists. Results from pharmaceuticals containing pilocarpine, such as Allergan's VUITY (1.25 % pilocarpine hydrochloride) (FDA-approved) and FOV tears (0.247 % pilocarpine hydrochloride, 0.78 % phenylephrine and others), have shown improvements in uncorrected near visual acuity (UNVA) [31–34]. Some of these pharmaceuticals have completed phase 3 trials, although detailed results are yet to be fully published. It is important to note that these drugs, to varying degrees, have exhibited side effects such as headaches, visual impairment, or blurred vision, recommending do not use for night driving [35].

Pharmaceutical strategies for lens softening show promise in presbyopia research, particularly those based on lipoic acid choline ester, aiming to restore dynamic accommodation. However, current results primarily induce improvements in distance-corrected near visual acuity (DCNVA) without achieving independence from other types of corrections [36]. Ongoing research is essential to further understand the potential of lens softening as a viable pharmaceutical approach to presbyopia.

1.2.2 – Surgical corrections

Intraocular Lenses (IOLs):

If we examine the most commonly utilized surgical correction method [37], IOLs implantation likely stands out as the predominant platform being one of the most cost-effective health-care procedures [38]. IOLs are artificial lenses used in both refractive lens exchange and cataract surgery to replace the eye's natural lens and correct refractive errors. The most prevalent cataract surgery involves the implantation of a monofocal IOL for distance correction [39,40], yet there persists a need for additional correction for intermediate and near distances [39,41].

The evolution of new types (based on the lens technology: refractive and diffractive) and designs of IOLs (multifocals, EDoF, enhanced monofocals) has facilitated presbyopia correction [42–45], consequently leading to increased independence from glasses. However,

with the division of light energy into different foci in bifocal or trifocal IOLs, some patients report experiencing dysphotopsias such as halos, starburst and glare, while others may manifest a loss of contrast [46–49]. In response to these described drawbacks, recent trends in the sector are inclining towards opting for EDoF or enhanced monofocal designs [50–53].

The difference between EDoF and enhanced monofocal designs is not clearly defined yet, although both provide an improvement at intermediate distance produced by an elongation of far-distance focus, without a higher compromise in far distance and photic phenomena of the multifocal IOLs [54]. The American National Standard Institute (ANSI) [55] provides several requirements to consider a design EDoF, while enhanced monofocal designs (termed as such after the launch of Tecnis Eyhance [56] by Johnson & Johnson) do not meet the classification criteria of either monofocals or EDof. A review conducted by Fernandez et al [57], analyzed the available monofocal enhanced designs with the conclusion that none of them met the four EDoF criteria, suggesting that another classification is needed in order to include this group in a standard.

Independently of the selected design, a persistent issue faced by patients and surgeons is the difficulty in determining which type (around 100 multifocal designs are available in the market [58]) would provide better visual performance and how patients they will see after the surgery, making the personalization of the process a challenge.

Accommodative IOLs represent another type of correction under constant research in recent years, but their functionality is highly dependent on proper ciliary body movement, which diminishes after implementation time and is associated with a reduction in far distance acuity [59].

Ablation patterns:

Among corneal ablation techniques, two distinct laser strategies have emerged, employing laser in situ keratomileusis (LASIK) or photorefractive keratectomy (PRK): monovision or multifocality. LASIK Monovision, a long-standing and extensively utilized approach, has demonstrated reliability, safety, and excellent visual performance at near distance [60–62].

Particularly, presbyLASIK has gained popularity as a multifocal corneal laser surgery for addressing presbyopia and ametropia. This technique offers two options based on the corneal zone where the ablation is performed. Central presbyLASIK employs a center-near design for corneal ablation, while peripheral presbyLASIK adopts a center-distance design, changing both corneal asphericity [63]. Different companies have developed their own techniques, each showing better results in specific types of baseline ametropia [64].

While both options are available, central presbyLASIK [65–67] has more substantial evidence of use than peripheral presbyLASIK [68], primarily due to a greater tissue removal in myopic cases, remaining as a limitation of peripheral presbyLASIK [63,69]. Nevertheless, according to several reviews , these techniques are not free of drawbacks, including issues such as loss of contrast, variations in high order aberrations and dry eye [63,64,69]. Despite

these disadvantage, the technique has demonstrated positive outcomes in UNVA, achieving spectacle independence [63,64,69]. However, adequate patient selection is imperative for the successful implementation of this technique, allowing for better control of the aforementioned disadvantages.

Corneal Inlays:

An alternative -and less common- surgical method for addressing presbyopia involves the implantation of corneal inlays with diameters ranging from 2 to 4 mm [70]. These inlays are placed either corneal pocket or within a flap created by femtosecond laser [71], with the depth of placement depending on the type of implant (from 150 to 300 μm) [70]. The corneal inlays are typically allocated to the non-dominant eye, enhancing intermediate and near vision and reducing the reliance on other correction methods.

Currently, there are three main types of corneal inlays available in the market, each with distinct working principles. Small aperture intracorneal inlays (SAICI), such as KAMRA, function by blocking the passage of light acting like a pinhole, and thereby increasing the depth of focus (DoF) [72,73]. The Raindrop Near Vision inlay reshapes the anterior curvature of the central cornea (2 mm) and induces a multifocal pattern [73]. Finally, refractive corneal inlays, currently considered the most promising type, include several commercial models like Flexivue, Invue and Icolens [74,75]. They feature a central zone without refractive power and a positive power induced in the periphery, resulting in a bifocal behavior.

Several reviews have examined the outcomes of the three types of inlays mentioned in this section [70,74,76,77], focusing on intermediate and near visual acuity with and without correction, patient satisfaction, and spectacle independence, among other factors. These reviews suggest an improvement in uncorrected near visual acuity (UNVA) but are associated with a reduction in uncorrected distance visual acuity (UDVA), loss of contrast sensitivity [78], and not achieving complete spectacle independence.

Recently, researchers from the Diffractive Optics Group at the University of Valencia have developed an alternative that combines the depth of focus principle of KAMRA with a trifocal diffractive pattern based on photon sieves [79]. This innovative solution, known as Diffractive Corneal Inlays (DCI) [80,81], resembles KAMRA but features micro-holes in the opaque zone, generating trifocal diffractive interference. Computational models and on-bench measurements assessing the visual performance of this design show promising results [81,82], but further in-vivo testing is necessary.

Other treatments:

Various attempts have been made over the years to restore functional accommodation in presbyopic individuals by sclera intervention, but its efficacy remains to be tested before it can be considered a primary option in the treatment of presbyopia. The main treatments focused on this domain include VisAbility scleral implants and Scleral Laser Anterior Ciliary Excision (Laser ACE) [83].

VisAbility scleral implants are grounded in the controversial accommodation model proposed by Schachar [84], aiming to increase the space between the ciliary muscle and the sclera to reactivate true physiological accommodation [83]. Preliminary studies on VisAbility (currently undergoing FDA clinical trials) indicated that up to 83 % of patients could perform near tasks without reading glasses after 24 months. However, some associated risks, notably anterior segment ischemia (ASI), were observed, presenting potential challenges [85].

The LaserACE procedure involves creating a matrix of micro-excisions using an Er:YAG laser on three critical zones of the sclera, penetrating to a depth of 85-90% of the scleral thickness (approximately 500-700 µm) [83]. This approach enhances flexibility and adaptability in the treated regions and surrounding tissues when the ciliary muscles contract, ultimately improving the accommodation process [83]. Studies examining the visual performance of patients treated with LaserACE demonstrated slight improvements at intermediate and near distances without other corrections after 24 months [86]. The primary risk factor associated with this treatment is the possibility of accidental micro-perforation of the sclera [83] Despite this risk, patient satisfaction in the mentioned study showed improvement with the treatment [86].

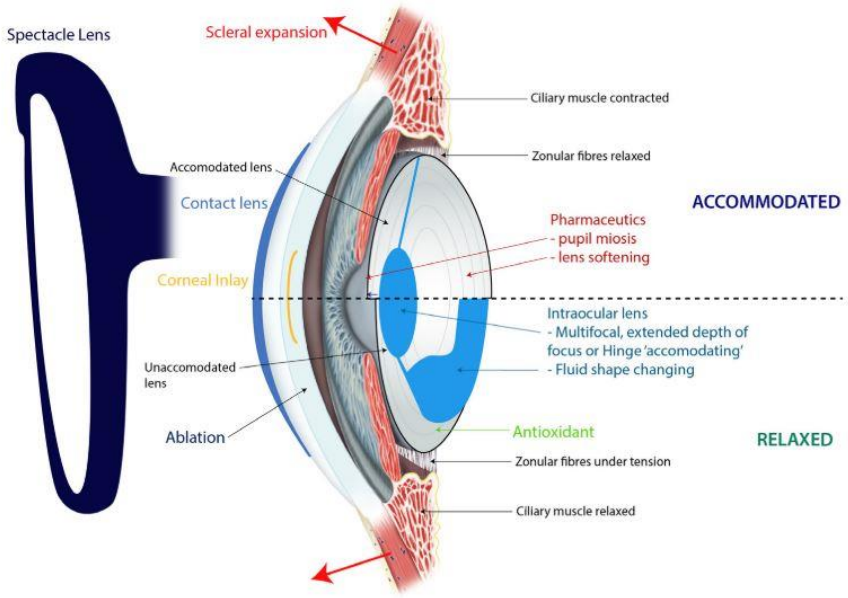

Figure 1.3. Presbyopia treatments targeting both internal and external locations. *Source: Wolffsohn et al.* [21].

1.3 – Strategies and technologies to correct presbyopia

In the preceding section, different platforms have been described in detail, each employing distinct strategies to address presbyopia or alleviate its symptoms. The present section delves into the core principles underlying optical treatments, with or without surgical process, offering insights into their primary advantages and drawbacks.

1.3.1 – Monovision

Monovision correction involves correcting one eye for far distance and the other for intermediate or near distance [87,88]. Typically, the dominant eye is chosen for distance correction, using commonly the sensory dominance determined with positive lenses [89]. The amount of addition most commonly used for this assessment is +1.50 D (since a higher value of 2.0 D may reduce drastically VA and contrast sensitivity [90]), but this is a variable decision made by each eye care professional (ECP) without clear consensus regarding the ideal amount of anisometropia [91].

Monovision can be achieved with CLs, which offer the advantage of being removable, or through a surgical treatment such as LASIK procedure or IOLs, which is less reversable.

Although far and near vision tend to be successfully achieved with monovision, other visual characteristics are impaired with this strategy. Monovision users are reported to experience stereopsis reduction [92], loss of contrast [90] and/or an additional correction to perform intermediate distance tasks [93]. Some risk complications, such as misperception motion [94,95] or blur suppression problems [96], may induce severe incidents.

1.3.2 – Alternating vision

The key concept underlying this strategy involves alternating optical power across the surface of the optical element. This modulation can occur smoothly or through different zones, the user necessitating a shift in visual gaze to focus on different specific distances. As discussed in section 1.2.1, PALs and occupational lenses are based on this concept, smoothly transitioning the optical zone from far to near distance in PALs and from intermediate to near distance in occupational lenses, without abrupt shifts. Although not widely established in the CLs market, the alternating vision strategy is utilized in bifocal RGP CLs using different zones. Certain RGP CL designs present this strategy, using the mechanical properties of eyelids and eye's gaze during near tasks, enabling vision through different zones of CLs. In these CLs, the central zone provides far distance vision, while the inferior zone, containing the near addition, facilitates near vision.

The visual performance achieved with this strategy is excellent in terms of optical quality. However, challenges related to reduced peripheral vision or professional near tasks that involve different gaze direction (e.g., plane pilot, electricians etc) may impact satisfaction with these lenses. In addition, it is necessary to adapt to a new way of looking with this type of corrections, which involves making total head movements versus eye movements, in search of focusing the area of interest through the proper correction zone.

1.3.3 – Simultaneous vision

Simultaneous Vision (SV) or simultaneous images stand out as one of the most widely adopted strategies globally for achieving spectacle independence in presbyopic patients, introducing multifocality. The working principle of SV involves the generation various focal points that provide the superimposition of focused and unfocused images of the same objects. Thus, objects located at different distances always have a focused or relatively

focused image on the retina, depending on the design. The main benefit inherent in this principle lies in the fact that there is no requirement for eye rotation or changes in gaze to provide vision at different distances [97]. This is facilitated by the intrinsic movements of these elements in tandem with the eye. Presbyopic users, in this manner, perceive a focused image for far, intermediate, or near vision, with the brain accepting one of them and adapting to the contrast reduction produced by the superimposition of images through adaptive mechanisms [98]. Several platforms employ this method to correct presbyopia, including IOLs, CLs and corneal ablations, each utilizing designs with distinct characteristics.

Depending on the optical principle generating the simultaneous images, designs can be categorized as refractive or diffractive. Refractive designs exhibit a variation in refractive power across the optical element's surface, either separated into concentric zones or smoothly continuous through aspheric surfaces. Conversely, diffractive designs combine a surface with diffractive rings and another purely refractive surface to generate SV images through interference. The diffractive pattern, through interferences and the arrangement and height of its echelettes, forms different focal points via various diffraction orders (0, 1, 2) employing the refractive surface. It is also necessary to report that a percentage of energy, in a range of 15-20 % depending on the design [99] , is lost in the high orders of diffraction.

Regardless of the optical technology generating multifocality, SV designs can be further classified into those producing well-defined focal points for different distances (bifocal, trifocal, or even tetrafocal) and those aiming to increase DoF by, for instance, introducing spherical aberration using aspheric surfaces (See Figure 1.4).

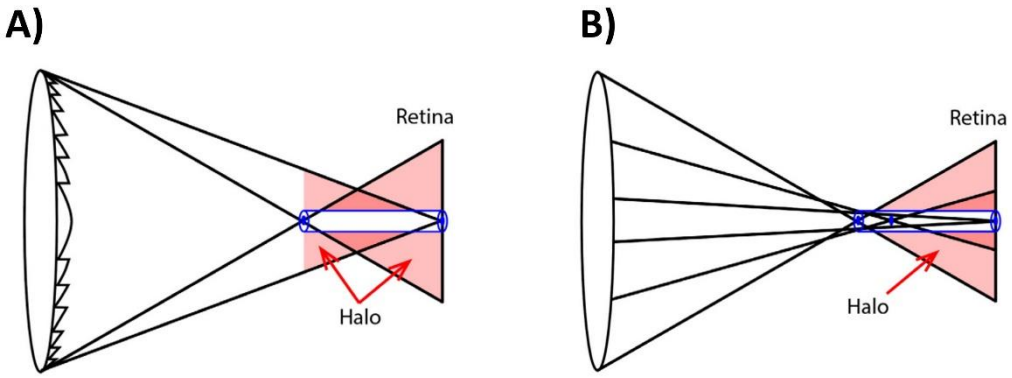

Figure 1.4. Different SV designs schemes: *(A) SV generated by specific focal points for different distances and (B) enhanced DoF by spherical aberration. Blue cylinders represent the areas between which there is sharp vision while red ones represent the halo contributions. Source: Optical Principles of Extended Depth of Focus IOLs. Alcon White Paper.*

In terms of the most implemented optical technology by each platform, IOLs feature both refractive-diffractive and refractive designs, including bifocals, trifocals, EDOF, or enhanced monofocals. Generally, bifocal and trifocal designs tend to be refractive-diffractive, while EDOF and enhanced monofocal tend to be purely refractive (see examples of through-focus energy distribution for different designs in Figure 1.5). However, for MCLs,

refractive designs are predominantly used, with center-near aspheric designs being the most common, although other options like bifocal annular, concentric multizone or steps-based designs are available in the market (explained in more detail in Section 1.4.2). On the other hand, corneal ablation surgeries are purely refractive patterns, including modifications of asphericity for specific purposes.

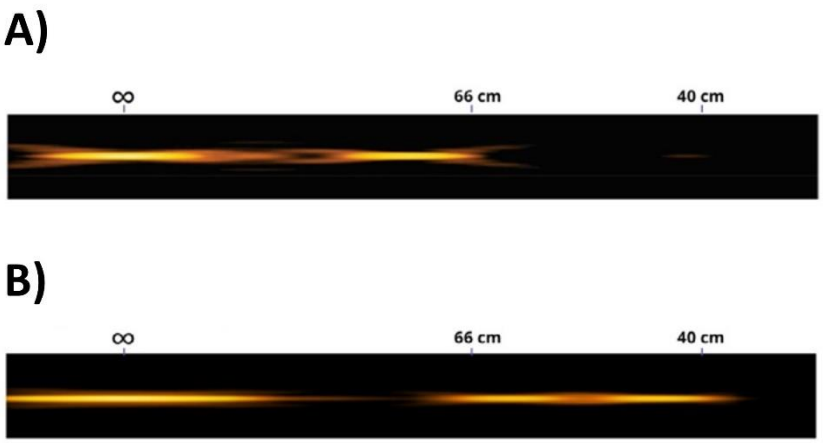

Figure 1.5. Simulated polychromatic through-focus energy distribution for different SV designs: *(A) EDOF diffractive IOL and (B) trifocal diffractive IOL. Source: Optical Principles of Extended Depth of Focus IOLs. Alcon White Paper.*

Due to the overlap of sharp and blurred images on the retina, SV inherently presents a contrast reduction due to the redistribution of light energy across different focal points. Depending on the physical characteristics and the chosen design, certain designs may exhibit more photic phenomena, such as bifocals or trifocals, while providing better near vision. EDOF or enhanced monofocal designs, on the other hand, are more optimized for intermediate vision, presenting fewer halos and glare, and better contrast.

It's noteworthy that the subject's pupil size is a crucial factor in these designs. While diffractive designs show higher pupil independence, refractive designs are highly pupil-dependent since a zone dedicated to specific vision may receive more or less light due to pupillary dynamics.

As described earlier, these designs require neuronal adaptation to mitigate far distance degradation, contrast reduction, and photic phenomena effects, which can vary among individuals. Numerous studies have investigated the mechanisms playing a significant role in both long-term and short-term adaptation. However, these mechanisms exhibit different behavior among subjects, making it challenging to predict results on a case-by-case basis. In fact, a considerable number of subjects reject multifocality from the beginning of wear.

Long-term adaptation has been documented using different SV corrections [100–102]. It has been reported that the adaptation occurs at different levels, but often, this adaptation is insufficient, leading to the removal of the optical element. The main limitation in this long-term adaptation studies is the lack of testing for different corrections. The short-term adaptation mechanisms, that remain not fully understood especially in specific commercial

designs, have been studied using generic designs through systems based on Adaptive Optics (AO) [103].A deeper understanding of this short-term adaptation mechanisms, achieved through the use of visual simulators, may improve final results by allowing for testing different designs and selecting the most suitable one for each patient.

In conclusion, simultaneous vision corrections present a significant opportunity due to their vast array and the substantial independence from spectacles they offer. However, conducting an in-depth study of the subject's needs, lifestyle, optical properties of their visual system, and managing their expectations is crucial for the success of this strategy.

1.3.4 – Combined Strategies

Other alternatives, such as mix and match or modified monovision, involved the combined use of different designs in one or both eyes to achieve a better overall result.

In the mix and match strategy, a combination of different designs of multifocal IOLs, of either distinct lens technology (refractive or diffractive) [104] or different optical near additions [105], are employed to compensate presbyopia. This approach is commonly utilized to find a binocular summation between far and near vision, including intermediate distance for presbyopic individuals. By combining multifocal IOLs with different characteristics among them, significant improvements in visual outcomes have been demonstrated, mitigating the drawbacks observed in bilateral implantation, such as reduced contrast and/or intermediate distance visual quality.

An additional refinement within the monovision approach, previously explained, is known as modified monovision. Commonly employed in contact lenses [106–108] and refractive surgeries (including corneal ablation or MIOLs) [109], this technique aims to stablish a continuous balance between far and near vision, mitigating the visual compromise associated with traditional monovision. This balance is managed by enhancing the DoF in the correction dedicated to either dominant eye, non-dominant eye or both [110].

Given the multiple options available in the market for MIOLs and MCLs, modified monovision offers various possibilities. In the area of MIOLs, a common choice is a combination of monofocal or EDOF lens for the dominant eye paired with trifocal MIOL for the non-dominant eye, which could also be referred to as Mix and Match. Focusing on MCLs, the Fitting Guides provided by manufacturers (see Section 1.4.3.2 for further information) often recommend a combination of MCL with lower addition for dominant eye and higher addition for non-dominant eye [106] during specific steps. Another parallel strategy in MCLs is termed “Balanced Progressive”, using a bifocal center-distance design for the dominant eye and a bifocal center-near design for the non-dominant eye [107]. Corneal ablation techniques extend their capabilities to include a comparable strategy known as Blended Vision, facilitated by PresbyLASIK [109]. This innovative approach increases the DoF for both eyes through the application of a corneal pattern that induces spherical aberration using PresbyLASIK technology.

Due to the extensive array of designs and possibilities within modified monovision, reaching a definitive conclusion on its superiority over others can be challenging. Nevertheless, one can anticipate improved outcomes, especially in terms of stereopsis and binocular summation, when compared with traditional monovision.

1.4 – Multifocal contact lenses (MCLs)

1.4.1 – General properties

Currently, there are over 140 million CL wearers globally [111], and this field is expected for continued growth. Soft CLs, being the most prevalent type, account for a significant percentage ranging from 85 to 95%, as reported by various authors [112,113]. Other CL types, such as RGP, scleral, and hybrid lenses, serve as valuable tools, primarily employed in addressing irregular corneas.

Soft CLs offer several advantages, including a high level of comfort, reversibility, cosmetic versatility, and excellent optical quality, making them a preferred choice for many users.

Within the realm of soft CLs, a diverse array of options is available in the market, taking into consideration factors such as material (conventional hydrogel or silicone hydrogel), replacement time (daily, bi-weekly, monthly) and mechanical properties [114]. These lenses cater to a wide spectrum of visual impairments, including myopia, hyperopia, astigmatism, and even presbyopia, being the latter a small percentage of the total [115,116]. The market trend is shifting towards hydrogel silicone and disposable contact lenses, aiming to enhance oxygen permeability and minimize episodes of hypoxia, enabling long-term uses. However, it is worth noting that these types of lenses come with their own set of challenges, including deposit generation, handling difficulties, and associated discomfort.

As explained in preceding sections, bifocal and MCLs are not the exclusive options for correcting presbyopia using this platform. Monofocal CLs utilizing monovision technique also play a role in presbyopia management. This section explores the multifaceted features, main designs, fitting processes (both mechanical and in terms of visual performance), and potential penetration challenges associated with MCLs, which are pivotal in addressing the intricate visual requirements linked with presbyopia.

1.4.2 – Main MCL designs

As outlined in earlier sections, various alternatives, excluding monovision, are available with different types of CLs (RGP and soft CLs) (refer to Figure 1.6). While translational or alternating designs are specific to RGP lenses, this discussion will focus only on designs related to soft CLs: bifocal and MCLs [117].

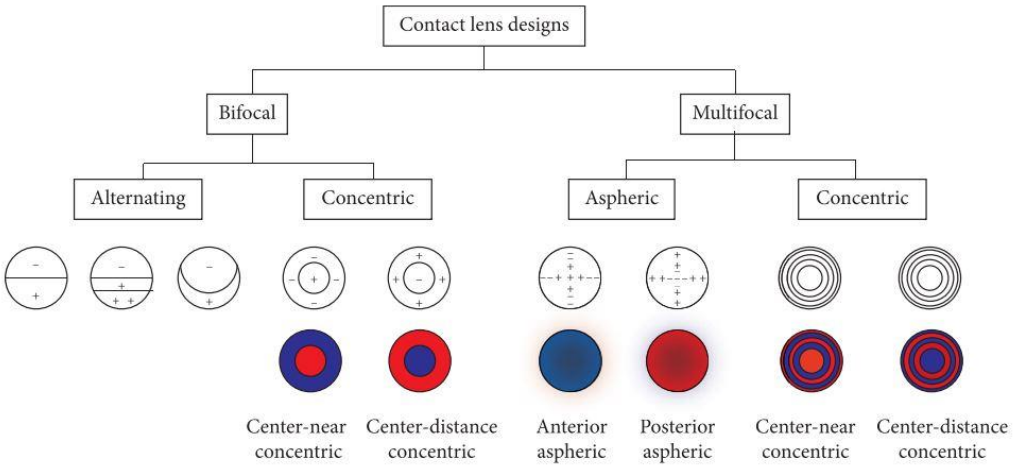

Figure 1.6. Main contact lens designs: *Bifocal and Multifocal classification according to Remon et al.* [117]*. + signs and red zones represent near zones while - signs and blue zones distance zones.*

Bifocal contact lenses are characterized by containing two distinct concentric optical zones with different focal points. Typically, these two foci are utilized for distance and near vision. If the annular zone provides far vision, the design is termed center-distance, whereas if this zone contains the near addition power, it is called center-near. Due to manufacturing constraints, the transition between zones may change smoothly rather than abruptly. These bifocal designs are often employed following a modified monovision strategy, known as "Balanced Progressive," with a center-near design in the non-dominant eye and a center-distance design in the dominant eye.

The most widely used designs for MCLs are currently aspheric and multizone concentric, with the first being the more prevalent among commercial MCLs. Within these designs, the aspheric center-near is the most typical, primarily due to the dynamic behavior of the pupil, which contracts to a miotic size in bright light and convergence looking at near target, leveraging the near zone power located at the center. Additionally, the arrangement of the aspheric surface introduces fixed negative spherical aberration (SA) to counterbalance the inherent positive SA of the eye (typically in the range of 0.10 D/mm2), thereby reducing to zero the entire optical system (eye + MCL) SA when the eye presents a value within normal ranges [118]. On the other hand, the aspheric center-distance design is not commonly employed for presbyopia correction, holding more value as a myopia management strategy for introducing positive SA.

Multizone concentric designs have been employed either center-near or center-distance independently since this type of design is more pupil-independent depending on the zone width. Similar designs to multizone concentric have been included in new center-near designs that employ power descendent steps (between 3 and 5) that run from the near addition zone to the distance power. Finally, a new type of design, denominated EDOF, has been launched recently with previous research studies successfully done with promising results [119–121], but no further details have been revealed yet regarding the design.

The MCL designs described above are highly beneficial for addressing presbyopia, increasing the DoF in this population. However, visual performance at near distances can be often compromised, with optimal benefits observed at intermediate distances. Due to the generation of distinct in-focus and out-of-focus images produced by SV, MCLs may result in far distance degradation, the presence of ghost images and associated loss of contrast, halos, and glare, which tend to be minimized after long-term adaptation [102,121]. Considering all the information presented about these designs, it is evident that a careful design selection, considering pupil size, pupil dynamics, inherent HOA, lifestyle, and expectations, will be crucial to ensure a successful fitting in terms of multifocality.

1.4.3 – Fitting processes

When discussing the adaptation of MCLs, two distinct types of adaptation must be considered. The first refers to the mechanical adaptation of the contact lens to the cornea of the presbyopic subject, which will be equivalent to that of other soft CLs. The second relates to the adaptation to the multifocal design, which may depend on the specific design and is associated with the behaviors described in the previous section:

1.4.3.1 – Mechanical Adaptation

The first step in assessing the adaptation of MCLs, in general terms, begins by ensuring that the mechanical adaptation of the MCL to the anterior surface of the cornea is correct. This mechanical adaptation has traditionally involved a series of CL parameters (ranging from basic ones like base curve (BC), total diameter (Ø) to more personalized ones like sagittal height) that must be taken into account in relation to the user's eye data. These parameters have been well described by the Contact Lens Evidence-based Academic Reports (CLEAR) group, establishing the correct way to calculate them in a publication that gathers all this information together [122]. Despite the great utility of this resource, it does not allow for a wide range of options in the field of soft MCLs, as most commercial lenses (outside of customized lenses) only have one or two values for BC and a single diameter in which they are manufactured.

The CLEAR guide also suggests an optimized evaluation protocol (based on a prospective study [97]), that will be explained in detail in Section 1.5.1 (Mechanical Evaluation).

It is worth noting that while a spherical soft contact lens must maintain its movement within acceptable limits, a MCL can cause a variety of adverse effects due to its multifocal design being decentered and in contact with movement. Conversely, a reduced movement is

associated with improved comfort and may induce conjunctival staining and indentation among other complications.

1.4.3.2 – Multifocal design lens selection: Fitting Guides (FG).

Regarding the selection of the most appropriate multifocal design for each individual, it is worth noting that it will have a significant impact on the success of the adaptation and the correction of their refractive error, along with the challenges associated with presbyopia.

Commercial manufacturers provide adaptation guides for their multifocal lenses with a series of recommended steps, considering subjective refraction (maximum positive accepted) and addition for proper adaptation. It is essential to determine the patient's sensory dominance, typically assessed using positive trial lenses, usually set at + 1.50 D. This information is crucial for proceeding with the subsequent steps, which involve considering different designs or refractive errors for each eye. These guides typically recommend initial lenses with specific refraction, dominance and addition (usually labeled as Low, Mid, and High, with the effective value not necessarily equivalent to the patient's spectacle addition [123]) and a series of modifications if the desired vision is not achieved at distance, near, or both. These modifications often involve adding or removing positive power or even changing the design by altering the addition in one or both eyes and may require several changes until the correct lens combination is found. Depending on the manufacturer, there may be different trends: using different designs in each eye for center-near and center-distance (Fig 1.7 A for high additions) or the same design and addition (Fig 1.7 B for additions up to +1.75 D).

A) **B)**

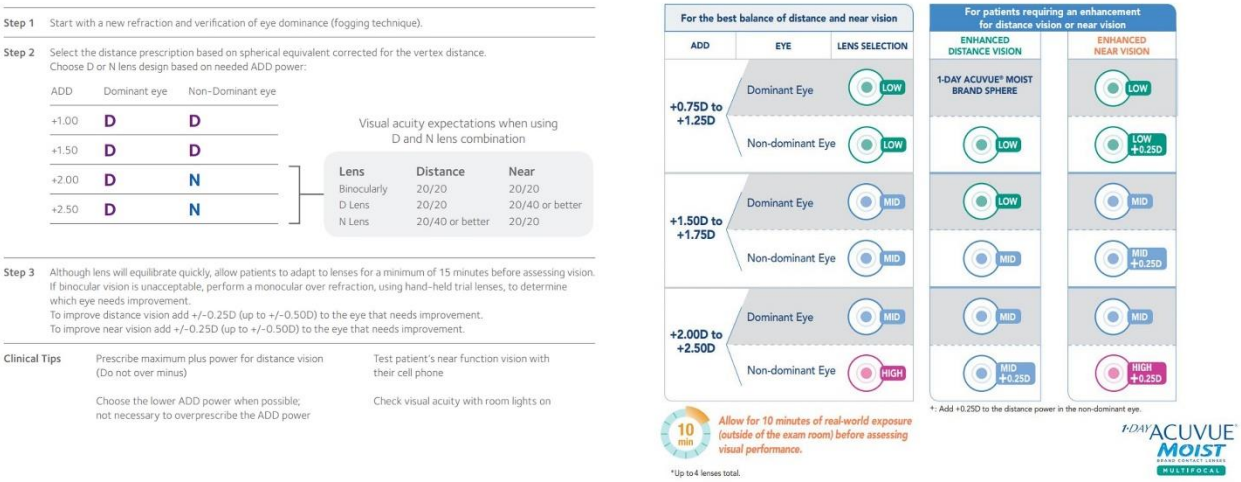

Figure 1.7. Two FG examples from different commercial brands: *(A) Biofinity from CooperVision and (B) 1-Day Acuvue Moist from Johnson & Johnson. The FG presents initial lenses according to addition values and different steps to enhanced visual performance, either far distance or near distance.*

While these FG can be a great help to initiate the adaptation and determine the initial pair of MCLs, they are far from being a method where professionals can leverage their knowledge and understand how each MCL design works. In fact, studies have shown that modifications to these FG can improve the process and even reduce the number of lens pairs that need to be tested to find the optimal one [124]. Understanding how each design works and having data on the power profile beyond these FG would help ECPs achieve a deeper understanding, translating into greater success in these adaptations, better visual performance, and fewer adverse effects associated with MCLs.

1.4.4 – Penetration problems

Despite the availability of various bifocal and multifocal designs in CLs, the utilization of CLs decreases significantly when individuals reach the presbyopic age. This trend is highlighted in the study conducted by Naroo et al [26], which observed a decline in the percentage of CL users from 66% to 52% and further to 25% in the age groups of 40–44, 45–49, and 65–70 years, respectively. The same study reported that only 25% of presbyopic CL users opted for a multifocal or multifocal toric design, a percentage closely aligned with the findings of Morgan et al. [28] (depicted in Fig. 1.8).

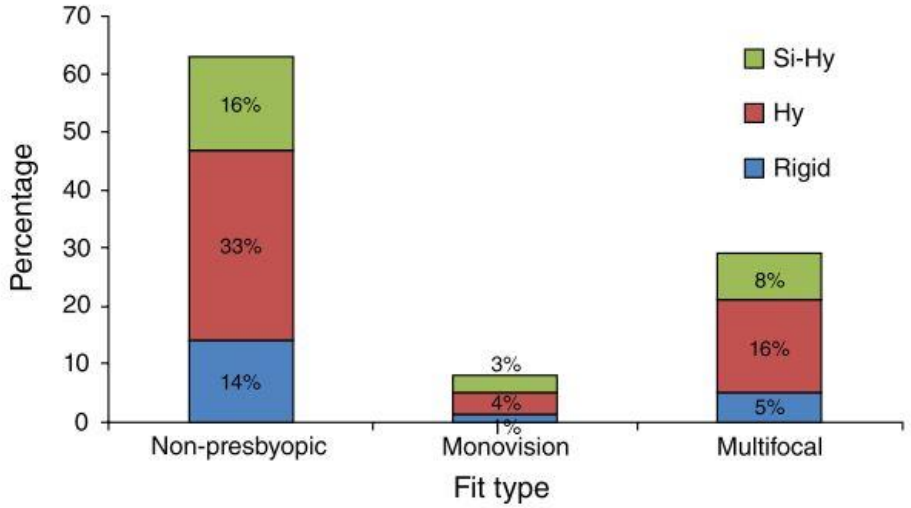

Figure 1.8. Percentage of presbyopic patients corrected with different CL types and strategies for each material: *Silicone Hydrogel (Si-Hy) in green, conventional hydrogel (Hy) in red and RGP (Rigid Gas Permeable) in blue. Graph from Pérez-Prados et al.* [116] *based on Morgan et al* [28].

Several factors may contribute to this decline, including ocular dryness and associated discomfort linked to the aging process, limited awareness of multifocal solutions among both patients and ECPs, unexpected visual performance issues, especially at crucial distances required by users, and the time-intensive fitting process, which often necessitates multiple visits to the ECP.

To reverse this trend and increase the adoption of MCLs over spherical CLs, it is imperative to gain a comprehensive understanding of MCL design and optimize the fitting process to minimize chair time. This involves addressing issues such as ocular dryness through

better material options, enhancing awareness and education about multifocal designs, and streamlining the fitting process to achieve successful and efficient adaptations, ultimately encouraging more individuals to adopt MCLs.

1.5 – Evaluation of MCLs

An important step inside the adaptation of MCLs is to note if this solution is truly able to address the presbyopia and refractive error with enough comfort to be maintained or not in time as an option. For this reason, both a correct mechanical adaptation, associated with comfort, and an adequate visual performance for the desired distances evaluations are critical to decide the success of adaptation. In the majority of cases, a correct mechanical adaptation will be associated with comfort, and conversely a poor mechanical adaptation may affect the visual performance obtained at different distances.

1.5.1 – Mechanical evaluation

As it was anticipated in the Mechanical Adaptation section (1.4.3.1), CLEAR group developed an optimized evaluation protocol (based on a prospective study [97]) for soft CLs adaptations after 10 minutes of wear, which includes a slit-lamp examination assessing three scores related to CL's movements (+ quick or large; 0 medium; or - slow or minimal) for: (1) post-blink movement in upgaze (B), (2) horizontal lag (L; CLs overlapping onto limbus)and (3) push-up recovery speed (P); (4) a fitting cross indicating the amount of decentration, and a 0 [poor] to 10 [don't feel] comfort scale. If these indicators are positive receiving a good score, with more importance in "B" and "P", the adaptation can be considered clinically correct (an example of good adaptation is presented in Fig. 1.9).

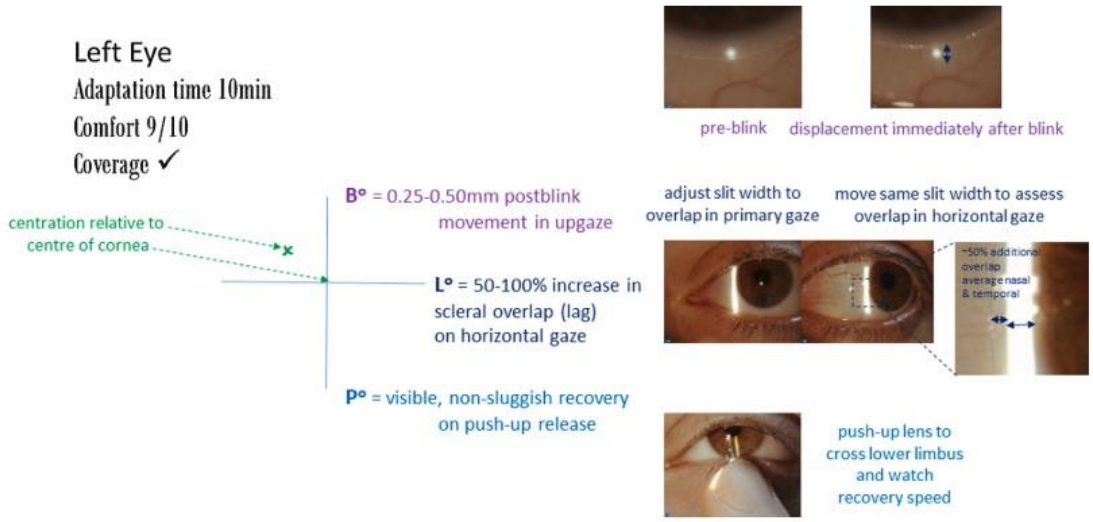

Figure 1.9. Optimized mechanical evaluation proposed by CLEAR group and consisted of slit lamp examination of: *post-blink movement in upgaze (B), horizontal lag (L), push-up recovery speed (P), a fitting cross indicated the decentration and a comfort scale. Source: Wolffsohn et al.* [122].

In case of the existence of an intolerant movement or another suspicious of irregular behavior, corneal and conjunctival staining assessment with fluorescein or lissamine green -depending on the complication- will be recommended to explore the ocular surface health after the use of CLs. The CLEAR group also recommends a guideline of more frequent complications associated with CLs [125] and the proper way to manage them, becoming a gold standard in the field.

1.5.2 – Comfort evaluation

The comfort evaluation with CLs has been a research target in the optometry field, since it supposes a primary reason resulting in dry out for CLs wearers. Comfort is a complex subjective variable with a great difficulty to judge and depending on multiple factors such as material, geometry, edge shape, etc.

Nowadays, one of the most utilized methods to assess comfort related to CLs wearing is the questionnaires based on Rasch model analysis. Questionnaires frequently utilize interval scales such as numerical rating scales, verbal rating scales or visual analogue scales. However, not all of these questionnaires are properly validated for assessing CLs discomfort [126].

The validated questionnaires that have been used concretely in CLs to measure discomfort may be distributed in integrally developed for CLs or for DED, with utilization in CLs. The questionnaires completely dedicated to CLs are CLDEQ (Contact Lens Dry Eye Questionnaire) [127] , CLDEQ-8 [128], being the latter a reduced and quicker version with only 8 items, both with moderate discrimination and accuracy, and belonging to a different family, the Contact Lens Impact on Quality of life (CLIQ) showing a good validity and repeatability [129]. In other hand, the dedicated DED questionnaire OSDI (Ocular Surface Disease Index) presents good discrimination and repeatability [130].

1.5.3 – Visual performance evaluation

The assessment of visual performance in bifocals and MCLs primarily focuses on addressing the challenges that these lenses aim to overcome. This involves achieving a DoF increment for intermediate and near vision and spectacle independence. Simultaneously, the evaluation considers potential drawbacks, such as ghost images, contrast loss, reduced stereoacuity and far distance degradation.

To analyze visual acuity (VA), assessments can vary conditions including different real distances of interest (typically at 4 m, 0.66, and 0.40 cm), changing optotype contrast (usually High and Low contrast), and adjusting lighting conditions (photopic and mesopic) to study visual acuity through pupillary dynamics.

In a similar way, defocus curves or through focus visual acuity (TF-VA) become valuable. These curves are commonly assessed using trial lenses ranging from +1.00 D to -4.00 D in 0.50 D steps, offering insights into visual performance across a broad range of distances. Despite providing valuable information, this method requires a significant amount of time and may

induce fatigue in the evaluated patient. It also aids in detecting shifts, allowing for fine-tuning through over-refraction, as recommended by some fitting guides.

Additionally, questionnaires like NVAQ (Near Visual Activities Questionnaire) [131], focusing on spectacle independence and comfort in various tasks with MCLs, or QoV (Quality of Vision) [132], evaluating the quality of vision provided by MCLs [133] serve as useful tools to understand the perceived benefits of these lenses.

Exploring the potential disadvantages of SV corrections, contrast reduction resulting from these designs can be studied through contrast sensitivity function testing, covering low to high frequencies under different lighting conditions [119,134,135]. To speed up the process, fast contrast sensitivity tests at a fixed visual acuity size, tailored to high frequencies, are being introduced[136]. Due to the introduction of diverse designs that may differ between eyes, stereopsis is evaluated to assess any potential reduction and quantify the amount of loss[108,137–139], considering the impact on daily activities.

Recent developments in optometry and ophthalmology have introduced technologies such as the "Lens Disturbance Analyzer" (Universidade do Minho, Portugal), which assesses the size and shape of light disturbances around a central source while wearing MCLs [133,140], helping to understand which designs may produce more significant photic phenomena. Furthermore, other emerging tools streamline classic tests like defocus curves or contrast sensitivity, using adaptive psychophysical methods and minimizing the exploration time, exemplified by the iPad application: Multifocal Lens Analyzer (MLA, QVision, Spain)[136].

1.6 – Visual simulators

The definition of a visual simulator in the optics context pertains to a device capable of replicating different optical elements and related experiences, aiming patients to test how their vision is through different options. This becomes particularly crucial in non-reversible treatments, such as IOLs implantation or corneal ablation with multifocality application, where patients might be unfamiliar with the expected result of his/her vision. However, which is the technology behind this possibility?

1.6.1 – Adaptive Optics

Typically, visual simulators have been based on Adaptive Optics (AO), even though its origins lie outside this topic. Initially developed to mitigate atmospheric distortion or turbulence affecting astronomical observations, AO emerged to rectify blurred images produced by telescopes[141,142]. In the astronomical context, AO works by sensing the wavefront to quantify distortion levels and then applying inverse corrections using deformable mirrors.

The evolution of this technology has evolved from astronomy to vision science in the field of optics and ophthalmology [143], sophisticating and embracing different questions,

such as comprehensive understanding of HOA in the human eye (addressing not only correction, but also inducing desired values) [144,145], retinal imaging [146] and simulations of optical elements at real time [147].

Nowadays, two different active compensator devices are commonly used following aberration measurements using Hartmann-Shack detectors: deformable mirrors and Spatial Light Modulators (SLM). Deformable mirrors and SLMs, under different working principles, modulate and manipulate the wavefront, offering the possibility to induce multifocal elements.

The continuous evolution of this technology has led to increasingly sophisticated developments, manifesting in more comprehensive systems (see Fig. 1.10). These advancements enable the exploration of complex properties, introducing possibilities such as binocular devices, the incorporation of polychromatic aberrations assessments [143] and integration of real optical elements in a cuvette inside AO system[148].

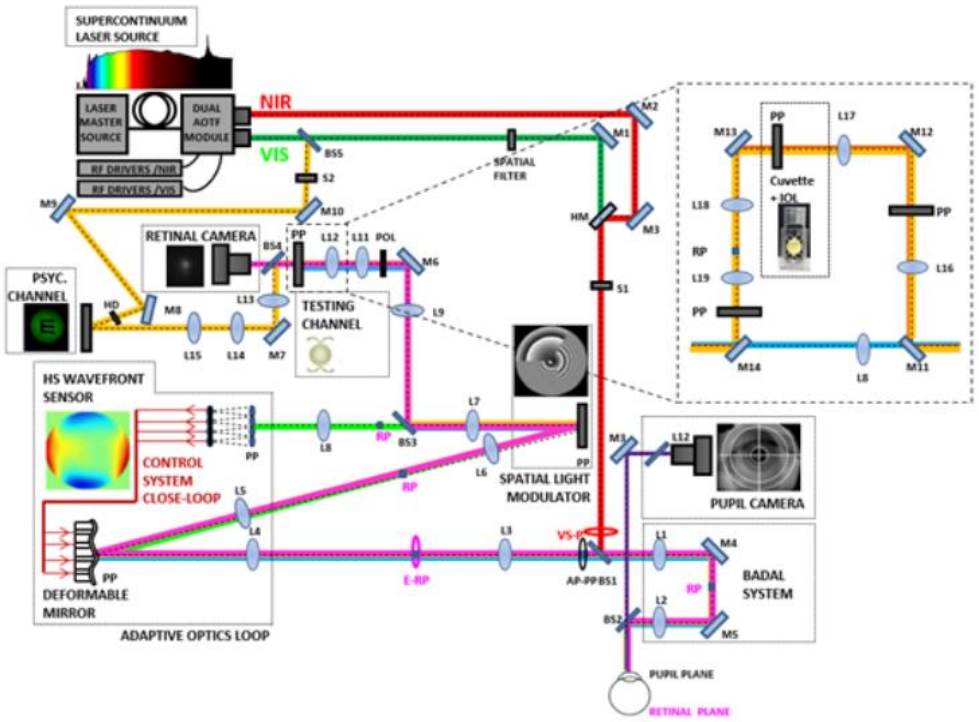

Figure 1.10. Schematic diagram of Adaptive Optics (AOII) system from VioBio Lab, which presents a deformable mirror and a SLM, as AO elements, IOL cuvette and a temporal multiplexing channel. *Source: Marcos et al. [143].*

1.6.2 – IOL Cuvette

Another type of technology employs a cuvette containing various real Intraocular Lenses (IOLs) and a projection system to simulate them in patients' eyes. This concept has

been tested by VirtIOL [149] KTH Royal Institute of Technology through various developments[150] and Viobio Lab [148], among others.

The main advantage of this technology is that it simulates a real optical element, similar to the one that will be implanted in the patient, providing a highly realistic experience. On the other hand, it has the disadvantage of lacking versatility to test different models, and the evaluation does not occur in a real vision environment.

1.6.3 – Temporal Multiplexing

Temporal multiplexing -previously explored in other industrial doctoral theses focused on its development[151], validation in visual simulations, and application in IOLs designs and corneal ablation[152] - represents an innovative approach distinct from AO. Originating from VioBio Lab (Institute of Optics, CSIC, Spain), this technology has even led to the establishment of a start-up, 2EyesVision SL.

Temporal multiplexing uses optotunable lenses, a concept well-supported by scientific evidence[153]. Temporal multiplexing induces optical power variations at speeds greater than the blur flicker fusion threshold of the eye, enabling the simulation of apparently static multifocal images on the retina. From an optical quality metric from a lens design, it is able to calculate how long the optotunable lens must stay in each optical power under temporal multiplexing to replicate the desired multifocal element.

1.6.4 – Commercial devices

While the development of complex AO and IOL cuvette systems, previously mentioned, is a current reality, these optical systems serve as valuable laboratory tools, remaining in general distant from commercialization in a clinical environment.

In order to overcome this limitation, different laboratories and companies have tried to translate these described setups and technologies to more compact devices with the potential for commercialization. Presently, the most prominent devices available in the market are SimVis Gekko , VAO (Voptica, Spain) and (Dezimal, Austria); as depicted in Fig.1.11 and Fig.1.12.

The temporal multiplexing technology has been commercialized into a device known as SimVis Gekko™, marking the first binocular and head-mounted visual simulator oriented to clinical use. SimVis Gekko™ has already demonstrated its capability to reproduce commonly used M-IOLs [154], multifocal corneal ablations [155] and MCLs [156]. While M-IOLs have received more attention, the potential for advancements and innovative contributions to the MCLs market lies in the less-explored territory of SimVis Gekko™. Further details regarding SimVis Gekko™ will be elucidated in the Methods section (2.1).

Figure 1.11. Use of SimVis Gekko visual simulator inside a clinical assessment.

VAO, a visual simulator based on SLM (AO), offers multiple functionalities, including objective and subjective refraction, HOA assessment and simulation of both generic and their own commercial M-IOLs (the simulation of lenses from other manufacturers is not available). VAO is a monocular, non-portable device with an internal screen for stimuli presentation, which has demonstrated reliability in simulating MIOLs and measuring subjective refraction, substantiated by scientific evidence [157,158].

On the hand, the RALV visual simulator employs Real M-IOLs under a projection system to experience postoperative vision before undergoing the surgery, aiding in the lens selection. RALV is a non-wearable device that uses an external screen with various positions at different distances. However, detailed information regarding the disposition of M-IOLs inside the instrument (whether in a cuvette or similar mechanism) has not been reported. The scientific evidence validating the device and ensuring the reliability of its outcomes is not openly available at present.

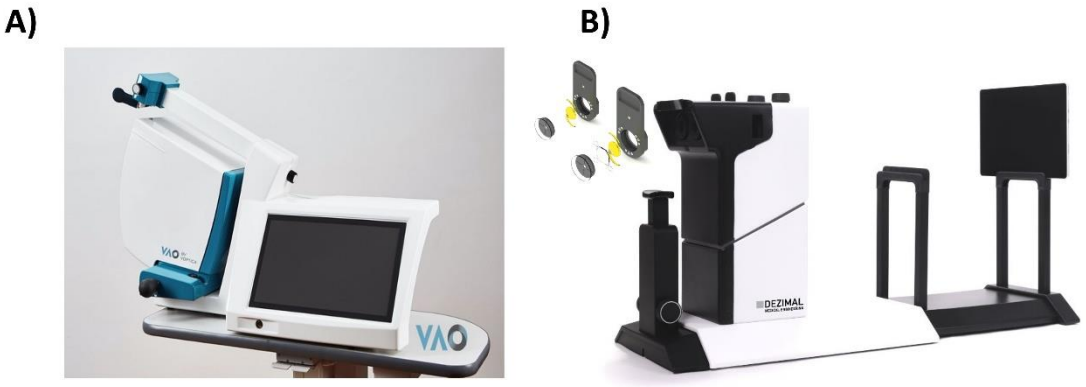

Figure 1.12. Main commercial visual simulator: (A) VAO (Voptica) and (B) RALV (Dezimal).

1.7 – Motivation of this thesis

The SimVis technology has already demonstrated to provide a high level of accuracy and reliability for the simulation of a wide range of commercial IOLs designs: enhanced monofocals, EDOF, bifocals and trifocals. In fact, these simulations have also been validated in patients with cataract showing strong correlation between pre- and post-operative results. Other optical corrections, such as multifocal corneal ablation and MCLs, have also been successfully simulated using manufacturers-provided information.

The market penetration of MCLs in presbyopic corrections presents a significant opportunity for improvement. This will undoubtedly be based on increased awareness of these corrections, improved visual performance following the fitting guides and further enhancement of assessments and fittings processes to reduce additional times. Achieving these milestones not only contributes to a reduction in chair-time, but also minimizes frustration levels for both ECPs and patients. SimVis technology can definitely play a crucial role in overcoming the challenges associated with MCLs, aiding ECPs in enhancing processes and associated visual performance.

This thesis aims to achieve this ambitious goal by obtaining accurate MCL simulations, understanding how to improve fitting guides using these simulations, and exploring the neural processes that may influence adaptation. By doing so, we hope to pave the way for a more effective and efficient approach to presbyopic corrections using CLs.

1.8 – Open questions

In this thesis, we have proposed a proceeding to obtain MCLs simulations using in-vitro measurements, optimized current visual performance assessments, and analyzed different strategies of presentation of SV corrections and how its short-term neural adaptation has occurred, to answer the following open questions:

1. Is it possible to obtain the SimVis simulation of any MCL design using in-vitro measurements and computational characterization? Are these MCLs simulations accurate enough in comparison with real MCLs?

2. Is it possible to use the SimVis MCLs simulations to replicate the Multifocal Fitting Guides for each commercial lens and manufacturer? Is it possible to use it to even optimize these Multifocal Fitting Guides?

3. Is it possible to develop a quick and automatized mechanism to induce a wide range of astigmatism magnitudes and axes? Could this mechanism allow to simulate MCLs with astigmatism avoiding trial lenses?

4. Is it possible to optimize classic visual performance tests using SimVis Gekko and an App based on adaptive methods, in a synchronizing way? Could this synergy reduce the time of assessment?

5. Could different strategies of presentation be used to change the first impression of multifocality and modulate the rejection of multifocal presbyopia corrections?

6. Is it possible to measure short-term neural adaptation to SV corrections in a real clinical environment? Could any attribute related to these SV corrections be a predictor for level of adaptation? Is it applicable to commercial SV lenses?

1.9 – Goals of this thesis

The main purpose of the thesis is to validate SimVis Gekko as a useful tool in contact lens practice for presbyopia. The specific goals are:

1. To replicate the fitting guides of MCLs using SimVis Gekko simulations obtained from in-vitro measurements.

2. To enhance classic visual performance tests performed in the MCLs evaluation using SimVis Gekko.

3. To understand the neural implications that play a role in multifocality presentation and short-term adaptation to SV.

1.10 – Hypothesis

The hypotheses of this thesis are:

- MCLs simulations based on in-vitro measurements allow us to replicate accurately fitting guides from different manufacturers and open to the chance to improve the fitting process to achieve an optimal solution.

- The development of a new automatized mechanism to induce astigmatism and the synchronization of SimVis with an App that includes adaptive methods, allows to optimize visual performance test and reduced chair-time.

- The smooth presentation of SV corrections after adaptation to blur reduces the multifocality rejection.

- SV corrections with low amount of addition and higher percentage of energy in near vision induce higher short-term neural adaptations

Chapter 2

Methods

This chapter presents the methods used in this thesis and, among them, the visual simulator used in all the measurements throughout the clinical and psychophysical tests. The methodologies adopted in the different projects of this thesis have been grouped in the following sections:

1. SimVis Gekko simulator and the quality control processes used to ensure the accuracy of each lens simulation.

2. Clinical and Psychophysical methods or tests employed in the different studies and how they were conducted.

3. The commercial instruments and software that were used to: (1) achieve the required characterization and obtain the lens simulations, (2) measure the visual performance through these lenses and other corrections, and (3) calibrate the displays and mechanisms used in the studies of this thesis.

2.1 – SimVis Gekko Visual Simulator

As previously mentioned, the primary motivation of this thesis, across various objectives, is to validate the current version of SimVis Gekko as a beneficial tool in MCLs fitting. We believe that SimVis Gekko can actively support the two key processes involved: 1) the MCLs selection and; 2) the clinical evaluation. Therefore, SimVis Gekko, the pivotal element of this thesis, is employed as a multi-purpose device for simulating MCLs, also with the aim of improving visual function assessments and serving as an essential apparatus in psychophysical experiments.

SimVis Gekko is the first commercial binocular and clinical visual simulator that operates under the principle of temporal multiplexing of optotunable lenses (OTL), as mentioned in section 1.6.3.. Other notable features of SimVis Gekko are that it is a wearable device, with a wide field of view of 20 degrees, and wirelessly controlled.

The Temporal Multiplexing principle [153] consists of inducing rapid and periodic optical power variations at speeds faster than the blur flicker fusion threshold of the eye (50 Hz), enabling the simulation of apparently static multifocal images on the retina [159,160]. This working principle is represented in figure 2.1, where we can observe two different states of optical power, 0 D (A) and 2 D (B) generated applying two different voltage signals on the OTL, and the apparent superposition of these states on the retina due to the high speed alternation, generating the simulation of a bifocal lens (C).

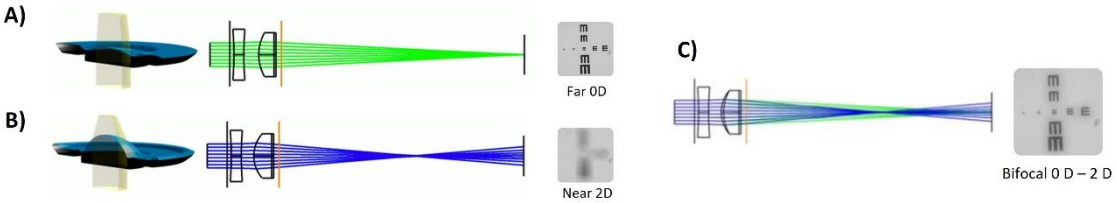

Figure 2.1. Temporal multiplexing principle: the working technology behind SimVis Gekko. Each state of the lens is represented individually: *A) Far 0D; B) Near 2 D and C) Apparent superposition under temporal multiplexing, to provide the simulation of a bifocal with 2 D of addition.*

While OTLs are the main optical component of the device, the optical modules of the SimVis Gekko are miniaturized chassis comprising other significant elements (two achromatic doublets, one field stop and six flat mirrors, (shown in Fig. 2.2 [151]) acting together as an erect 1:1 relay, an optical projection system with magnification one and without image inversion. This arrangement allows the OTL plane to be conjugated onto the pupil plane of the eye, without inversion nor magnification, or other aberrations such as astigmatism, distortion, or coma.

In SimVis Gekko, the subjects' refraction is corrected using trial lenses placed in dedicated external trial lens holders, and the simulation produced by the OTL represents the multifocal pattern of the intraocular lens only. The device provided a pair of color LEDs to guide the alignment process, allowing centration on the corneal apex and taking into account

the interpupillary distance. With this alignment mechanism, each patient's pupil must be vertically and horizontally centered with respect to the optical axis of the respective SimVis Gekko optical channel, achieved through mechanical adjustments made by various wheels.

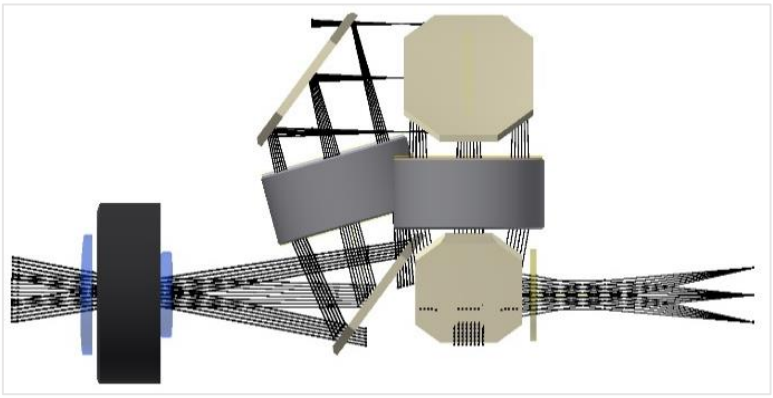

Figure 2.2. SimVis Gekko module scheme with the main optical elements and the followed optical path. *The main optical elements are: OTL, six flat mirrors and two achromatic doublets. Source: Barcala et al [151]*

Both the OTL and the LEDs are controlled by an electronic circuit powered by a Lithium battery. The electronic circuit, through custom firmware, can send and receive various commands from a host device, typically an iPad (Apple Inc, USA), using Bluetooth. The information for each simulation is taken from a cloud network through a backend service containing the lenses associated with each SimVis Gekko and selected in a SimVis Gekko App using the iPad. In this thesis, we used customized SimVis Gekko devices that can be controlled using Matlab (MathWorks, USA) with a dedicated toolbox, and through Bluetooth connection to a PC (process described in section 2.7.1).

Finally, several modifications were made in this thesis to the custom firmware, to provide more versatility in the introduction of simulations. While in normal clinical use the simulations are introduced abruptly, these modifications allowed for smooth transitions with distinct variable inputs: number of linear steps of the smooth transition, optical starting point of the transition, and the duration of the transition. These modifications in the firmware were used in the psychophysical experiment described in chapter 7.

2.2 – SimVis Gekko Quality Assurance Processes

A series of quality assurance processes are essential to ensure proper functionality. These processes pertain to two primary aspects: the components of SimVis Gekko's optical modules and the SimVis Gekko simulations.

2.2.1 – Quality control and calibration of SimVis Gekko

As previously mentioned, the main active elements of SimVis Gekko are the OTL, and optimal performance of these components is crucial for accurately simulating a wide variety of optical elements:

Dynamical behavior of OTLs:

The dynamical behavior associated with OTLs is an important factor that requires compensation to ensure their proper function. This behavior may vary even within the same model of OTL [161], necessitating the measurement of this dynamical behavior for each OTL prior to assembly in each SimVis Gekko. A custom high-speed focimeter is utilized to measure the transient response of each OTL and determine the necessary compensation to achieve the desired performance [162,163]. Once each OTL is characterized, this correction will be applied in future simulations, resulting in accurate and predictable behavior.

Static and dynamic quality check:

A calibration setup (Cal-03) enables us to calibrate the correspondence between the OTL digital counts (associated with potential variations) and optical diopters for each optical module, thereby identifying the best focus images using a binary noise stimulus for 0 D (far distance) and 2 D through an algorithm, for different digital count values, referring to this process as “static check”. Using the static quality check calibration, generic bifocal lenses are generated and analyzed with image acquisition, and the dynamic quality is recorded [153,164].

Binocularity evaluation and field of view (FoV)

The binocularity correspondence between each optical module is verified using a calibration setup (Cal-04), ensuring that it falls within acceptable range, in accordance with the American Standards for Binoculars [165]. During this process, the field of view must exceed 20 degrees, binocularly, to pass the control.

2.2.2 – Obtaining and validating SimVis simulations

Another crucial aspect to consider within the quality processes is the methodology for achieving accurate and reliable simulations of SimVis Gekko and its implications [161,166,167]. The comprehensive process, depicted in the flowchart of Fig 2.3, starts with the target lens data (IOL or MCL), typically using the phase map as initial input [154,161]. In instances where this information is not provided by the manufacturer, it can be measured directly using commercial devices, as detailed in Chapter 3 for MCL elements.

With the phase map for a specific optical diameter of the multifocal element, the Through Focus Visual Strehl (TF-VS), ranging from -1 D to +4 D in 0.05 D increments, is obtained using a dedicated Matlab script. From the TF-VS of each lens design, a set of temporal coefficients is calculated, indicating the duration that OTL of the instrument must remain at each optical power under temporal multiplexing.

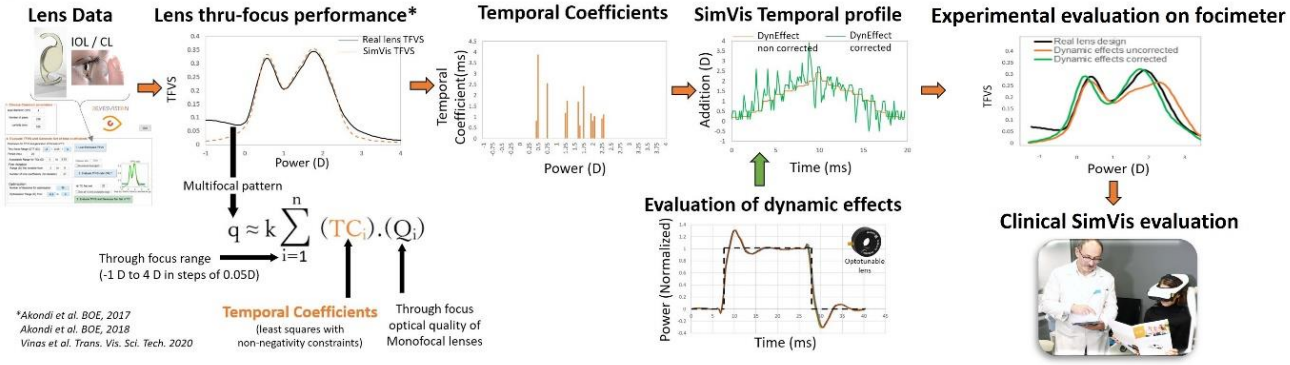

***Figure 2.3*. Obtention and validation of SimVis technology simulation:** *TF-VS calculation, temporal coefficients obtention, on-bench validation and clinical evaluation of the simulations.*

Upon applying the compensation for the measured dynamic effects, we obtain the final SimVis Gekko temporal profile (20 ms per cycle) to replicate the desired multifocal element. Subsequently, an experimental TF-VS evaluation of this SimVis Gekko temporal profile is performed on bench using the high-speed focimeter, comparing it with the theoretical TF-VS, with these differences assessed in terms of Root Mean Square Error (RMSE).

The on-bench validation is successfully achieved if the following quality terms are met: differences lower than 0.20 D of shift for the location of the TF-VS peaks and a RMSE less than 0.05 between theoretical and experimental TF-VS in the dioptric range of interest: -1.00 D to + 4.00 D. After a satisfactory on-bench evaluation, this lens simulation is validated for clinical use.

2.3 – Commercial Multifocal Contact Lenses

Four families of daily commercial soft MCLs from different manufacturers were used in Chapters 3 and 4: MyDay (CooperVision, USA), 1-Day Acuvue Moist (Johnson & Johnson, USA), Dailies Total1 (Alcon, USA) and Biotrue ONEday (Bausch + Lomb, USA). The different parameters of the lenses studied can be seen in Table 2.1. MCLs with a wide range of distance powers and additions labeled as Low, Mid or High were used. The Biotrue ONEday MCL has only Low and High labeled additions available.

Table 2.1: **Nominal parameters of the four daily commercial soft MCL families used in this thesis:**




Parameter	MyDay	1-Day Acuvue Moist	Dailies Total1	Biotrue ONEday
Manufacturer	CooperVision	Johnson & Johnson	Alcon	Bausch+Lomb
Add	Low Mid High	Low Mid High	Low Mid High	Low High
Material	Stenfilcon A	Etafilcon A	Delefilcon A	Nesofilcon A
Refractive index (546 nm)	1.40	1.40	1.42	1.37
Lens design	Aspheric	Aspheric	Aspheric	Aspheric
Water content (%)	54	58	33	78
Base Curve (mm)	8.4	8.4	8.5	8.6
Diameter (mm)	14.2	14.3	14.1	14.2
Central thickness (mm) @ -3.00 D	0.08	0.084	0.09	0.1

These MCLs were used for different purposes, clearly differentiated. In chapter 3, the MCLs were characterized in-vitro and computationally and used to study its visual performance in comparison to SimVis Gekko simulations. On the other hand, the same real MCLs were used in chapter 4 to compare the visual performance obtained with the selection offered by the commercial Fitting Guide of each manufacturer and by SimVis Gekko, using a custom-developed metric based on VA obtained with their simulations.

2.4 – Commercial instruments and devices

During the different studies undertaken in this thesis, we have utilized a wide range of commercial instruments and devices. This range includes from sophisticated metrology equipment used for precise in-vitro measurements of multifocal elements, to routine clinical instruments integrated to everyday optometric practice.

2.4.1 – Nimo TR1504

NIMO TR1504 (Lambda-X, Belgium) is an optical mapping device which allows measuring the power profile of CLs [168–171] and IOLs [172] (showed in Fig 2.4 A). It is based on the patented quantitative deflectometry technique, combining the Schlieren principle with a phase shift method [173] (depicted in Fig 2.4 B). It uses a light source of 546 nm to measure beam deflections and obtain power maps. Its accuracy and repeatability are 0.05 D for spherical soft CLs powers and between 0.04 D to 0.2 D for MCLs [173,174].

The previously described MCLs families were measured with NIMO TR1504 to obtain their power profile maps, a process widely explained in Chapter 3. These MCLs were placed in a cuvette of the device with saline solution, as recommended in the instrument guidelines.

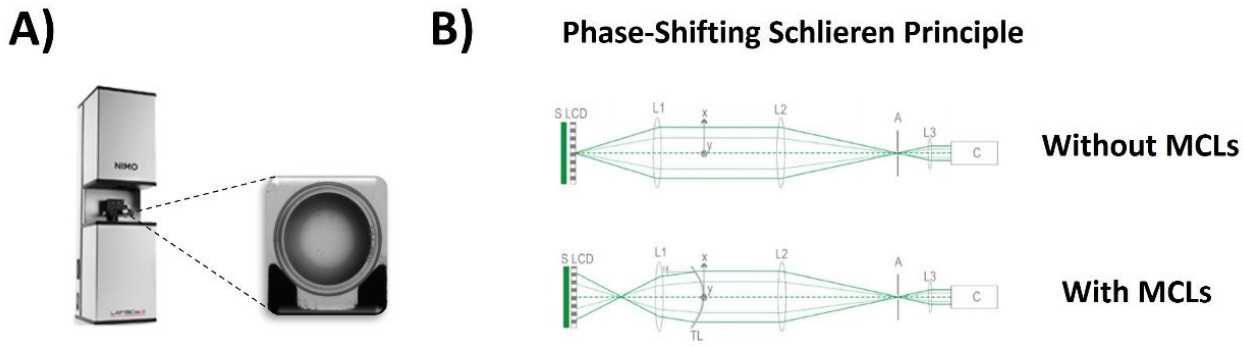

Figure 2.4. Nimo TR1504: *A) CLs cuvette to in-vitro measurement and B) Phase-Shifting Schlieren principle scheme of NMO TR1504 with and without MCL optical element. Adapted from Joannes et al. [173].*

2.4.2 – Auto Lensmeter Nidek LM-500

The fast and automatic lensmeter, illustrated in Figure 2.5, is based on a Hartman-Shack sensor with a lenslet of 108 points, that enables to measure optical power in monofocal, PALs and CLs. The optical power is expressed in spherocylindrical notation with a maximum resolution of 0.12 D of power and 1 deg of orientation. This lensmeter was utilized to measure different amounts and orientation of astigmatism generated with an automatized Stokes lens (further details in Chapter 6).

Figure 2.5. Auto Lensmeter Nidek LM-500.

2.4.3 – PlusOptix Power Refractor II

The PlusOptix Power Refractor II (PlusOptix, Germany) is a device with the capability to measure binocular refraction and the components of the accommodation triad (accommodation, convergence and pupil size) dynamically in real time, allowing to follow up across different time intervals during tests. This technique is based on transillumination tests using eccentric infrared lights for its measurements [175].

In this thesis, the main use of this device was to measure the patient's pupil size in the examination conditions, especially in the measurements related to Chapter 3 and 5. In Chapter 3, this assessment is crucial to assure correspondence between the pupil size wearing real MCLs and the pupil of the SimVis Gekko MCLs simulations.

2.4.4 – Displays

Two calibrated TV screens were used in the different studies performed in the thesis. A 48.5-inch screen (LG model 49UH770V, 3840 x 2160 pixels, refresh rate of 60 Hz) was utilized at optometric cabinet as optotypes display, including all subjective refractions (except those conducted in chapter 4 at University of Alicante) and the overall measurements carried out in Chapter 3. In other hand, the psychophysical experiments were displayed on a 3D TV screen (LG model 49UH850V, 3840 x 2160 pixels, refresh rate of 60 Hz) with the maximum luminance level fixed at 200cd/m^2 and located at 4 m and 2 m from the subject for the experiments described in Chapter 7 and 8, respectively.

For measurements closer than 4 m, we have displayed the optotypes chart in two different iPads. An iPad Pro 12.9inch (3rd Generation) with a resolution of 2732x2048 pixels, was used for intermediate and near VA at real distances in chapter 3 with the maximum luminance level fixed at 200 cd/m^2, while an iPad 10.2inch (8th Generation) with a resolution of 2.160 x 1.620 pixels was used as screen located at 4 m, using MLA App in Chapter 5 with two different luminance protocols: 85 cd/m^2 and 212 cd/m^2.

2.4.5 – ColorCal Colorimeter

ColorCal (Cambridge Research Systems, UK) is a calibrated colorimeter controlled by a PC through a software interface. This interface allows for the measurement of CIE chromaticity coordinates and luminance. The instrument is powered via USB and uses a suction cup to isolate direct measurements from the desired screen, preventing interferences from other light sources.

All displays previously described in this section were calibrated with ColorCal and have their gamma correction applied to each RGB channel.

2.5 – Clinical methods of evaluation

In the studies conducted in this thesis, we have employed clinical optometric methods commonly used in regular clinical practice. These methods include those aimed at measuring

refractive errors (both objective and subjective), examining the ocular health and those dedicated to visual performance assessment.

Visual Acuity at real distances:

The VA measurements at different distances, a classic method widely used in a large number of evaluations, was used in this thesis both in the exams of refractive error and in the evaluation of the visual performance of real MCLs and their respective simulations in chapters 3 and 4. Specifically in these studies, the evaluated distances were Far (4m), intermediate (0.66m), and near (0.40m) using ETDRS charts. A representation of VA measurement at far and near distances is shown in figure 2.6 A and B, respectively.

Through Focus Visual Acuity curves (TF-VA), or Defocus Curves:

A similar methodology was employed to measure VA across a greater range of distances using TFVA in chapters 3, 4 and 5. TFVA is considered the gold standard in visual performance using positive and negative trial lenses to change the virtual distance of the optotypes without physically moving them. An illustrative example of this method is depicted in Fig. 2.6 C).

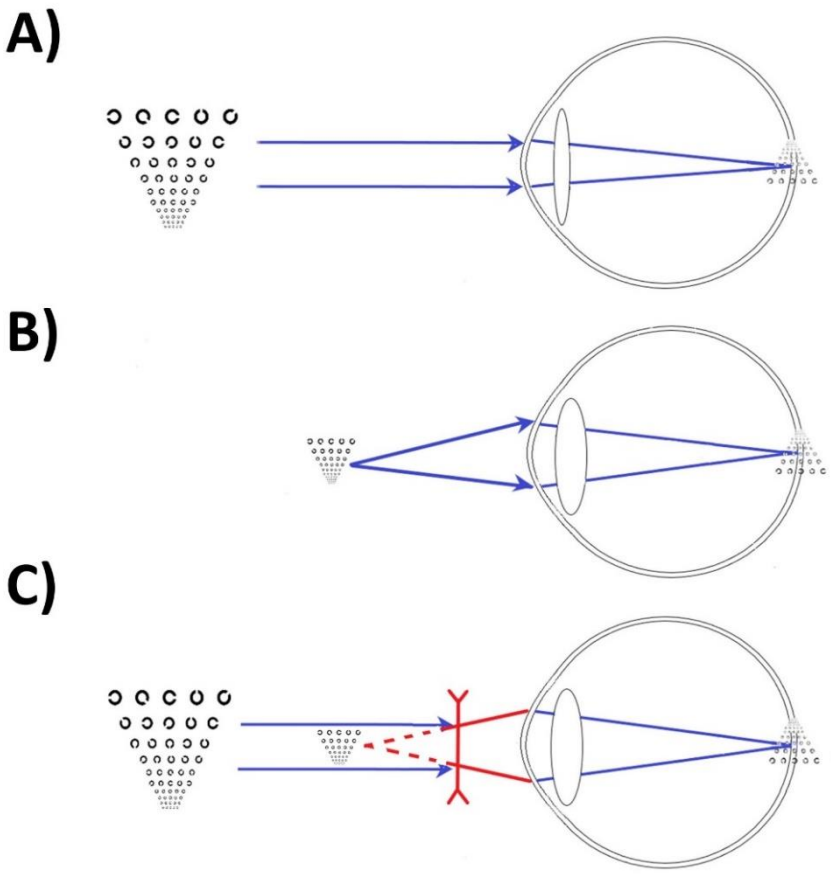

Figure 2.6. Strategies for VA measurements: *A) VA optotypes at real far distance, B) VA optotypes at real near distance and C) VA optotypes at virtual near distance formed by negative trial lens (from far distance optotypes). Adapted from: Clavé et al.* [176].

The evaluated range of TFVA was from a minimum of +1.00 D to -3.00 D, in 0.50 D increments. The primary advantage of this method is the time saved, as it eliminates the need to physically move the optotypes, and the results are comparable to VA at real distances [176]. The TFVAs included in chapter 5 have used the Multifocal Lens Analyzer (MLA) application (described in section 2.7.4) to analyze the time reduction obtained by the synergy of adaptive methods and power variations introduced by SimVis Gekko.

Objective and subjective refraction:

Objective refraction, using an autorefractometer ARK1 (Nidek, Japan), and a subjective refraction exam was carried out to each patient evaluated in this thesis. The subjective refraction assessment has included monocular examination using trial frame with a fogging method, biocular and binocular refinement to assure accommodation control.

Slit lamp examination:

A routine examination was conducted with the objective of assessing the health of various ocular structures (eyelids, tear film, conjunctiva, cornea, etc.) as part of the comprehensive optometric evaluation prior to the inclusion of each patient in the studies. A more specific examination, adhering to CLEAR guidelines for soft CLs (previously explained in section 1.5.1), was carried out for the MCLs wearers included in Chapter 3 and 4.

Contrast sensitivity:

The contrast sensitivity function was examined, using CSV-1000 (VectorVision, USA), to evaluate the visual performance obtained with various real MCLs in chapter 4. In this test, the subject must identify the location of a grating pattern between two lines of eight patches each (two alternative force choice 2-AFC), shown in Figure 2.7.

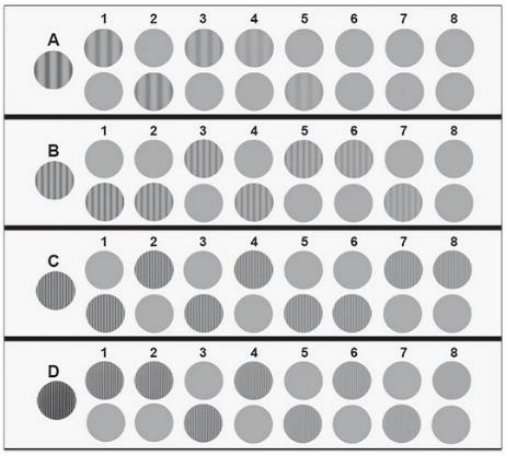

Figure 2.7. CSV-1000 Chart. *Each block of two circles lines corresponds to different spatial frequencies. The circles associated with each number present lower contrast as the number increases, being number 8 the higher value of CS.*

As the circles move further to the right, the contrast decreases, making it more challenging to see and thus indicating greater sensitivity. There are four blocks of these two lines of circles, each displaying a different spatial frequency: 3, 6, 12, and 18 cycles per degree (cpd). The contrast sensitivity function is obtained from the results of each block.

In Chapter 5, contrast sensitivity was studied through focus for high frequencies using VA tasks with fixed size optotypes and varying contrast. The implementation of this test was made possible using the MLA App displayed in an iPad at 4 m, which provides the test incorporating an adaptive method, and SimVis Gekko which induces power changes for through focus evaluation.

2.6 – Psychophysical methods of evaluation

Psychophysics is a field of study that investigates perception and sensation through behavior measurement [177]. The psychometric function, a key concept utilized in this field, measures performance on tasks based on stimulus strength. This function indicates the probability of detecting a stimulus or completing a specific task [178]. The psychometric function provides the perceptual threshold, defined as the stimulus characteristics that yield 50 % of probability of detection or resolution.

2.6.1 – Adaptive Methods

Adaptive procedures, which adjust trial placement based on previous results, were developed to efficiently determine the perceptual threshold These measurements typically focus on the location of the perceptual threshold among others. [177]. Depending on the strategy employed to identify the perceptual threshold, we can distinguish between the staircase and QUEST methods.

Staircase Method

The staircase method aims to identify the threshold by increasing or decreasing the stimulus intensity based on the subject's previous response. If the stimulus is not detected, the intensity increases in a fixed step (during each reversal or the complete test) and conversely, whether the stimulus is detected, the intensity of the stimulus decreases (example of Staircase Method shown in 2.8 A). The threshold is typically reached near the final trials and accuracy can depend on various factors. The number of trials can be fixed or dependent on several reversals, which are defined as a change in the staircase direction due to a transition between a positive to a negative response (or vice versa).

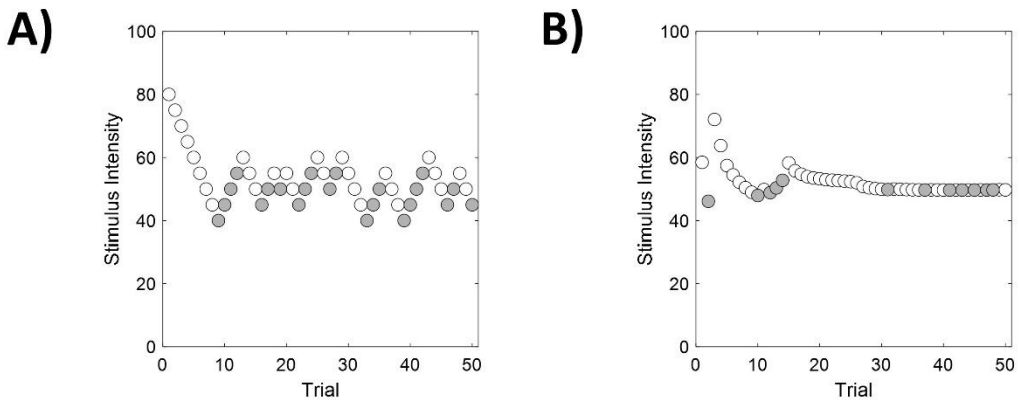

Figure 2.8. Example of psychophysical measurements using adaptive methods for a stimulus intensity threshold of 50*: A) Staircase method and B) QUEST Algorithm method.*

The staircase method was utilized using MLA App in chapter 5 to measure VA and CS in combination with SimVis Gekko. The app completed the measurement for each defocus amount after 5 reversals.

Quick Estimation by Sequential Testing (QUEST) Method

The QUEST method operates similarly to staircase methods, but it employs a Bayesian algorithm to identify the threshold[179,180]. This algorithm takes into account each response from subject so far, adjusting the intensity of the stimulus based on detection or non-detection and varying the step size accordingly (example of QUEST Method shown in 2.8 B). The algorithm allows for the modification of various variables in order to optimize threshold acquisition, depending on the properties of the stimulus and the desired convergence. QUEST can reach the threshold more quickly than the staircase method and with a higher level of accuracy, enabling a reduction time without compromising the result.

The QUEST method was utilized in one of experiments in Chapter 8 to adjust variations on the far energy percentage in bifocal lenses (intensity of the stimulus) and determine the perceptual threshold after adaptation to different SV corrections.

2.6.2 – Perceptual Scoring Methods

A quantitative subjective metric, known as perceptual scores (PS), was utilized in Chapters 4, 5, 7 and 8 in both clinical and psychophysical studies. This metric, frequently used in visual sciences research [103,181], serves to quantify and associate visual perception related to a specific correction or type of vision. This method translates the subjective visual perception to a numerical scale between two shown and well-defined extremes prior making the judgement. In these studies, a perceptual scale ranging from 0 to 10 in 1-point steps, was used, where 0 represents blurry vision and 10 represents sharp vision.

PS were employed to describe perceptual satisfaction at different distances (far, intermediate and near) in Chapter 4 for both the current presbyopia correction and different

MCLs corrections. In the same chapter, PS were also utilized to assess the lifestyle needs in visual tasks of each distance for presbyopic patients participating in this study. In chapter 5, PS were also used to describe the comfort, visual experience and overall satisfaction of visual function tests conducted with two different methods. PS were used to determine the visual perception in chapter 7 and 8, with different corrections presented using various ways and under different adaptation conditions. Due to the subjective nature of PS, we conducted between 3 or 5 repetitions per condition to calculate the intrasubject standard deviation.

2.7 – Software

Specific software was employed during the development of various studies including to this thesis:

2.7.1 – Control of simulations by Matlab

A custom toolbox of Matlab functions was developed by 2EyesVision to enable remote control of customized SimVis units and establish a communication protocol. This toolbox contains, besides the primary functionalities available when the SimVis is controlled by iPad, some other additional features for automatization. It allows for the integration of SimVis corrections within Matlab scripts to conduct psychophysical experiments. All the experiments related to Chapter 7 and 8 were carried out using this Matlab toolbox and custom SimVis units.

2.7.2 – PsychToolBox 3.0.

The PsychToolBox 3.0. [182–184] is a comprehensive Matlab toolbox for implementing automatized psychophysical experiments. As an open-source toolbox, it offers various psychophysical methods, such as QUEST algorithms and the ability to control the spatiotemporally presentation of stimuli. These features were employed in the experiments discussed in Chapter 8.

2.7.3 – Optonet Vision Unit

The Optonet Vision Unit (Optonet Ltd, UK) is a software platform that allows for a wide variety of optotypes, and stimuli used in optometric tests to be displayed on a single computer (connected to a screen). These tests range from subjective refraction to binocular vision examinations. In addition, it also enables quick and easy calibration to ensure that your tests are being conducted correctly.

Optonet Vision Unit was used, as calibrated optotype platform displayed on a TV, to perform the different clinical measurement for Chapter 3 and all the subjective refractions conducted in this thesis (except those conducted in chapter 4 at University of Alicante).

2.7.4 – Multifocal Lens Analyzer (MLA) App

As previously mentioned, the MLA App (Qvision, Spain) is an iPad application that uses adaptive methods to perform a variety of visual performance measurements at fixed

distances (either 2 or 4 m) [136,185]. These measurements are used to create a defocus curve range using trial lenses. The MLA offers two types of tests: VA and CS, both of which incorporate a crowding effect (as depicted in Fig.2.9 A and B). CS is measured using a VA task but with a fixed optotype size that corresponds to a high spatial frequency. Patients' responses are selected using a mobile phone App that serves a controller.

The combined use of MLA and SimVis Gekko, which induces varying amounts of defocus by altering the virtual optotypes distance, was assessed in chapter 5.

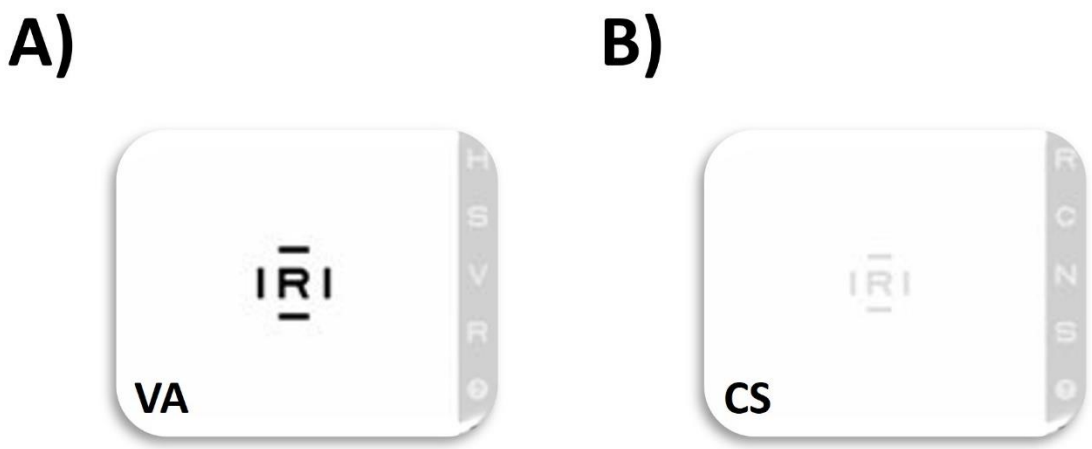

***Figure 2.9*. Examination screens for different tests of MLA App:** *(A) Visual acuity and (B) Contrast Sensitivity, both with crowding effect.*

2.8 – Clinical and Psychophysical measurements in patients

In the studies conducted for this thesis, all the subjects were volunteers. All subjects participated in accordance with the Helsinki Declaration guidelines, and the studies received approval from the Ethics Committee corresponding of each respective institution: CSIC and ISABIAL (University of Alicante).

All subjects received a thoughtful explanation of the purpose of each study and signed an informed consent form.

Chapter 3

Simulation of daily soft multifocal contact lenses using SimVis Gekko

In this chapter, we describe the comprehensive process to obtain SimVis simulations of daily soft MCLs from in-vitro measurements and computational characterization, with the information provided by these measurements, to clinical validation.

This work is the result of a cooperative collaboration among various institutions: Instituto de Optica Daza de Valdés (CSIC), 2EyesVision SL, Universidad de Valencia, Universidad Politécnica de Valencia and Universidad de Alicante.

The entire process described in this paper is composed of (1) in vitro measurements of 4 families of MCLs using NIMO TR1504, (2) computational characterization of these MCLs through TF-VS metric, (3) calculation and on-bench validation of MCLs simulations and finally, (4) clinical validation of these simulations in 8 presbyopic patients with refractive error of myopia and hyperopia and various addition amounts.

The author of this thesis (1) performed the in vitro measurements (in collaboration with Diego Montagud-Martínez), (2) calculated the computational characterization (TF-VS), (3) obtained and validated on-bench using a high speed focimeter and (4) supervised the clinical validation of the MCL simulations, (5) collected all data, (6) analyzed and discussed the results (in collaboration with Enrique Gambra, Diego Montagud-Martínez, Walter D. Furlan and David P. Piñero) and (7) prepared the manuscript (in collaboration with all co-authors).

The customized Matlab script to obtain the TF-VS metric from *in-vitro* measurements was developed by Lucie Sawides and Alberto de Castro. The clinical measurements were conducted by Amal Zaytouny.

This work is based on the original manuscript by Esteban-Ibañez et al. “Simulation of daily soft multifocal contact lenses using SimVis Gekko: from in-vitro and computational characterization to clinical validation” published in Scientific Reports. The co-authors of this scientific contribution are Diego Montagud-Martínez, Lucie Sawides, Amal Zaytouny, Alberto de Castro, Irene Sisó-Fuertes, Xoana Barcala, David P. Piñero, Walter D. Furlan, Carlos Dorronsoro and Enrique Gambra.

A part or the entire work was presented as an oral contribution at the IMOS 22, BER Summer School 23, Jornada de Doctorandos Física UCM (2023) and OPTOM 24.

3.1 – Introduction

Presbyopia is commonly defined as the loss of capability to focus correctly, using the crystalline lens, at intermediate or near distances. This usually occurs at 45 years old and progresses with age to the point of losing the ability completely. This condition has been explained as a loss of crystalline lens elasticity by several authors [1,2].

Due to the global increase in the aging population, the number of people affected by presbyopia is constantly growing, expecting to reach 2.1 billion worldwide in 2030 [6]. Different correction strategies are available to compensate this condition and overcome its symptoms, using different platforms such as spectacles, intraocular lenses (IOLs), contact lenses (CLs) and corneal laser refractive surgery (PresbyLASIK) treatments.

Despite the existence of bifocal and multifocal designs in CLs (MCLs), the percentage of CL users decreases when the presbyopia is reached. Within the presbyopic CL users only between 25 - 29 % wore a multifocal or multifocal toric design [27,28]. Both facts can be explained by various reasons: ocular dryness and associated discomfort, unawareness of multifocal solutions, unexpected visual performance and time-consuming fitting process to obtain a success adaptation, leading to several visits to eye care practitioner. Some of these unexpected visual performance aspects can be related to photic phenomena (i.e. glare and dysphotopsias), contrast decrease or an insufficient near vision to perform routinary tasks [186].

Visual simulators can help patients understand how their vision would be like with different MCL designs, allowing clinicians to recommend the most suitable option considering patient's visual needs and expectations, thus improving the process. There have been a few attempts to produce commercial visual simulators based on different technologies (adaptive optics, projection of a real lens in a cuvette…), but most of them have not yet validated its ability to replicate commercial corrections. Moreover, these devices only offer monocular simulation, many of them displaying visual stimuli on an internal screen, and all of them are designed as tabletop devices.

The SimVis Gekko visual simulator (2EyesVision SL, Spain), based on temporal multiplexing using optotunable lenses, has already demonstrated its ability to accurately simulate multifocal IOL designs using data from the public-literature of visual quality metrics [147,154,187]. Moreover, the potential impact of SimVis technology for the CL market, exploiting its ability to simulate all kinds of multifocal corrections binocularly, has already been successfully demonstrated in a previous study performed in clinical settings using 1-Day Acuvue Moist MCLs [156].

Information on the power profile of the MCLs is needed to achieve correct simulations. Potentially, this information can be obtained from CL manufacturers, from public data about the MCLs designs or metrology measurements. MCLs can be characterized by measuring their power profile across the surface lens using dedicated devices for this purpose. To the best of our knowledge, three commercial devices have been used to measure MCL power profiles in

different studies: NIMO TR-1504 (Lambda X, Belgium) [188], SHSOphthalmic (Optocraft, Germany) [189] and Phase Focus Lens Profiler (Phase Focus Ltd, UK) [190]. Nevertheless, the measurements obtained by these instruments are not free of drawbacks such as repeatability problems, calibration processes required and accuracy uncertainties with the devices compared to data provided by manufacturers. These discrepancies may be attributed to variations in the manufacturing process that diverge from the theoretical design [123], assuming a closer approximation to the final lens design which can also vary with the nominal power [188]. Moreover, most of the MCLs measured in the literature are monthly replacement designs, while the market trends towards a greater use of daily replacement and silicone hydrogel materials [191].

Our main objective in this study was to obtain accurate SimVis Gekko simulations of different daily commercial soft MCL designs from four manufacturers. For this goal, first, we obtained an in-vitro and computational characterization of these MCLs using NIMO TR-1504 and a dedicated algorithm, and then we clinically validated the SimVis Gekko simulations, obtained from these characterizations, in a small group of patients in a pilot study.

Finally, the obtention of these simulations could provide eye care practitioners with a powerful tool to non-invasively demonstrate the benefits and disadvantages of each MCL design. It allows patients to actively participate in the fitting process, test multiple MCL designs instantly in a single session and speed up the overall process.

3.2– Methods

3.2.1– MCL characterization

3.2.1.1– MCLs measured: Four different families

Four families of daily commercial soft MCLs from different manufacturers were studied: MyDay (CooperVision, USA), 1-Day Acuvue Moist (Johnson & Johnson, USA), Dailies Total1 (Alcon, USA) and Biotrue ONEday (Bausch+Lomb, USA). The different parameters of the lenses studied have been seen in Table 2.1 (Section 2.3). MCLs with distance powers of -4.00 D, -2.00 D, 0.00 D, +2.00 D and +4.00 D and additions Low, Mid and High were measured. Powers of -4.00 D and +4.00 D were also measured only in MyDay and Dailies Total1, as a comprehensive characterization, because there is no literature data for their power profiles, as far as we know. The Biotrue ONEday MCL had only Low and High additions available.

3.2.1.2– NIMO TR1504 device

The MCLs were measured with the instrument NIMO TR1504 (Lambda-X, Belgium), an optical mapping device which allows measuring the power profile of CLs [173]. It is based on the patented quantitative deflectometry technique, combining the Schlieren principle with a phase shift method. It uses a light source of 546 nm to measure beam deflections and obtain power maps. Its accuracy and repeatability are 0.05 D for spherical soft CLs powers and between 0.04 D to 0.2 D for MCLs [173,174].

3.2.1.3– MCLs power profile measurement process

First, a calibration of the device was performed, following the method recommended by the manufacturer using standard calibration lenses. Then, each MCL was taken out of the blister pack and placed in a cuvette with saline solution at room temperature. The parameters of each MCL unit (see Table 2.1 in Methods section) were introduced into the device's software and the MCL was centered using the device's camera. The power profile was measured across a 6 mm diameter optical zone: from MCL center (0 mm) to 3 mm of semi-diameter. To check the repeatability, the measurement process -removing and re-introducing the MCL in the cuvette- was repeated 2 more times. The power profiles, obtained for each MCL addition and distance power, were processed with a moving average filter with a window size of 5. The results of multiple repetitions were averaged to calculate the final power profiles.

3.2.1.4– Computational process: Obtaining phase map and theoretical Through-Focus Visual Strehl

The average power profile of each MCL design for all distance powers was used to compute the Through-Focus Visual Strehl (TF-VS) for 5 different diameters (from 3 mm to 5 mm in a 0.50 mm step) using a custom algorithm in Matlab (MathWorks, USA). Note that through these TF-VS, only the pure multifocal pattern of the MCLs is considered. Essentially, the 2-dimensional wavefront aberration map (phase map) was calculated point-by-point so that its curvature resulted in the power profile measured for each MCL design, and Fourier Optics was used to calculate the modulation transfer function (MTF). TF-VS is an optical quality metric that quantifies the volume under the MTF at all spatial frequencies weighted by the human contrast sensitivity function and has been recognized as a good predictor of visual acuity [192,193]. Furthermore, it has been validated as an input metric for SimVis Gekko simulations [154,161,166]. This metric was then evaluated in a range from -2.00 D to +4.00 D in 0.05 D. Phase maps were obtained for each MCL design (for each family and addition) and the TF-VS was calculated for each optical diameter.

3.2.2– Validation of SimVis Gekko simulations

3.2.2.1– Computational calculation of SimVis simulations

From the TF-VS of each lens design, a set of SimVis temporal coefficients were calculated based on the equation described by Akondi et al. [161,166]. The set of time coefficients describes the lens simulation with SimVis Gekko, indicating how long the tunable lenses of the instrument must stay in each focus (in 0.1 D steps) under temporal multiplexing to replicate the desired multifocal element. Mathematically, the temporal coefficients stand for the weighting factors of a series of monofocal point spread functions (PSFs) for different optical powers (additions), tuned to match the TF-VS of the MCL design. The number of temporal coefficients varies according to the lens design.

3.2.2.2– On-bench TF-VS validation

Each MCL SimVis Gekko simulation was experimentally evaluated on-bench with a high-speed focimeter [161,162] provided with a camera working at 3823-fps (IL5S; Fastec Imaging, USA) and an optotunable lens (Optotune, Switzerland, EL-3-10). The measurements were carried out in two different sessions with a room temperature fixed at 26 °C. The TF-VS ratio was computed from the experimental measurements obtained with the high-speed focimeter for the SimVis lens simulation, using specific custom Matlab programs. The time spent at each optical power is calculated (in 0.1 D steps), and the differences with respect to the theoretical TF-VS were assessed in terms of Root Mean Square Error (RMSE). The on-bench validation was successfully achieved if the following quality terms were reached: differences lower than 0.20 D shift for the location of the TF-VS peaks and a RMSE less than 0.05 between theoretical and experimental TF-VS in the dioptric range of interest: -1.00 D to +4.00 D.

3.2.2.3– SimVis Gekko visual simulator

SimVis Gekko [153,194] is a see-through and head mounted clinical visual simulator with the capability to mimic binocularly any multifocal design behavior, such [147,154,187] (including patients with mild cataract opacification [195]), CLs [156,167] and presbyLASIK patterns [155]. SimVis Gekko simulates these multifocal elements working under temporal multiplexing using optotunable lenses [166], generating fast and periodic optical power changes at a speed greater than the defocus flicker fusion of the human eye. A SimVis Gekko ™ device (v.0.8, 2022), with a pupil entrance of 3 mm, was used in the pilot study to clinically validate six MCL design simulations from three manufacturers in volunteer subjects.

Subjects' refraction was corrected using trial lenses placed in the dedicated external trial lens holders attached to SimVis Gekko. Each patient's pupil was centered vertically and horizontally with respect to the optical axis of the respective SimVis Gekko optical channel by using mechanical adjustments and a pair of color LEDs to guide the alignment process, allowing centration on the pupillary reflex and considering then the interpupillary distance.

3.2.2.4– *Subjects*

Eight presbyopic subjects (2 males and 6 females) participated in the pilot study (see Table 3.1). All subjects received a thoughtful explanation of the purpose of the study and signed an informed consent. The protocol conducted in this study was approved by the Consejo Superior de Investigaciones Cientificas (CSIC) Ethics Committee.

Table 3.1. Subjects' data related to age, gender, and ocular parameters: *evaluated eye, refractive error (Sphere, Cylinder and Axis), near addition and mean pupil diameter (matched simulation pupil size using SimVis Gekko).*

Subject	Age (y)	Gender	Evaluated Eye	Refractive Error (D, D, deg)	Addition (D)	Pupil diameter (mm) (SV simulation)
S#1	45	F	OS	-2.75 – 0.50 x 160	+0.75	3.90 (4.00)
S#2	45	F	OD	+2.50	+1.00	4.40 (4.50)
S#3	48	M	OS	-4.00 – 0.50 x 100	+0.75	2.80 (3.00)
S#4	47	F	OS	+2.00 – 0.50 x 180	+1.25	2.90 (3.00)
S#5	62	F	OS	+2.75-0.50 x 100	+2.25	3.10 (3.00)
S#6	61	F	OS	+1.75-0.50 x 110	+2.00	3.50 (3.50)
S#7	53	M	OD	-3.25-0.25 x 165	+1.75	3.50 (3.50)
S#8	50	F	OS	-1.50-0.50 x 90	+2.00	3.80 (4.00)

Subjects were distributed in two different groups according to their near addition: young presbyopes (46.3 ± 1.3 years) including subjects with a near add from +0.75 D to +1.25 D and old presbyopes (56.5 ± 5.9 years) including subjects with a near add from +1.75 D to +2.50 D. Each addition group had 2 hyperopes and 2 myopes with a spherical refractive error equal to or higher than 1.50 D in absolute terms. The exclusion criteria were astigmatism higher than 0.75 D, contraindications for CL use, previous ocular surgery and/or pathology.

3.2.2.5– *Clinical Validation measurements (Pilot Study)*

Prior to clinical validation, a complete optometric examination (anamnesis, subjective refraction, near addition quantification, ocular dominance and slit lamp examination) was carried out for all subjects to obtain the required information and ensure that all of them met the inclusion criteria. Clinical measurements consisted of monocular Through-Focus Visual Acuity (TF-VA) curves with trial lenses ranging from +1.00 D to -4.00 D (in 0.50 D steps). Monocular visual acuity (VA) was also measured at real distances (4 m, 0.66 m and 0.40 m). These measurements were performed for SimVis Gekko simulated MCL and for Real MCL Biotrue ONEday, MyDay and Dailies Total1 designs considering the subject's addition. 1-Day Acuvue Moist was not included in the pilot study as this MCL design had already been clinically validated for all additions using SimVis Gekko in Barcala et al. [156]. We evaluated only the dominant eye in subjects fitted with Low addition MCLs and the non-dominant eye in subjects fitted with High addition MCLs, following the recommendations of the fitting guide of each brand.

The VA charts of ETDRS optotypes were displayed into Optonet Vision Unit (Optonet Ltd, United Kingdom) in a calibrated screen: 48.5-inch screen (49UH770V, LG) for 4 m distance

and iPad Pro 12.9-inch for 0.66 m and 0.40 m distances. VA measurements were performed in a dark room where only the display with the optotypes was illuminated. The luminance of the display was 200 cd/m^2, measured with ColorCal Colorimeter (Cambridge Research Systems, UK), as recommended by ISO 10938:2016 [196].

The Plusoptix Power Refractor II (Plusoptix, Germany) was exclusively used to measure the patients' pupil size three times. The light conditions during these pupil size measurements were the same as those applied in the clinical evaluation of real MCLs visual performance. Since MCL performance depends on the pupil size, we selected the mean pupil size for each subject to determine the appropriate MCL SimVis simulations. The developed simulations were applied using the closest value to the real pupil size, rounded to the nearest 0.50 mm step. If the subject had a sphero-cylindrical refraction (obtained from subjective refraction exam), it was corrected with trial lenses with SimVis Gekko and the composition of spherical error and tear film meniscus with the Real MCL, since astigmatism was less than 0.75 D in all subjects.

For real MCL evaluation, we waited for 10 minutes for a correct CL settlement, before evaluating the fitting quality according to the CLEAR clinical guideline [122]. A randomized criterion was established to choose the evaluation order for the lens tested (SimVis simulation or Real MCL) and brands examined.

3.2.2.6– Data Analysis

The Depth of Focus (DoF), estimated as the range of values with a Strehl ratio higher than 0.12 (VS>0.12) [197,198] , was calculated for the theoretical TF-VS for 3 mm, 4 mm and 5 mm of diameter, in each SimVis Gekko simulation obtained computationally, to analyze behavioral changes between different diameters and additions.

Two different metrics were used to compare the SimVis Gekko simulations with the Real MCLs in TF-VA terms using a dedicated Matlab script: partial correlation ($r_{xy,z}$) [199], where the SimVis Gekko simulation TF-VA was defined as *x*, the Real MCL TF-VA as *y*, and the defocus value as z; and RMSE between the SimVis Gekko simulation TF-VA and the Real MCL TF-VA.

3.3 – Results

3.3.1– MCLs characterization

Figure 3.1 shows the absolute power profiles measured for each lens family, addition and distance power of MCLs (a total of 42 power profiles and 126 measurements) as a function of the semi-diameter up to a maximum of 3 mm. The average of the three repetitions is shown in figure 3.1; the standard deviation was less than 0.10 D along all the semi-diameters for each MCL design.

The two typical MCL designs followed by most of manufacturers are shown in figure 3.1: Dailies Total1 (Fig.3.1.A), MyDay Low and Mid Addition (Fig.3.1B) and 1-Day Acuvue Moist (Fig.3.1C) with an aspheric center-near design with a power decrease towards the MCL periphery, while MyDay High Addition (Fig.3.1B) and Biotrue ONEday (Fig.3.1D) have a concentric center near design with different number of steps between designs, four and three, respectively. For a comprehensive analysis and better comparison between MCL designs, relative power profiles (subtracting the distance power, in order to reveal the multifocal contribution) are presented in figure 3.2, including the average across distance powers for each MCL design (in black lines).

While 1-Day Acuvue Moist and Biotrue ONEday families show a very similar power profile across distance powers, Dailies Total1 and MyDay exhibit differences in the relative power profiles across distance powers. The latter families present relative power profiles with more power for negative distance powers and less power for positive distance powers, with a maximum difference of 1.61 D between the -4.00 D and the +4.00 D lenses for the MyDay High Addition.

Considering the average power profiles, addition differences across MCL families can be observed. The lowest and highest addition are found for 1-Day Acuvue Moist (0.37 D) and Biotrue ONEday (1.09 D) in low addition designs, for MyDay (0.90 D) and Dailies Total1 (1.03 D) in mid addition designs, and for Biotrue ONEday (1.27 D) and Dailies Total1 (1.45 D) in high addition designs, respectively.

The theoretical TF-VS, calculated using the average power profiles across distance powers for each MCL design, are shown in Figure 3.3 for 3 mm, 4 mm and 5 mm optical diameters. There is a tendency to vary from a more monofocal performance, provided by near addition, for 3 mm of optical diameter, towards an increase in the DoF as the optical diameter increases, shifting the main peak towards the distance power (except for MyDay High Addition).

If we analyze the TF-VS for different additions, we can observe an increase in the DoF (VS > 0.12), as the addition increases. The DoF, for the 4 mm optical diameter, between low and high addition changes from 1.90 D to 2.85 D for Dailies Total1, 1.80 D to 2.30 D for MyDay, 1.65 D to 2.40 D for 1-Day Acuvue Moist and 2.35 D to 2.40 D for Biotrue ONEday.

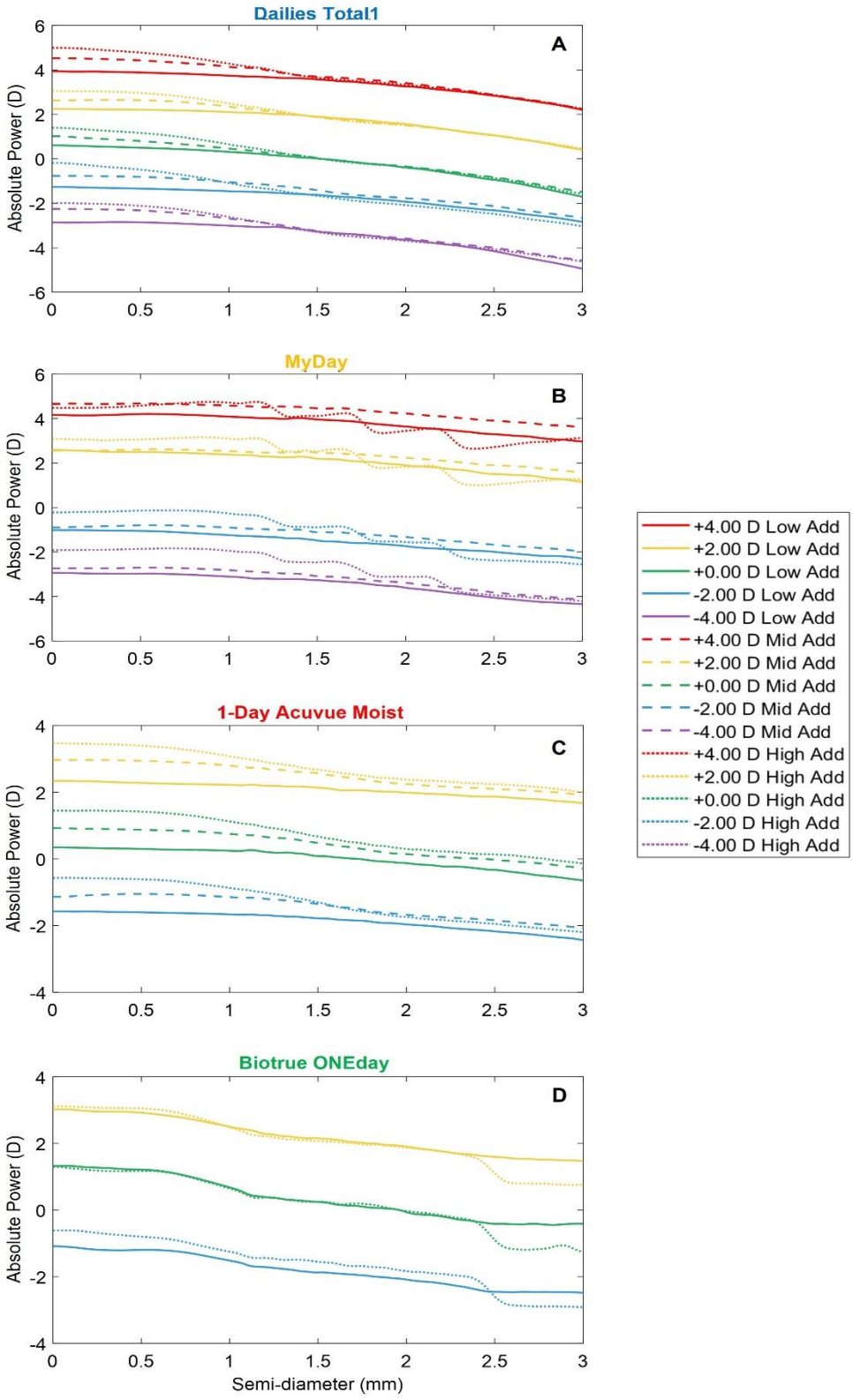

Figure 3.1. Absolute power profiles measured with NIMO TR-1504 across 3 mm of semi-diameter for each MCL family*: (A) Dailies Total1, (B) MyDay, (C) 1-Day Acuvue Moist, and (D) Biotrue ONEday. The different additions are represented for each family with solid lines (Low Addition), dashed lines (Mid Addition) and dotted lines (High Addition) with different colors according to the labeled distance power: red (+4.00 D), orange (+2.00 D), green (0.00 D), blue (-2.00 D) and purple (-4.00 D).*

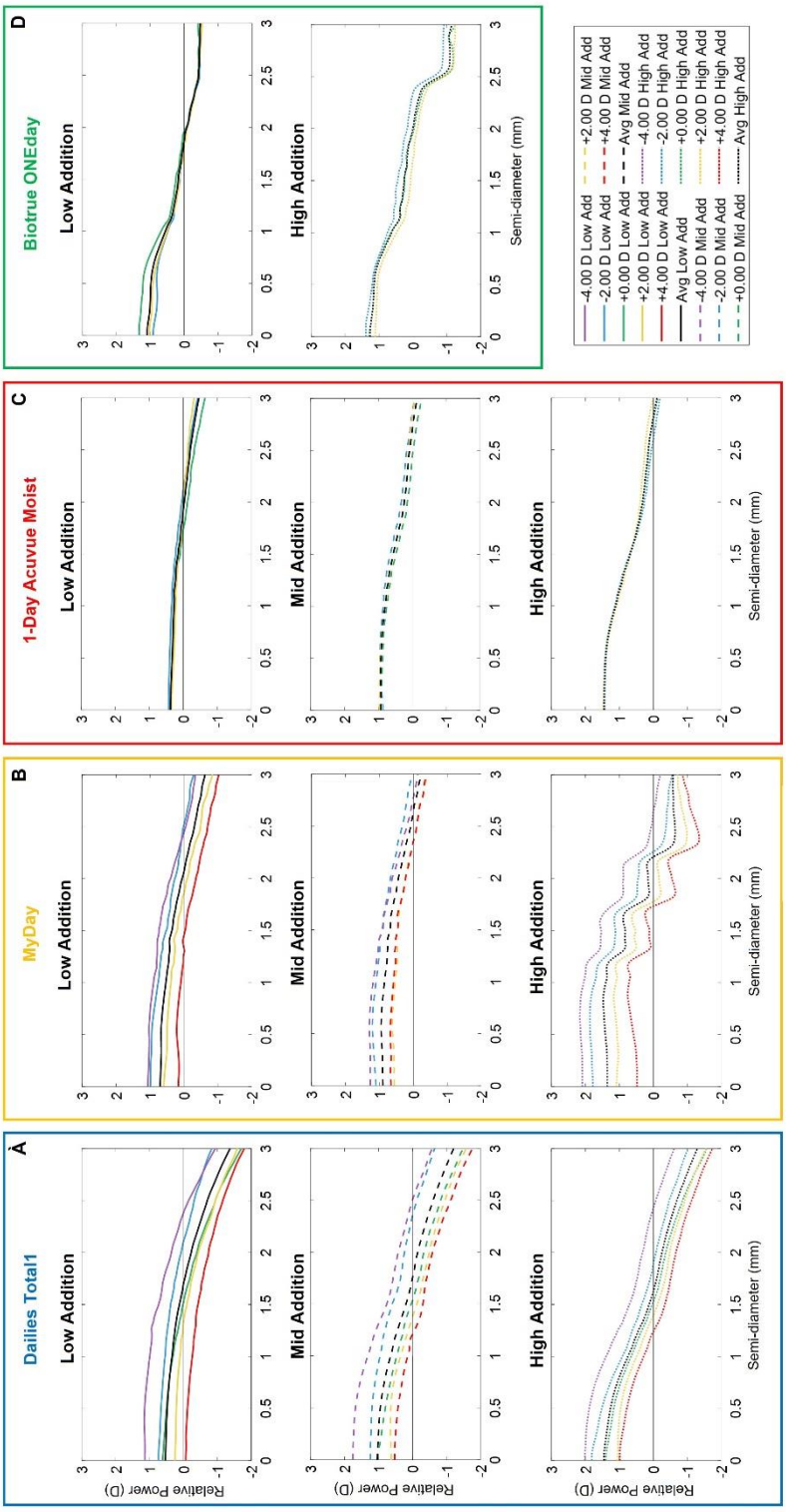

Figure 3.2. Relative power profiles obtained through NIMO TR-1504 measurements across 3 mm of semi-diameter for each MCL family*: (A) Dailies Total1, (B) MyDay, (C) 1-Day Acuvue Moist, and (D) Biotrue ONEday. The different additions are represented for each family with solid lines (Low Add), dashed lines (Mid Add) and dotted lines (High Addition) with different colors according to the labeled distance power: red (+4.00 D), orange (+2.00 D), green (0.00 D), blue (-2.00 D) and purple (-4.00 D). The average (Avg) relative power profile across all distance powers is represented in black solid line for each lens design.*

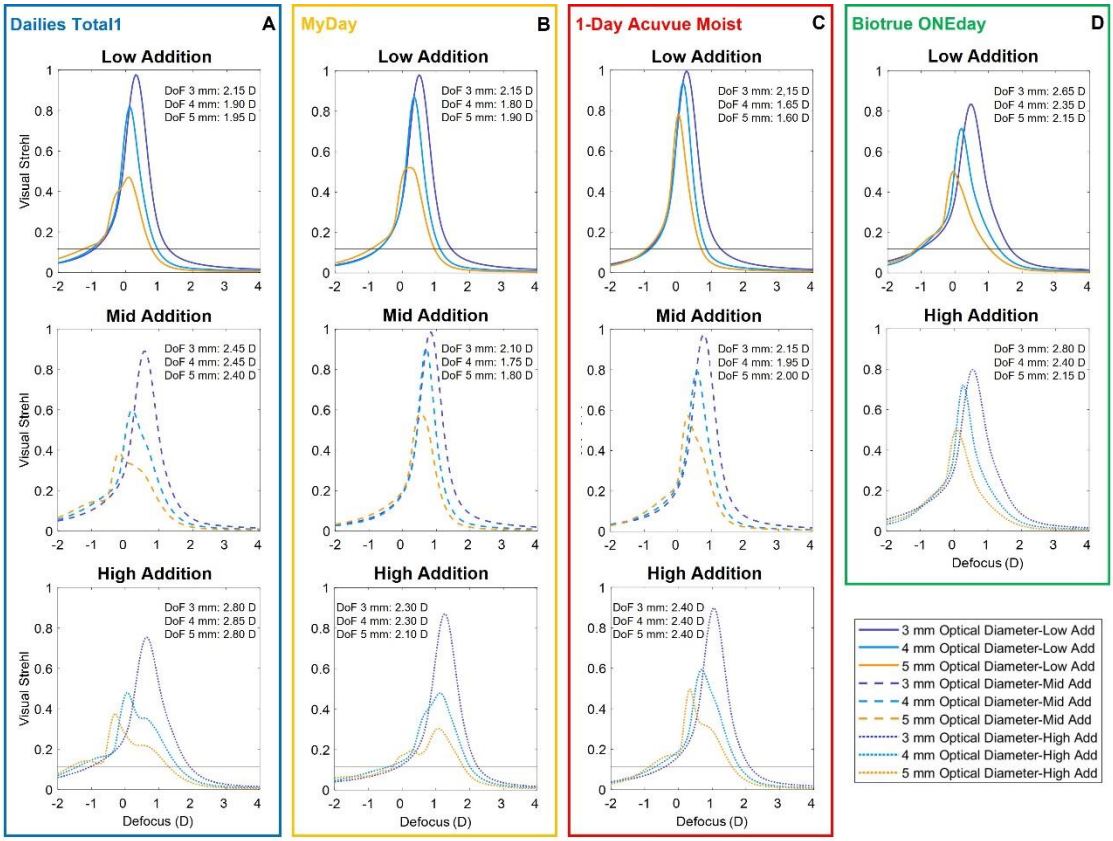

Figure 3.3. Theoretical TF-VS computationally calculated to simulate MCLs with SimVis Gekko for each family: *(A) Dailies Total1, (B) MyDay, (C) 1-Day Acuvue Moist, and (D) Biotrue ONEday. The TF-VS for each family is represented with solid, dashed and dotted lines for low, mid and high additions, respectively, with different colors for optical diameter zone of 3 mm (purple), 4 mm (blue) and 5 mm (yellow). The DoF estimated as the range where VS > 0.12 is shown for each MCL design for the three optical diameters*.

3.3.2– Clinical validation of the SimVis Gekko simulations

The measurements performed in the clinical validation with the SimVis Gekko simulations of MCLs are shown in figures 3.4 and 3.5. TF-VA and VA are presented comparing the results obtained with SimVis Gekko simulations (solid lines and black circle markers) and with real MCLs (dashed lines and black triangle markers) for low and high additions. The mean pupil size across all patients when wearing real MCLs for low and high addition was 3.44 ± 0.78 mm and 3.47 ± 0.29 mm, respectively, while the mean pupil size used for SimVis simulations was 3.57 ± 0.75 mm and 3.48 ± 0.41 mm for the same additions.

The comparative metrics reveal a range of partial correlation ($r_{xy,z}$) and RMSE between 0.905 and 0.978 and 0.033 logMAR and 0.062 logMAR for all lens designs studied. Mean differences of VA in real distances between Real MCL and SimVis Gekko simulations (Real MCL VA – SimVis VA) were calculated across all distances for each manufacturer, being 0.023 ± 0.036 logMAR for Dailies Total1, 0.018 ± 0.037 logMAR for MyDay and 0.04 ± 0.026 logMAR for Biotrue ONEday. In addition, mean values of 0.012 ± 0.036 logMAR

in low addition and 0.041 ± 0.023 logMAR in high addition were obtained. The overall mean differences, considering the three distances evaluated, were 0.016 ± 0.033 logMAR, 0.020 ± 0.041 logMAR and 0.040 ± 0.020 logMAR for 4 m, 0.66 m and 0.40 m, respectively.

In order to carry out a comprehensive analysis between SimVis Gekko simulations and Real MCL, comparative results for each refractive error group and addition are shown in figure 3.5, including bars that report the VA differences between methods in each TF-VA step. Partial correlation and RMSE metrics are also calculated: for the low addition design in the hyperope group and across all manufacturers, $r_{xy,z}$ and RMSE are 0.929 ± 0.058 and 0.084 ± 0.039 logMAR, while the results are 0.964 ±0.013 and 0.094 ± 0.052 logMAR in the myope group for the same addition. Otherwise, the partial correlations and RMSE for high addition in the hyperope group and myope group are 0.857 ± 0.74, 0.967 ± 0.034 and 0.084 ± 0.039 logMAR, 0.055 ± 0.001 logMAR across manufacturers, respectively.

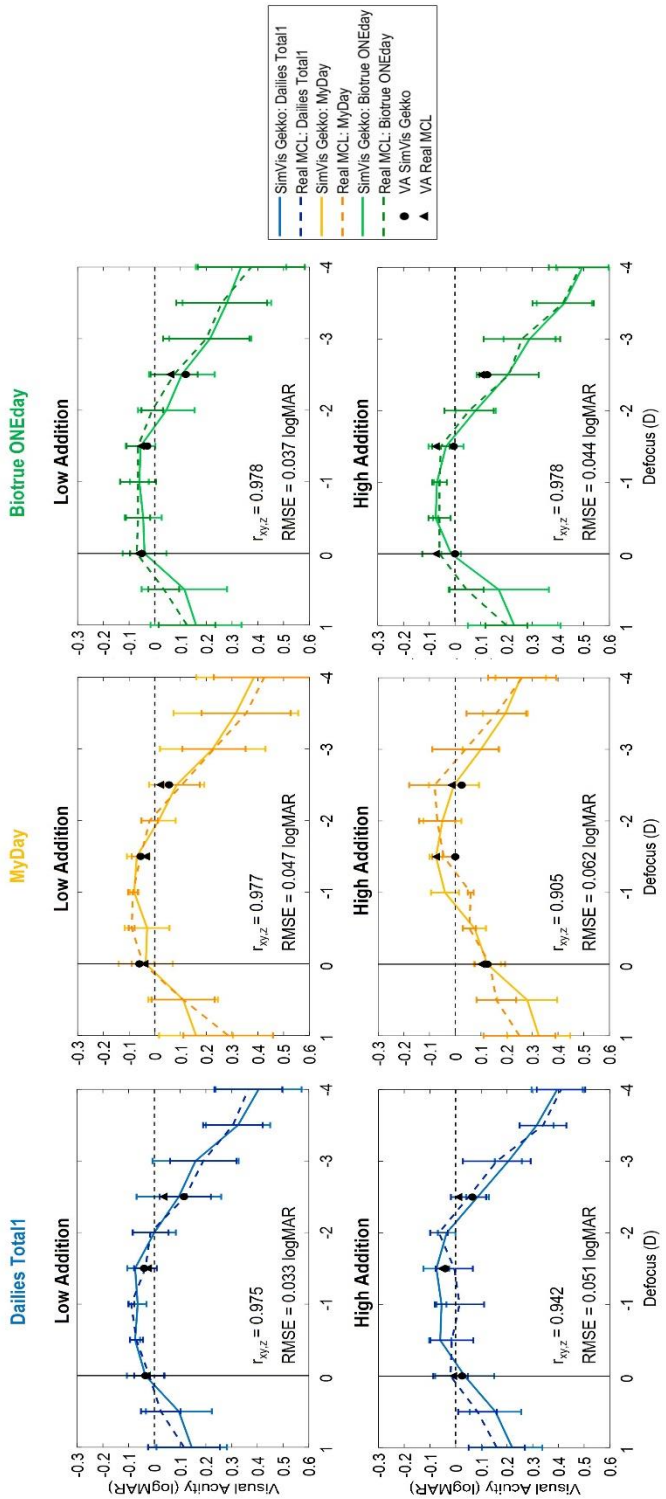

Figure 3.4. Clinical validation of simulated MCLs using SimVis Gekko for each addition group (n = 4). *TF-VA curves and real distances VA measurements with both the three families of real MCLs and the respective MCLs simulations using SimVis Gekko: (A) Dailies Total1 (blue color) (B) MyDay (yellow color) and (C) Biotrue ONEday (green color); for low (upper row) and high addition (bottom row). The TF-VA (with standard deviation in each 0.50 D step) and real distances VA are represented by dashed lines and black triangles for Real MCLs and solid lines and black circles for the simulated MCLs, respectively. The degree of correlation between methods for each MCL design is provided in each graph by partial correlation ($r_{xy,z}$) and RMSE metrics.*

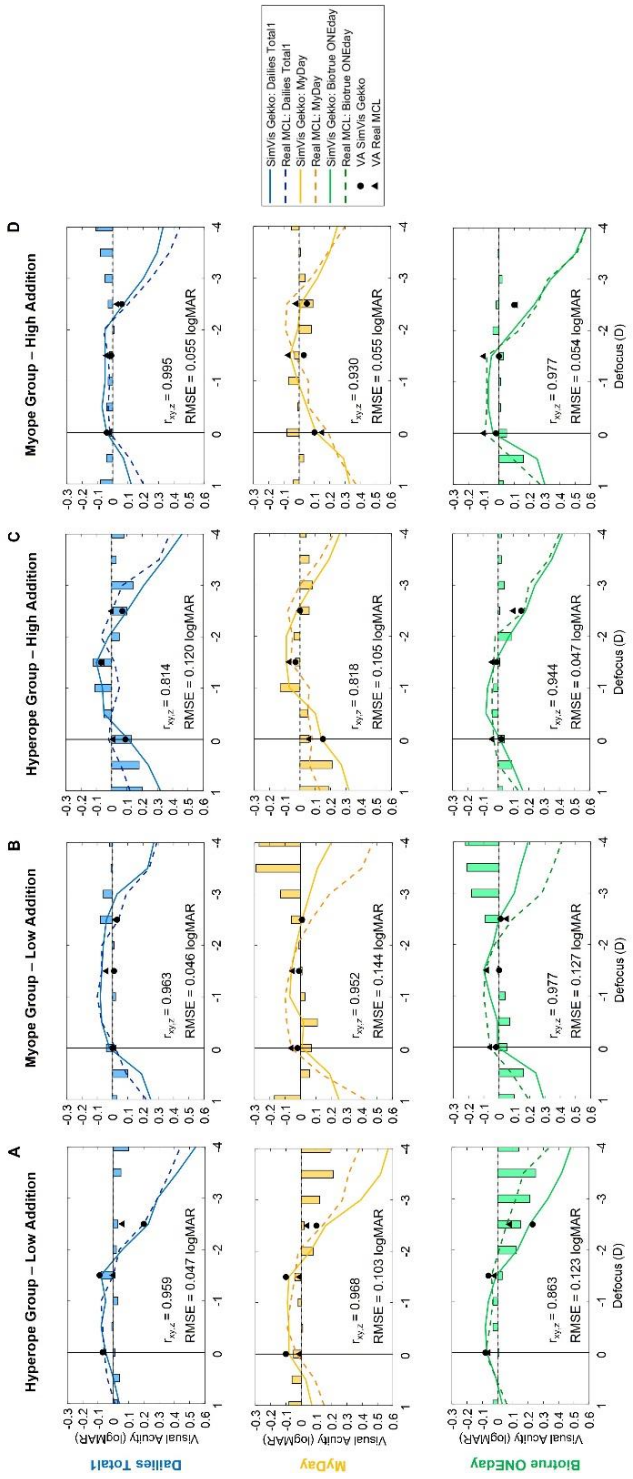

Figure 3.5. Clinical validation of simulated MCLs using SimVis Gekko for each subgroup: refractive error and addition*. TF-VA curves and real distances VA measurements with both the real MCLs and the respective MCLs simulations using SimVis Gekko for different sample groups (n = 2), considering addition and also the sign of the refractive error: (a) Hyperope-Low Addition, (b) Myope-Low Addition, (c) Hyperope-High Addition and (d) Myope-High Addition, with Dailies Total1 (blue color; upper row), MyDay (yellow color; middle row) and Biotrue ONEday (green color; bottom row). This figure follows the same representation and metrics as Fig.3.4.*

3.4 – Discussion

An in-vitro and computational characterization of daily soft MCLs from four different manufacturers is reported, using the NIMO device and a dedicated algorithm based on the in-vitro measurements, respectively. These characterizations were employed as an independent input source (not provided by any manufacturer) to obtain the corresponding SimVis Gekko simulations. Finally, the MCL simulations have been clinically validated in a pilot study with volunteer subjects having different refractive errors and additions.

The absolute power profiles (see Fig. 3.1) show a consistent behavior with respect to distance powers and additions, except for Biotrue ONEday which had similar designs for low and high additions up to 2.5 mm of semi-diameter. MyDay results reveal different designs for low/mid (continuous aspheric design) and high additions (concentric rings).

The relative power profiles (see Fig. 3.2) highlight differences with the distance power for Dailies Total1 and MyDay families, while 1-Day Acuvue Moist and Biotrue ONEday families present equivalent profiles across distance powers, coinciding with the results obtained by Kim et al. [188] using NIMO TR-1504. These differences across distance powers have been previously reported in other studies [188,200] , where a higher value of positive spherical aberration have been found for positive distance power, while a higher amount of negative spherical aberration have been found for negative distance powers [188] . This phenomenon might be explained based on the strategy followed by some manufacturers of considering the eye's inherent spherical aberration and compensating it with the amount introduced by their MCLs to improve visual performance [118,201] . SimVis Gekko only simulates the addition profile, not the refractive correction component nor the interaction between the lens and the eye spherical aberration. Therefore, we decided that averaging across all distance powers considering the symmetry between positive and negative measured distance powers, would be the fairest estimation to represent the addition for each lens design.

The theoretical TF-VS, calculated using the average relative power profiles, shows two distinct behaviors: (1) nearly monofocal with a low DoF (low /mid addition), addressed to presbyopes with residual accommodative amplitude, and (2) a more multifocal behavior, increasing with pupil size, for older presbyopes. For high addition designs, the CLs behave as multifocal with most energy devoted to the far focus for 5 mm pupil diameters, except MyDay which prioritizes near vision (see Fig. 3.3). These differences between designs for the same addition label, especially high, are consistent with the different strategies followed by each manufacturer in their fitting guides, as they can opt for a symmetric addition in both eyes (Dailies Total1 and Biotrue ONEday) or a different addition depending on whether it is dominant or non-dominant eye (1-Day Acuvue Moist and MyDay).

The clinical validation shows that the SimVis Gekko simulations for different additions and lens families have a good agreement with real MCLs when measuring TF-VA curves and VA at real distances (see Fig. 3.4). As the TF-VS changes significantly with pupil size, simulations for every MCL design were obtained and used in the clinical validation between

3 mm and 5 mm (in 0.5 mm steps). The good agreement observed between the results obtained with the MCLs and SimVis Gekko simulations suggest that considering a sampling of the lens design simulated with SimVis Gekko every 0.5 mm pupil size provides an accurate simulation of the lens design. The low addition designs had slightly better agreement than high additions designs in both partial correlation ($r_{xy,z}$) and RMSE in the TF-VA curve, this small difference being probably due to higher variability when using lenses with a significant multifocal behavior. The differences in real distance VA between methods, although small, showed better VA with the real MCLs, for each manufacturer and addition across the three tested distances, with a maximum difference of 2 logMAR letters for MyDay and high addition respectively. Similarly, the largest difference between methods considering the distance, across all designs and manufacturers, was observed at 0.40 m, also with a value of two letters. Although the tendency seen was VA is better with real MCLs, the total of these differences was within the variability of repeated VA measurements: 0.04 ± 0.06 logMAR [202] .

Moreover, a comparison between groups of subjects with the same addition and refractive error sign (n = 2) was conducted to assess the impact of relative profile differences on clinical simulations (see Fig. 3.5). Despite finding good correspondence between simulations and real MCLs results, better partial correlation and RMSE were observed for the myopic group with both low and high additions, with larger differences seen in the case of high additions. Among the hyperopic designs, there were three of them with higher differences between methods with a $r_{xy,z}$ below 0.90 and RMSE beyond 0.10 logMAR: Biotrue ONEday Low Addition, MyDay High Addition and Dailies Total1 High Addition. This fact can be explained by the differences in the amount of spherical aberration between designs for hyperopes or myopes and how this spherical aberration interacts with the spherical aberration of the eye. However, this effect cannot be completely modeled with the SimVis Gekko, where we have used the average relative power profile to obtain the simulation of MCLs. Otherwise, the residual accommodation amplitude could have an influence in the spherical aberration value according to the refractive error group, since these differences between refractive groups occur mainly in young presbyopes, as in Biotrue ONEday family while it does not happen for the high addition design of the same lens family, despite having almost an identical power profile. Furthermore, it is crucial to consider the potential impact of variability within the small subject groups as a limitation of the pilot study that could affect the pupil size, amount of refractive error or even fatigue doing the measurements. In any case, it has to be noticed that these behaviors, although systematic, do not occur in the region of the defocus range where the SimVis Gekko simulation is expected to be really accurate, but in the two extremes of the defocus curve range (above +0.00 D and below -2.50 D), where it does not have such an impact on visual performance and the defocus is higher increasing the variability in VA results [203] .

3.5 – Conclusion

In summary, the designs of four daily commercial soft MCLs from different manufacturers and different additions have been characterized using a commercial device (NIMO TR-1504) and the results have been used to produce a visual simulation of the corrections with SimVis Gekko. Clinical comparison between the visual acuity with the simulation and with the real MCL on eye for hyperopes and myopes with different additions were conducted. The good agreement in all the reported cases -even when considering separately groups with different refractive error, lens design and addition- confirms the validity of the simulation approach. SimVis Gekko simulations capture with a high degree of accuracy the multifocal performance of the lens, while there is still some room for fine tuning by calculating dedicated simulations for each refractive group.

After validation of SimVis Gekko's accuracy in simulating the performance of daily commercial soft MCLs, a study could be conducted to assess its potential use in clinical practice. This would allow for quick and accurate testing of different lens designs without the need to fit multiple MCL units. Furthermore, incorporating other clinical measurements using SimVis Gekko, such as contrast sensitivity or photic phenomena analysis, would provide a higher qualitative comprehension of the correlation with real MCLs.

In the future, a project with a larger sample size using these simulations could be carried out to replicate or even modify fitting guides of each manufacturer based on addition in order to streamline the process, save chair-time and enable testing of various designs in a single session.

Chapter 4

Improving replication of MCLs fitting guides through SimVis Gekko in a clinical environment

In this chapter, we implemented all the Fitting guide steps from 4 manufacturers daily MCL designs using SimVis Gekko with the simulations obtained and clinically validated in Chapter 3. Twelve subjects were evaluated with several steps of this Fitting Guides for each manufacturer using a new metric (3D-VA) that determined if the subject preferred the Fitting Guide recommended step considering its addition or other. Both steps were clinically evaluated for each manufacturer using the corresponding real MCLs and comparing them.

This work is the result of a cooperative collaboration among various institutions: Instituto de Óptica Daza de Valdés (CSIC), 2EyesVision SL and Universidad de Alicante.

The author of this thesis (1) designed the study and conceptualized the methodology (in collaboration with David P. Piñero, Enrique Gambra and Carlos Dorronsoro), (2) imparted the training of SimVis Gekko to researchers from University of Alicante, (3) developed the 3D-VA metric, (4) supervised the clinical measurements results (5) provided the 3D-VA metric values and SimVis prescription combination of MCLs (6) collected and organized the results, (7) analyzed and discussed the results (in collaboration with all co-authors) and (8) performed the statistical analysis.

The clinical measurements were conducted by Ainhoa Molina-Martin and Elena Martinez-Plaza (Universidad de Alicante).

This work is based on the original manuscript by Esteban-Ibañez et al. “Improving replication of MCLs fitting guides through SimVis Gekko in a clinical environment” submitted to Scientific Reports. The co-authors of this scientific contribution are Ainhoa Molina-Martin, Elena Martínez-Plaza, Carlos Dorronsoro, Enrique Gambra and David P. Piñero.

4.1 – Introduction

This doctoral thesis primarily focuses on the potential of Multifocal Contact Lenses (MCLs) as a reliable alternative for presbyopia compensation, a condition affecting a significant population [6]. Despite their potential, MCLs' market penetration is still far from expectations, with only a range between 24% and 29 % of CLs users adopting them when developing presbyopia [27,28], while monofocal lenses and monovision remain more popular. This trend can be attributed to factors such as lack of knowledge, the complexity of the adaptation process, and insufficient visual performance of multifocal CL designs.

Manufacturers recommend their fitting guides (FG) to address these adaptation issues. These FG, which include an initial choice nomogram of MCLs combination based on the patient's addition and steps to optimize vision at different distances, are often helpful. However, the eventual need to test multiple trial lenses can prolong the adaptation process, leading to patient disinterest and consequent dry out of these MCLs.

While these FG are useful, they can be inadequate in specific cases, such as in patients on the boundary between two near additions or having non-standard eyes with different spherical aberration values [118]. Moreover, these FG often lack detailed information about how lens profiles change at each step, leaving many optometrists without necessary information to contribute to the adaptation process. User needs and vision preferences at different distances should also be considered in these FG to optimize adaptation [204]. Despite attempts to improve these FG [124], the underlying philosophy still remains the same.

The implementation of these FG within a clinical visual simulator, such as SimVis Gekko, which can accurately simulate MCLs from various manufacturers and designs (see Chapter 3), could enhance the fitting process. This approach could shorten the adaptation time, allow testing of a larger number of steps in a single session (even from different manufacturers), and help find the optimal design and lens combination for each patient in a customized solution.

The main clinical question of the study detailed in this chapter is the feasibility of automatically implementing the fitting guides in SimVis Gekko and whether this could optimize the performance of the initial lenses suggested by each manufacturer's fitting guide nomogram. Additionally, we propose and aim to validate a metric based on SimVis Gekko inputs and lifestyle needs to determine the fitting guide step with the best visual performance for each subject.

To achieve these goals different steps of the FG were evaluated through SimVis Gekko by obtaining VA at different distances for each step. If the visual performance was found to be better compared to other steps not recommended by the FG for this patient, both corrections (the ones proposed by the FG and by SimVis Gekko) were clinically evaluated using real MCLs to analyze a more comprehensives clinical outcomes.

4.2– Methods

4.2.1– Subjects

Twelve presbyopic subjects participated in this study (see Table 4.1). Subjects were distributed in two different groups according to their near addition: low addition (48.5 ± 2 years) including subjects with a near add from +0.75 D to +1.50 D and mid - high addition (53.8 ± 3.6 years) including subjects with a near add from +1.75 D to +2.50 D. Regardless of their group classification, each subject followed the fitting guide corresponding to their specific near addition.

The research protocol was approved by the Health Department of Alicante (ISABIAL CEIM, General Hospital, Alicante, Spain) under the reference CEIm PI2022-052 – ISABIAL 2022-0092 and was conducted in agreement with the Declaration of Helsinki. Before enrollment, all subjects were thoroughly briefed about the study's objectives and provided their written informed consent.

Subjects with astigmatism greater than 1.00 D, contraindications for contact lens use, or a history of ocular surgery and/or pathology were excluded from the study.

The study was conducted over 5 sessions distributed on different days. The initial session involved an optometric examination and SimVis Gekko clinical evaluations. The subsequent four sessions were dedicated to the clinical evaluation of one or two real designs from each manufacturer, with one session allocated per manufacturer.

Table 4.1. *Data of patients participating in the study, including age, refractive error (Sphere, Cylinder and Axis), near addition and pupil size measured in photopic conditions.*

Subject	Age (y)	Refractive Error (D, D, deg)	Addition (D)	Pupil Size (mm) (Photopic 160 lx)
S#1	47	-5.75 – 0.75 x70	1.25	OD: 2.8
		-5.75 - 0.50 x130		OS: 3.2
S#2	51	-1.25	1.25	OD: 2.9
		+0.00 – 1.00 x80		OS: 2.8
S#3	48	+1.25	1.00	OD: 2.6
		+1.25		OS: 2.8
S#5	51	-3.00 – 0.50 x45	1.25	OD: 2.9
		-4.00 – 0.25 x175		OS: 2.7
S#6	47	-1.25	1.25	OD: 2.9
		-1.00		OS: 3.4
S#7	55	-3.25 – 0.50 x165	2.50	OD: 2.6
		-3.00 – 0.75 x15		OS: 3.1
S#8	55	-5.25	2.00	OD: 3.1
		-5.75		OS: 3.0
S#9	59	-4.25	2.25	OD: 3
		-3.75		OS: 3.1

S#10	47	+0.50 – 0.75 x110	0.75	OD: 3.1
		+0.75 – 0.50 x70		OS: 3.1
S#11	48	-0.75	1.75	OD: 2.9
		-1.00 – 0.50 x15		OS: 3.4
S#12	53	-1.00 – 0.50 x180	2.00	OD: 3
		-0.50 – 1.00 x175		OS: 2.9
S#13	53	+1.25 – 0.75 x90	2.25	OD: 2.4
		+1.25 – 0.50 x70		OS: 2.6

4.2.3– SimVis Gekko visual simulator

The SimVis Gekko visual simulator was employed to simulate commercial daily MCLs from 4 different manufacturers in a clinical environment. SimVis Gekko served as a prescription tool to determine the preference between two different designs included in the fitting guides of each manufacturer. This prescription was based on clinical measurements that served as inputs for and a novel metric developed for this study. This metric provided the combination of MCLs chosen by the SimVis Gekko-based prescription (a detailed description is provided in section 4.2.5) which could be the same or different than the MCLs suggested by the manufacturer's fitting guide.

4.2.3– Real multifocal contact lenses and simulations

The real MCLs and their corresponding simulations by SimVis Gekko used in this study were the same as those utilized Chapter 3 for all the available near additions: Dalies Total1, MyDay, Biotrue ONEday and 1-Day Acuvue Moist. These simulations were obtained from *in-vitro* and computational methods and were clinically validated for Low and High Additions. Simulations for Mid additions were also incorporated into this study.

The pupil size for the simulations was adjusted to match the real pupil size of the subjects, ranging from 3 to 5 mm in 0.5 steps (rounded to the closer 0.5 mm). In cases where the rounded pupil size differed between the two eyes, the minor pupil size was set. Applying these criteria and the pupil size data shown in Table 4.1, all subjects were assigned a 3 mm pupil diameter for both eyes.

The refractive error of each subject was corrected using MCLs for real lenses, while trial lenses at SimVis holders were used to correct it for SimVis Gekko simulations.

4.2.4– Fitting guides

The initial steps of classic fitting guides (FG) of each manufacturer were considered to select the pair of MCLs according to near addition and eye dominance for each subject. These selected combinations of MCLs, referred to as 'Classic Fitting Guide', were one of the prescription methods used in this study.

The initial steps of the fitting guides for each manufacturer are described in Table 4.2.

Table 4.2. Fitting guide initial steps according to near addition and dominant eye for each manufacturer: *Dalies Total1, MyDay, Biotrue ONEday and 1-Day Acuvue Moist.*

Fitting guides for each manufacturer			
Initial Steps	Dailies Total1	Initial Steps	MyDay
Low Addition (up 1.25 D)	Dominant: Low Non-Dominant: Low	Low Addition (0.75 – 1.25 D)	Dominant: Low Non-Dominant: High
Mid Addition (1.50 – 2.00 D)	Dominant: Mid Non-Dominant: Mid	Mid Addition (1.50 – 1.75 D)	Dominant: Low Non-Dominant: Mid
High Addition (2.25 – 2.50 D)	Dominant: High Non-Dominant: High	High Addition (2.00 – 2.50 D)	Dominant: Low Non-Dominant: High
Initial Step	Biotrue ONEday	Initial Steps	1-Day Acuvue Moist
Low Addition (0.75 – 1.50 D)	Dominant: Low Non-Dominant: Low	Low Addition (0.75 – 1.25 D)	Dominant: Low Non-Dominant: Low
		Mid Addition (1.50 – 1.75 D)	Dominant: Mid Non-Dominant: Mid
High Addition (1.75 – 2.50 D)	Dominant: High Non-Dominant: High	High Addition (2.00 – 2.50 D)	Dominant: Mid Non-Dominant: High

Often, these fitting guides also include additional steps to enhance visual performance at specific distances. These enhancements may involve a change in the design (addition) or the inclusion of ± 0.50 D increments. However, for the purpose of this study, only the initial steps were taken into account.

4.2.5– 3D-VA Metric

A new metric (3D-VA) was developed to determine the optimal combination of MCLs for each subject (at least among the two options tested in this study), using a reduced number of inputs measured through SimVis Gekko simulations (including the visual preferences of the subjects).

The main inputs for this metric are the VA at far, intermediate and near distances, obtained through the different SimVis Gekko simulations that each subject evaluates. The metric also incorporates additional information regarding the importance each subject assigns to each distance in their lifestyle, which is used to weigh the corresponding VA value on a perceptual scale from 0 to 10 in increments of 1. The best-corrected visual acuity (BCVA) at each distance is considered to establish the maximum achievable value with the SimVis simulation, adjusting it according to the weight assigned to each distance. If the VA at any distance deviates significantly from the BCVA, a penalization factor is applied in the final metric output, indicating that the simulation does not meet the subject's needs.

The output of the metric is normalized to a range from 0 to 1, representing the module of the results for the three distances after applying the weights. A score of 0 indicates that the simulation does not match the VA needs in any distance, while a score of 1 signifies a perfect match.

In this study, the 3D-VA metric was calculated for the initial steps corresponding to the subject's addition and the closest subsequent step (i.e. FG: Low Add and Other: Mid Add, FG: Mid Add and Other: High Add; FG: High Add and Other: Mid Add). The evaluated step with the best 3D-VA value was prescribed as the SimVis Gekko Fitting pair of MCLs.

4.2.6– Clinical measurements procedures.

Optometric examination

Prior to the main clinical measurements of the study, all subjects underwent a complete optometric examination: anamnesis, subjective refraction, near addition quantification, ocular dominance stereopsis and slit lamp examination. These procedures ensured that all subjects met the inclusion criteria and provided the necessary information for the study.

Clinical measurements consisted of binocular VA defocus curves using trial lenses ranging from +1.00 D to -3.00 D (in 0.50 D steps) and binocular CSF for photopic and mesopic conditions (using CSV-1000, as described in Methods section) were also evaluated to obtain baseline results.

SimVis Gekko 3D-VA measurements

We employed the 3D-VA metric, which uses inputs from SimVis Gekko simulations (as described in section 4.2.5), to determine the SimVis Gekko CLs prescription for each subject. This prescription was made between the two initial steps for each manufacturer in a randomized order. VAs were measured using printed logMAR charts, and the best 3D-VA metric was chosen as SimVis Gekko prescription for each manufacturer. Figure 4.1 (Session 1) represents the two different prescription methods: Classic Fitting Guide (A) and SimVis Gekko Fitting (B). Each subject was measured simulating 2 different steps per manufacturer, with a total of 8 combinations of MCLs.

If the SimVis prescription did not match with the classic fitting provided by the Fitting guide of a certain manufacturer, we clinically measured the two steps using real MCLs to evaluate visual performance and determine the best option. Conversely, if the SimVis Gekko prescription matched with FG, only the CL model selected by both methods was measured (that was interpreted as a match between Classic FG and SimVis Gekko Fitting.

Clinical measurements with real multifocal contact lenses

The pair of MCLs selected by FG and SimVis Gekko were clinically evaluated using real MCLs from each manufacturer in a randomized order for manufacturer and method of prescription. This evaluation determined visual performance through different clinical tests, as depicted in Figure. 4.1 C (Session 2). As indicated before, if the pair of MCLs is the same for both methods, only one pair of MCLs was evaluated in Session 2. The clinical measurements evaluated in Session 2, following a 2-hour period of adaptation, included:

Fitting verification

Slit lamp examination to assess the proper settling of the MCLs, following the CLEAR guideline for soft contact lenses. If any of the adaptations were unacceptable, MCLs were removed immediately.

Binocular Defocus curves and VA at real distances

The binocular defocus curves were measured from +1D to -3D in 0.5D steps, following the method described in section 2.6 (Methods). The VAs at real distance were measured at 4, 0.66 and 0.4 m.

Binocular CSFs

The binocular CSFs at far distance for photopic (85 cd/m^2) and mesopic (3 cd/m^2) conditions were assessed with CSV-1000, also following the method described in section 2.5 (Methods).

NVAQ Questionnaire

The 10 question items of the Near Visual Questionnaire that evaluate spectacle independence were used, when the subject was wearing each combination of real MCLs.

Stereopsis

The Stereopsis was measured using the TNO test with anaglyphs filters placed in the trial frame.

Perceptual Scores of Visual Satisfaction.

The perceptual score of satisfaction at each distance with each combination of MCLs was evaluated, with perceptual scores ranging from 0 to 10, 0 being the worst visual performance and 10 the best visual performance.

Direct preference.

If the combination of MCLs differed between the two methods, subjects were asked the following direct preference question after the removal of the last combination: *Which combination of MCLs provides you a better visual performance at different distances?* Subjects were required to choose one option in a mandatory manner.

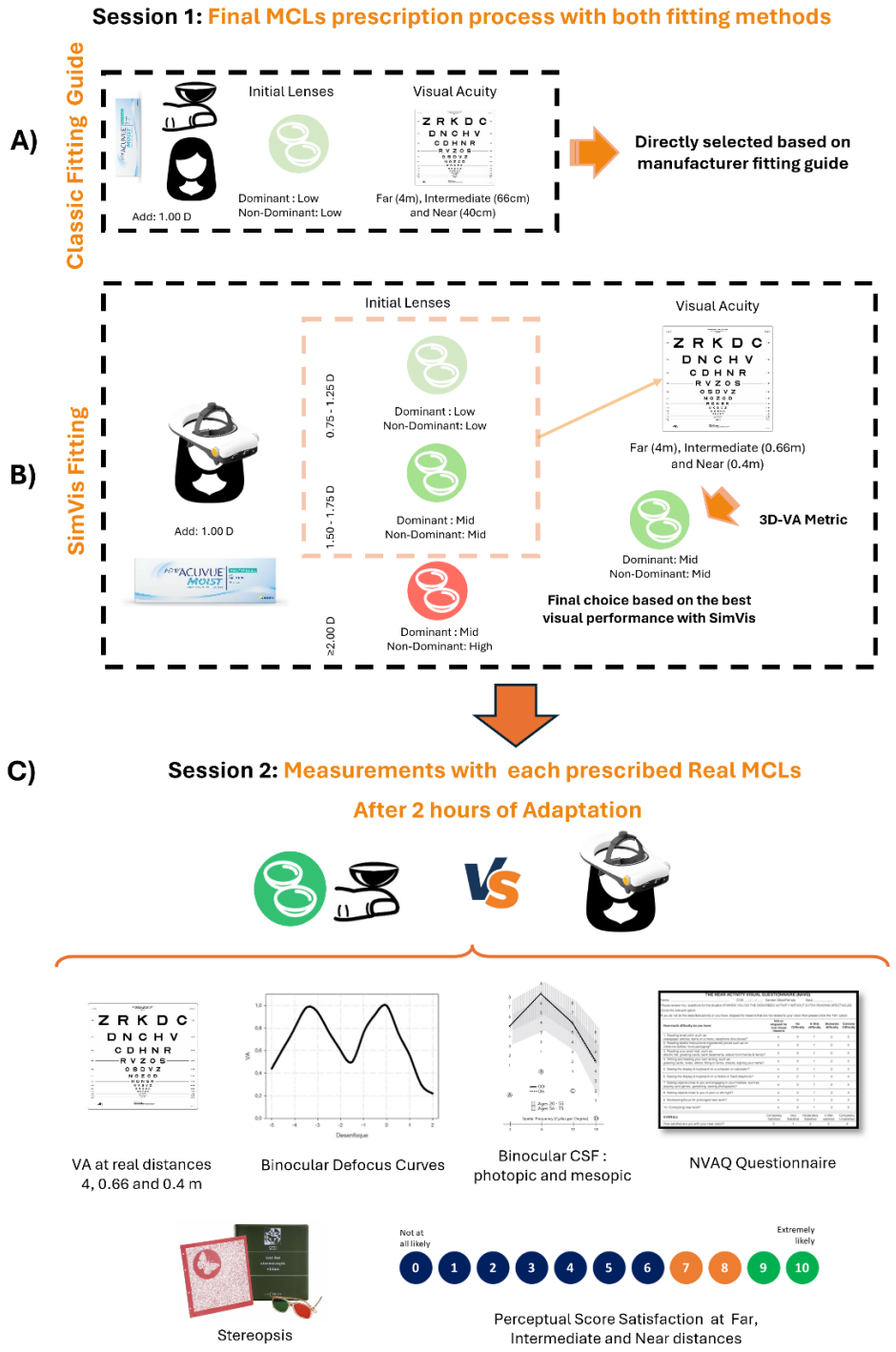

Figure 4.1. Clinical flowchart for each session conducted in the study. *Session 1: Prescription of each combination of MCLs following the classic fitting guide (A) and with SimVis Gekko simulations using 3DVA (B). Session 2 (C): Clinical measurements with the combination of real MCLs prescribed by both methods if they were different. The clinical measurements were VA at real distances, binocular defocus curve, binocular CSF, NVAQ questionnaire, Stereopsis (TNO) and Perceptual Score Satisfaction at different distances.*

Metric calculations based on clinical measurement:

The clinical measurements with real MCLs (VA at real distances and Perceptual Scores of Visual Satisfaction) were utilized to obtain the 3D-VA and Perceptual Satisfaction module of three distances, respectively. These metrics were calculated for Classic Fitting Guides prescriptions and SimVis Gekko fitting prescriptions.

4.2.6– Statistical analysis

The clinical measurements and calculated metrics were analyzed using IBM SPSS Statistics Version 28 (IBM Corp, USA). Descriptive statistics, including the mean and standard deviations, were reported for the clinical measurements of all FG prescription pairs of MCLs and SimVis Gekko prescriptions (only whether they were different).

Due to the small sample, a non-parametric test for paired groups (Wilcoxon signed-rank test) was performed to analyze different between clinical results and calculated metrics obtained with FG and SimVis prescription.

Spearman's correlation was used to analyze the relation between the calculated metrics.

Throughout the entire analysis, a significance level of $p < 0.05$ was applied to define statistical significance.

4.3– Results

4.3.1–SimVis Gekko evaluation.

The 3D-VA metric results obtained from VAs with SimVis Gekko simulations of MCLs combinations following the corresponding classic fitting guide step (FG) and other steps (O) are described in Table 4.3 for each manufacturer. The FG step presented higher 3D-VA in 29 cases (60.42 %) (with 13 presenting a small difference (<0.05)), while O steps had better 3D-VA in 19 cases (39.58 %) (with 6 presenting small differences).

The mean 3D-VA for FG and O steps was, respectively, 0.42 ± 0.24 and 0.37 ± 0.23 for Dailies Total1, 0.44 ± 0.21 and 0.44 ± 0.26 for MyDay, 0.35 ± 0.21 and 0.32 ± 0.19 for Biotrue ONEday, 0.38 ± 0.24 and 0.39 ± 0.22 for 1-Day Acuvue Moist and 0.39 ± 0.22 and 0.38 ± 0.23 across all manufacturers.

Table 4.3. 3D-VA metric values obtained with SimVis Gekko simulations for Classic Fitting guide step (FG) and other steps (O) for each subject (S) and manufacturer.

SimVis Gekko Evaluation																
S	Dailies Total 1				MyDay				BioTrue ONEday				1-Day Acuvue Moist			
	Addition Step		3DVA SimVis Gekko		Addition Step		3DVA SimVis Gekko		Addition Step		3DVA SimVis Gekko		Addition Step		3DVA SimVis Gekko	
	FG	O	FG	O	FG	O	FG	O	FG	O	FG	O	FG	O	FG	O
S1	Low	Mid	0.8	0.84	Low	Mid	0.79	0.98	Low	High	0.74	0.66	Low	Mid	0.69	0.72
S2	Low	Mid	0.41	0.35	Low	Mid	0.59	0.35	Low	High	0.35	0.33	Low	Mid	0.32	0.44
S3	Low	Mid	0.57	0.55	Low	Mid	0.55	0.41	Low	High	0.53	0.42	Low	Mid	0.46	0.54
S4	Low	Mid	0.42	0.3	Low	Mid	0.58	0.54	Low	High	0.38	0.28	Low	Mid	0.27	0.61
S5	Low	Mid	0.61	0.46	Low	Mid	0.51	0.55	Low	High	0.46	0.27	Low	Mid	0.62	0.4
S6	High	Mid	0.05	0.19	High	Mid	0.13	0.09	High	Low	0.05	0.22	High	Mid	0.09	0.09
S7	Mid	High	0.69	0.64	High	Mid	0.63	0.69	High	Low	0.48	0.52	High	Mid	0.73	0.54
S8	High	Mid	0.07	0.02	High	Mid	0.09	0.1	High	Low	0.04	0.03	High	Mid	0.03	0.02
S9	Low	Mid	0.54	0.47	Low	Mid	0.47	0.58	Low	High	0.39	0.49	Low	Mid	0.56	0.37
S10	Mid	High	0.32	0.22	Mid	High	0.28	0.36	High	Low	0.24	0.2	Mid	High	0.2	0.31
S11	Mid	High	0.43	0.32	High	Mid	0.3	0.55	High	Low	0.43	0.41	High	Mid	0.43	0.54
S12	Mid	High	0.11	0.13	High	Mid	0.32	0.11	High	Low	0.07	0.03	High	Mid	0.13	0.11

The manufacturer which obtained the best 3D-VA values across subjects, through SimVis Gekko simulations, was MyDay for both FG and O steps. Nevertheless, all manufacturers presented mean values in the range of 0.32 to 0.44.

4.3.2– Real Multifocal Contact lenses evaluation.

Clinical measurement results of classic fitting guides prescription (FG)

The results of the clinical measurements obtained with real MCLs following the FG, for each manufacturer, are presented in Figures 4.2, 4.3, 4.4 and table 4.3. All results are distributed in low addition and mid-high addition groups (n = 6). Mid and High addition categories were combined into a single group because they exhibited similar behavior and had an equal number of subjects as low addition group.

Fig. 4.2 represents the results of binocular defocus curves for low addition group (solid lines) and mid-high addition group (dashed lines) for each manufacturer: Dailies Total1 (A; blue lines), MyDay (B; orange lines), Biotrue ONEday (C; green lines) and 1-Day Acuvue Moist (D; red lines). A trend towards a decrease at far and intermediate defocus curve vergences between low and mid-high designs can be observed, but there is not a high benefit at near vergences among them. VA at real near distance was worse for high addition group in all manufacturers except 1-Day Acuvue Moist.

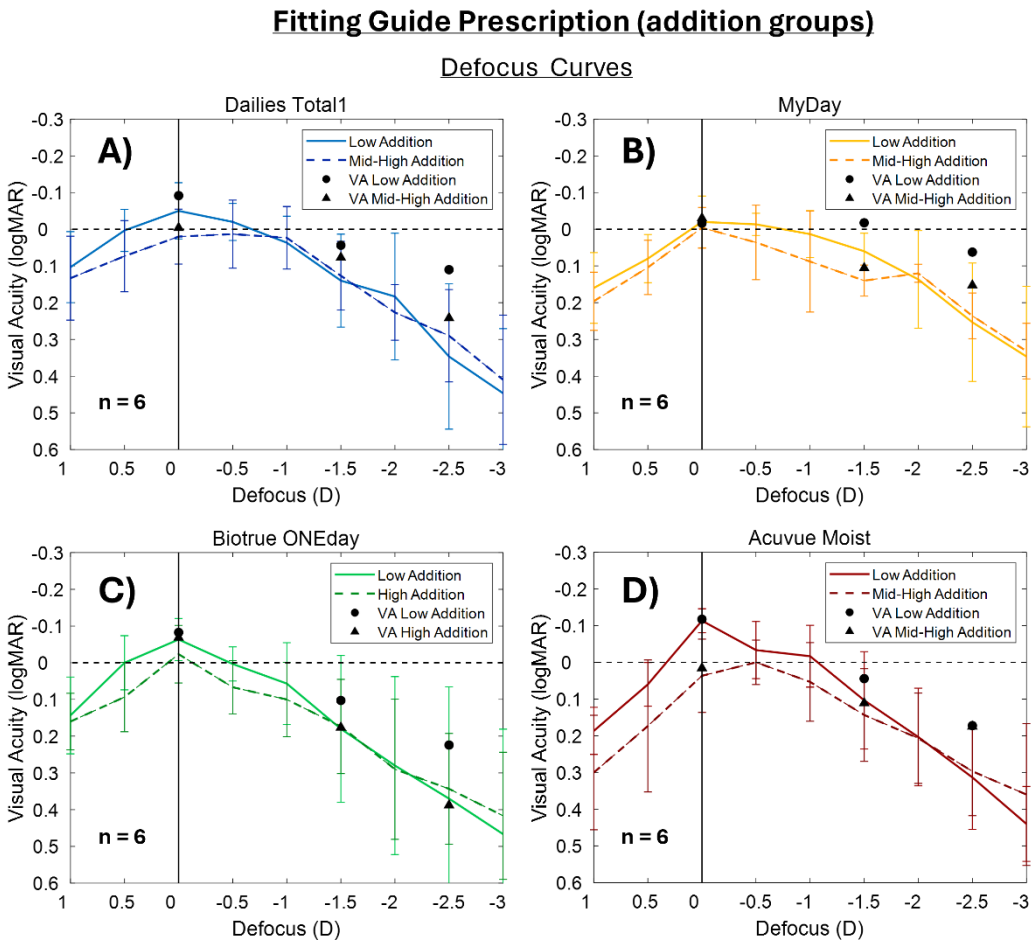

Figure 4.2. Defocus curves results and VA at real distances with real MCLs following initial Fitting Guides steps for each manufacturer (n = 6): *(A) Dailies Total1 (blue color) (B) MyDay (yellow color), (C) Biotrue ONEday (green color) and (D) 1-Day Acuvue Moist (red color); for low (solid lines and black circles) and mid-high addition (dashed lines and black triangles). Standard deviations of defocus curves are represented for each defocus value.*

Fig.4.3 illustrates the binocular CSF for photopic (left column) and mesopic (right column) light conditions for each addition group and manufacturer following the same representation as in Figure 4.2. These results exhibit a general decrease in contrast sensitivity for mid-high additions in all manufacturers, which is more evident in medium spatial frequencies (6 and 12 cpd) in mesopic conditions.

Fig.4.4 shows the results of binocular defocus curves (A and B) and CSF for photopic (C and D) and mesopic (E and F) for all manufacturers and single lens (represented by black lines), enabling us to compare these designs. The left and right columns represent low addition and mid-high groups, respectively.

Although a trend can be observed in the behavior between low and mid-high addition in the defocus curves (described above), some differences can be observed between the designs of the different brands, presenting all of them better VAs than single lens at near vergences.

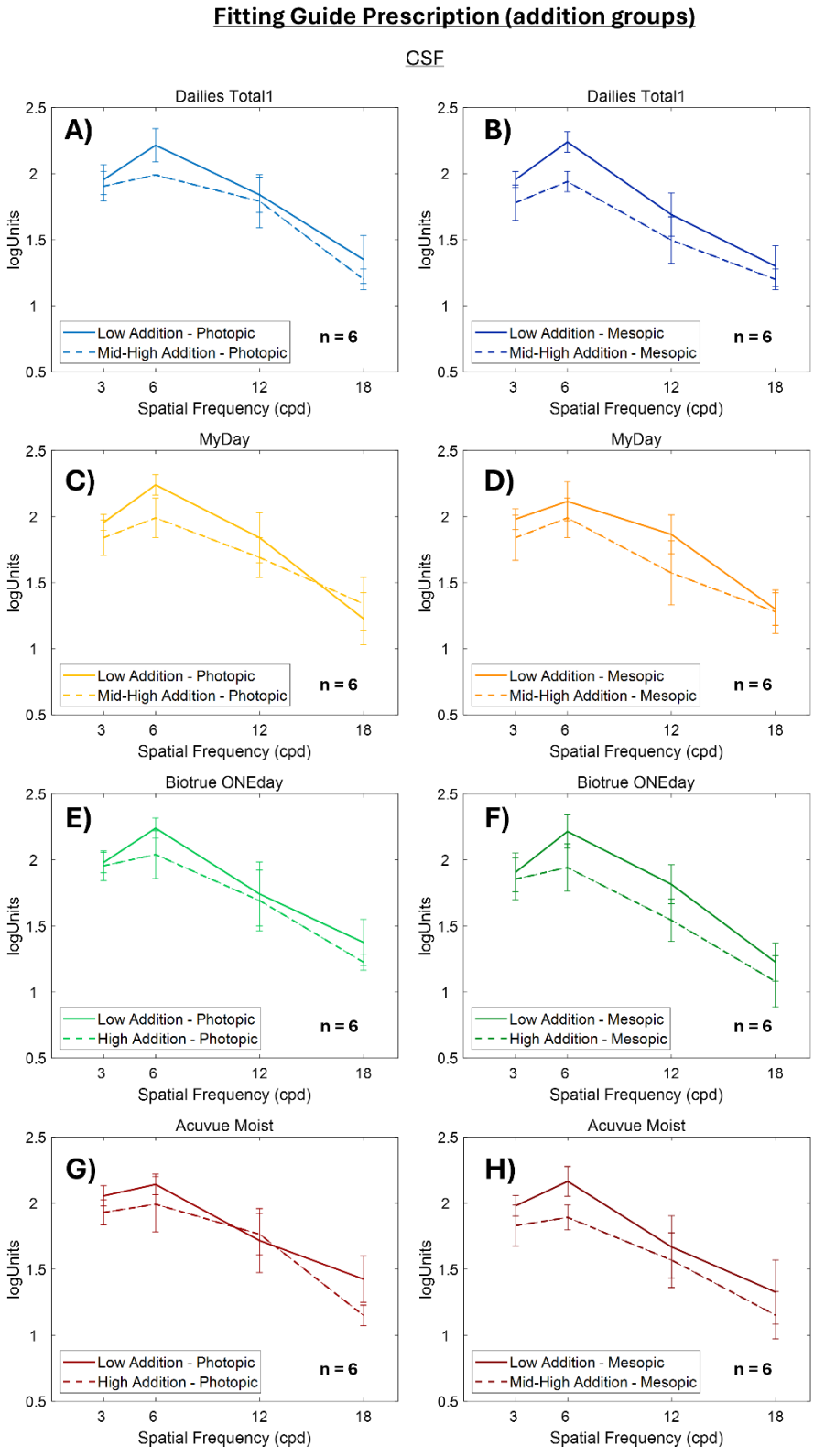

Figure 4.3. CSF results with real MCLs following initial Fitting Guides steps for each manufacturer (n = 6): *(A and B) Dailies Total1 Photopic and Mesopic conditions (C and D) MyDay Photopic and Mesopic conditions, (E and F) Biotrue ONEday Photopic and Mesopic conditions and (G and H) 1-Day Acuvue Moist Photopic and Mesopic conditions; for low (solid lines) and mid-high addition (dashed lines). Standard deviations of CSF are represented for each spatial frequency.*

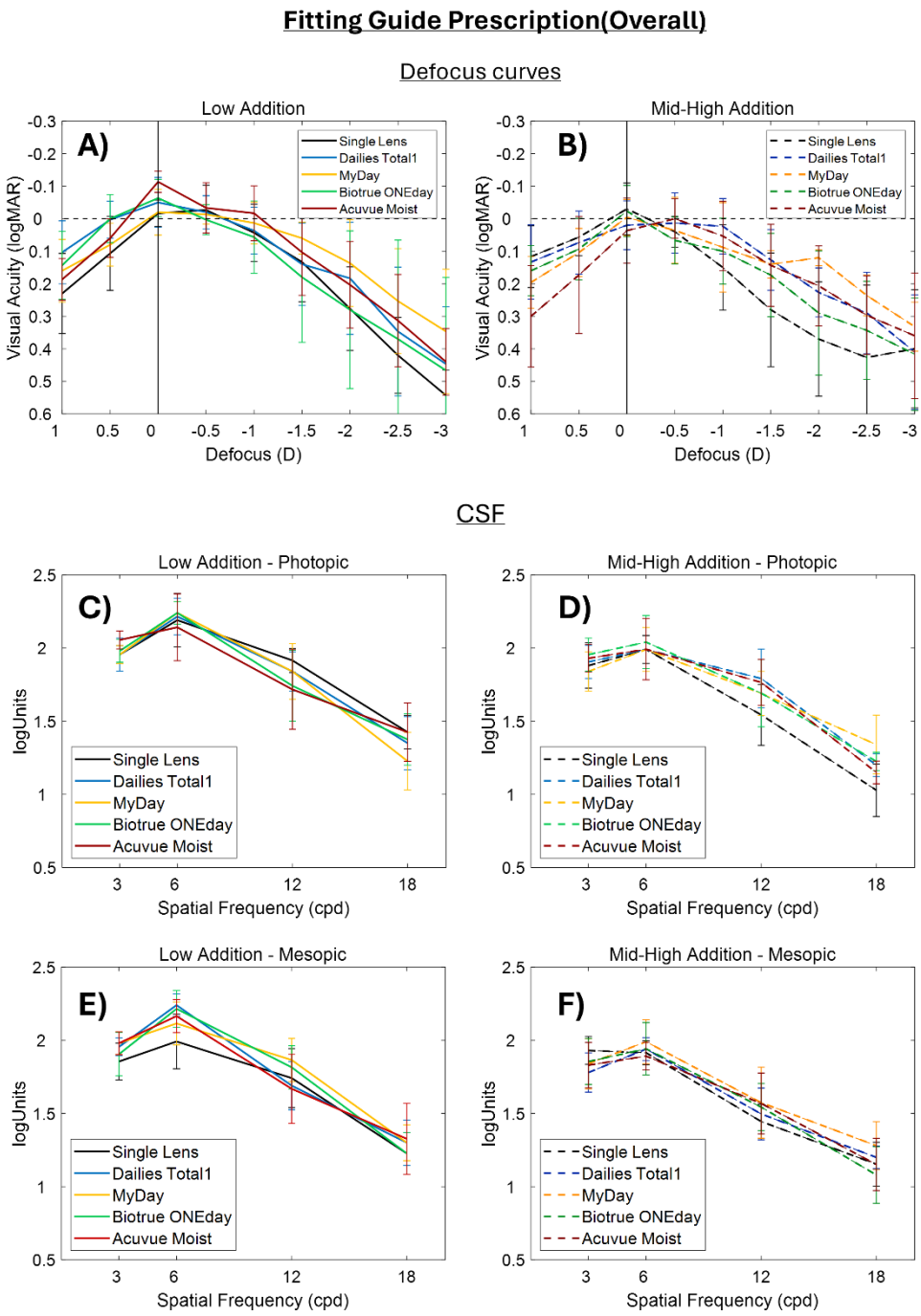

Figure 4.4. Defocus Curves and CSF with real MCLs following initial Fitting Guides steps for each addition group (n = 6): (A) Low Addition defocus curves, (B) Mid-High Addition defocus curves, (C) Low Addition Photopic CSF, (D) Low Addition Mesopic CSF, (E) Mid-High Addition Photopic CSF and (D) Mid-High Addition Mesopic CSF; for each manufacturer with its corresponding color and black lines represents single lens. Standard deviations of defocus curves and CSF are represented for each defocus value and spatial frequency, respectively.

For low addition, MyDay presented a wider depth of focus in comparison with others designs, also presenting a decrease in far vision. 1-Day Acuvue Moist for low addition showed a good balance between the highest VA at far distance and a good range of depth of focus.

The designs with mid-high addition demonstrated comparable VA at far distance. However, more variability was observed at near vergences. Among them, Biotrue ONEday presented less depth of focus compared to 1-Day Acuvue Moist and Dailies Total1, while the best behavior at near distances was MyDay. The differences between the mid-high addition and single lens were deeper in this group.

Regarding CSF for photopic and mesopic, there were no clear trends between manufacturers for low or mid-high additions, but all of them improve the behavior of singles lens.

Table 4.4 showed the rest of clinical measurements (VA and PS at 4, 0.66 and 0.40 m, NVAQ and stereopsis) for each addition group and manufacturer. These results were also worse for mid-high additions compared to low addition for all the measured variables.

Table 4.4. Clinical results with real MCLs following FG steps for different addition groups: Low and Mid-High additions. *The mean, standard deviation, and the statistical differences between methods of clinical variables are presented for each manufacturer and addition group.*

Clinical measurement results of fitting guides prescription for each manufacturer									
Dailies Total1									
Addition Group		**VA 4 m**	**VA 0.66m**	**VA 0.4m**	**PS 4 m**	**PS 0.66m**	**PS 0.4m**	**NVAQ**	**Stereopsis**
Low Addition	Mean	-0.09	0.04	0.11	9.17	7.50	6.50	12.00	130.00
	SD	0.04	0.12	0.13	0.75	3.15	2.95	12.25	58.99
Mid-High Addition	Mean	0.00	0.08	0.24	8.33	8.00	6.00	12.00	320.00
	SD	0.06	0.17	0.15	1.03	2.45	2.10	6.87	123.94
MyDay									
Addition Group		**VA 4 m**	**VA 0.66m**	**VA 0.4m**	**PS 4 m**	**PS 0.66m**	**PS 0.4m**	**NVAQ**	**Stereopsis**
Low Addition	Mean	-0.02	-0.02	0.06	8.67	9.50	8.17	6.83	80.00
	SD	0.08	0.12	0.06	1.03	0.84	1.47	6.18	30.98
Mid-High Addition	Mean	-0.03	0.11	0.15	7.00	7.17	7.33	9.50	200.00
	SD	0.04	0.10	0.10	2.10	2.48	3.01	8.83	145.33
Biotrue ONEday									
Addition Group		**VA 4 m**	**VA 0.66m**	**VA 0.4m**	**PS 4 m**	**PS 0.66m**	**PS 0.4m**	**NVAQ**	**Stereopsis**
Low Addition	Mean	-0.08	0.10	0.22	8.83	7.67	6.17	16.00	200.00
	SD	0.06	0.14	0.19	0.75	1.75	2.71	12.33	61.97
High Addition	Mean	-0.07	0.18	0.39	7.17	5.67	3.83	20.83	380.00
	SD	0.07	0.21	0.23	2.23	3.27	3.37	11.63	159.50
1-Day Acuvue Moist									
Addition Group		**VA 4 m**	**VA 0.66m**	**VA 0.4m**	**PS 4 m**	**PS 0.66m**	**PS 0.4m**	**NVAQ**	**Stereopsis**
Low Addition	Mean	-0.12	0.04	0.17	8.83	8.67	7.58	9.67	170.00
	SD	0.05	0.11	0.12	0.98	1.37	1.56	8.38	79.75
Mid-High Addition	Mean	0.02	0.11	0.17	5.33	8.33	6.83	12.17	180.00
	SD	0.10	0.14	0.11	1.03	1.63	2.32	7.73	65.73

Comparison of clinical results between prescription methods: Classic Fitting Guide and SimVis Gekko.

The clinical measurement results comparing the combination of MCLs prescribed by the Classic Fitting Guide and SimVis Gekko are represented in Figure 4.5 for defocus curves and VA at real distances, Figure 4.6 for CSF and Table 4.5 for the rest of clinical variables. The sample groups did not have the same size (between 3 and 7 subjects), as the cases in which SimVis Gekko prescribed other steps of FG were unequal among manufacturers. The SimVis Gekko prescription for 1-Day Acuvue Moist in subject 11 could not be measured using real MCLs because it was not available, but the rest of measurements were normally conducted in this subject.

Figure 4.5 shows results of defocus curves and VA at real distances for classic Fitting Guide (represented by the color of each manufacturer) and SimVis Gekko (represented by coral color) for each manufacturer. Dailies Total1 (A), MyDay (B) and BioTrue ONEday (C) presented comparable behavior among them without significant statistical differences in each defocus or real distance.

Comparison between prescription methods: Defocus Curves

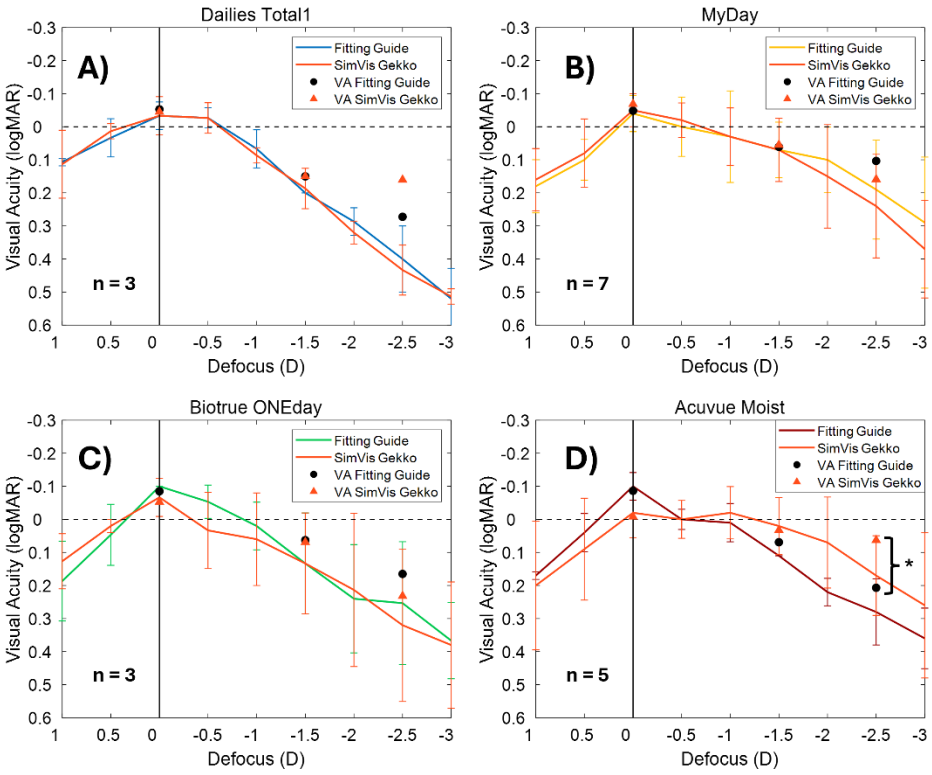

Figure 4.5. Defocus curves results and VA at real distances with real MCLs: comparison between prescription methods (Classic Fitting Guide vs SimVis Gekko): *(A) Dailies Total1 (blue color) (B) MyDay, (C) Biotrue ONEday and (D) Acuvue 1-Day; for Fitting guide (solid lines with each manufacturer color and black circles) and SimVis Gekko (solid lines and triangles with coral color). Standard deviations of defocus curves are represented in each 0.5 D defocus value.*

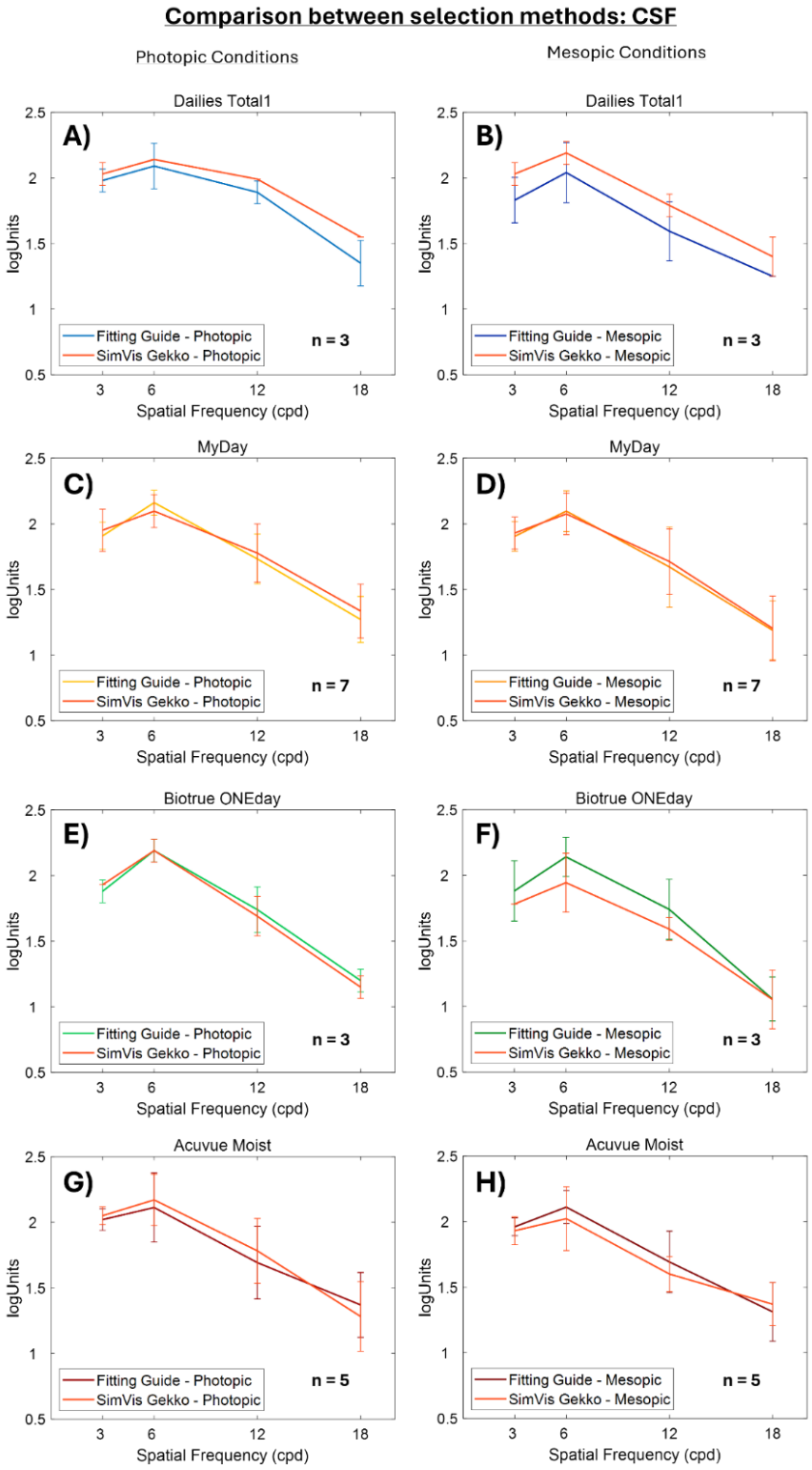

Figure 4.6. CSF with real MCLs: comparison between prescription methods (Classic Fitting Guide vs SimVis Gekko): *(A and B) Dailies Total1 Photopic and Mesopic conditions (C and D) MyDay Photopic and Mesopic conditions, (E and F) Biotrue ONEday Photopic and Mesopic conditions and (G and H) 1-Day Acuvue Moist Photopic and Mesopic conditions; for Fitting guide (solid lines with each manufacturer color) and SimVis Gekko (solid lines with coral color). Standard deviations of CSF are represented in each spatial frequency.*

On the other hand, for the 1-Day Acuvue Moist (D) results of defocus curves obtained with the SimVis Gekko prescription presented an increased benefit at near vergences without significant statistical differences, while the VA acuity at near was better for SimVis Gekko (0.06 (SV) vs 0.21 (FG) logMAR), showing significant statistical differences ($p< 0.05$).

Figure 4.6 shows the CSF with real MCLs for both methods, FG and SimVis Gekko. Results are similar across methods, with SimVis Gekko showing slightly better contrast sensitivity for all spatial frequencies in photopic and mesopic conditions for Dailies Total1. However, there were no significant statistical differences in the CSF between FG and SimVis methods for any manufacturer.

Finally, Table 4.5 shows the rest of the data collected for both FG and SimVis Gekko methods. Comparing the results across methods, statistically significant differences were only found for the NVAQ for both the 1-Day Acuvue Moist (6.80 (SV) vs 15 (FG)) and All Manufacturers (8.61 (SV) vs 12.72 (FG) logMAR).

Table 4.5. Comparison of clinical results with real MCLs prescribed by different methods: Fitting Guide and SimVis Gekko. *The mean, standard deviation, and the statistical differences between methods of clinical variables are presented for each manufacturer and overall.*

Comparison of clinical results between prescription methods: Fitting Guide and SimVis Gekko									
Dailies Total1									
RCL prescription method		**VA 4 m**	**VA 0.66m**	**VA 0.4m**	**PS 4 m**	**PS 0.66m**	**PS 0.4m**	**NVAQ**	**Stereopsis**
Fitting Guide	Mean	-0.05	0.15	0.27	9.33	9.33	5.67	17.00	280.00
	SD	0.05	0.04	0.06	1.15	0.58	1.53	2.65	183.30
SimVis Gekko	Mean	-0.05	0.15	0.16	9.67	9.33	8.33	7.33	160.00
	SD	0.04	0.04	0.05	0.58	0.58	0.58	0.58	69.28
Statistical Differences	p-value	0.79	1.00	0.11	0.32	1.00	0.10	0.11	0.18
MyDay									
RCL prescription method		**VA 4 m**	**VA 0.66m**	**VA 0.4m**	**PS 4 m**	**PS 0.66m**	**PS 0.4m**	**NVAQ**	**Stereopsis**
Fitting Guide	Mean	-0.05	0.06	0.10	154.29	9.14	8.00	7.71	7.14
	SD	-0.04	0.04	0.10	170.00	10.00	7.67	7.33	6.83
SimVis Gekko	Mean	-0.07	0.05	0.16	7.86	7.71	7.29	8.29	188.57
	SD	-0.06	0.04	0.17	7.67	7.33	7.00	8.50	210.00
Statistical Differences	p-value	0.07	0.75	0.46	0.83	1.00	0.78	0.49	0.16
Biotrue ONEday									
RCL prescription method		**VA 4 m**	**VA 0.66m**	**VA 0.4m**	**PS 4 m**	**PS 0.66m**	**PS 0.4m**	**NVAQ**	**Stereopsis**
Fitting Guide	Mean	-0.09	0.06	0.16	7.67	6.67	6.67	13.00	280.00
	SD	0.01	0.15	0.21	1.53	4.04	4.16	15.39	183.30
SimVis Gekko	Mean	-0.05	0.07	0.23	7.67	7.33	5.33	13.67	340.00
	SD	0.05	0.05	0.15	2.52	2.08	2.52	10.69	242.49
Statistical Differences	p-value	0.18	0.65	0.18	1.00	0.65	0.59	0.79	0.65
1-Day Acuvue Moist									
RCL prescription method		**VA 4 m**	**VA 0.66m**	**VA 0.4m**	**PS 4 m**	**PS 0.66m**	**PS 0.4m**	**NVAQ**	**Stereopsis**
Fitting Guide	Mean	-0.09	0.07	0.21	8.20	8.20	6.30	15.00	168.00
	SD	0.01	0.11	0.10	1.64	1.30	1.64	6.04	65.73
SimVis Gekko	Mean	-0.01	0.03	0.06	7.80	8.40	7.60	6.80	132.00
	SD	0.08	0.15	0.03	1.64	0.89	1.95	7.43	65.73
Statistical Differences	p-value	0.08	0.27	0.04	0.58	0.32	0.14	0.04	0.18
Total (All manufacturers)									
RCL prescription method		**VA 4 m**	**VA 0.66m**	**VA 0.4m**	**PS 4 m**	**PS 0.66m**	**PS 0.4m**	**NVAQ**	**Stereopsis**
Fitting Guide	Mean	-0.07	0.08	0.17	8.22	7.94	6.58	12.72	200.00
	SD	0.03	0.12	0.13	1.70	2.49	2.45	8.78	141.09
SimVis Gekko	Mean	-0.05	0.07	0.14	8.11	8.11	7.22	8.61	193.33
	SD	0.05	0.12	0.17	1.97	1.78	2.18	6.55	146.33
Statistical Differences	p-value	0.23	0.50	0.35	0.85	0.87	0.16	0.02	0.83

Comparison of calculated metrics and direct preference for Real MCLs prescribed with Classic Fitting Guide and SimVis Gekko.

The results of calculated metrics using the clinical measurements with real MCLs, 3D-VA and Perceptual Satisfaction Module (PSM), and direct preference between methods for each subject and manufacturer, are collected in table 4.6, 4.7 and 4.8, respectively.

A higher value of these metrics for the Real MCLs prescribed by SimVis Gekko are represented using green color, while red color means that the FG presented a better result. Inside this color code, light colors represent a difference between methods smaller or equal to 0.05 in the 3D-VA metric.

Table 4.6 revealed that the combination of real MCLs prescribed by SimVis Gekko was better, equal or worse in terms of 3D-VA across manufacturers for 11 (61.11 %), 3 (16.67 %), and 4 subjects (22.22 %), respectively.

Table 4.6. 3D-VA metric values obtained with Real MCLs for Classic Fitting guide step (FG) and SimVis Gekko (SV) option for each subject (S) and manufacturer. *Green color code represents a better value for SV option, while red color code represents a better value for FG. Gray color indicates the same value for both methods. Lighter color indicates that the difference between SimVis 3D-VAs values of each method was equal or smaller than 0.05.*

Real CLs Evaluation: 3DVA																
S.	Dailies Total 1				MyDay				Biotrue ONEday				1-Day Acuvue Moist			
	Addition Step		3DVA Real CL		Addition Step		3DVA Real CL		Addition Step		3DVA Real CL		Addition Step		3DVA Real CL	
	FG	O	FG	SV	FG	O	FG	SV	FG	O	FG	SV	FG	O	FG	SV
S1	Low	Mid	0.61	0.63	Low	Mid	0.68	0.76	Low	High	0.63	-	Low	Mid	0.63	0.76
S2	Low	Mid	0.87	-	Low	Mid	0.86	-	Low	High	0.82	-	Low	Mid	0.67	0.67
S3	Low	Mid	0.75	-	Low	Mid	0.83	-	Low	High	0.6	-	Low	Mid	0.48	0.79
S4	Low	Mid	0.49	-	Low	Mid	0.87	-	Low	High	0.63	-	Low	Mid	0.77	0.65
S5	Low	Mid	1	-	Low	Mid	1	1	Low	High	1	-	Low	Mid	0.97	-
S6	High	Mid	0.53	0.69	High	Mid	0.69	-	High	Low	0.56	0.63	High	Mid	0.81	-
S7	Mid	High	0.95	-	High	Mid	0.76	0.77	High	Low	0.83	0.73	High	Mid	0.67	-
S8	High	Mid	0.5	-	High	Mid	0.81	0.76	High	Low	0.62	-	High	Mid	0.22	-
S9	Low	Mid	0.99	-	Low	Mid	0.98	1	Low	High	1	0.69	Low	Mid	1	-
S10	Mid	High	0.92	-	Mid	High	0.9	1	High	Low	0.92	-	Mid	High	0.99	0.99
S11	Mid	High	0.27	-	High	Mid	0.37	0.5	High	Low	0.31	-	High	Mid	0.23	-
S12	Mid	High	0.25	0.27	High	Mid	0.39	-	High	Low	0.34	-	High	Mid	0.55	-

If we do not count the cases which had a difference less or equal than 0.05 in the SimVis Gekko 3D-VA, the results of 3D-VA with SimVis Gekko prescriptions were better, equal or worse for 8 (66.67 %), 2 (16.67 %) and 2 (16.67 %) subjects for all manufacturers, respectively.

When considering all manufacturers and prescription methods in relation to Real 3D-VA, it was observed that the combination of MCLs with a higher real 3D-VA corresponded to either the first (4/12) or second (6/12) highest values of SV 3D-VA (between the eight evaluated combinations, FG and O for all manufacturers) in 83.33 % of subjects (10/12).

Table 4.7 showed that the combination of real MCLs prescribed by SimVis Gekko had better PSM in 11 subjects (61.11 %), and worse PSM in 7 (38.89 %) subjects for all manufacturers. Without the cases of < 0.05 differences in the SimVis Gekko 3D-VA, the results of PSM with SimVis Gekko prescriptions were 8 subjects (66.67 %) with better PSM and 4 subjects (33.33 %) with worse PSM.

Table 4.7. Perceptual Satisfaction Module (PSM) metric values obtained with Real MCLs for Classic Fitting guide step (FG) and SimVis Gekko (SV) option for each subject (S) and manufacturer. *Green color code represents a better value for SV option, while red color code represents a better value for FG. Independently of color (green or red), light color indicates that the difference between SimVis 3DVAs values of each method was equal or smaller than 0.05.*

Real CLs Evaluation: Perceptual Satisfaction Module (VAS)																
S.	Dailies Total 1				MyDay				Biotrue ONEday				1-Day Acuvue Moist			
	Addition Step		PSM		Addition Step		PSM		Addition Step		PSM		Addition Step		PSM	
	FG	O	FG	SV	FG	O	FG	SV	FG	O	FG	SV	FG	O	FG	SV
S1	Low	Mid	8.5	9.04	Low	Mid	9.68	9.35	Low	High	7.75	-	Low	Mid	8.5	9
S2	Low	Mid	5.74	-	Low	Mid	8	-	Low	High	6.88	-	Low	Mid	7.14	6.78
S3	Low	Mid	9.68	-	Low	Mid	9.04	-	Low	High	9	-	Low	Mid	8.84	9
S4	Low	Mid	7.77	-	Low	Mid	7.77	-	Low	High	6.22	-	Low	Mid	7.72	7.89
S5	Low	Mid	7.7	-	Low	Mid	9.11	6.4	Low	High	7.7	-	Low	Mid	8.68	-
S6	High	Mid	8.04	9	High	Mid	7.89	-	High	Low	3.83	7.14	High	Mid	7.89	-
S7	Mid	High	8.68	-	High	Mid	6.06	8.39	High	Low	8.68	7.96	High	Mid	7.94	-
S8	High	Mid	8.72	-	High	Mid	10	9.68	High	Low	5.66	-	High	Mid	7.19	-
S9	Low	Mid	10	-	Low	Mid	9.38	9.7	Low	High	9.7	6.16	Low	Mid	9.68	-
S10	Mid	High	6.35	-	Mid	High	5.8	4.08	High	Low	6.66	-	Mid	High	6.22	7.39
S11	Mid	High	5.45	-	High	Mid	3.79	6.22	High	Low	3.87	-	High	Mid	5.8	-
S12	Mid	High	8.49	9.38	High	Mid	7.76	-	High	Low	8.49	-	High	Mid	7.41	-

Table 4.8 presents the number (and percentage) of subjects that directly preferred the pair of real MCLs prescribed according to SimVis or FG across manufacturers, being 11 (61.11 %) for SimVis prescriptions and 7 (38.89 %) for FG. Without the cases of < 0.05 differences in the SimVis Gekko 3D-VA, the pairs prescribed by SimVis Gekko were preferred in 8 (66.67 %) subjects, while the FG prescriptions were preferred in 4 (33.33 %) subjects.

Table 4.8. Direct preference between Real MCLs prescribed by Classic Fitting guide step (FG) and SimVis Gekko (SV) option for each subject (S) and manufacturer. *Green color code represents SV option preference, while red color code represents FG preference. Independently of color (green or red), light color indicates that the difference between SimVis 3D-VAs values of each method was equal or smaller than 0.05.*

Real CLs Evaluation: Direct Preference																
S.	Dailies Total 1				MyDay				Biotrue ONEday				1-Day Acuvue Moist			
	Addition Step		Preference		Addition Step		Preference		Addition Step		Preference		Addition Step		Preference	
	FG	O	FG	SV	FG	O	FG	SV	FG	O	FG	SV	FG	O	FG	SV
S1	Low	Mid			Low	Mid	-		Low	High	-	-	Low	Mid		
S2	Low	Mid	-	-	Low	Mid	-	-	Low	High	-	-	Low	Mid		
S3	Low	Mid	-	-	Low	Mid	-	-	Low	High	-	-	Low	Mid		
S4	Low	Mid	-	-	Low	Mid			Low	High	-	-	Low	Mid		
S5	Low	Mid	-	-	Low	Mid	-	-	Low	High	-	-	Low	Mid	-	-
S6	High	Mid			High	Mid	-	-	High	Low			High	Mid	-	-
S7	Mid	High	-	-	High	Mid			High	Low			High	Mid	-	-
S8	High	Mid	-	-	High	Mid			High	Low	-	-	High	Mid	-	-
S9	Low	Mid	-	-	Low	Mid			Low	High			Low	Mid	-	-
S10	Mid	High	-	-	Mid	High			High	Low	-	-	Mid	High		
S11	Mid	High	-	-	High	Mid			High	Low	-	-	High	Mid	-	-
S12	Mid	High			High	Mid	-	-	High	Low	-	-	High	Mid	-	-

The overall results across all manufacturers, considering only > 0.05 differences in SV 3D-VA, revealed that the SimVis prescription was better or equal than FG in 83% (10/12) of cases in terms real 3D-VA, 66.67 % (8/12) for PSM and 66.67 % (8/12) for direct preference.

Spearman correlation coefficient showed a moderate correlation between 3D-VA metric measured with SimVis and with Real MCLs for FG steps ($\rho = 0.33$; $p = 0.02$) and the 3D-VA metric measured with Real MCLs and PSM measured also with Real MCLs ($\rho = 0.30$; $p=0.04$).

4.4 – Discussion

In this study, we included the FG of daily MCLs from 4 manufacturers to be simulated using SimVis Gekko. We used clinical measurements obtained through these SimVis Gekko simulations as inputs for a new metric. This new metric was designed to evaluate whether alternative steps, not recommended by the FG for this subject, could potentially enhance visual performance for each subject. Lastly, we conducted a comprehensive set of clinical measurements that were assessed using real MCLs for both the step prescribed by FG step and suggested by SimVis Gekko using its new 3D-VA metric.

A total of 96 clinical simulations using SimVis Gekko have been performed, including the recommended FG step and other steps for 4 manufacturers in 12 subjects. The 3D-VA metrics

calculated with these simulations revealed that in the 39.58 % (27.08 % for differences higher than 0.05) of cases the initial FG steps are not the optimal option considering the subjects' distance preferences. This could be considered as the range of patients that would need to be reexamined in more than one session in a clinical routine trying other steps to find the optimal combination of MCLs. These results agree with Merchea et al. [124] findings, where the proper adaptation with the FG was achieved in 65.1 %, 33.7 % and 1.2 % of patients for 1, 2 and 3 combinations of MCLs, respectively.

Clinical measurements with real MCLs following the initial steps recommended by FG primarily revealed differences in behavior among addition designs. The group with mid-high addition exhibited a decrease in both far and intermediate distances on defocus curve, without any benefit at near distances. This observation was further confirmed also with a decrease VA at near real distance. This tendency can be considered normal, as the low addition group retains residual accommodation, and the low addition does not degrade the far distance image so much. In contrast, high addition designs introduce a higher level of blur degradation that impacts far distance and may be insufficient for good performance at very close distances. This trade-off has been seen in Simultaneous Vision designs across different studies [205] .

Similarly, CSF demonstrated poorer values at 6 and 12 cpd with mid-high additions compared to low addition, particularly under mesopic conditions. This can be attributed to a decrease in the contrast in retinal images [206], which increases with the addition of the design and is amplified under mesopic conditions. These conditions, which lead to an increase in pupil size, enhance the multifocal behavior and reduce the contrast. However, among all manufacturers, MyDay and Dailies Total1 designs exhibited the smallest changes between low and mid-high addition.

Comparing the clinical results obtained with real MCLs prescribed by the initial FG step and SimVis Gekko, there were similar visual performance for the majority of the variables. Differences in visual function variables might be expected due to SimVis Gekko's prescription shift towards higher or lower additions, but the smaller sample size could potentially minimize this effect. Nevertheless, 1-Day Acuvue Moist exhibited better VA with MCLs prescribed by SimVis at near real distance (Figure 4.5 D), without a significant decrease in far distance, and better result in NVAQ questionnaire. It makes sense because the SimVis Gekko prescriptions changed towards superior additions in all the cases of this manufacturer, obtaining better results in variables related to near distances and without degradation at far distance, indicating that the compromise is accepted.

The SimVis prescriptions for all manufacturers also exhibited better results of NVAQ questionnaire, indicating that these prescriptions produced more comfort and independence for near activities.

The calculated metrics (3D-VA and PSM) based on clinical measurements obtained with MCLs and direct preference consistently showed agreement in determining which

prescription method yielded better results. These methods were very similar to each other. We analyzed trends to identify which method performed better across all cases and considering differences greater than 0.05 in 3D-VA SV to test the resolution of this metric.

Analyzing the metrics and direct preferences, it can be stated that Dailies Total 1 and 1-Day Acuvue Moist exhibited very high preference (or equity) percentages for lenses prescribed by SimVis, with ranges of 100 and 60-80 %, respectively, even including small differences in the 3D-VA metric. In contrast, MyDay and Biotrue ONEday showed poorer results, which improve when we analyze differences greater than 0.05 in 3D-VA between steps, reaching ranges of 60-100 % and 50 %, respectively, for different metrics.

Spearman correlations indicate a moderate correlation between 3D-VA obtained with SimVis and Real CL for the steps of the FG (which have a larger sample size). Although there is a quantitative difference between them, they exhibit a trend that can be used to decide preferences between steps. Additionally, it also appears to be a moderate correlation between PSM and 3D-VA metrics for the FG steps using real MCLs, suggesting the possibility of using perceptual scores at different distances as a decision method with SimVis, similar to 3DVA, with a more perceptual implication.

Although the final goal is to enhance the adaptation for each patient, we have analyzed the preferences based on various metrics per manufacturer and overall. However, a limitation of this study is the small sample size for each subgroup of each manufacturer (with FG and SV steps), which prevents us from observing clearer trends in clinical outcomes with real MCLs. Additionally, it would be ideal to separately analyze cases where SimVis recommends an addition higher or smaller than FG to better understand it and improve the metric.

4.5 – Conclusion

In summary, simulations of daily MCLs from 4 different manufacturers, considering various additions, have been integrated in SimVis Gekko and evaluated in a clinical research clinical setting.

By incorporating SimVis Gekko, including all FG steps and using a novel metric that has margin for improvement, evaluating more subjects, we could potentially increase the percentage of satisfied MCLs wearers from 72.92% to a minimum of 91.67 %. This improvement has the potential to enhance the adoption of these types of CLs among the presbyopic population and elevate their visual performance.

While our research environment explored its applicability, individual optometrists may discover its applications in their clinical practice, adapting the process collaboratively with their patients.

Chapter 5

Evaluating visual function tests through SimVis Gekko and Multifocal Lens Analyzer App synergies

In this chapter, we describe the development a new synergy between a visual function tests App (Multifocal Lens Analyzer, MLA) based on adaptive method and SimVis Gekko to perform defocus curves (introducing optical defocus with the optotunable lenses) of Visual Acuity and Contrast Sensitivity in fast and accurate manner. This synergy combination was compared with the use of MLA with trial frame and trial lenses in presbyopic subjects.

This work is the result of a cooperative collaboration among various institutions: Instituto de Optica Daza de Valdés (CSIC), 2EyesVision SL and Qvision.

The author of this thesis (1) designed the study and conceptualized the methodology (in collaboration with Xoana Barcala, Irene Sisó-Fuertes, Enrique Gambra, Carlos Dorronsoro), (2) calibrated the iPad Screen for different light conditions, (3) performed the preliminary measurements by himself, (4) supervised the clinical measurements, (5) collected and organized the results and (6) analyzed and discussed the results (in collaboration with all co-authors), (7) analyzed and discussed the results (in collaboration with all co-authors) and (8) performed the statistical analysis.

The development of a customized MLA App version to synchronize with SimVis Gekko was performed by Manuel Rodriguez-Vallejo. The development of a customized SimVis app version to link with MLA App was carried out by Yassine Marrakchi. The clinical measurements were conducted by Amal Zaytouny.

This work was presented as a poster contribution at the PhDay CSIC (2023) and OPTOM 24.

5.1 – Introduction

Visual function tests allow for the characterization of the visual system performance by considering various properties [207]. In the study of multifocality, the most important function tests are likely to be the VA, which provides a quantitative representation of vision, and CS, which offers a qualitative evaluation that VA cannot capture [208,209].

VA tests are probably the most measured outcome in the visual sciences field. Nevertheless, these VA tests have not incorporated new developments in their methodology, optotype design, or standardization process. In fact, different optotypes charts, based on letters or numbers, printed or retro-illuminated on digital screens, are used in the clinical routine without standard, at least outside of clinical trials. As a gold standard assessment in multifocality corrections [176,210,211], the estimated exploration time of a VA defocus curve using trial frames, with 11 steps (from +1.00 to -4.00 D), is approximately 18.7 minutes [136], being an unacceptable amount of time if you want to test different multifocal designs in a single session. The implementation of adaptive methods through a digital test, controlling light conditions and with randomized letters, can be a great solution for time reduction [136].

A similar problem exists with the clinical measurement of CS because the complete exam involving several spatial frequencies (CSF)[212] takes between 30 and 60 min [213]. This time is multiplied if we have the intention to measure the CSF for different distances (CSF defocus curve) or light conditions (photopic and mesopic conditions)[214]. Furthermore, the useful information in these types of designs is reduced to medium-high spatial frequencies since they are the most affected by multifocal defocus.

The development of digital tests to firstly reduce the time of exploration of these tests [185] and subsequently introduce them in the evaluation of multifocal performance through defocus curves [136], has been the objective of a group of researchers with consecution of MLA app (Qvision, Spain). The MLA app uses adaptive methods to measure visual test function with a considerable reduction of time but maintaining the use of trial frame and its associated disadvantages. Other research groups have explored the use of an electronic trial frame to change refractive errors rapidly, but with other purposes [215].

SimVis Gekko has demonstrated its capability to simulate multifocal corrections using optotunable lenses [156,195], a new optical component having demonstrated versatility and speed [216], which positions the instrument as a potential tool for assessing visual function. Furthermore, the ability to simulate multifocal corrections and evaluate their visual performance in an optimized manner could offer several benefits to eye care practitioners.

For this reason, the main aim of this feasibility study is to demonstrate an initial approach of combining SimVis Gekko and MLA app to evaluate visual function to test through defocus curves in presbyopic subjects. This first approach will not be considered performing any multifocal simulation with the SimVis Gekko. We will show that this combination of novel techniques is not only viable but also presents several advantages compared to the standard methods used in clinical practice [217,218].

5.2– Methods

5.2.1– Subjects

Five subjects with presbyopia participated in this feasibility study. The subjects' average age was 52.4 ± 6.11 years. Inclusion criteria required at least 1.50 D of addition), a refractive error between +5.00 D and -6.00 D, less than 3 D of astigmatism and an interocular refractive error difference lower than 2 D. Conversely, the exclusion criteria encompassed the presence of ocular pathologies in the anterior and posterior pole, amblyopia or other binocular disorders and a history of ocular surgery.

Related general and ocular information about the subjects included in this study is collected in Table 5.1:

Table 5.1. Data related to age, gender and ocular parameters, including refractive error (Sphere, Cylinder and Axis), binocular best corrected distance visual acuity (BCDVA), addition and pupil diameter at 85 cd/m²*. (measured with the optotype screen as a light source at that luminance, with the rest of the room in darkness).*

Subject	Age (y)	Gender	Refractive Error (D, D, deg)	BCDVA (logMAR)	Addition (D)	Pupil diameter (mm)
S#1	54	M	OD: -0.50 – 0.50 x 130 OS: +0.25 – 0.25 x 90	-0.10	+2.00	OD: 4.50 OS: 4.50
S#2	46	F	OD: +3.00 OS: +4.75 – 1.00 x 60	-0.10	+2.00	OD: 4.10 OS: 4.60
S#3	54	M	OD: +1.25 OS: +2.25 – 0.50 x 180	-0.10	+2.00	OD: 4.70 OS: 4.80
S#4	47	F	OD: -2.75 x 95 OS: -2.75 x 90	-0.10	+1.50	OD: 6.20 OS: 6.40
S#5	61	F	OD: – 0.50 x 90 OS: -0.25 – 0.50 x 160	-0.10	+2.50	OD: 5.20 OS: 5.80

The research protocol of this study, which was in compliance with ethical standards, received approval from the Ethics Committee of the "Consejo Superior de Investigaciones Cientificas (CSIC)". Before being enrolled in, all volunteers were informed of the goals of the study and gave their informed consent.

5.2.2– Multifocal Lens Analyzer

The Multifocal Lens Analyzer App (MLA) (previously described in Section 2.7.4) was employed in this study to display optotypes in the screen of an iPad and using its adaptive psychophysical method to save time in visual function assessments. This adaptive method used 5 reversals to determine thresholds.

One of the methods employed in this study was the use of the MLA with a conventional trial frame and physical trial lenses to change the virtual vergence of optotypes at each defocus curve step. The MLA control and subject responses records are provided by an additional MLA app (MLA remote control) running on a mobile phone.

5.2.3– SimVis Gekko visual simulator

The binocular SimVis Gekko visual simulator, which has been detailed in previous sections, was utilized in this study as one method to change the defocus value quickly and automatically, eliminating the need of positive and negative trial lenses at each step of the defocus curve, which streamlines the process.

An additional -4.00 D optical power was incorporated into each trial lens holder of SimVis Gekko. This was done to extend the negative range of optical powers introduced by optotunable lenses. Taking into account the extra -4.00 D optical power, the refractive error of each subject was introduced into the trial lenses holders for each eye, applying SimVis Gekko distometry to the final amount.

A custom application specifically designed for this study was developed. This application was synchronized with the MLA application (replicating MLA remote controller) to record the subject responses and send the appropriate optical power to the optotunable lenses for each defocus curve step.

5.2.4– Measurements procedure

The visual function tests (VA and CS) were assessed with the MLA App using two different methods for introducing the defocus optical power: (1) SimVis Gekko and (2) Trial Frame with physical trial lenses.

The iPad with the MLA app was fixed using a tripod at 4 m from the examination seat. MLA was used to measure VA and CS monofocal defocus curves from +1.00 D to -4.00 D in 0.50 D steps, in presbyopes without multifocal elements. Both VA and CS utilized Sloan optotypes (logMAR) with crowding effect. CS test employed a VA task with a fixed size of 0.3 logMAR (corresponding to a high spatial frequency of approximately 20 cpd) and contrast variations [136].

Both the sequence of evaluation method, and the visual function test within each method, were randomized for each subject. The full measurement duration and a set with satisfaction questions, related to each method, were collected in the unique evaluation session. The evaluation scheme followed in the session is represented in Fig. 5.1.

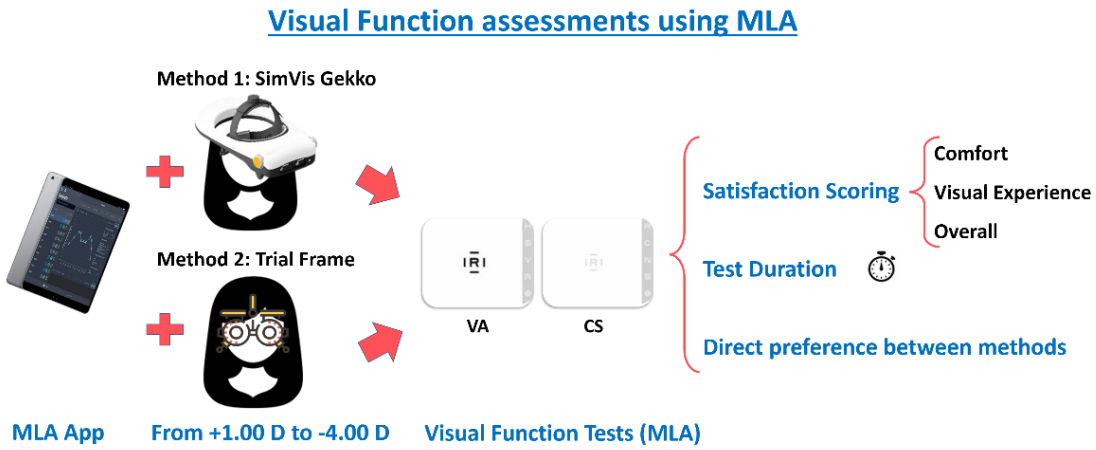

Figure *5.1*. *Flowchart scheme of evaluation measurements.* *The only difference is the method used to induce optical defocus: SimVis Gekko (upper pathway) and trial frame (bottom pathway)*

Preparation:

A standard optometric exploration was carried out prior to the study measurements in order to determine if the inclusion and exclusion criteria were met. The optometric exam included monocular subjective refraction with both biocular and binocular refinement, the determination of near addition amount, slit lamp exploration, stereopsis and measurement of pupil diameter size at 85 cd/m^2.

MLA tests:

Visual tests were assessed using each method, considering the randomized orders. Different brightness conditions protocols were implemented in the iPad MLA App for each method, following previous gamma calibrations. The trial frame protocol was set at 85 cd/m^2 while SimVis Gekko protocol was set at a higher luminance to compensate for the internal transmission loses.

Test duration

The duration time in each visual function test measured with each method was recorded using a chronometer without the subject's knowledge, for later analysis.

Satisfaction scoring

At the end of each method (for both VA and CS tests), the subjects were asked to score their satisfaction regarding three features: Comfort, Visual Experience and Overall. The question was: *How satisfied are you in terms of "Comfort"/ "Visual Experience"/ "Overall" with this method of evaluation?*

The satisfaction score was assessed on a scale from 0 (very unsatisfied) to 10 (very satisfied) in steps of 1, for the responses to all questions.

Direct preference

After the entire evaluation session, subjects were asked about their preferred method for visual function assessments: SimVis Gekko or Trial Frame.

5.2.5– Statistical analysis

Three different metrics were used to compare the visual function tests using MLA with (1) SimVis Gekko and (2) trial frame (with trial lenses) using a dedicated Matlab script and IBM SPSS Statistics Version 28 (IBM Corp, USA). These metrics included: partial correlation ($r_{xy,z}$), where the MLA + SimVis Gekko tests (VA and CS) were defined as x, MLA + trial frame as y, and the defocus value as z; RMSE to quantify the differences between the two methods across the entire defocus curves and the Wilcoxon signed-rank test to analyze the differences in each visual function test between methods at each defocus value.

Both satisfaction scoring and time consumed using each method (MLA + SimVis Gekko or MLA + Trial Frame) were compared. The time consumed was compared for each visual function test. These comparisons were performed using the Wilcoxon signed-rank test with IBM SPSS Statistics Version 28. The statistical significance level was set at $p<0.05$.

5.3– Results

5.3.1– Visual Function Tests

The results of defocus curves for visual function tests across subjects, using MLA and each method (SimVis Gekko and trial frame), are represented in Fig. 5.2 for both Visual Acuity (A) and Contrast Sensitivity (B).

The measurements obtained with SimVis Gekko method (red line) and trial frame method (blue line) show a good agreement, with $r_{xy,z}$ values of 0.99 and 0.97 for VA and CS, respectively.

On the other hand, the RMSE metric revealed an error of 0.14 logMAR and logU between the defocus curves of SimVis Gekko and Trial Frame for VA and CS, respectively.

However, VA and CS visual function tests demonstrated statistical differences between methods at specific defocus curve values. The VA test exhibited better values using the SimVis method at the extreme defocus curve values of +1.00, -3.00, -3.50 and -4.00 D (p-value <0.05). The CS test also showed statistically significant better values with SimVis Gekko, but only at the positive defocus value: +1.00 and +0.50 D.

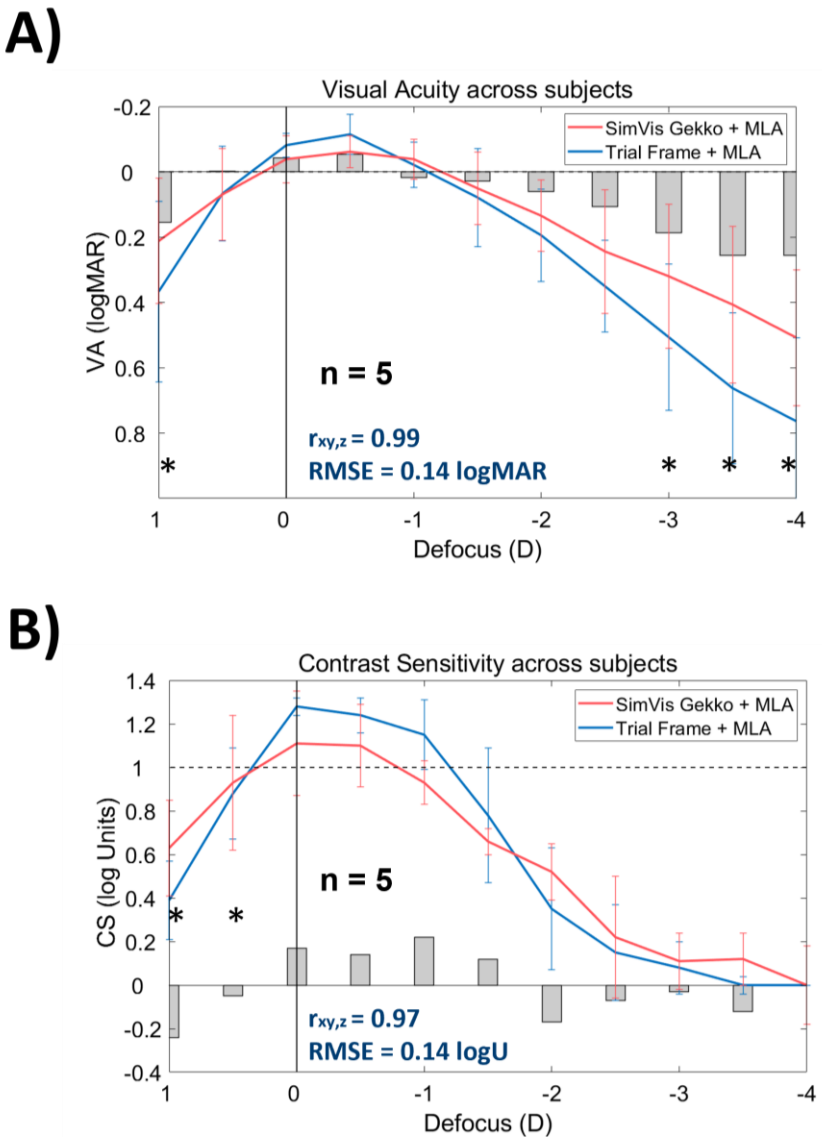

Figure *5.2*. *Defocus Curves of VA (A) and CS (B) obtained with MLA and SimVis Gekko (represented by red line) and trial frame (represented by blue line) (n = 5).* *Each point of defocus curves represents the average across subject with the standard deviation. The gray bars exhibit the difference among methods at this defocus step. The values of* $r_{xy,z}$ *and RMSE are set at each graph. The * symbols represent defocus steps where were significant statistical differences between methods for both VA and CS tests (Wilcoxon signed-rank test).*

5.3.2– Test duration

The average time using MLA and each method are depicted in Fig 5.3 for VA and CS tests. The combination of MLA and SimVis Gekko lasted an average of 7.61 ± 2.20 min and 13.03 ± 5.80 min, while MLA and trial frame lasted 11.47 ± 5.32 min and 15.21 ± 3.69 min for VA and CS tests, respectively. The Wilcoxon tests only revealed a difference statistically significant between the time of evaluation of VA among methods (p=0.043), but not for the evaluation of CS.

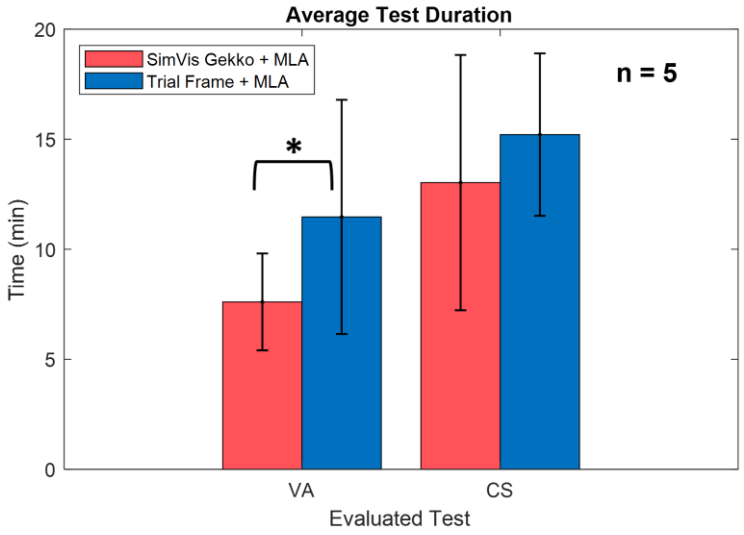

Figure *5.3. Average consumed time using SimVis Gekko (red bars) and trial frame (blue bars) in the evaluation of VA (left group) and CS (right group) (n = 5).* *Standard deviation is represented in each bar. Statistically significant differences are highlighted with an asterisk symbol.*

5.3.3– Satisfaction scoring

Figure 5.4 collects the average satisfaction scores across subjects using SimVis Gekko (red bars) and trial frame (blue bars) for Comfort (7.20 ± 0.84 vs 5.80 ± 0.84), Visual Experience (6.00 ± 1.41 vs 5.60 ± 0.89) and Overall (7.40 ± 1.67 vs 5.80 ± 0.84). SimVis Gekko showed better scores in the three features, but there were differences statistically significant among methods for none of them (p = 0.10, p = 0.71 and p = 0.14).

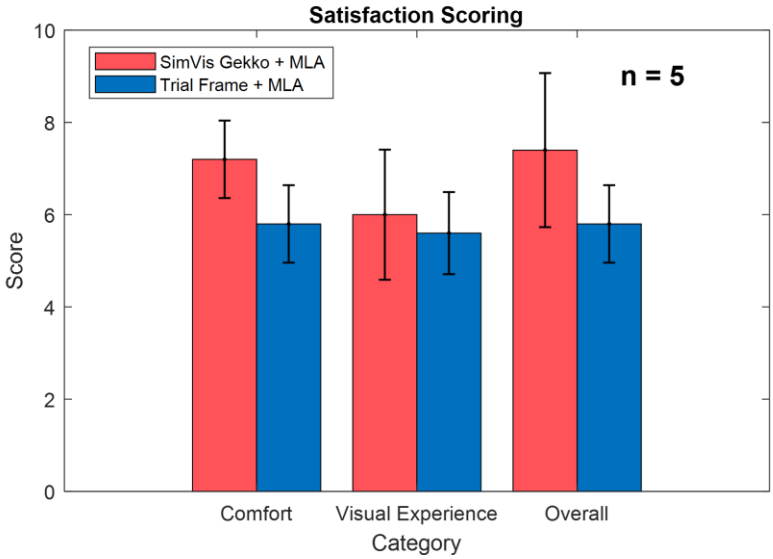

Figure *5.4. Average satisfaction scores using SimVis Gekko (red bars) and trial frame (blue bars) in the evaluation of Visual function tests for Comfort (left group), Visual Experience (central group) and Overall (right group) features (n = 5).* *Standard deviation is represented in each bar.*

5.3.4– Direct preference

Four out of five subjects preferred the combination of MLA and SimVis Gekko as evaluation method of visual function tests.

5.4– Discussion

In this study, we assessed VA and CS defocus curves using MLA App and two different methods to change the optotypes virtual distances. These methods were the standard method (with trial frame) and SimVis Gekko and were tested in five presbyopic subjects. The main purpose of this feasibility study was to demonstrate that SimVis Gekko enables to measure defocus curves of several visual function tests, reducing the exploration time and yields results comparable in accuracy to the standard method of trial frame.

Despite the introduction of new more standardized visual function tests and the application of adaptive psychophysical methods, the MLA app is still dependent on a trial frame to measure defocus curves. The traditional trial frame presents several disadvantages when clinicians want to measure defocus curves over an extended period for different function tests and types of multifocal elements. These disadvantages are primarily related to the need to change trial lenses at each defocus curve step, the time-consuming nature of this action and the potential issues with the stability of the axis of the astigmatism lenses during the test. Furthermore, if the patient has spherocylindrical prescription, the combination of three trial lenses can negatively impact the visual experience and increase weight over a significant period.

To address these issues, SimVis Gekko is here introduced as a method to vary optical power. This method showed results comparable to the trial frame for both evaluated visual function tests (Figure 5.2). The VA test revealed similar defocus curve shapes using both the Trial Frame and SimVis Gekko with a partial correlation and RMSE of 0.99 and 0.14 logMAR, respectively. The main statistical differences between methods were found in the high defocus interval from -3.00 to -4.00 D and the positive defocus value of +1.00 D, with the maximum difference (0.26 logMAR) at -3.00 D and -3.50 D with better VA for SimVis Gekko (Figure 5.2 A). These differences can be attributed to the increased variability at high defocus amounts [203] (associated with a high standard deviation) and a possible enhanced depth of focus produced by the fixed pupil entrance of SimVis Gekko [210], being smaller than the pupil size of all subjects.

Similarly, the CS defocus curves also showed good agreement using both methods (shown in Figure 5.2 B), with a partial correlation of 0.97 and a RMSE of 0.14 log Units. The differences among methods revealed a trend shift, with higher values of CS with the trial frame from 0.00 to -1.50 D, changing to slightly superior values of CS using SimVis Gekko for the intervals from +1.00 to +0.50 D and -2.00 to -3.50 D. The maximum average difference

was 0.22 log Units for -1.00 D defocus step, but only the positive interval (+1.00 to +0.50 D) exhibited statistical differences. The described differences can also be attributed to the depth of focus provided by the fixed pupil of SimVis Gekko (+1.00 to +0.50 D and -2.00 to -3.50 D), and the varying light condition protocols that didn't fully compensate for contrast loss of SimVis Gekko, compared to trial frame, at the interval from 0.00 to - 1.50 D.

In terms of test duration, the use of SimVis Gekko with the MLA app resulted in a reduction of exploration time for both visual function tests: VA and CS (Figure 5.3). The average time saved with the SimVis Gekko, compared to the trial frame, was 3.86 min (SV: 7.61 min; TF: 11.47 min) and 2.18 min (SV: 13.03 min; TF: 15.21 min) for VA and CS, respectively. Nevertheless, statistically significant differences were only found in the reduction of time for VA defocus curves ($p<0.05$). The CS tests showed higher exploration times than VA for both methods, likely due to the increased difficulty of recognizing low contrast letters, which increasing the subject's time and repeatability variability [214].

The average satisfaction scoring revealed that SimVis Gekko outperformed in all features (depicted in Figure 5.4). Notably, there were higher differences for comfort (1.40 score) and overall satisfaction (1.60 score), although these differences were not statistically significant, with p-values of 0.10 and 0.14, respectively. The overall satisfaction scoring was highly correlated with the direct preference among methods, with four out of five subjects selecting SimVis Gekko as their preferred choice.

Upon analyzing the results, the use of SimVis Gekko with the MLA App demonstrated a reduction of one-third of the time compared with the trial frame, providing clear benefits. A modest reduction was observed for the CS test. Moreover, the comparison of results for VA and CS in this feasibility study revealed comparable behaviors and similar shapes, with minor differences in selected intervals in presbyopic patients without multifocal simulations. Despite these differences, the combination of SimVis Gekko and the MLA App could serve as useful tool to evaluate visual performance and compare different multifocal simulations with the same device. For this purpose, future studies will need to evaluate this combination by comparing different multifocal designs (IOLs and MCLs) to validate the method with a larger sample.

5.5 – Conclusion

This feasibility study introduces the potential use of SimVis Gekko in conjunction with the MLA App as an effective method to perform defocus curves of different visual function tests (VA and CS), significantly reducing time while maintaining or improving satisfaction rates. The ability to evaluate defocus curves and compare visual performance while SimVis Gekko is simulating multifocal elements could improve the fitting process of MCLs.

Chapter 6

Development and calibration of a programmable astigmatism correction system based on motorized Stokes Lenses

In this chapter, we developed and calibrated a new astigmatism correction system from scratch. The automatic and programmable system was based on Stokes Lenses moving by servomotors with the objective of being implemented in SimVis Gekko modules. The entire chapter reports in detail the working principle of the system and the calibration carried out using a lensmeter for the Stokes Lens System and a customized Optical Quality Bench for the combination of Stokes Lens System and SimVis Gekko module.

The author of this thesis (1) performed the literature search of Stokes Lens principle, (2) designed the methodology (in collaboration with Enrique Gambra), (3) ensembled the Stokes Lens systems , (4) linked the servomotors with the Arduino microcontroller, (5) programmed the Stokes Lens control code in Matlab (6) conducted the calibration with lensmeter, (7) acquired the images from the Optical Quality Bench (in collaboration with Maria Pilar Urizar), (8) collected all data and (9) analyzed and discussed the calibration results (in collaboration with Enrique Gambra and Maria Pilar Urizar).

The custom image processing algorithm to characterize the axis and magnitude of the astigmatism induced by the Stokes Lens implemented in a SimVis Gekko module using the Optical Quality Bench was developed by Maria Pilar Urizar and Gonzalo Guerrero. The mechanical design of Stokes Lens prototype was conducted by Jose Ramon Alonso. Lastly, the migration of the Stokes Lens control code from Matlab to Arduino Firmware and the compensation of sphere with the optotunable lens was carried out by Yassine Marrakchi.

6.1 – Introduction

As mentioned before, visual function tests are pivotal measurements in the study of multifocality, and specifically in the MCLs due to the number of designs that must be checked to find the most proper one. Moreover, in many patients these designs include multifocal toric designs, which may increase the number of factors to be taken into account in the adaptation.

The effect of uncorrected astigmatism has been previously studied in adaptation aftereffects [219] and cataract surgery with an undesired outcome [220], but this has not yet been studied, to our knowledge, for visual performance using multifocal toric CLs. However, the impact of different increments of astigmatism axis rotation on multifocality and what is the limit for not providing an uncomfortable visual performance have not been widely studied yet. This analysis could be the key to a deeper understanding of the relation between multifocality and astigmatism.

Different developments and strategies have been proposed to develop an optical system capable of continuously varying the astigmatism correction. Some of these systems are based on the Alvarez [221–223] or Stokes lens [224,225] principles, the latter being the most widely used option for more than 100 years due to its versatility. The Stokes lens principle achieves a variable magnitude of astigmatism by using two pure cylindrical lenses of equal power and opposite sign. These lenses start with their astigmatism axes at 180 deg and rotate the same angle but in opposite direction to induce different astigmatism magnitudes. The use of this principle has been extensively explored by different authors for different applications such as: astigmatism correction at optical devices [226,227], astigmatism measurements using it in conjunction with a manual focimeter [228] and clinical applications as subjective refraction tool implemented in a manual Risley prism holder [229,230].

On the other hand, cylindrical optotunable lenses have been developed as an investigational product [231,232]. However, the fact they are not a commercial component and the limited speed they present prevent us from using them for the multifocal correction simulations in the SimVis Gekko system.

In this chapter we analyze the combination of a Stokes lens system for astigmatism correction with the optotunable lens of SimVis Gekko. From one side the combination of the Stokes lens system with the MLA development could significantly improve the visual performance evaluation and accelerate the defocus curve process previously described in in Chapter 5. On the other side, in a research environment, this combination could also be employed to analyze the implication of uncorrected or not totally compensated astigmatism in multifocality rejection. In terms of refractive error correction, the Stokes lens system compensates astigmatism, while the spherical error of the patient and the residual sphere of the lens is corrected by the optotunable lens. To achieve that, the optotunable lens must have sufficient dioptric range to simulate a multifocal pattern and induce the request spherical offset at the same time.

For this reason, the main purposes of this study were: (1) to develop an automated and programmable astigmatism correction system based on the Stokes lens principle with the possibility to incorporate it into the SimVis Gekko, (2) to characterize its optical performance, accuracy and reliability using the gold standard method (lensmeter); and (3) to develop an alternative method to measure the astigmatism axis of each Stokes lens as well as the whole system for calibration purposes of the combined optical system (Stokes lens + SimVis Gekko optical module).

6.2– Methods

6.2.1– Stokes Lens system

Stokes Lens system design:

A programmable astigmatism correction system was developed, based on the Stokes Lens mechanism (Fig.6.1 A and B show the schematic mechanical drawing and experimental prototype respectively. An exploded view of the system is depicted in Figure 6.1 C for clarification.

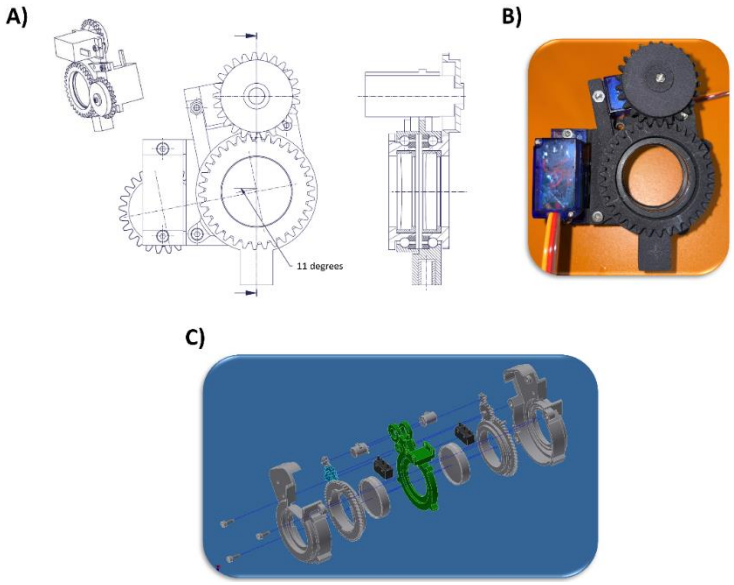

Figure 6.1. Automated Stokes Lens System. *A) Sketch of the mechanical design. B) Image of the assembled prototype used in this study and C) Exploded view of each component that comprised the Stokes lens system, except for the servomotors.*

The core of the system consists of two symmetric sintered pieces, each one containing a pure cylindrical lens with the same optical power but opposite sign: ± 2.50 D (Ø1" LJ1363RM-A and LK1487RM-A, Thorlabs, Germany). Each lens was centered and fixed (after marking its astigmatism axis) in their compartment orientated at 180 deg. The lens compartments featured a gear wheel with 34 teeth) which allowed to independently rotate each lens of 180 deg when combined with the wheel of a servo motor (DM-S0090D, Dooman RC Hooby, China) with 25 teeth. The servo motors were positioned on the superior and lateral sides of the system core.

Stokes Lens principle:

The astigmatism correction system was designed based on the Stokes Lens principle. The Stokes Lens principle facilitates the generation of variable and continuous astigmatism in a cross-cylinder format. The maximum astigmatism achievable is twice the value of each individual cylindrical lens, thereby inducing a spherical component which in this case is +2.50 Sph - 5.00 D Cyl. Different magnitudes of astigmatism are generated by rotating each cylindrical lens at the same relative angle (θ) but in opposite directions. This rotation starts from a parallel position at 180 deg (neutral position, where no astigmatism is induced due to the optical power cancellation between lenses) to a relative angle of 45 deg, which generates the maximum astigmatism and displaces the axis of astigmatism of the two lenses perpendicularly to each other.

The spherocylindrical notation (S, C, α; Sphere, Cylinder and axis), widely used in the clinical field, can be expressed in vectorial notation using three independent variables between them (M, J0, J45; Spherical Equivalent, Vertical Astigmatism and Oblique Astigmatism) [233] (Equations 1):

$$M = S + C/2 \tag{1.1}$$

$$J0 = -C/2(\cos 2 \propto) \tag{1.2}$$

$$J45 = -C/2(sin\ 2 \propto) \tag{1.3}$$

This notation enables us to characterize the Stokes Lens as a system constituted by two independent lenses. The final value of each variable in the system is the cumulative sum of the two lenses (L_1 and L_2). The M and J0 variables of the system are cancelled between lenses due to their opposing signs, being J45 the unique contribution to the astigmatism magnitude. The contribution of J45 is composed of two components: $J45_{L1}$ and $J45_{L2}$.

Using the previously presented notation and Equation 2, we can solve the relative angle θ needed to induce the desired total astigmatism (TA), in cylinder notation, and obtain the Equation 3, being C the cylinder power of each lens (with positive sign):

$$TA = -2\sqrt{(J45L1 + J45L2)^2} \tag{2}$$

$$\theta = \frac{\sin^{-1}\left(\frac{TA}{-2 * C}\right)}{2} \tag{3}$$

Knowing the angle θ for each desired astigmatism diopters, we can deduce the position of each lens (δ1 and δ2) to induce it at 45 deg, and the desired final axis (FA) with the final positions of each lens (δ1f and δ2f), following the Equations (4) and (5), respectively.

$$\delta 1 = 180 - \theta \quad (4.1)$$

$$\delta 2 = 0 + \theta \quad (4.2)$$

$$\delta 1f = \delta 1 + (FA - 45) \quad (5.1)$$

$$\delta 2f = \delta 2 + (FA - 45) \quad (5.2)$$

Astigmatism correction control:

Equations (3) and (4) enable to rapidly induce the desired astigmatism magnitude in our system by only programming the variation of the variables: θ and FA. For this purpose, we utilized a dedicated Arduino firmware, controlled by Matlab functions, to adjust the position of each servomotor. This adjustment moved each lens to its precise position, varying from the neutral position, depending on the required astigmatism.

The Matlab functions calculated the angular position of each servomotor, (sending different electrical pulses) taking into account the transfer relation (0.735) between the servo and the main piece wheels due to the different number of teeth. This approach enabled a range of movement of 198 deg. The servomotors were controlled with an electrical Pulse Width Modulation (PWM) signal, in such a way that the variable angular position of the lenses was controlled with the pulse range of the PWM signal. The pulse range was set between 0.5 ms to 2.5 ms, where 1.5 ms corresponds to the neutral position of each lens.

These functions used the input variables of the spherocylindrical notation (S, C, α) to send the appropriate pulses to the servomotors and positioned the lenses in the correct position for each astigmatism magnitude.

6.2.2– Lensmeter

The Nidek LM-500 lensmeter previously explained in detail in section 2.4.3, was used as gold standard method to measure spherocylindrical powers characterizing the Stokes Lens system. The lensmeter measurement protocol employed negative cylinder notation with a resolution of 0.12 D. The Stokes Lens system was positioned above the lensmeter's measurement component without contact and secured on a horizontally oriented optical post to streamline the measurement process.

6.2.3– Implementation of Stokes Lens system into SimVis Gekko modules.

Two Stokes Lens systems were integrated into SimVis Gekko optical modules, excluding the simulator chasing (as illustrated in Figure 6.2. The servomotors were connected to an Arduino microcontroller on the SimVis Gekko custom PCB (Printed Circuit Board) and controlled using the I2C (Inter-Integrated Circuit) protocol.

The entire binocular system was installed on the Optical Quality Bench for its characterization. This setup was used to evaluate the potential application of astigmatism correction with the left module of SimVis Gekko and the Stokes Lens system jointly. During these characterization measurements, the spherical power induced by the Stokes Lens system was directly compensated by the optotunable lens, resulting in the generation of pure cylindrical power.

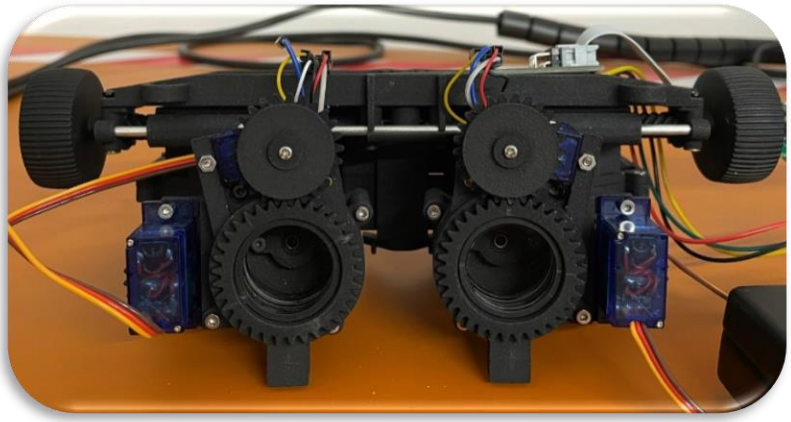

Figure 6.2. Stokes Lens systems ensembled into SimVis Gekko modules. *The implementation of Stokes lens systems to the SimVis Gekko modules was carried out using three screws. The servomotors were included in the SimVis Gekko electronics to allow their control.*

6.2.4– Optical Quality Bench setup

Optical Quality Bench setup:

An optical quality bench (OQB), available at 2EyesVision, was used to characterize the pure cylindrical astigmatism induced by the SimVis Gekko optical modules with the Stokes lens system attached to it. The OQB (shown in Fig. 6.3) allows to analyze the optical quality of SimVis Gekko head-mounted device when it is set at different static imaging configurations. The optical quality of the SimVis Gekko is obtained by analyzing the image acquired through the SimVis Gekko of a stimulus placed in front of it. The OQB allows to adapt the stimulus used depending on the parameter to be analyzed. In this case a small circular spot center in the field of view of the SimVis Gekko was used, in order to have a better resolution of the astigmatism optical power. The OQB consists of a stimuli visualization screen (see in Fig 6.3 A), a pair of cameras (CS165MU/M, Thorlabs) with adjustable focal fixed at infinity and located in the pupil exit plane of each SimVis Gekko module, and a holder to settle the SimVis Gekko optical modules (represented in Fig 6.3 B). The visualization screen was placed at 1 m

collimated by a pair of +1 D trial lenses placed in front of the pupil entrance of the SimVis optical modules.

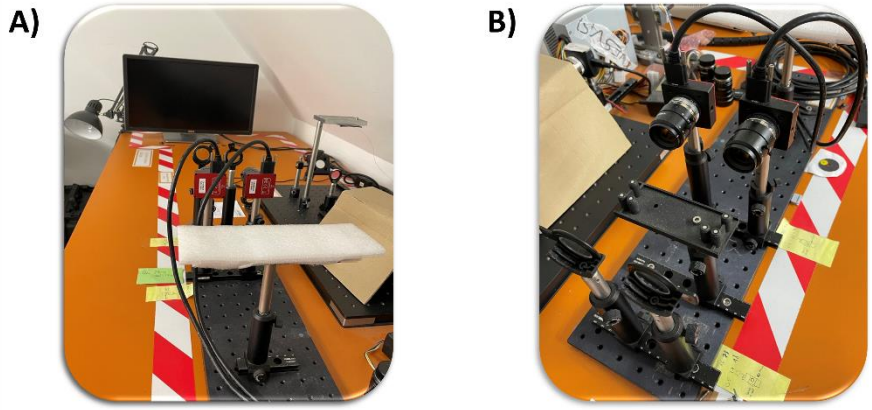

Figure 6.3. Optical Quality Bench setup: *Visualization Screen (A), cameras and holder to settle SimVis Gekko modules (B).*

The Thorlabs camera software was used to acquire images of a dot stimulus through SimVis Gekko and the astigmatism correction, generating different pure astigmatism magnitudes.

Image processing algorithm:

A dedicated image processing algorithm was developed using Matlab to characterize the magnitude of astigmatism induced by the SimVis Gekko optical modules with the Stokes Lens system at the OQB.

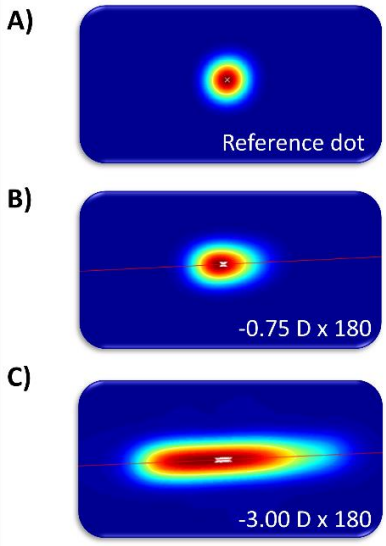

Figure 6.4. Images obtained through the application of the processing algorithm on the images acquired with the OQB, illustrating: *A) the reference dot without induced astigmatism obtained when the Stokes lens system was decoupled fom the SV binocular system, B) pure astigmatism of -0.75 D x 180 deg induced with the astigmatism system at the SV and C) pure astigmatism of - 3.00 D x 180 deg induced with the astigmatism system at the SV. The red solid line indicates the long axis of the ellipse, which corresponds to the astigmatism axis.*

The algorithm fits the imaged spot to an ellipse (see examples in Figure 6.4). The long axis of this fitted ellipse exhibited the axis of the induced astigmatism, while the ratio between the lengths of the long and short axis indicated the astigmatism magnitude. The fit to the ellipsoid was performed by applying an intensity threshold to the image and fitting the corresponding points of the image to an ellipsoid. The intensity threshold applied was varying within a range, thus obtaining a set of fitted ellipsoid for the same spot, allowing us to obtain the average of them and reduce the error. Moreover, to obtain a better resolution of the astigmatism measurement in the OQB a significantly small circular spot was used (only having a few pixels of radius), to increase the capability of image processing of the algorithm, a first step of image expansion was incorporated to the code.

6.2.5– Measurement procedure

The characterization measurements of the Stokes Lens system were conducted using the gold standard method (Lensmeter) and the Optical Quality Bench (OQB) developed by the company.

Lensmeter:

The lensmeter described, was used to characterize the Stokes Lens system by itself, and thus to validate it as a reliable and accurate method to implement in SimVis Gekko device. Figure 6.5 shows a picture where the Stokes Lens system from the left optical module of the SimVis Gekko was placed into the lensmeter.

Figure 6.5. Stokes lens System displaced into Lensmeter for its characterization. *The Stokes Lens system was positioned using a horizontally oriented optical post that was fixed into a rail to avoid any displacement.*

Once the Stokes Lens system was fixed with the neutralization of the astigmatism magnitude, different astigmatism axis and optical powers were induced through the Matlab function driving the astigmatism control system. Firstly, a fixed astigmatism optical power was fixed (-0.75 D and - 3.00 D) and the angle was varied in steps of 5 deg starting at 180 deg and decreasing until 0 deg. This measurement was repeated three times. Then, the astigmatism angle was fixed at two different positions (180 deg and 45 deg) and, at each of them, the astigmatism magnitude was varied in steps of 0.12 D starting from -5.00 D until 0 D. The steps were continuous without changing to the neutral position.

Optical Quality Bench setup:

The same methodology as the previous section was performed, only for astigmatism axis variations, using the OQB with the Stokes Lens system attached in the left SimVis Gekko optical module (represented in Figure 6.6 A and B). The induced astigmatism of -0.75 D and - 3.00 D was fixed, and the astigmatism axis was changed using the Matlab driving functions. An image was acquired using the camera in each astigmatism axis step and recorded for consequent processing.

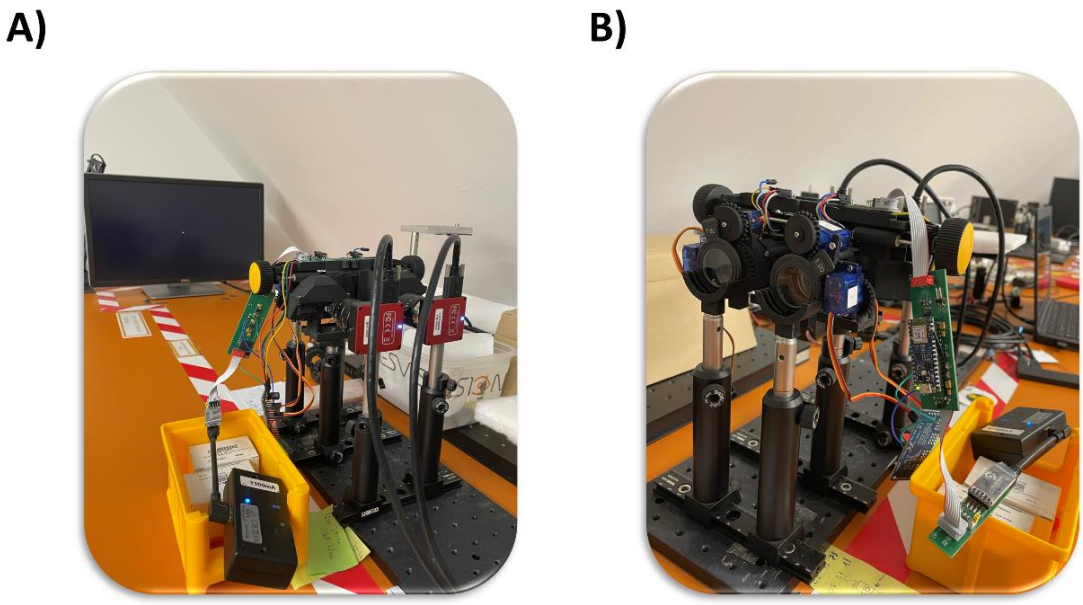

Figure 6.6. SimVis Gekko modules incorporating the Stokes Lens Systems into the Optical Quality Bench for astigmatism axis characterization: *A) Back view with the modules, cameras and the dot stimulus displayed on the screen; B) Front view with the modules, trial lenses to compensate the 1 m distance and cameras.*

These results were compared with the results from the lensmeter in order to validate the OQB and its capability to detect astigmatism axes.

6.3– Results

6.3.1– Stokes Lens system characterization with lensmeter

Astigmatism axis variation characterization

Figure 6.7 presents the results of the characterization of the Stokes Lens system with the lensmeter. This characterization is performed by varying the axis of astigmatism, for two fixed astigmatism magnitudes. These two fixed values of astigmatism are shown with blue lines (-0.75 D) and yellow lines (-3 D). The measured axis angle in comparison with the expected astigmatism axes are represented in Figure 6.7 A with the standard deviation for the three repetitions measured. Figure 6.7 B depicts the error at each angular position obtained as a function of the astigmatism axis.

An offset error (-2 deg) that would minimize the general deviation has been represented in red dashed line. The measured spherical and cylindrical optical power induced in each astigmatism axis position are shown in Figure 6.7 C with dashed and solid lines respectively.

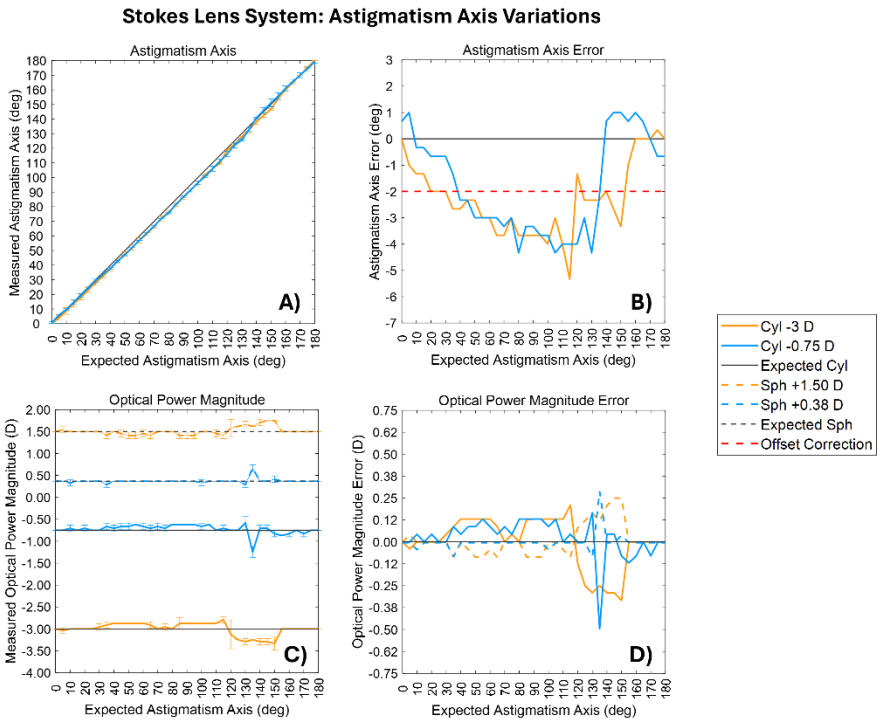

Figure 6.7. Measurements of the Stokes Lens system with Lensmeter under varied astigmatism axes for two specific astigmatism values: *A) Comparison of average measured (standard deviation) and expected astigmatism axis, B) Error between measured and expected astigmatism axis, C) Measured optical powers at each astigmatism axis degree and D) Error between measured and expected optical powers at each astigmatism axis. Referenced astigmatism values of - 0.75 D and - 3.00 D are shown by blue and yellow lines for cylinder (solid) and sphere (dashed). Expected values are indicated with black lines. An offset correction for astigmatism axis is represented by a red dashed line.*

Figure 6.7 D illustrated the errors of each magnitude as a function of the astigmatism axis. In all cases, the error was below 5 deg (axis) and 0.4 D (magnitude).

Optical power magnitude variation characterization

The characterization of the optical power variation for two fixed astigmatism axes of the Stokes Lens system with the lensmeter, is represented in Figure 6.8. The two fixed astigmatism axes are 180 deg and 45 deg, represented with blue and red lines respectively. Figure 6.8 A and C display the measured optical power with respect to the expected optical power for both sphere and astigmatism magnitudes. The corresponding errors are represented in Figure 6.8 B and D respectively.

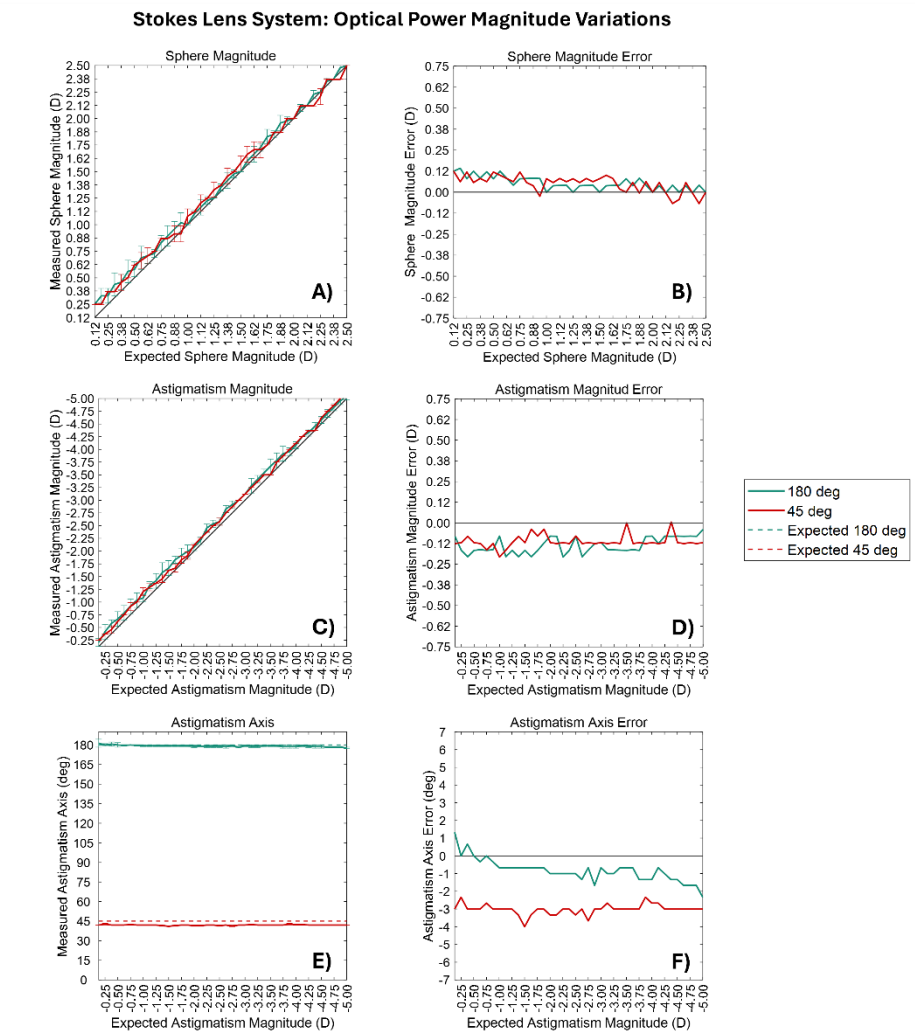

Figure 6.8. Measurements of the Stokes Lens system with Lensmeter under varied optical powers for two astigmatism axis values: *A) Comparison of average measured (standard deviation) and expected spherical powers, B) Error between measured and expected spheres, C) Comparison of average measured (standard deviation) and expected cylindrical powers, D) Error between measured and expected cylindrical powers, E) Measured astigmatism axes at each astigmatism magnitude and F) Error between measured and expected astigmatism axes at each astigmatism magnitude. Referenced astigmatism axis values of 180 deg and 45 deg are shown by green and red lines for cylinder. Expected values are indicated with dashed lines with the same astigmatism axis color.*

The measured astigmatism axis for each magnitude of astigmatism (solid lines) are represented in Figure 6.8 E comparing with the expected astigmatism axis (dashed lines) for 180 deg and 45 deg. The astigmatism axis error in each astigmatism magnitude is indicated in Figure 6.8F.

6.3.2– Stokes Lens system characterization with Optical Quality Bench

Astigmatism axis variations characterization

The results for astigmatism axis variations of the Stokes Lens system, obtained by comparing the two measurement methods (Lensmeter and Optical Quality Bench) are represented in Figure 6.9. Figure 6.9 A shows the measured astigmatism axis compared to the expected astigmatism axis for -0.75 D and -3 D measured by lensmeter, light blue and light orange lines, and OQB, dark blue and dark orange lines, respectively. A direct difference comparison of measured astigmatism axes between methods is represented in Figure 6.9 B for -0.75 D (gray lines) and -3 D (purple lines).

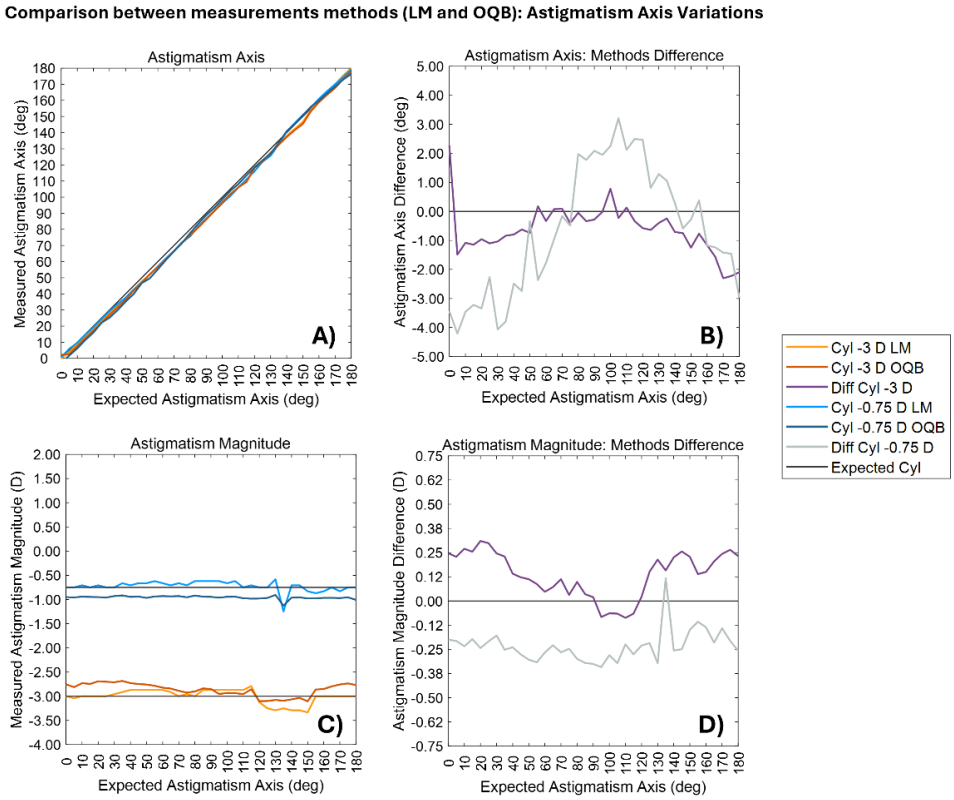

Figure 6.9. Comparative analysis of Lensmeter and Optical Quality Bench in measuring the Stokes Lens system under varied orientations for two specific astigmatism values: *A) Comparison of average measured and expected orientation for both methods, B) Orientation differences between methods at each expected orientation, C) Comparison of average measured and expected astigmatism magnitude for both methods, D) Astigmatism magnitude differences between methods at each expected orientation. Referenced values of - 0.75 D and - 3.00 D are shown by blue and yellow lines for lensmeter (light color) and OQB (dark color). Differences between methods are shown in purple and gray solid lines for -3.00 D and -0.75 D, respectively.*

The same representation is used in Fig 6.9 C and D to show the measured astigmatism magnitude for -0.75 D and -3 D for both methods, as well as the differences among them.

6.4– Discussion

An automated and programmable Stokes Lens system based on the Stokes lens principle was developed and characterized against the gold standard method and an alternative custom method developed by the company. The characterization made with these methods revealed a high accuracy and reliability of the approach for most of the measured conditions.

To our knowledge, this is the first time that an automated, fast and programmable Stokes lens system has been developed. A manual version or an adaptation using another element of clinical use, such as Risley prism mount, was employed for different measurements purposes by other researchers from University of Valencia. Our proposal is based on a custom mechanical assembly with two servomotors allowing quick changes in the angular position of each lens that can be easily programmed. The system not only shows very promising results, but also has a reduced size (which allows for the assembly of miniaturized systems), and a competitive cost. However, the selected servomotors showed some limitations.

When analyzing the validation of the Stokes Lens system for astigmatism axis variations using the lensmeter as gold standard, a similar behavior was observed for both fixed astigmatism magnitudes. Figure 6.7 B showed an average error higher than 2 degrees for the interval of 40-140 deg with the maximum magnitude at 115 deg (5.5 deg for -3.00 D). An offset of two deg could compensate and reduce this small systematic error. Similarly, the errors between the measured and expected powers values showed a general good agreement in sphere and cylinder. However, an exception was noted in the range of 120 – 150 deg with a maximum difference of -0.5 D (at 130 deg for the cylinder of -0.75 D). The peak at 130 deg, and nearby astigmatism axes, was attributed to one of the servos reaching its operational limit of a 2.5 ms PWM pulse. This resulted in a performance that deviated from expected. The utilization of servos with a higher range of degrees (>270 deg) would avoid situations close to the limit range. Another solution could be a characterization of the error of each servo on this range to compensate it. The average standard deviation of all astigmatism axes, across three measurements, showed a low variability: 1.01 and 1.17 deg for -0.75 and -3.00 D, respectively.

The error results for power magnitude variations measured by lensmeter revealed a similar behavior for the two fixed astigmatism axes (180 deg and 45 deg). The sphere error was less than 0.125 for all optical power magnitudes, while the astigmatism error was systematically situated between -0.125 and -0.20 D. The astigmatism axis errors for each optical power variation were constant with an average difference of 1 deg and 3 deg for the fixed astigmatism axis at 180 deg and 45 deg, respectively.

The development of an algorithm to evaluate the astigmatism axis of astigmatism using a custom-made optical quality bench (OQB) allowed to characterize one of the Stokes Lens systems implemented in a SimVis Gekko module, whose optotunable lens compensates for

the spherical power induced by the Stokes lens. The results of differences between methods for astigmatism axis variations showed small differences (Figure 6.9 B), with maximum differences of 2 deg and 4 deg for -3.00 D and -0.75 D, respectively. The trend was consistent, showing a negative difference between methods for most of astigmatism axes values at -3.00 D. However, the differences fluctuated between negative and positive values at -0.75 D. The differences in astigmatism magnitude between methods were less than 0.30 D for both astigmatism cylinders of -3.00 D and -0.75 D. The different trend was primarily negative for -3.00 D and positive for - 0.75 D. The OQB method produced comparable results in angles (error below 5 deg) and astigmatism magnitude (error below 0.35 D), inducing small offset in comparison with lensmeter. This achievement will be very useful for production and calibration tasks, enabling the assembling and calibration of the Stokes lens in the optical modules of the SimVis Gekko.

The Stokes Lens system that was developed exhibited maximum errors of 5 deg in astigmatism axis and -0.50 D in cylindrical power (an isolated case at 130 deg, corresponding to the extreme range of the servos), with 0.25 D being the second highest magnitude. These magnitudes represent the minimum clinically significant step used in routine clinical practices, such as with phoropters or trial frames with trial lenses for astigmatism axis and magnitude.

The implementation of the automated Stokes Lens system, equipped with servomotors that have a higher range of degrees, into SimVis Gekko, could improve the visual performance testing and open new research lines. However, validation in a clinical environment would be needed for this purpose.

6.5 – Conclusion

A system for correcting astigmatism, both automated and programmable, was developed based on the principle of the Stokes lens. This system was characterized using both the gold standard method and a custom method developed within the company. The results obtained from these characterization methods demonstrated the accuracy and reliability of this approach under most of the conditions tested.

6.6 – On-going and future work

Although it is outside the scope of this thesis, the Stokes lens system is already being used with the SimVis Gekko modules in measurements of visual perception of astigmatism for different magnitudes and axes.

In these on-going measurements Astigmatisms of ±0.5, ±1.5 and ±3 D were induced at 0, 30, 45, 90, 120, 135 and 180 deg (42 conditions in total) in one patient. The astigmatisms were induced with Stokes lenses through SimVis Gekko modules and programmed with MATLAB. The presented stimulus was a video sequence of natural images (explained in detail in Chapter 7) displayed on a TV. During the measurements, the observer had to make perceptual judgements of the image using Perceptual Scores, with 10 being the best and 0 the worst score, respectively. The measurements lasted less than 20 minutes.

In Fig. 6.10, the variation of the Perceptual Scores with the magnitude and axis of the induced astigmatism is observed. Thus, the Stokes lenses incorporated in the SimVis allow subjective measurements of patient's visual perception for different astigmatism magnitudes and axes.

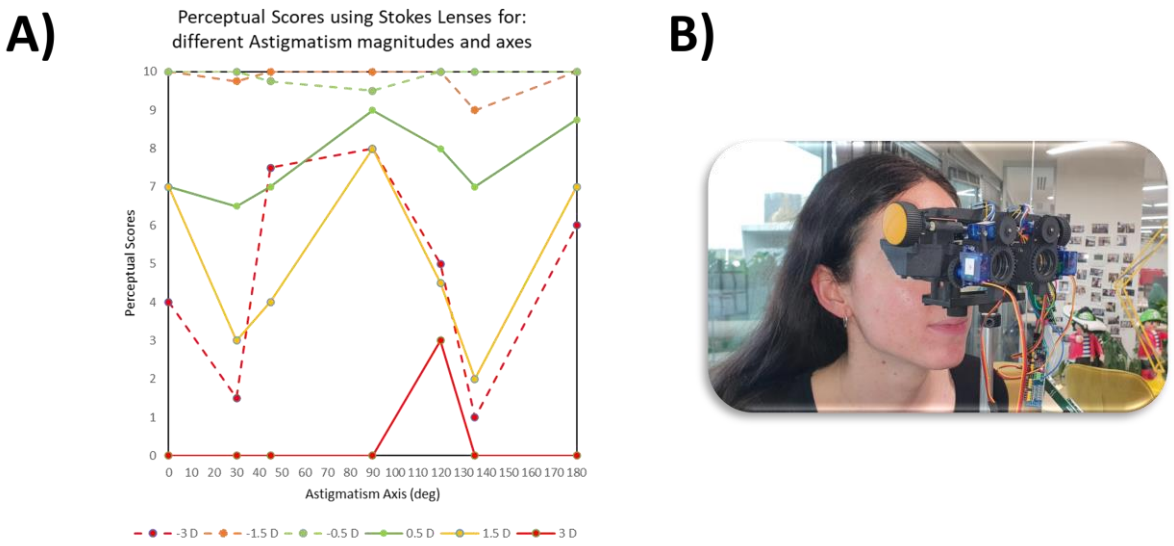

Figure 6.10. Ongoing clinical measurements using Stokes Lens System: *A) Perceptual Scores results in one patient for different astigmatism magnitudes and axes. B) Stokes Lens Systems implemented in SimVis Gekko modules for the clinical measurements.*

However, a larger sample and a greater number of repetitions per patient will be necessary to extract results from this ongoing study. In addition, it is intended to also study how the performance of the different multifocal designs would be affected when the axis of induced astigmatism presents a deviation with the axis of the subject's astigmatism.

Chapter 7

Perceived image quality of natural video sequences through simulated bifocal corrections: effect of energy balance and adaptation state

In this chapter, we studied the perceived image quality of natural video sequences of bifocal corrections under different adaptation conditions. Experiment 1 focused on the study of energy balance of bifocal corrections for different adaptation conditions based on: a previous adaptation state, type of transition (between the adaptation state and correction) and transition time. Experiment 2 studied the perceptual differences produced by energy balance and addition variations through a fixed adaptation condition.

The author of this thesis (1) designed the experiments (in collaboration with Carlos Dorronsoro, Enrique Gambra and Lucie Sawides) (2) programmed the Experiment codes in Matlab, (3) performed the preliminary measurements by himself, (4) explained and conducted the experiments with patients, (5) collected the data (6) analyzed and discussed the results (in collaboration with all the co-authors), (7) performed the statistical analysis (in collaboration with Laura Barrios) and (8) prepared the manuscript (in collaboration with Carlos Dorronsoro and Enrique Gambra).

The custom Matlab toolbox to introduce SimVis Gekko simulations using “smooth” transitions was developed by Yassine Marrakchi.

This work is based on the original manuscript by Esteban-Ibañez et al. “Perceived image quality of natural video sequences through simulated bifocal corrections: effect of energy balance and adaptation state” in preparation. The co-authors of this scientific contribution are Yassine Marrakchi, Lucie Sawides, Enrique Gambra and Carlos Dorronsoro.

Experiment 1 of this work was presented as a poster contribution at OPTICA Fall Vision Meeting 2022 (Rochester, USA), and as oral contribution at Visual and Physiological Optics (VPO) 2022 (Cambridge, United Kingdom) and OPTICA Vision and Color Summer Data Blast 2022 (Online). Experiment 2 of this work was presented as an oral contribution at VI International Symposium of Young Optometrists (SIYO) 2022 (Online).

7.1 – Introduction

Presbyopia, a common age-related vision impairment, can be corrected by applying different methods to address blurred vision at intermediate and near distances [8]. A substantial portion of these correction modalities operates based on the principle of simultaneous vision (SV), extensively explained in previous sections, offering users independence from traditional spectacles.

However, the neural mechanisms underlying the visual processing of different images, provided by these corrections, are still not perfectly understood. Research regarding this topic observed that there is an optimization of this visual processing, derived from a neural adaptation to SV corrections. Traditionally, this neural adaptation was attributed to a brain prioritization of sharp images, suppressing blurred ones to enhance the visual performance expected by the superimposition of images[98]. An alternative explanation for this phenomenon could be that it represents an adjustment to the contrast reduction resulting from the overlay of sharp and blurred images [234]. Nevertheless, there is a clear consensus that SV corrections entails a visual compromise, yielding an improvement in intermediate-near range vision at the expense of a degradation in far vision.

Previous studies using customized Adaptive Optics (AO) systems have revealed how adaptation mechanisms work in pure defocus[103], in astigmatic blur [219] or in high order aberrations[235,236]. The short-term adaptation to SV has been investigated also using an AO system by Radhakrishnan et al.[103], who compared short-term adaptation to SV with pure defocus effects using convolved images. Radhakrishnan et al. concluded that the SV degradation was smaller than pure defocus and subjects experienced adaptation aftereffects following these SV corrections. Also, long-term neuroadaptation has been explored in various studies for both multifocal intraocular lenses (MIOLs)[100] and multifocal contact lenses (MCLs)[101,102], but it involves more complex study designs. Furthermore, better visual performance, on average for most users, does not guarantee that it is the optimal solution for each individual. Therefore, the analysis of short-term adaptation to several options of types and designs of SV can provide useful information to predict the long-term visual performance of a combination of MIOLs or MCLs.

The recent emergence of visual simulators for clinical use, such as SimVis Gekko (2EyesVision SL, Spain), may facilitate the investigation of short-term adaptation in SV. SimVis Gekko's ability to accurately simulate a large number of binocular corrections (both generic and commercial) in a controlled real-world environment enables the execution of complex psychophysical experiments. Furthermore, the use of multifactorial metrics with SimVis Gekko [237], based on perceptual scores, to evaluate various multifocal corrections can provide a broader insight into the achievable performance for each correction, emphasizing better the differences among them than other types of metrics as visual acuity.

Regardless of the adaptation to SV, it is known that many patients do not have sufficient visual satisfaction with multifocality -or at least certain types of multifocality- when adapted

with MCLs (short-term) or M-IOLs (long-term). This effect also occurs when using SimVis Gekko in short-term periods. We wonder if some patients experience insufficient visual satisfaction because they are comparing their sharp vision with the vision given by SV corrections abruptly. Therefore, we are considering whether there is an optimal way to present these corrections to minimize such rejection in order to predict more accurately the potential satisfaction with multifocal solutions. Our hypothesis, based on a preliminary study, is that the smooth presentation of the correction coming from a previous blurred adaptation state may favor greater acceptance of multifocality [238].

This study aims to investigate diverse strategies for presenting multifocality, additionally exploring variations in energy balance and addition within bifocal corrections and assessing their impact on perceptual judgments. We explore how changes in energy balance influence subjects' perceptual judgments across various conditions, including transition type and time, and prior adaptation state. Subsequently, the relationship between energy balance and addition in bifocal corrections is examined, focusing on fixed conditions and evaluating the compromise between near and far vision benefits for each correction.

7.2 – Methods

In this study, two experiments were conducted in which the subjects saw through SimVis Gekko, a clinical visual simulator. SimVis Gekko simulated several bifocal and monofocal optical corrections, presented through different transitions, while the subjects watched a display showing a stimulus with a continuous video format.

Their perceptual response to the image quality provided by these different corrections after various perceptual adaptation processes was evaluated. In both experiments, the perceptual judgement was carried out using the same methodology, based on a previously shown reference scale.

Experiment 1 focused on exploring the impact of using various presentation strategies (different adaptation states, type of transitions and transition times) for bifocal corrections with different energy balances and one single addition (3 D).

Experiment 2 aimed to investigate specifically the interaction between the energy balance and the addition of bifocal corrections for a fixed presentation strategy. This section describes in detail the evaluated conditions for each experiment.

7.2.1– Subjects

Twelve subjects took part in this study: 10 of them participated in Experiment 1 , 11 in Experiment 2, and 9 in both experiments (See Table 7.1 for details). The average ages were 32.6 ± 10.21 years and 31 ± 10.96 years for experiments 1 and 2. Only one of the subjects was presbyope and participated in both experiments. Regarding the distribution of refractive errors, 6 participants were myopic, 4 were emmetropic and 2 were hyperopic. Only the left eye (OS) of each subject was evaluated in both experiments.

The research protocol was approved by the Ethics Committee of the Consejo Superior de Investigaciones Cientificas (CSIC) and was performed in accordance with the guidelines of Declaration of Helsinki. Prior to the enrollment, all subjects received a comprehensive explanation of the study and provided informed consent.

Exclusion criteria included astigmatism greater than 1.25 D, severe systemic disease, previous ocular surgery, and/or ocular pathology.

Table 7.1. *Age, gender, evaluated eye and refractive error (Sphere, Cylinder and Axis) of the subjects participating in the experiments.*

Subject	Experiments	Age (y)	Gender	Evaluated Eye	Refractive Error (D, D, deg)
S#1	1-2	27	M	OS	+1.00
S#2	1-2	39	M	OS	-6.00 – 1.25 x 110
S#3	1-2	26	M	OS	-3.00 – 0.25 x 170
S#4	1-2	37	F	OS	+0.00
S#5	1-2	40	F	OS	-2.50 – 0.75 x 5
S#6	1-2	28	M	OS	+0.25
S#7	1-2	33	F	OS	+0.00 – 0.50 x 180
S#8	1-2	21	M	OS	-4.75 – 0.50 x 180
S#9	1-2	54	M	OS	+2.00
S#10	1	21	M	OS	+0.00
S#11	2	18	M	OS	-1.50
S#12	2	18	M	OS	+0.25 – 0.25 x 180

7.2.2– SimVis Gekko visual simulator

As mentioned in previous chapters, SimVis Gekko [153,194] is a clinical visual simulator capable of replicating diverse multifocal designs from any solution (IOLs [147,154,195], CLs [239,240], and presbyLASIK patterns[155]). In this chapter, we used the SimVis Gekko ™ device (v.0.8, 2022) to simulate different generic monofocal and bifocal patterns within the left eye during two psychophysical experiments. The SimVis Gekko simulator was controlled by Matlab (MathWorks, USA), enabling optimized and precise control over the optical simulations required in each experiment trial. A dedicated firmware of the instrument was developed for this study with the aim of expanding the simulation capabilities beyond those

offered by the commercial version of the instrument, making it able to introduce potentially any lens simulation.

A battery of comprehensive calibrations was carried out on bench, before the experiments, in order to ensure the accuracy of the SimVis Gekko employed in this study. The entire set of optical simulations was validated using a high-speed focimeter[161,162] considering and compensating temperature effects of the tunable lenses[164].

The refractive error of the left eye of the subjects was corrected using trial lenses in a dedicated lenses holder, while their right eye was occluded throughout the session.

7.2.3– Stimuli

The stimulus used in all sessions was a video sequence (https://www.youtube.com/watch?v=CVS63LN6ZrE; 4K, 60Hz, 30 minutes) showing an evolving urban scene with people, cars, and signs. The video is continuous, without jumps, ensuring similar but sufficiently different stimuli for each evaluated trial. A Japanese environment, with signs unintelligible to the participants, was chosen to include, but not overemphasize, reading visual hints. The video was displayed on a calibrated TV screen (LG model 49UH850V, 3840 x 2160 pixels) located 4 m away from the subjects, with an angular subtense of 13.09° x 7.45°. The maximum luminance level was fixed at 200cd/m^2.

7.2.4– Experimental procedures

The experiments, as well as the conditions tested, are described in figure 7.1. Each curve represents a different condition.

Setup

Figure 7.1 A illustrates the setup employed in both experiments, previously described in section 7.2.3. Subjects viewed monocularly (OS) the 4K natural video at 4 m, while wearing SimVis Gekko on their head and different optical corrections were simulated.

Experiments 1 and 2 followed a similar procedure and used the same perceptual judgement (explained below). However, experiments 1 and 2 had different combinations of condition tested (adaptation state, transition type and time, test correction addition and test correction energy balance). Experiment 1 had more variety of transitions and test correction energy balances, while experiment 2 focused more on the impact of test correction additions.

Custom scripts were programmed in Matlab to control and randomize the conditions in both experiments, being different for each subject.

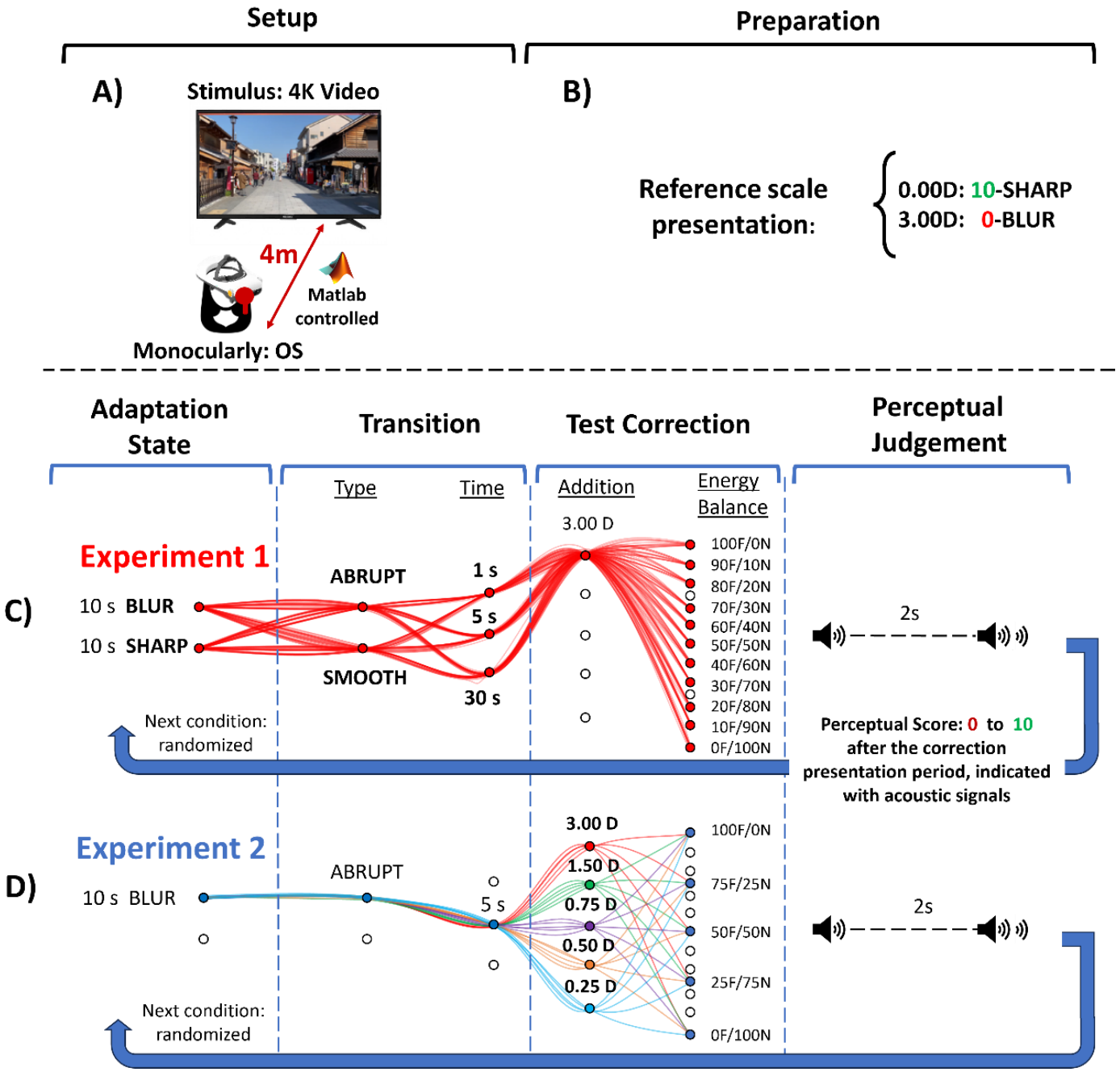

Figure *7.1*. *Flowchart of the procedures and conditions for Experiments 1 and 2*. *Panel A describes the setup. Panel B describes the reference criterion, the scale used in the judgements and explained to the subject before each experiment. The upper itinerary (C) represents each evaluated condition in Experiment 1, while the bottom itinerary (D) represents Experiment 2 conditions. Each condition of itinerary presents the Adaptation, Transition, Test correction and Perceptual Judgement sections. After the perceptual judgement, the next condition starts in a randomized order. A total of 132 (66 per adaptation state) and 25 conditions are represented in this flowchart for Experiment 1 and 2, respectively.*

Preparation

Prior to starting the experiment (Experiment 1, experiment 2 or both) a reference criterion was provided to the subject (See panel B in Fig.7.1). Following this criterion the best achievable perceptual score, 10, was associated with the SHARP visual condition and the lowest score, 0, was associated with a BLUR visual condition of 3.00 D. These visual conditions were shown to subjects, simulating them with SimVis Gekko while watching the video stimulus on the TV.

Experiment 1

The flowchart illustrated in Fig 7.1, panel C, outlines the sequence followed during Experiment 1. Each curve represents a different condition characterized by a set of parameters: an adaptation state, a transition and a test correction.

Adaptation State

Each condition started with an adaptation state of 10 s (either SHARP or BLUR) while the video continued playing and the subject watched the screen. The adaptation states matched with the maximum and minimum from reference scale (see “preparation” in the previous section)

Transitions

The adaptation was followed by the presentation of a test correction (all the test corrections are described in the next section). Different transitions between the adaptation state and the test correction were evaluated in experiment 1. The transition type can be SMOOTH or ABRUPT. The SMOOTH transition is a linear transition between the adaptation state and the test correction (See Fig.2 A) lasting 1, 5 or 30s (transition). Each Smooth transition is implemented in 15 quick steps that progressively reduce the weight of the adaptation state and increase the weight of the test correction. The ABRUPT transition can be understood as an instantaneous transition (in just one step) between the adaptation state and the test correction (See Fig.2 A). In ABRUPT transitions, we define the transition time (also 1, 5 or 30 s) as the time between the transition and the perceptual judgment. The monofocal corrections were presented only using ABRUPT transitions.

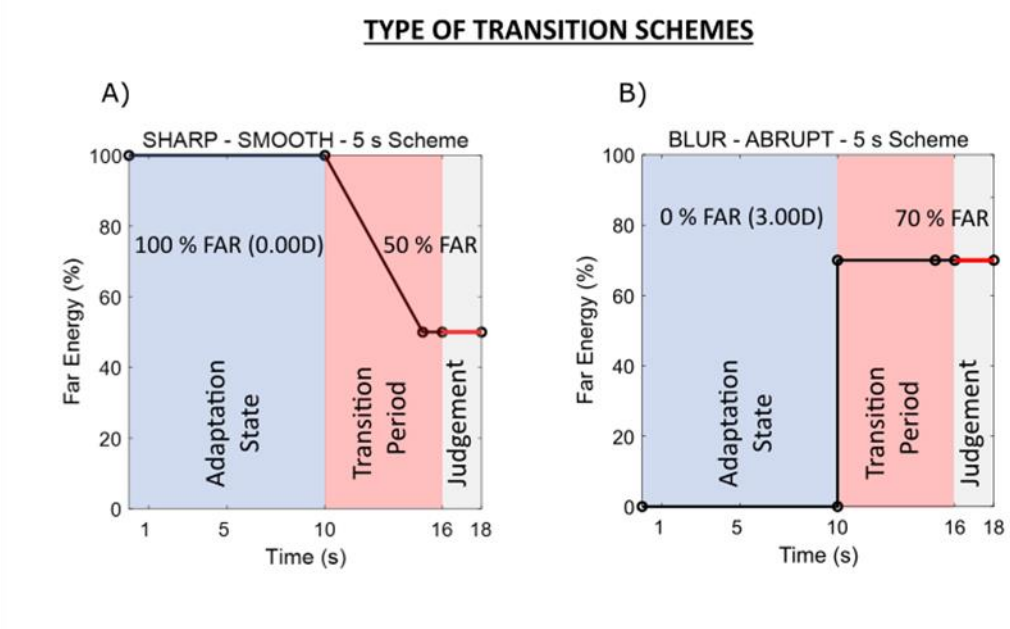

Figure *7.2. Schemes of the transition types assessed in the experiments for each condition*. *These schemes represent the Far Energy percentage of the simulated correction through the time in each phase of the procedure: Adaptation State (blue color), Transition Period (red color) and Judgement (gray color). A) SMOOTH transition between a SHARP (0.00 D) Adaptation State of 10 s and a bifocal correction with 50% of energy in FAR (0.00) and 50 % in NEAR (3.00 D). B) ABRUPT transition between a BLUR (3.00 D) Adaptation State of 10 s and a bifocal correction with 70% of energy in FAR (0.00) and 30 % in NEAR (3.00 D). In all cases, once the final bifocal correction is applied, it remains for 1 s and after that the subjects have 2 seconds to make a Judgement, indicated by the red line.*

Test corrections

The test corrections optically simulated were: two monofocal corrections, at far -0.00D- and at near -3.00 D- and nine generic bifocal corrections with an addition of 3.00D. These bifocal corrections had different energy distribution between far (F) and near (N) vision, ranging from 90 % to 10 % in steps of 10 %. Combined with the monofocal lenses, the range expands from 100F/0N to 0F/100N in steps of 10 % energy balance intervals.

Perceptual judgements

One second after the end of the transition, the subject had 2 seconds to perceptually judge the image quality from 0 to 10 in increments of 1 perceptual score. Acoustic signals indicated the start and end of this interval. Subsequently, the next condition starts in a randomized order.

Summary of the conditions.

In total, there were 132 conditions (11 corrections x 2 type of transitions x 3 transition times) per adaptation state (SHARP and BLUR) in experiment 1. Each condition was repeated 3 times. Each subject's measurements were obtained during 6 experiment sessions with each session lasting 30 minutes. The entire process was programmed in Matlab, to control times,

induce SimVis Gekko simulations, follow randomization tables and collect the perceptual scores for each subject.

Experiment 2

Experiment 2 followed a similar procedure, but with different conditions. The differences between experiments can be seen in Fig.7.1, Panel D. Experiment 2 focused on studying the effect of the addition, reducing the number of conditions (less adaptation states and transitions parameters). Each color represents a different addition value.

Preparation, Adaptation state and transition

Same preparation, reference criterium and scale, as in experiment 1. In all cases but 9 subjects had performed experiment 1 before experiment 2, and the preparation phase was just a reminder, asking the observers to use the same criteria already used in experiment 1. The adaptation state was fixed to BLUR. The transition type was fixed to ABRUPT and the Transition time to 5s. These parameters were chosen after showing a greater effect in preliminary tests of experiment 1 [238].

Test Corrections

Five different amounts of addition (0.25 D, 0.50 D, 0.75 D, 1.50 D, and 3.00 D) were used in the test corrections of experiment 2, what represents the main change with respect to experiment 1 (that only used an addition of 3D).

Only five energy balance distributions were tested: Three bifocal energy balances (75F/25N, 50F/50N and 25F/75N), and the two monofocal extremes (represented as 100F/0N and 0F/100N). The 100F/0N correction was evaluated 5 times. The 0F/100N corrections were evaluated as pure defocus: 0.25 D, 0.50 D, 0.75 D, 1.50 D and 3.00 D.

Summary of conditions

In total, there were 25 test corrections. As only one adaptation state (BLUR) and one transition (ABRUPT) were judged, the number of conditions in experiment 2 is equal to the number of corrections. As previously mentioned, Figure 7.1 shows all the conditions, with each addition represented by a different color. As in experiment 1, each condition was repeated three times. Each subject followed a different randomized order in a single measurement session that lasted around 30 minutes.

7.2.5– Perceptual Cost and Perceptual Benefit of bifocal corrections

Experiments 1 and 2 provide perceptual scores for several corrections under different adaptation conditions. From these same data, we can obtain information with greater clinical application value if we calculate the Bifocal Perceptual Cost at Far and the Bifocal Perceptual Benefit at Near. Figure 7.3 illustrates the process.

The Bifocal Perceptual Cost at Far is calculated by subtracting the perceptual score of each correction, which has been measured at far, from the perceptual score of the far monofocal lens, that is, the perceptual score of the 100F/0N correction.

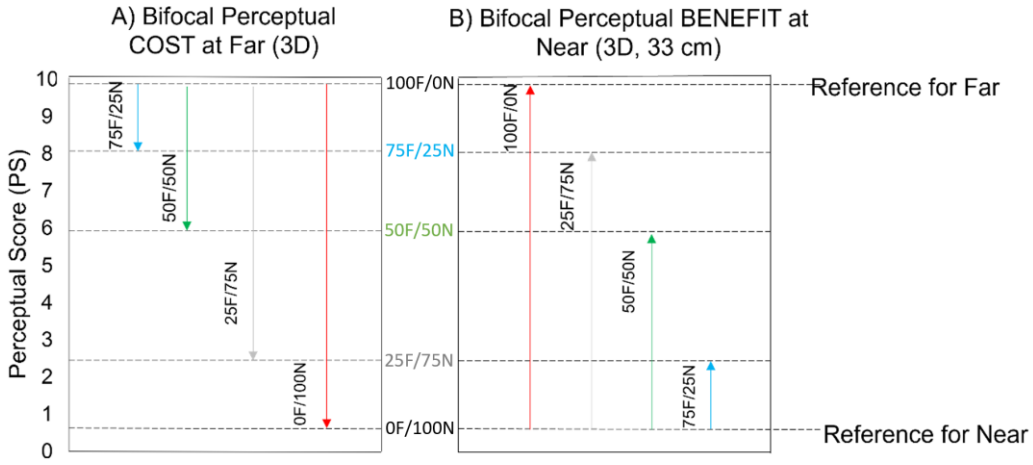

Figure *7.3.* Calculation of the COST and BENEFIT associated to a bifocal lens. A) Bifocal perceptual cost at far and B) Bifocal Perceptual Benefit at near (See text for details).

For the calculation of the Bifocal Perceptual Benefit at Near, two things are changed in the calculation compared to Bifocal Perceptual Cost at Far. Firstly, the reference is changed, which becomes the far monofocal correction, evaluated at near distance. On the other hand, the distance changes, which becomes the distance at which the near energy is focused. In the case of Experiment 1, 33 cm corresponds to 3D.

Although it has not been measured at near, we can assume that a 75F/25N correction at far, with 3D of addition, is equivalent, in terms of optical quality, to a 25F/75N correction at 33 cm of distance, because both have 75 % of the energy in focus, and 25 % of the energy. And therefore, both have the same perceptual score. As will be discussed later, this is an abstraction, as it assumes the pure perceptual score, without considerations associated with distance, the patient's visual needs at near, previous adaptation or experience, which can be very different between near and far. But it allows an estimation of the perception of the image quality provided at near different corrections, isolated from other phenomena.

In the same way, as seen in Figure 7.3, we can obtain the near perceptual scores for all evaluated corrections in all experiments. By subtracting the estimated PS at near from the new reference (far monofocal lens evaluated at near), we can determine the bifocal benefit at near.

The results between far and near have an inverse relation: when a correction works better at near, it performs worse at far. But they are not related by a linear function, and its dependence changes with the evaluated correction. A simple example is the 50F/50N correction. In the figure, we see that it has a PS at far of 6. Therefore, we estimate a PS at near of 4. A very interesting parameter is the difference between cost and benefit, which in this chapter we denominate Perceptual Gain. In the case of 50F/50N, the perceptual gain of using a bifocal correction is +2, representing a positive compromise of 2 perceptual points: The patient sacrifices 4 points at far, to gain 6 points at near.

7.2.6– Statistical analysis

The datasets gathered in Experiments 1 and 2 were analyzed using IBM SPSS Statistics Version 28 (IBM Corp, USA). Descriptive statistics, including the mean PS across subjects, standard deviations and 95% confidence intervals, were reported for each evaluated condition. As the experiments involved repeated measurements, we employed a mixed-effects linear model [241] with PS as the dependent variable.

For Experiment 1, the statistical model included fixed effects such as far energy distribution, type of transition, transition duration, and adaptation state. The random effect considered was 'Subject'. Additionally, we conducted pairwise comparisons, taking into account the adaptation state and comparing the three transition times. These analyses allowed us to determine the significance and impact of the different parameters on perceived image quality.

In Experiment 2, the model included as fixed effects the far energy distribution and the addition, with 'Subject' as the random effect. We also conducted pairwise comparisons, considering the addition parameter and comparing each far energy distribution.

Throughout the analysis, we applied a significance level of $p<0.05$ to define statistical significance.

7.3– Results

7.3.1– Experiment 1

The Perceptual Scores collected throughout all sessions of Experiment 1 are presented in Figure 7.4, for the 2 adaptation states (SHARP or BLUR) and the 2 types of transition (ABRUPT or SMOOTH) employed. Each data point in this figure represents the mean PS across 11 subjects for each energy balance (correction), and the error bars a 95% confidence interval. Each curve represents a different duration of the transition (1, 5 or 30 s). The different panels stand for different combinations of adaptation states and transition types: A) SHARP-ABRUPT; B) SHARP-SMOOTH; C) BLUR-ABRUPT; and D) BLUR-SMOOTH conditions.

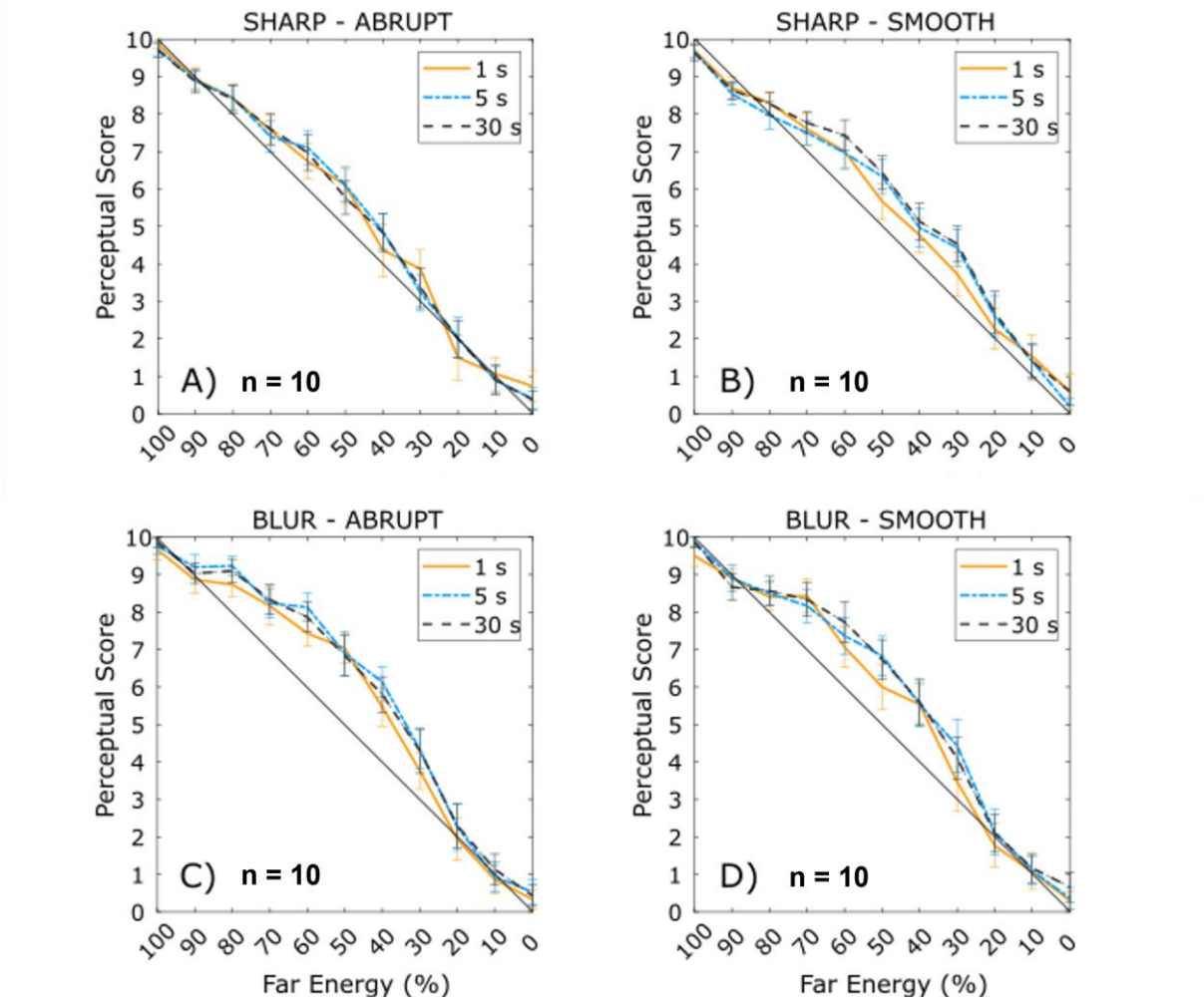

Figure *7.4. Perceptual Scores (PS) for each correction condition across subjects (n=10) in Experiment 1.* *Different data series represent transition times: 1 s (orange solid line), 5 s (blue dotted line) and 30 s (black dashed line). Each panel represents the combination of adaptation state and type of transition: A) SHARP-ABRUPT; B) SHARP-SMOOTH; C) BLUR-ABRUPT; and D) BLUR-SMOOTH. Each point represents the mean PS with 95% confidence interval bars. A diagonal solid line denotes a linear decrease between PS and Far Energy % as reference.*

Although the perceptual score is a highly subjective measurement, the dataset from experiment 1 demonstrates remarkably consistent and systematic results.

We observed a consistent decrease in PS with the reduction of the far energy percentage in the simulated bifocal correction. This decrease was expected and is consistent across all parameters: adaptation state, transition type and transition time.

The black line represents a linear response between perceptual score and energy balance. We observe important deviations from linearity in all conditions for intermediate values of far energy. The conditions with SHARP adaptation have a much more linear behavior than the conditions with BLUR adaptation. Regarding the influence of the transition time, the curves corresponding to 5 s and 30 s appear to overlap, while the difference with the 1 s is very small. Although the statistical significance of these differences will be examined later, ultimately, it depends on the variability among repetitions and subjects.

The standard deviation across subjects and repetitions averaged ±1.15 perceptual score across conditions and does not differ excessively for different conditions. The maximum value of standard deviation was 1.24 for BLUR-SMOOTH-1 s condition, while the minimum value was 1.05 for SHARP-SMOOTH-5 s and SHARP-SMOOTH-30 s.

The mean intrasubject deviation across repetitions and conditions is 0.93 perceptual points (on a scale of 10), indicating that the subjects are very consistent in their responses, as in previous studies [103,242–244]. That mean intrasubject deviation is smaller, although very similar to the mean intersubject deviations across repetitions and conditions (1.15). These low individual differences show that the trends are consistent across subjects, and that they all performed the experiment in a similar way.

The differences between each adaptation state are better seen in Figure 7.5, which shows the same data with a different representation. Now, the curves are smoothed to illustrate the trends in a better manner. They are 5th degree polynomial interpolations of the average data from the graphs in Figure 7.4. In this case, they are represented for each combination of transition parameters (type and transition time), with each data series corresponding to an adaptation state (SHARP or BLUR).

The panels on the left (A, C, D) represent ABRUPT transitions with filled markers and solid lines, and the panels on the right represent SMOOTH transitions, represented by empty markers and dashed lines. The two top graphs (A and B) represent 1 second transitions, the two middle graphs (C and D) represent 5 second transitions, and the two bottom graphs (E and F) represent 30 second transitions. In each panel, the effect of the type of adaptation (SHARP or BLUR) is directly compared. Adaptation to SHARP is represented with squares, and adaptation to BLUR is represented with triangles.

The effect of the transition is small. The transition type (ABRUPT or SMOOTH; left column versus right column) does not significantly affect the result. Similarly, the difference produced by the change in transition times (top, middle, and bottom graphs) is also subtle. However, it is clearly evident that the adaptation to BLUR has a significantly greater impact compared to

the adaptation to SHARP. Nevertheless, this representation allows us to appreciate that this effect does not happen in all cases. In certain conditions, an inversion in the curve is observed when adaptation to SHARP results in larger effects, particularly for SMOOTH transitions and corrections with higher energy at near. This inversion was systematically produced at the same point, around 30F/70N energy balance, for all transition times (panels B, D and F).

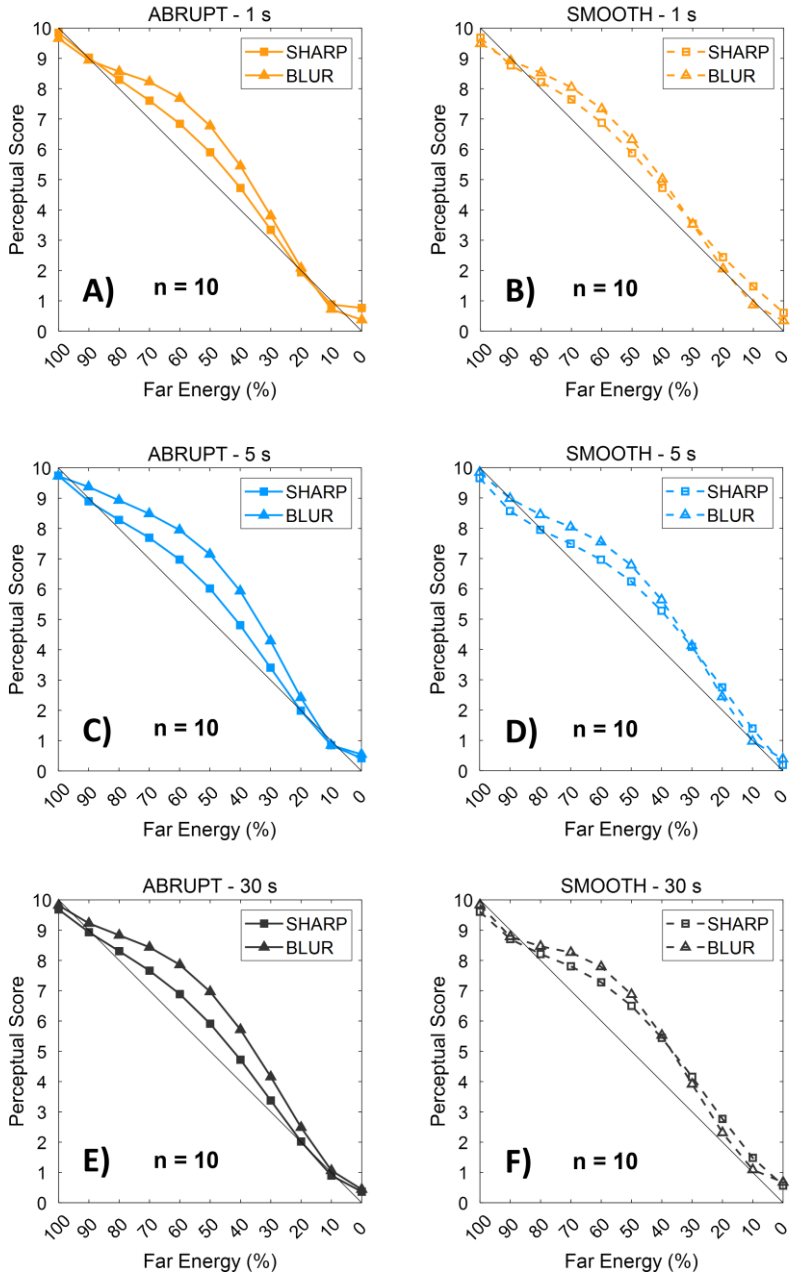

Figure *7.5. Perceptual Scores (PS) for each correction condition across subjects (n=10) in Experiment 1, comparing the results for each adaptation state.* *Each dataset corresponds to various adaptation states: SHARP (squares) and BLUR (triangles). Each panel represents the combination of type of transition and transition time: A) ABRUPT - 1 s; B) SMOOTH - 1s; C) ABRUPT - 5 s; D) SMOOTH - 5 s; E) ABRUPT - 30 s; and F) SMOOTH - 30 s. ABRUPT transitions are represented by solid lines and filled markers, while SMOOTH are represented by dashed lines and empty markers .Each point represents the mean PS with 95% confidence interval bars. A diagonal solid line denotes a linear decrease between PS and Far Energy % as reference.*

Statistically, the implications of each parameter as fixed effect, using the mixed-effects linear model, are summarized in Fig.7.6 in a graphical overview. The analysis revealed that there were significant differences -red dots- for the energy balance (Fig. 7.6 A) in both adaptation states, for the type of transition only in BLUR adaptation (Fig. 7.6 B), and for the transition time also in BLUR adaptation (Fig. 7.6 C).

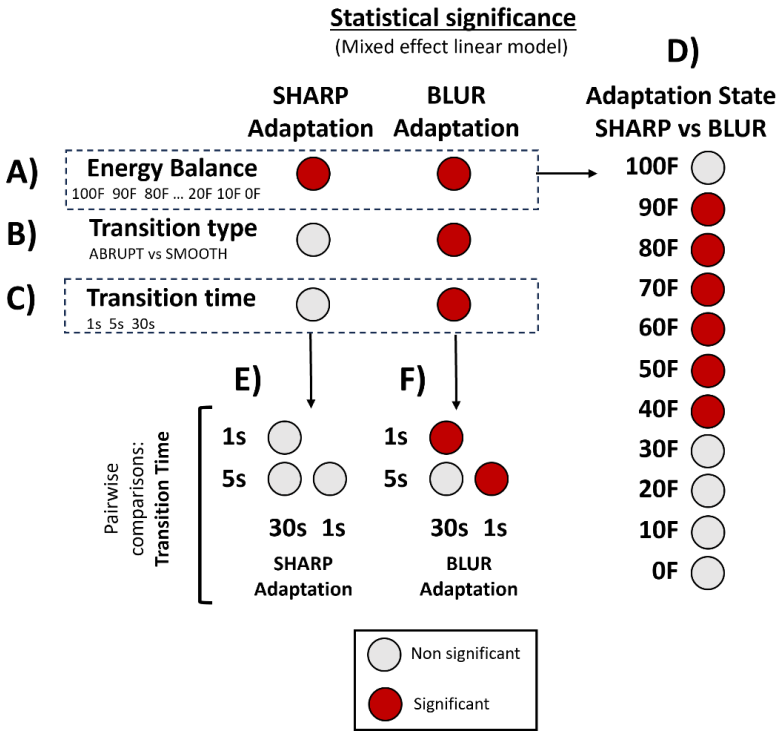

Figure *7.6. Graphical maps of statistical relations among parameters evaluated in Experiment 1.* *Statistical significances for each Adaptation State are represented for each parameter: A) Energy Balance, B) Transition Type and C) Transition Time. Statistical significances of each energy balance between Adaptation States are reported in panel D). Pairwise comparisons between transition times are represented for SHARP adaptation (E) and BLUR adaptation (F). The red circles represent statistical significances relations between the related parameters, while the gray circles represent non-significant relations among them.*

These results reinforce what was seen in the previous figures, with the adaptation state causing the most important differences in the perceptual scores. The energy balances that showed significant differences between adaptation states (D) were those within the 90F - 40F range, which correspond to the energy balances present in commercial lenses. The differences shown in the transition times for BLUR adaptation were analyzed with pairwise comparisons, showing that the 1s time presented differences compared to 5 and 30 seconds. But the conditions with transition time 5s were not statistically different to the conditions with 30s.

Figure 7.7 shows the bifocal perceptual cost at far (worsening of the perceptual score compared to 100F/0N in focus) vs the bifocal perceptual benefit at near (improvement

compared to 100F/0N at near distance) for the different conditions, in a distribution similar to Figure 7.4 (average across subjects).

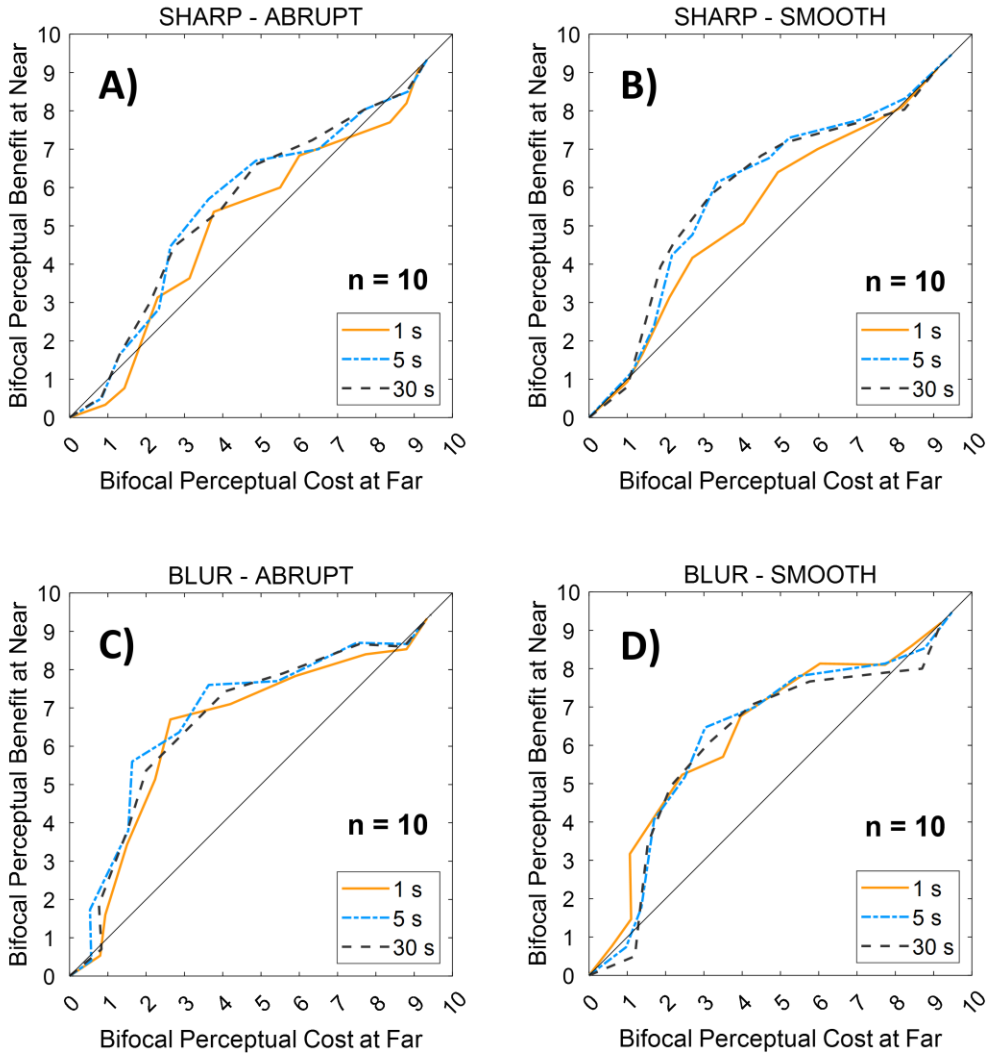

Figure *7.7. Bifocal Perceptual Benefit at Near vs Bifocal Perceptual Cost at far for each correction (considering its Bifocal Perceptual Cost at far across subjects (n=10) in Experiment 1, comparing the results for each transition times.* *This figure is the equivalent to Fig.7.4 considering Bifocal Perceptual Benefit at Near vs Bifocal Perceptual Cost at far. Each dataset corresponds to various transition times: 1 s (orange), 5 s (blue) and 30 s (black). Each panel represents the combination of adaptation state and type of transition: A) SHARP-ABRUPT; B) SHARP-SMOOTH; C) BLUR-ABRUPT; and D) BLUR-SMOOTH.*

Compared to that figure, this representation in terms of cost and benefit has a direct clinical interpretation. The curves continue to have great consistency among themselves and show now a more marked separation with respect to linearity (diagonal line). The benefits are manifestly higher to the costs in practically all corrections except those in the limits of the scale (benefit or cost 0-1 or 9-10, corresponding to monofocal or almost monofocal corrections, which have a cost of 10 when in focus, and 0 when out of focus).

Conditions with a transition time of 1s have less benefit than 5 s or 30 s (which also look very similar to each other), especially for SHARP adaptation. Again, the BLUR- ABRUPT

conditions have much more adaptation than the SHARP-ABRUPT conditions. The conditions with SMOOTH transitions present an intermediate behavior to these two extremes.

This adaptation effect is better seen in figure 7.8, where a direct comparison is made between the SHARP and BLUR adaptation states (similar to Figure 7.5). BLUR causes a much larger adaptation than SHARP for all types of transitions and adaptation times, although this adaptation is smaller for SMOOTH transitions, especially for 5 and 30 seconds, where SHARP and BLUR present similar results.

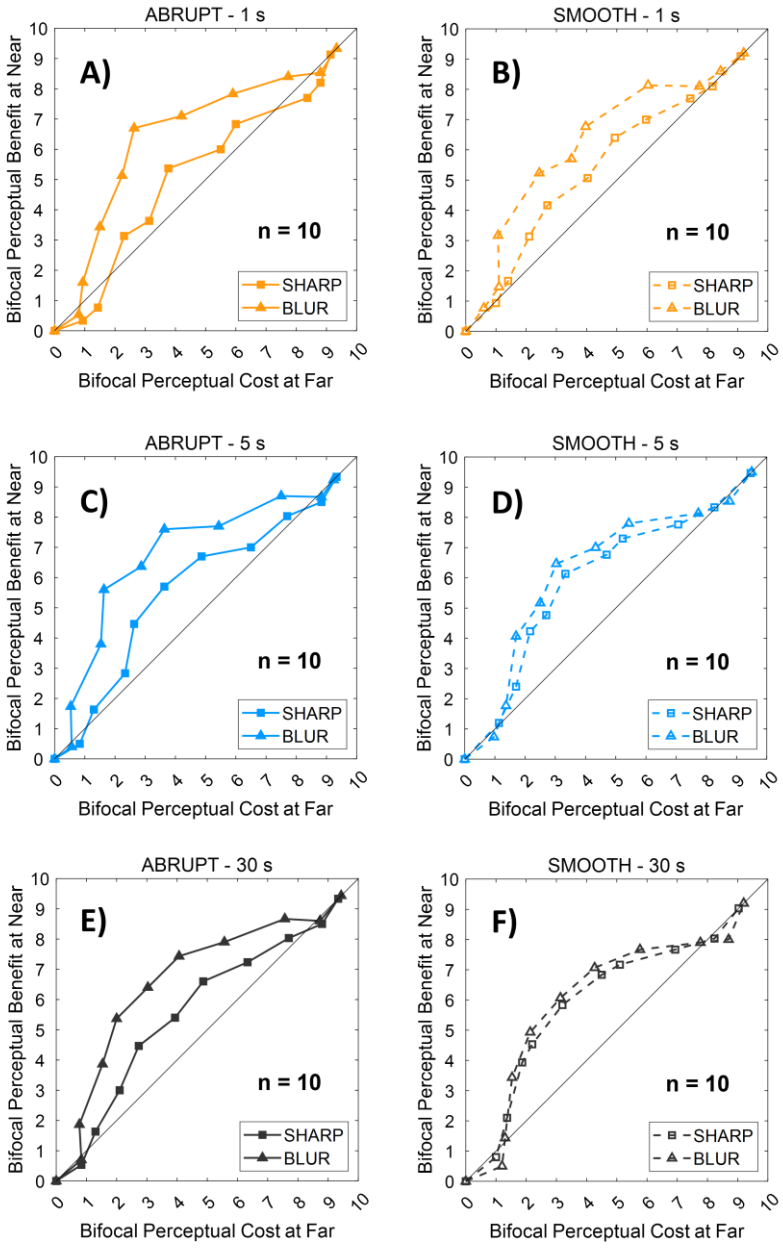

Figure *7.8. Bifocal Perceptual Benefit at Near vs Bifocal Perceptual Cost at far for each correction (considering its Bifocal Perceptual Cost at far across subjects (n=10) in Experiment 1, comparing the results for each adaptation state.* *This figure is the equivalent to Fig.7.5 considering Bifocal Perceptual Benefit at Near vs Bifocal Perceptual Cost at far. Each dataset corresponds to various adaptation states: SHARP (squares) and BLUR (triangles). Each panel represents the combination of type of transition and transition time: A) ABRUPT - 1 s; B) SMOOTH - 1s; C) ABRUPT - 5 s; D) SMOOTH - 5 s; E) ABRUPT - 30 s; and F) SMOOTH - 30 s.*

Figure 7.9 shows the Perceptual Gains, difference between perceptual Benefit and perceptual Cost, generated for each evaluated correction. As anticipated by Figure 7.8, the Perceptual Gain is greater than zero in all conditions, except for energy balances close to monofocality. Remarkably, the Perceptual Gains reaches 4 perceptual points in BLUR adaptation with ABRUPT transitions, but it is very significant even in the worst conditions (SHARP adaptation and short times, 1 s). There is a very noticeable asymmetry in the curves, which have a maximum around a perceptual cost of 3. Moreover, perceptual costs around 0-1 and 8-9 do not produce any positive Perceptual Gain.

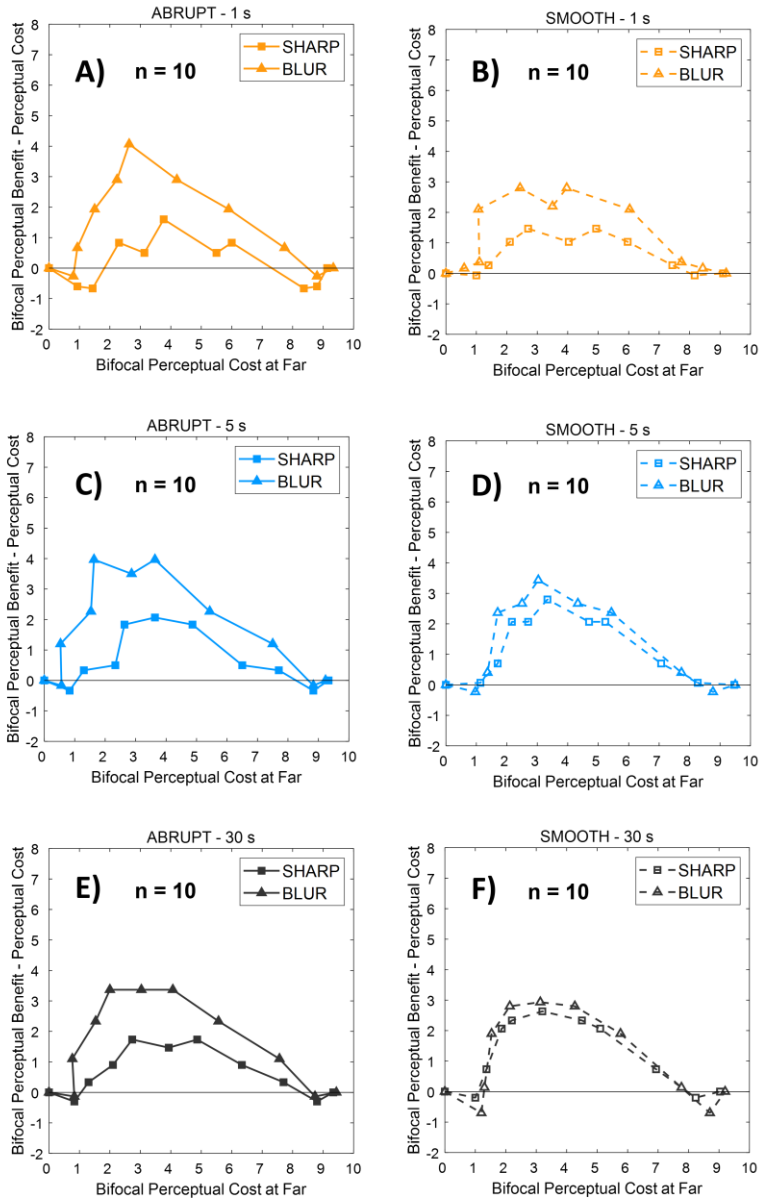

Figure *7.9. Perceptual Gain (Bifocal Perceptual Benefit – Bifocal Perceptual Cost) for each correction (considering its Bifocal Perceptual Cost at far) across subjects (n=10) in Experiment 1, comparing the results for each adaptation state.* *This figure is the equivalent to Fig.7.5 considering Perceptual Gains. Each dataset corresponds to various adaptation states: SHARP (squares) and BLUR (triangles). Each panel represents the combination of type of transition and transition time: A) ABRUPT - 1 s; B) SMOOTH - 1s; C) ABRUPT - 5 s; D) SMOOTH - 5 s; E) ABRUPT - 30 s; and F) SMOOTH - 30 s.*

It is also very significant in Figure 7.9 that, again the SMOOTH transition conditions in 5 s and 30 s hardly show differences with the adaptation state (SHARP and BLUR). This seems to suggest that a sufficiently long SMOOTH transition makes the subject's previous adaptation irrelevant. On the contrary, a SHARP transition makes the subject's responses very dependent on the previous adaptation.

Figure 7.9 clearly shows that the subject's response is influenced by the adaptation process that precedes the perceptual judgment. In Figure 7.10 A, all the perceptual gains are represented, illustrating the range of variability induced by the different adaptation and transition parameters. Given the wide range of conditions studied, this band captures the variability that can be expected from neuronal adaptation processes, at least in the short-term.

However, Figure 7.10 A does not show the energy distributions of the bifocal corrections, something of critical interest from the lens design perspective. Figure 7.10 B is an alternative representation in which the perceptual gains are plotted directly against the energy balances (Far Energy %). It is now clear that the large perceptual gains observed in Fig. 7.10 A correspond to energies at far 40%, 50%, and 60%, which happen to be the typical energies at far of commercial intraocular lenses and contact lenses. Figure 7.10 B clearly shows, again, that energies close to monofocality (10%, 20%, 80%, and 90%) have irrelevant or even negative benefits.

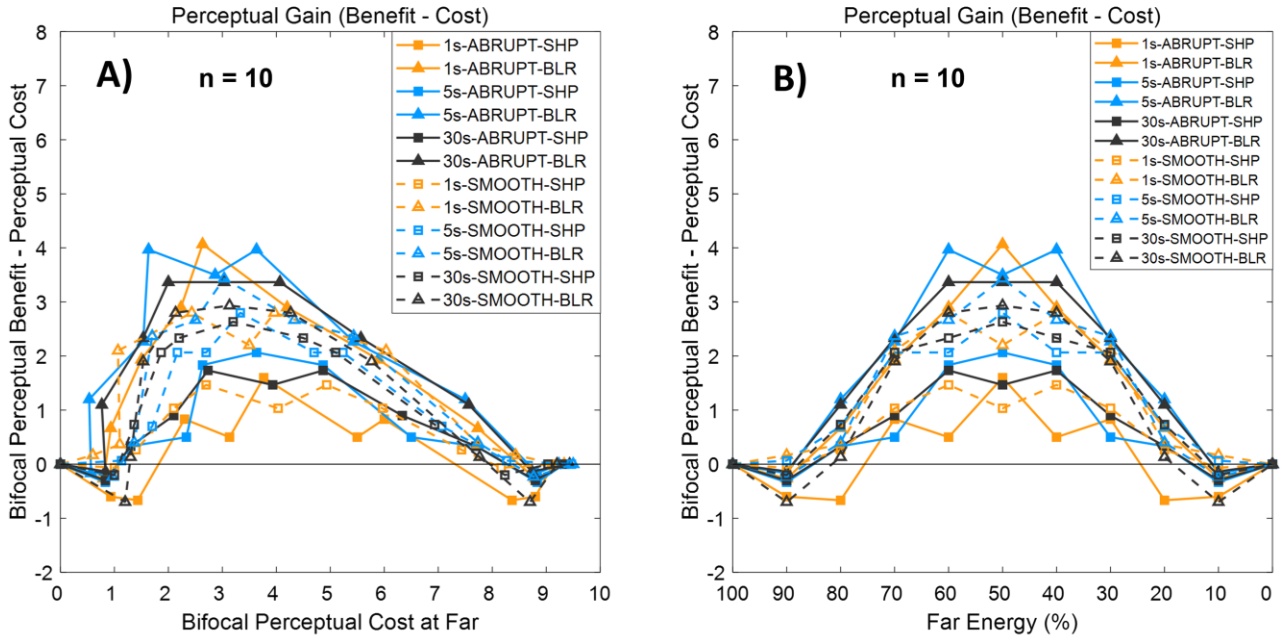

Figure *7.10. Perceptual Gain (Bifocal Perceptual Benefit – Bifocal Perceptual Cost) for each correction and all conditions across subjects (n=10) in Experiment 1, representing in the x-axis:* *A) Bifocal Perceptual Cost at far and B) Energy Balance (Far Energy %). Each dataset corresponds to each condition (transition time - transition type - adaptation state) that followed the previous representations.*

All the previous figures, and Figure 7.10 C, in particular, represent results averaged across subjects, and a significant trend representative of all subjects. However, it is noteworthy that there are some individual differences. Figure 7.11 shows a graph similar to Figure 7.10 but with the extreme subjects, the ones providing the minimum (Subject S#2; panel A) and maximum (Subject S#2; panel B) perceptual gains.

In Figure 7.11 A, a large percentage of the conditions have a negative gain, even those with intermediate energy balances as parameter. But, even in this subject with minimum gains, there are many conditions with perceptual gain above 2, and some conditions with a gain greater than 4. In contrast, in Figure 7.11 B, almost all conditions have a positive gain, and some reach values above 6. This figure illustrates that even with the same design (energy balance) and adaptation, subjects perceive the images in different ways, and get different perceptual gain from the different bifocal cost at far, and bifocal benefit at near.

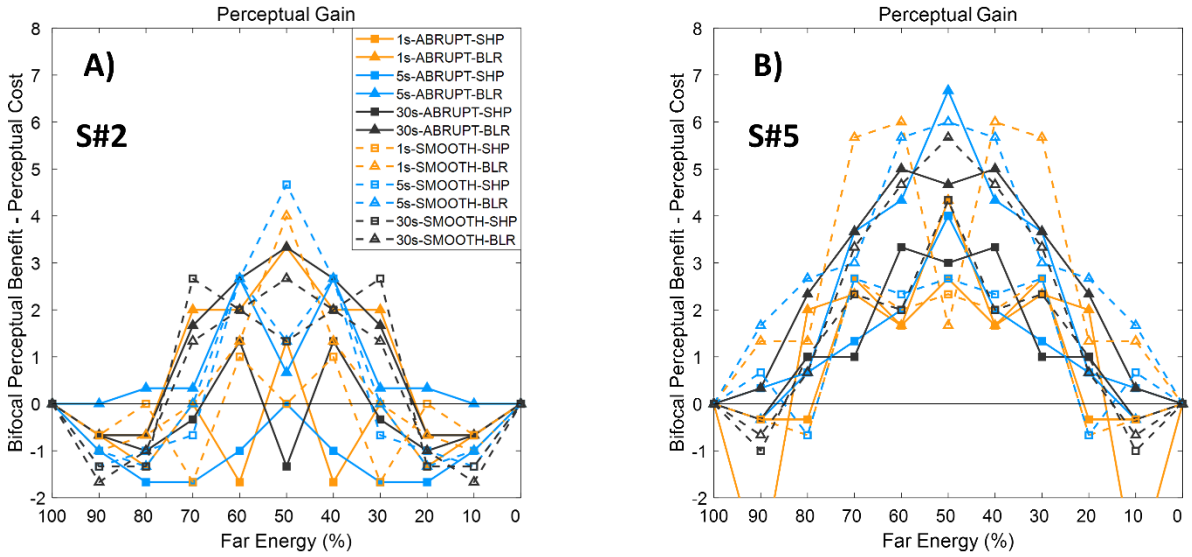

Figure *7.11. Perceptual Gain for each correction and all conditions in Experiment 1, represented by Energy Balance (Far Energy %) for:* *A) Subject (#2) with the minimum perceptual gains and B) Subject (#5) with the maximum perceptual gains. Each dataset corresponds to each condition (transition time - transition type - adaptation state) that followed the previous representations.*

Figure 7.12 represents the ratio benefit / cost, for all conditions, versus each bifocal design (percentage of far energy). All the adapting conditions are represented for each percentage of far energy. In this representation, a ratio equal to 1 indicates that the benefit is equal to cost, relative to a far monofocal. This is what happens monofocal corrections for near (0F/100N) and those close to it (10F/90N and 20F/80N). In these corrections, whatever is lost at far is gained at near, and vice versa.

A ratio greater than 1 indicates a benefit greater than the cost. This happens in intermediate bifocal corrections (70F/30N, 60F/40N, 50F/50N, 40F/60N, and 30F/70N). Some of these designs reach a ratio of 3 at some conditions. This means that the perceptual points that are lost at far are multiplied at near, which represents a very favorable transaction.

On the contrary, a ratio less than 1 indicates that the benefit is less than cost. This occurs in 90F/10N (and just one adapting condition of 80F/20N). It does not necessarily mean that this correction will be rejected, as it provides some near vision in exchange for a loss of far vision, but it indicates that from the point of view of perceptual image quality, the balance is more unfavorable.

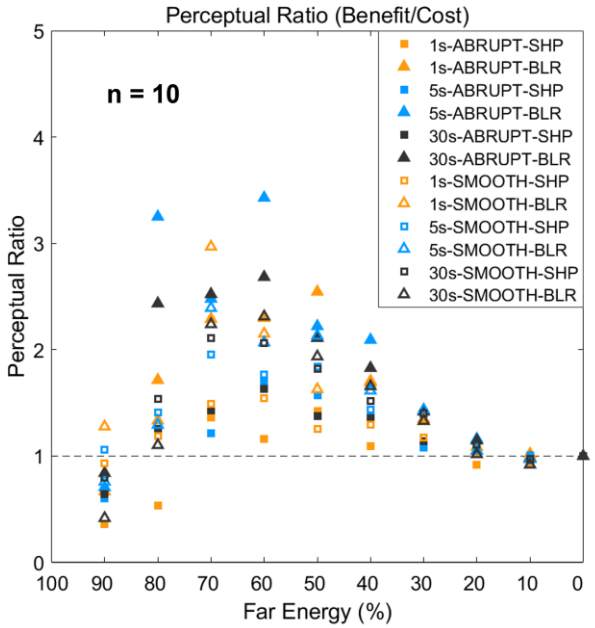

Figure *7.12. Perceptual Ratio (Bifocal Perceptual Benefit/Bifocal Perceptual Cost) for each correction and all conditions across subjects (n=10) in Experiment 1, considering Energy Balance (Far Energy %).* *Markers above the dashed line of perceptual ratio = 1 represent corrections with a higher benefit than cost, while corrections below that line represent corrections with a higher cost than benefit.*

7.3.2– Experiment 2

Experiment 2 focused on evaluating the perceived image quality across various corrections with different energy balances and addition values. This is in contrast with Experiment 1, where the addition value was fixed, and different transition conditions were evaluated.

Figure 7.13, panel A, represents the perceived quality at far, perceptual score (PS) obtained, for each energy balance and addition. Each curve represents a different correction (a different energy balance at far: from 100F/0N -monofocal at far-, 75F/25N, 50F/50N, 25F/75N, 0F/100N -monofocal at near-. Each point represents the average PS across eleven subjects and three repetitions (the bars stand for 95 % confidence intervals). The graph shows

a decrease in perceptual scores as near addition increases (except for the flat response of 100F/0N -orange line-, which is expected, as it is a monofocal lens without addition). PS also decreases as the energy at far decreases. The maximum decrease of perceptual score with addition is obtained for 0F/100N (red curve; monofocal at near), and it is almost linear, which is also expected as the perceptual judgements are performed at far distance. On the other hand, the bifocal curves (blue, green and gray curves) retain the perceptual score to some extent when the addition increases. The amount of energy at far is critical, with 75F/25N -in blue- being close to monofocal at far, 25F/75N -in gray- being close to monofocal at near, and 50F/50N being in the middle. Interestingly, at low additions, the 25F/75N curve -gray- is worse than the pure monofocal at near -red-.

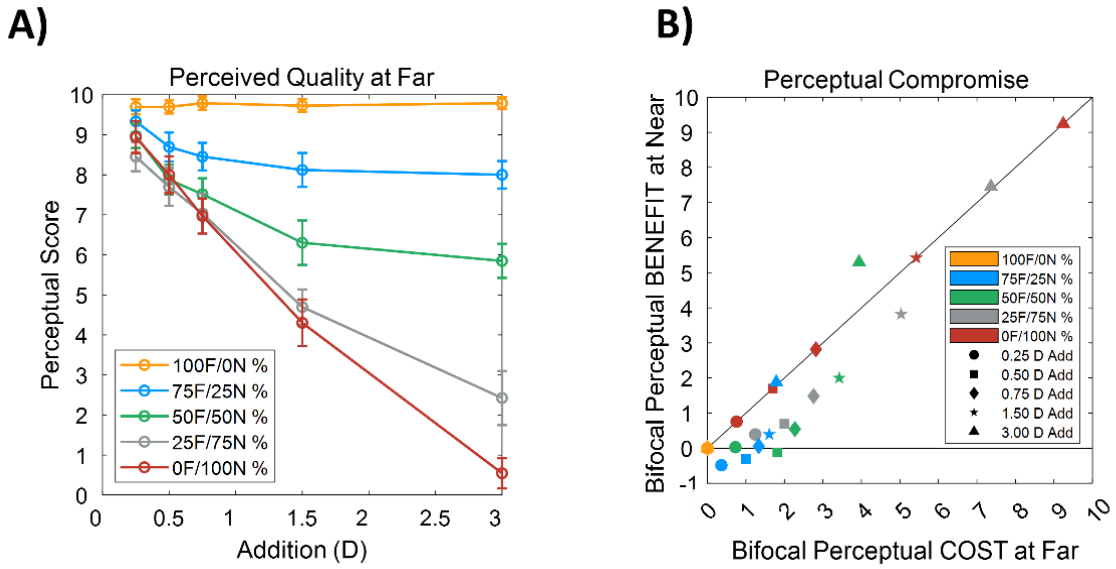

Figure *7.13. Results of experiment 2 across subjects (n=11):* *A) Perceived Quality at Far (Perceptual Scores through simulated corrections with different amount of addition and energy balance): average across subjects and 95% confidence interval bars. The energy balance of each data series is represented by different colors: yellow (100F/0N %), blue (75F/25N %), green (50F/50N %), gray (25F/75N %) and red (0F/100N %). B) Perceptual compromise for each assessed correction: bifocal perceptual benefit at near vs bifocal perceptual cost at far. In this graph, energy balances are color-coded as in the previous one and the addition amount is represented by geometric shapes: circles (0.25 D), squares (0.50 D), diamonds (0.75 D), stars (1.50 D), and triangles (3.00 D). The diagonal line represents the points where the Near Benefit and Far Cost are equal.*

Figure 7.13 B displays the corresponding bifocal perceptual benefit at near versus each bifocal perceptual cost at far, for each of the conditions of Experiment 2. Only the intermediate energy balance (in this case 50F/50N) for the 3D series has a benefit greater than the cost (5.5 versus 4). The rest of the values in the 3D series – which are close to near or far monofocality – have benefits similar to the costs, showing a neutral effect of the bifocal correction. This 3D series agrees with similar results from Experiment 1 (Figure 7.8 C, for the central point of the 5s curve – dashed black line -, also with 3D addition). But Figure 7.13 also contains data from other additions (1.5, 0.75, 0.50, and 0.25, in addition to 3). Surprisingly, no other symbol is above the diagonal. There are other values on the diagonal (with red

symbols), but they are not actually bifocal corrections, only the near monofocal correction 0F/100N.

It is remarkable that in bifocal corrections with an addition less than 3, the bifocal perceptual benefit at near is always less than the bifocal perceptual cost at FAR. That is, what happens at 3D additions is not extrapolatable to other additions. Just as the addition plays a fundamental role in image quality, it also plays a role in the perception of images.

Regarding the statistics of Experiment 2, the intrasubject variability was 0.56 Perceptual Scores (Standard deviation), showing an even higher repeatability than in experiment 1. On the other hand, the intersubject variability is slightly higher (0.89 Perceptual Scores) but maintaining under 1 point.

The fixed effects of the mixed linear model demonstrated varying behaviors related to far energy balance, addition, and their interactions, as illustrated Figure 7.14. It is worth noting that as the addition increases, the number of significant pairwise comparisons between corrections also increases. For an addition of 0.25 D, there are 5 significant pairwise comparisons. This number increases to 6 for 0.50D, 7 for 0.75D, and 9 for 1.5D of addition. When the addition reaches 3D, all pairwise comparisons (10 out of 10) are significant. This confirms that the near addition of bifocal corrections plays a crucial role in the observed effects.

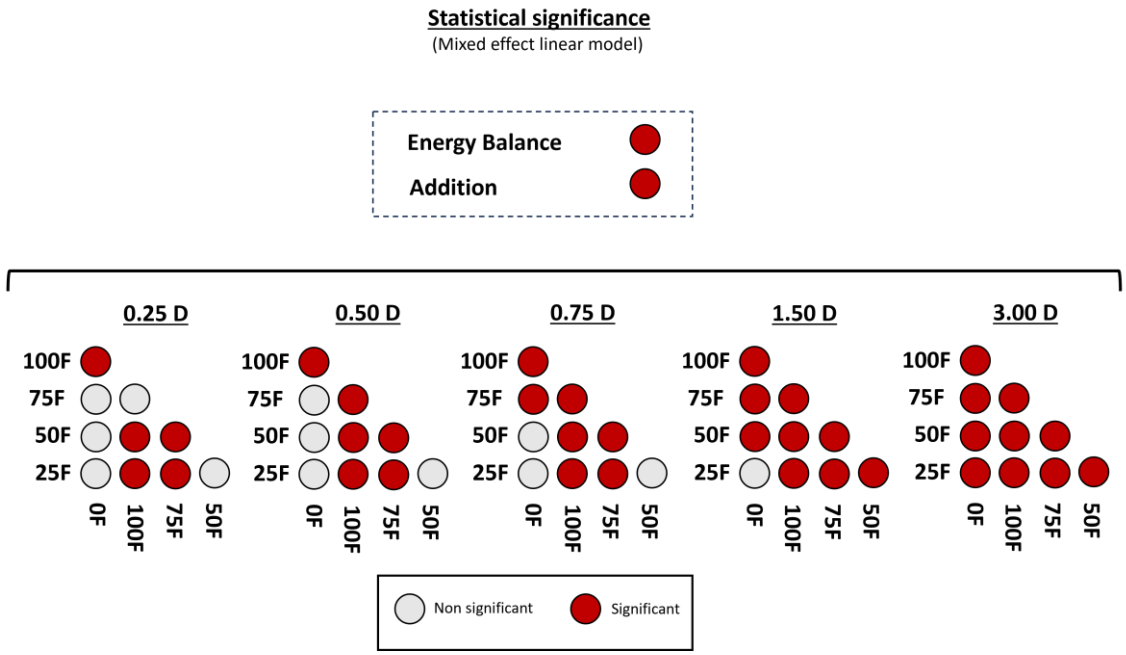

Figure 7.14. Graphical maps of statistical relations among conditions evaluated in Experiment 2*. For each addition amount, the disparities between different Far Energy corrections are illustrated within each block. Red circles indicate statistical significance between the associated conditions, while the gray circles not statistical significances.*

7.4 – Discussion

In this study, we investigated the effect of energy balance and addition of bifocal corrections on subjective perceptual judgments of image quality. By using the SimVis Gekko device (see-through and with wide field of view) the visual experience was more natural, and closer to the clinic, than in previous experiments of perceptual quality of multifocal images [153,181,245]. However, there is a good correspondence between this study and previous studies in the perceptual score obtained with different energy balances. For example, the reference condition in many studies, 50F/50N bifocal corrections after adaptation to SHARP, presented very similar perceptual scores, 3 on a scale of 5 in Radhakrishnan et al. [103] compared to 6 on a scale of 10 in our study.

This study included a large number of adaptation conditions (with a total of 157 randomized conditions for both experiments , each repeated three times), across several dimensions -adaptation state (SHARP or BLUR), transition type (ABRUPT or SMOOTH), and transition time (1s, 5s or 30s)-, providing complementary information to previous psychophysical measurements of adaptation to multifocal corrections [103,242,244]. Besides, the measurements were performed with optical induction of the bifocal design, instead of digital manipulation of the images, and without manipulating the optical aberrations of the eye.

Robustness and Variability

The task of assessing perceptual scores of image quality is highly subjective and therefore associated with a lot of variability. It could depend on many factors that are beyond our experimental control, such as fatigue, attention, or mood. Furthermore, the presence of ocular aberrations, or the use of a head-mounted clinical device (SimVis Gekko) instead of an optical table with bite bar could be a source of additional variability with respect to previous studies [103,242–244].

Furthermore, this study uses natural image sequences as stimuli, which could introduce additional variability and differences in the results, compared to using a high-contrast static image of a face. This study tends to capture the overall impression provided by a correction, rather than a comparison based on specific image features.

But both experiments conducted in this study, with randomized repetitions, reported low intrasubject variability (0.93 PS and 0.56 PS in experiment 1 and 2, respectively), demonstrating the robustness of the method. At the same time, the intersubject variability also presents low values: 1.15 PS in experiment 1 and 0.89 PS in experiment 2. The lower number of adapting conditions can explain the lower variability found in experiment 2.

The energy balance is the most important parameter in bifocal corrections. Experiment 1 demonstrates a consistent reduction in Perceptual Scores as the far energy percentage of

simulated bifocal correction decreases. This trend is consistent across all conditions (adaptation states, transition types and transition times; see Fig. 7.4 and Fig 7.5) and all subjects. However, the reduction is not linear, and the perceptual score provided by the subjects increases significantly at intermediate energy balances, in an amount that strongly depends on the adaptation.

The fact that curves with very similar shapes are measured in Experiment 1 validates the methodology and the perceptual task used, as it makes evident that the responses of all subjects, and all the repetitions, are very systematic. A mixed linear model, using Subject as a random effect and therefore modeling the variability between subjects confirms the strong correlation across observations.

Adaptation conditions and effect of the adaptation

This study also shows that the same design can produce different perceptual results, depending on the previous adaptation. As seen in figs 7.5 (for Perceptual Scores), 7.8 and 7.9 (for Perceptual Benefit and Gain), adaptation seriously affects the perceptual results obtained, and in a systematic and predictable way. It is worth noting that the predictable perceptual behavior obtained comes from an average across subjects. Figure 7.11 shows that there are important and unpredictable individual differences in the magnitude of the adaptation.

The perception of the image is seriously affected by previous exposure to blur. Other studies also revealed improvements in other visual test outcomes and neural adjustments following pure defocus adaptation[246–248]. BLUR adaptation produces a higher perceptual score than SHARP adaptation, being statistically significant for the energy interval of far energy between 90 to 40% (Fig. 7.6 D), interestingly the range of far energies normally found in commercial lenses.

BLUR adaptation generates the maximum level of adaptation and perceptual score (that could be understood as acceptance of multifocality). The interest in this result goes beyond a study of adaptation, as it has clinical implications. Once the correction is fitted or implanted in the eye, it will induce blur in the image, and the amount of blur can vary due to many reasons: the observation distance, the pupil diameter or, in the case of CLs, variability of the lens producing oscillating optical quality.

It is not clear and cannot be deduced from these experiments what exactly the effect of adaptation would be for subjects to their own lens design. This topic has been directly addressed, although partially, in some previous studies [103,242–244]. In this study it can only be estimated indirectly, but more completely thanks to the higher number of conditions included. It is clear from Figures 7.4 to 7.12, that adaptation produces a certain range of responses, and this study provides useful numerical information to quantify the maximum and the minimum of that range, by establishing a large sample of possible (and often extreme) adaptation conditions that could occur. That diversity of adaptation conditions can give an

idea of the range of representative values of perceptual score in different circumstances of real life with a given correction.

Although the adaptation times are short, below 30 s, the statistical analysis shows that statistically significant differences between 1 s and 5 s and between 1 s and 30 s but does not report statistically significant differences between 5 s and 30 s, indicating that most of the adaptation takes place in the first few seconds (between 1 s and 5 s), at least for the adaptation conditions, corrections and timelines involved in this study.

Effect of the Addition

The experiment demonstrates that in addition to energy balance, variations in the addition of bifocal lenses also determine the perceived image quality. Other studies have investigated the effect of the addition in bifocal lenses, either directly or as an adaptation, on perceptual judgments. Interestingly, low additions (between 0.25 and 0.75 D depending on the study), generate more degradation of the image, greater reductions in perceptual scores, and also a larger adaptation. At high additions, there is a recovery (1 to 2D) and a stabilization (>2.5D) in image quality and perceptual score, and a reduction in adaptation[103,244].

In our Experiment 2 (Fig.7.13 A), we detect a faster drop in perceptual scores for low additions (0.50 D) and an attenuation of the drop for higher additions, accentuating this effect for 75F/25N and 50F/50N. But there is no recovery or stabilization. Similarly, Figure 7.13 B shows that low additions produce little benefit and much cost, worse than the 3.00 D addition evaluated in Experiment 1.

Implications on presbyopic lens designs

Following the logic of this study in terms of perceptual costs and benefits, a presbyopia correction could be understood as an investment of perceptual points, being profitable when the gain (benefit - cost) is more than 0 (i.e. when the ratio is more than 1). Figure 7.13 B provides detailed information of which bifocal designs work best. Designs with energy at distance between 70 and 30% provide high gain (up to 4.07 for 50 %) and ratios up to 3.43 (for 60 %). Very high or very low energies, as well as low additions, do not produce a positive gain (the cost exceeds the benefit).

In other words, the return on the investment is not linear in Experiment 1 and depends on the amount of perceptual points invested (Figures 7.8, 7.9 and 7.10), and excess of energy at near does not translate into a beneficial correction, because the cost is not recovered. Interestingly, our results show that when the energy at near is too small, the invested perceptual costs at far are not fully recovered at near (Figures 7.8, 7.9 and 7.10).

The findings of this study, while primarily focused on bifocal solutions, can be extrapolated to more intricate multifocal solutions. Full range multifocal commercial lenses typically have additions around 3D and distribute the energy among a few intermediate and near foci, besides the far vision focus. The usual energies at far vision are 60-40% that of a monofocal lens. This paper demonstrates that this distribution results in an optimal near-far

compromise and the highest perceptual gain. However, the costs and gains involved are substantial, and some patients may be reluctant to accept this cost-benefit trade-off if the resulting image quality, both at near and at far, does not meet their expectations in absolute terms.

In contrast, EDOF or monofocal plus lenses generally have a low addition and a significantly displaced energy balance towards the near focus. These lenses are widely accepted for distant vision, according to clinical experience. Few patients express dissatisfaction with the far image quality, but these lenses often underperform in terms of near functionality. This paper shows that energies of 90-80% provide high perceptual scores, indicating good acceptance for far vision, but with low gains, suggesting limited improvements in near vision. These observations are solely based on image quality and perception, but not functional vision at different distances. Patients with EDOF lenses undoubtedly appreciate the residual intermediate vision provided, even if it comes at a significant perceptual cost. Furthermore, although according to this study EDOF or monofocal plus lens designs may be less beneficial than full range corrections, the absolute costs involved are minimal, making the transaction more viable. EDOF lenses represent a modest perceptual investment that offers new functionality at a low perceptual price, although with lower profitability. Conversely, full range lenses represent a more beneficial perceptual investment in relative terms, offering a higher benefit-to-cost ratio, but also entailing higher absolute costs.

Individual differences and clinical implications

It is widely recognized that individual differences exist in the preference for one multifocal design over another. In some optical elements like MCLs, this does not pose much of a problem other than investing time to find the suitable one. However, in MIOLs, the implant is not removable (only in extreme cases the lenses are explanted), with some patients accepting it, others needing periods of neuroadaptation, and others rejecting it. This paper shows that individual differences are consistent across a large number of conditions, indicating that the measurements are systematic (although noisy, like other perceptual measures) and that the origin of the individual differences lie in the criterion used, derived from the adjustment or tuning of perceptual mechanisms.

In clinical visual simulations, due to adaptation the response of the patient could depend on their previous exposure to blur. The prior state of adaptation seems to have a minimal effect if the transition is SMOOTH and lasts between 5 and 30 seconds. In a preoperative evaluation with SimVis Gekko, where several designs can be tested in a short period of time, the evaluation with a 30-second SMOOTH transition will provide more stable results, making them independent of the previous state, which could be BLUR, their own correction, or another previous simulated correction.

Next steps

Although the experiments conducted in this study have given us a valuable understanding of different corrections and their adaptation, the results at close distance are not measurements, but estimations that only take into account the component of image quality. The same conditions could be directly measured at a close distance to take into account other important factors such as reading distance, convergence, visual expectations at near, or visual tasks at near. Furthermore, the lenses studied here are pure bifocal lenses with only two design parameters (energy balance and addition), while commercial designs present more complex optics. The results of this study are likely representative of commercial designs and can help to understand and interpret their perception in terms of perceptual cost at far and perceptual benefit at near.

7.5 – Conclusion

In conclusion, our experiments provide valuable insight into multifocality presentation strategies, energy balance and addition variations in vision correction using SimVis Gekko. Based on the study's findings, presenting multifocal corrections after a BLUR adaptation state, using an ABRUPT transition lasting more than 5 seconds, appears to enhance the acceptance of a wide range of corrections, particularly those with intermediate to high energy distribution in near vision. This benefit provided by the BLUR adaptation state can be matched in some way through SMOOTH transitions for 5-30 seconds. This could serve as an alternative to quickly test different corrections regardless of the previously presented state.

Furthermore, it is clear that more pronounced visual degradation occurs in corrections with low additions, which do not offer significant benefits at near distances. In addition, it has also been shown that the behavior of visual corrections can be described as a trade-off between benefit and cost that is not always linear. This helps to better understand the visual behavior provided by the different energy balances Lastly, there is a pressing need for future research that systematically controls various SV corrections (including commercial lenses) as both adaptation and post-adaptation tests using SimVis Gekko. This research would offer a deeper understanding of the neural recoding process and its potential to enhance user satisfaction with SV corrections.

Chapter 8

Short-term adaptation aftereffects induced by simulated generic and commercial simultaneous vision corrections

In this chapter, we studied the short-term adaptation aftereffects produced by different SV corrections simulated using SimVis Gekko under psychophysical experiments with clinical application. Among them, we studied the aftereffects induced by generic bifocal lenses with different parameters (energy balance and addition) and commercial lenses, including IOLs and MCLs with different designs.

The study presented in this chapter was designed and conceptualized during the research stay in Marcos Lab (University of Rochester), while the measurements with patients were conducted at the Instituto de Óptica “Daza de Valdés” (CSIC).

The author of this thesis (1) designed the experiments (in collaboration with Susana Marcos), (2) programmed the Experiment codes in Matlab (in collaboration with Victor Rodríguez-López), (3) conducted the experiments with patients, (4) collected the data (5) analyzed and discussed the results (in collaboration with all the co-authors), (6) performed the statistical analysis (in collaboration with Laura Barrios) and (7) prepared the manuscript (in collaboration with Carlos Dorronsoro and Susana Marcos).

This work is based on the original manuscript by Esteban-Ibañez et al. “Short-term adaptation aftereffects induced by simulated generic and commercial simultaneous vision corrections” in preparation. The co-authors of this scientific contribution are Victor Rodríguez-López, Enrique Gambra, Carlos Dorronsoro and Susana Marcos.

This work was presented as a poster contribution at the Association for Research in Vision and Ophthalmology (ARVO) annual meeting 2024 (Seattle, USA).

8.1 – Introduction

Simultaneous vision (SV) solutions are increasingly becoming a popular choice for correction of presbyopia, both in the form of M-IOLs and MCLs [205]. These lenses superimpose on the retina a focused and an out of focus version of the same image, in the simpler version produced by a far and a near foci of the lens. Multifocal lenses therefore increase the focal range in eyes that have lost the ability to accommodate, at the expense of reducing contrast at any given distance.

However, debate exists on the extent to which patients adapt to multifocal vision, and whether this adaptation occurs in the short-term, long-term or both. Furthermore, as lens design parameters may vary, including the percentage energy split between far, near and intermediate foci and the magnitude of the near add, and those will impact retinal image quality, a further question arises on to what extent adaptation is dependent on the actual lens design. If adaptation to SV occurs, gaining insights on the factors that influence adaptation will help to improve selection, management, and counseling of multifocal lens prescriptions.

Seminal work by Webster et al. [248,249] demonstrated the presence of aftereffects that occur following short periods of adaptation to images either artificially sharpened or blur. This short-term adaptation is explained as a rapid recalibration of the visual system to maintain constancy in spatial visual perception. Interestingly, similar recalibrations have also been shown in color vision [250]. Subsequent work has shown aftereffects following adaptation to image degradation produced by astigmatism [219] and high order aberrations [144]. Besides, subjects appear to be long-term adapted to both the magnitude and orientation of their native aberrations [236,251,252], suggesting bias to the degradation matching that produced by their own optics.

To our knowledge, the short-term neural adaptation to SV corrections has only been directly studied by Radhakrishnan et al [103]. In that prior work subjects viewed monocularly through an Adaptive Optics Visual Simulator that corrected their high order aberrations images that were digitally treated to simulate the effect of a generic pure bifocal lens. The study revealed short-term adaptation effects, which differed across energy balances and near adds. . Particularly, the largest aftereffects (at far) occurred with designs with more energy at near (energy balance 25F/75N), while adds above approximately 0.5 D produced constant aftereffects, for a given energy balance.

While this prior work provides first evidence of short-term adaptation effects to SV, the measurement conditions are very different from real settings. First, the study used convolved images to represent the effect of the lens. Although it has been shown that convolved images captured well the degradation produced by the aberrations of the eye [253,254], and by optical treatments [103,255], they fail at capturing the effect of interactions between the lens design and the natural aberrations of the eye and . between chromatic and monochromatic aberrations [254]. Second, pure SV corrections represent a generic lens where near and far

corrections combine across the entire pupil, but they do not represent any specific lens profile. Instead, visual simulators have been shown to mimic realistically the actual through focus optical performance, and/or spatial lens profile, including those commercially available. Third, the previous work was performed in a monocular bench-top adaptive optics visual simulator, with around 2-deg visual stimuli. However, for SV simulations in a more realistic environment, a binocular approach with a wider visual field would be required.

The SimVis Gekko has previously demonstrated in this thesis (chapter 7) to be particularly useful for conducting psychophysical experiments with clinical applications due to its design as head-mounted device offering a wide visual field. Furthermore, since the optotunable lenses are fully programmable, it is possible to expose the eye to rapid changes in visual experience through a sequence of lenses, allowing both a rapid testing of different treatment options in the clinic, implementation of psychophysical paradigms aiming at testing visual performance, perceived visual quality, and, as in the current study, spatial neural adaptation with different lens designs. In a previous study, simulated pure bifocal lenses with different energy balances and near additions were perceptually evaluated after a period of blur adaptation (3.00 D) [238]. SimVis Gekko can not only simulate generic lenses, but it can also be programmed to replicate the optical quality of commercial SV lens models [154,156], that can be used binocular in adaptation experiments, under natural aberrations, and in clinical environments.

The primary purpose of this study is to assess the short-term adaptation aftereffects of generic and commercial SV lenses, utilizing the binocular simulator SimVis Gekko to simulate the lens profiles in an adaption study, as well as blur in images uses as tests in the psychophysical paradigm. We investigated adaptation aftereffects and the relation between the magnitude of the effect and lens design parameters. In a second experiment, we evaluated the shifts in the perceptual judgments of image quality following a short period of adaptation to SV lenses.

8.2– Methods

8.2.1– Subjects

Six subjects participated in this study, that involved two psychophysical experiments. The data related to these subjects is collected in Table 8.1. The subjects (three myopes, one hyperope and two emmetropes with refractive error ranging from +2.25 D to -6.00 D) had an average age of 29.7 ± 5.2 years.

Exclusion criteria included astigmatism greater than 1.25 D, severe systemic diseases, a history of ocular surgery, or any ocular pathology.

Table 8.1. Age, gender, and ocular parameters of the subjects, including the evaluated eye and refractive error (Sphere, Cylinder and Axis).

Subject	Age (y)	Gender	Evaluated Eye	Refractive Error (D, D, deg)
S#1	28	M	Both	OD: +2.25
				OS: +1.00
S#2	40	M	Both	OD: -6.00 – 1.00 x 40
				OS: -6.00 – 1.25 x 110
S#3	29	M	Both	OD: -4.50 – 0.75 x 20
				OS: -5.50 – 0.75 x 165
S#4	26	F	Both	OD: +0.25
				OS: +0.25
S#5	28	F	Both	OD: -4.50 -0.50 x 170
				OS: -3.25 -1.00 x175
S#6	27	F	Both	OD: -0.25
				OS: -0.25

The research protocol adhered to ethical guidelines and was approved by the Ethics Committee of the Consejo Superior de Investigaciones Cientificas (CSIC) and was performed in agreement with the Declaration of Helsinki. Prior to the enrollment, all subjects were given a thorough explanation of the study's objectives and provided their informed consent in writing.

The total duration of the study ranged between 4 and 5 hours distributed in three sessions with the necessary pauses on three days close to each other. These sessions comprised an optometric exam and two psychophysical experiments.

8.2.2– Apparatus: SimVis Gekko visual simulator

The SimVis Gekko visual simulator was used in two psychophysical experiments simulating both generic bifocal lenses and commercial SV lenses, including IOLs and CLs.

Subjects, wearing the SimVis Gekko on their head, were seated in a chair and positioned in a chin rest, looking towards the stimulus screen placed 2 m away. The accommodating vergence amount (0.50 D) was compensated in both experiments.

8.2.3– Stimulus

The stimulus presented in both experiments was a grayscale face image subtending an angle of 4x4 degrees and was used both during the adaptation period and the test. The stimulus was displayed on a calibrated 4K TV screen with gamma correction. During adaptation the stimulus was jittered (randomized movements within a range of ±3 pixels in the horizontal and /or vertical direction, every 20 ms) to avoid local light adaptation [219,236,256]. A complete description of the stimulus sequence in combination with simulated conditions for each experiment is described in Section 8.2.4.

8.2.4– Experiments

The two experiments conducted in this study followed a similar sequence of stimuli, adaptation and test presentations. The main difference between experiments was the psychophysical task performed by the subjects. In Experiment 1 subjects performed a 2AFC task with a QUEST paradigm to find the threshold between sharp and blur. In Experiment 2 they made direct perceptual judgements of image quality.

Experiment 1

Adaptation conditions

Twenty different SimVis Gekko lens simulations were used as adaptation conditions in Experiment 1, that were shown for 60 s before each experimental run (explained in detail later).

These adaptation conditions included 4 generic bifocal lenses with different energy balance % for Far(F)/Near(N) (100F/0N, 75F/25N, 50F/50N and 25F/75N), with 5 near addition values (0.50, 0.75, 1.50, 2.25 and 3.00 D). The 100F/0N in fact represents a monofocal lens, with all the energy for far.

Additionally, 4 commercial SV lenses were utilized: Trifocal diffractive IOL (representing the FineVision by PhysIOL/BVI, FV), a non-diffractive EDoF IOL (Vivity by Alcon Research Labs, VV), a center near refractive MCL with Low Addition (MyDay Low addition by CooperVision, MDL) and high addition MCL (MyDay High addition by CooperVision, MDH). These lenses were simulated considering a pupil size of 3.4 mm for commercial IOLs and 4 mm for commercial MCLs.

Test conditions

The test conditions (i.e. sequence of images presented in a QUEST algorithm with 20 trials in Experiment 1) were a sequence of 20 simulated generic pure bifocal lenses, with the energy balance (Energy at far/Energy at near) varying between 100F/0N and 0F/100N, in1% steps. The corresponding near adds (0.50, 0.75, 1.50, 2.25 and 3.00 D) matched the near add of the adaptation image. For the test of adaptation to commercial SV lenses, the near add of the test image were 0.75, 1.50 and 3.00 D.

Experimental procedure

In Experiment 1 (see experimental overview in Figure 8.1), subjects adapt for 60 s to a given lens (see Adaptation conditions) Then, they judge the perceived quality of a sequence of images (see Test conditions), in a 2AFC task (image too sharp or too blurred) using a Bayesian adaptive psychometric algorithm (QUEST) [179,180], which proposes the energy balance (test condition) for each new trial, considering the history of responses of the subject in each experimental run. After 20 trials, the algorithm provides the Energy Balance Threshold, i.e. the energy distribution far/near that produces a neutral image quality perception (i.e. neither too sharp nor too blurred).

Each condition was evaluated in a different experimental run, with a total of 32 randomized conditions (adaptation + test). Each experimental run (Figure 8.2) begins with 60 s of short-term adaptation to an adaptation condition (vision through a simulated lens using SimVis Gekko). The stimulus is presented with randomized jitter (3 pixels of randomized displacement). After the adaptation, the stimulus is then replaced by a gray background for 0.5 seconds. Subsequently, the test simulation is introduced, and a static stimulus was shown for 0.5 s, after which, the subject has a 1 s interval, signaled by acoustic signals, to answer whether the presented stimulus is perceptually SHARP or BLURRED (2AFC). Once the subjects make the judgement, the QUEST algorithm calculates the next test condition. If the subject's response was SHARP, the far energy in the bifocal balance decreases for the next trial, whereas if it was BLURRED, the far energy increases. In between trials there was a re-adaptation period of 3 s.

The procedure for each experimental run was repeated for the different adaptation conditions (See Figure 8.1).

Beyond the Energy Balance Thresholds (provided by the QUEST algorithm), other metrics obtained from the set include the Perceived Image Quality Threshold (PIQT) and the Perceived Degradation Thresholds (PDT). PIQT is defined as the percentage of far vision and near vision in a bifocal lens required to perceive blur neutrality. PDT is defined as 100 - PIQT. The Shift in the Perceived Degradation Threshold (SPDT) is calculated as the adaptation aftereffects for each adaptation condition, considering the adaptation to a monofocal lens (100F/0N) as the baseline.

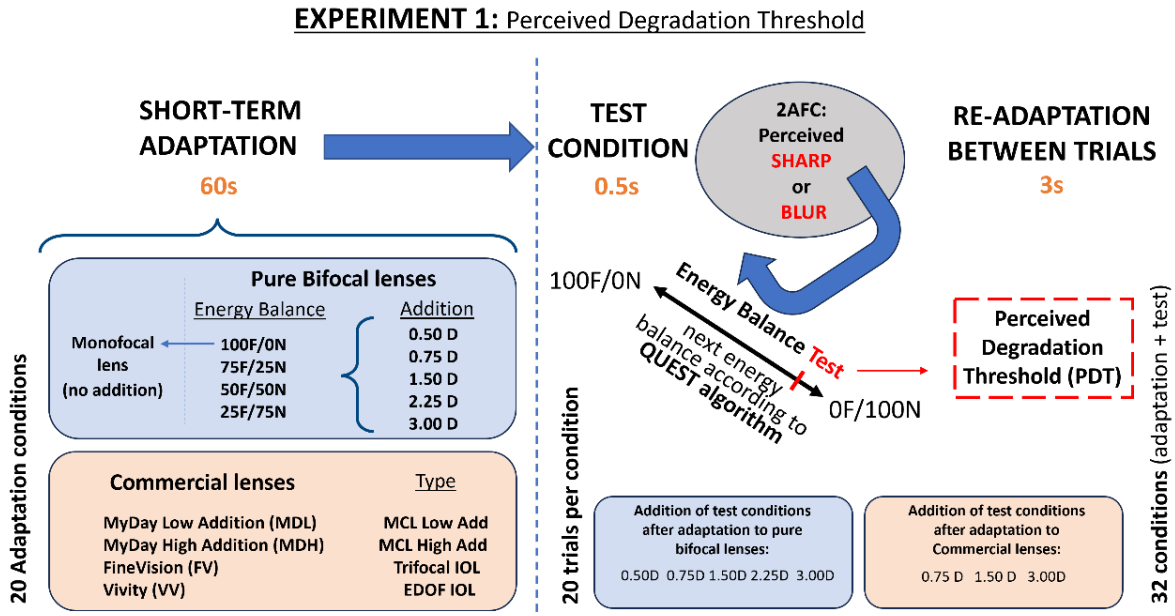

Figure 8.1. Flowchart conditions assessed in Experiment 1: Perceived Degradation Threshold (PDT). *The left side of figure represents the short-term adaptation (60s) conditions for different simulated lenses: the monofocal lens and bifocal lenses block (blue color) and commercial lenses block (orange color). The right side represents the test section and its bifocal correction conditions. The energy balance in the bifocal test correction was varied according to QUEST responses of the subject (perceived SHARP or BLUR image). The near addition test was 0.50, 0.75, 1.50, 2.25 and 3.00 D for monofocal lens and bifocal lenses and 0.75, 1.50, and 3.00 D for commercial lenses. 3s of top-ups re-adaptations was introduced after each 2-AFC of the QUEST (20 trials). A total of 32 randomized conditions (combination of adaptation + test) were evaluated.*

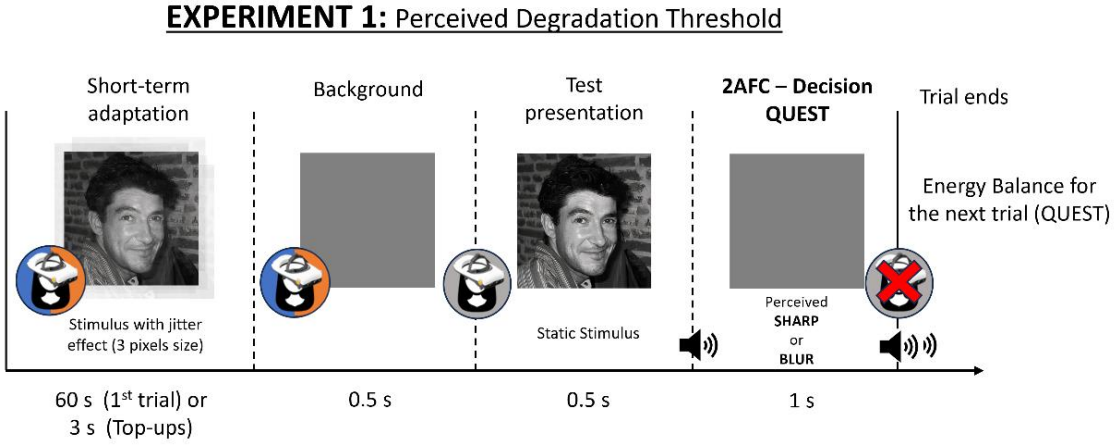

Figure 8.2. Sequence for each QUEST trial in Experiment 1: Perceived Degradation Threshold (PDT). *Characteristics of stimulus showed in each trial and the type of simulation with SimVis Gekko (described by orange/blue and gray icons, representing pure bifocal lenses/commercial lenses and test corrections, respectively). The subject adapts for 60 s to a given lens, while looking at the stimulus through the system simulating the lens. The stimulus is jittered (3 pixels size); 3 s re-adaptation are given between subsequent trials. The stimulus is removed maintaining the simulated adaptation during 0.5 s. Then, the simulated test correction (gray icon) is introduced, and the static stimulus is presented for 0.5 s. The stimulus is removed, and the subject has to respond if it was perceived SHARP or BLUR (2AFC) in an interval of 1 s defined by sound signals. After that the test simulation ends. Considering the 2AFC responses, QUEST determines the energy balance for next trial.*

Experiment 2

Experiment 2 mirrored the sequence of stimuli and simulation presentations from Experiment 1, but the task was based on perceptual judgements, as depicted in Fig. 8.3.

Adaptation conditions

Only the monofocal lens and the commercial SV lenses were simulated as adaptation conditions.

Test conditions

In experiment 2, the test conditions involved generic bifocal lenses simulated with energy balance of 75F/25N, 50F/50N and 25F/75N and near additions of 0.75, 1.50 and 3.00 D.

Experimental procedure

Each condition, which includes both adaptation and the test, consisted of 5 randomized repetitions of perceptual scores evaluation from 0 (blur) to 10 (sharp) in steps of 1 perceptual point. These judgements followed the sequence illustrated in Fig. 8.4. The 9 test conditions were evaluated for the 5 adaptation conditions, with a total of 45 conditions.

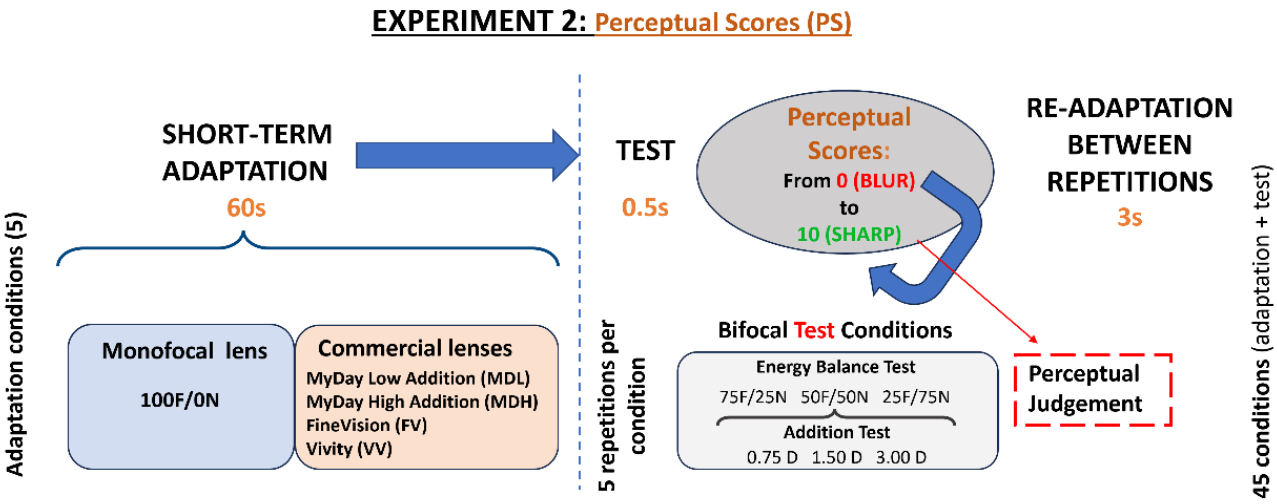

Figure 8.3. Flowchart of conditions tested in Experiment 2: Perceptual Scores (PS). *The left side of figure represents the short-term adaptation (60 s) section for different simulated lenses: the monofocal lens (blue color) and commercial lenses block (orange color). The right side represents the test section and its bifocal correction conditions. The energy balance in the bifocal test correction was 75F/25N, 50F/50N and 25F/75N. The near adds in the test conditions were 0.75, 1.50, and 3.00 D for monofocal lens and commercial lenses. 3 s of top-ups re-adaptations were introduced after each perceptual judgement (5 repetitions). A total of 45 randomized conditions (combination of adaptation + test) were evaluated.*

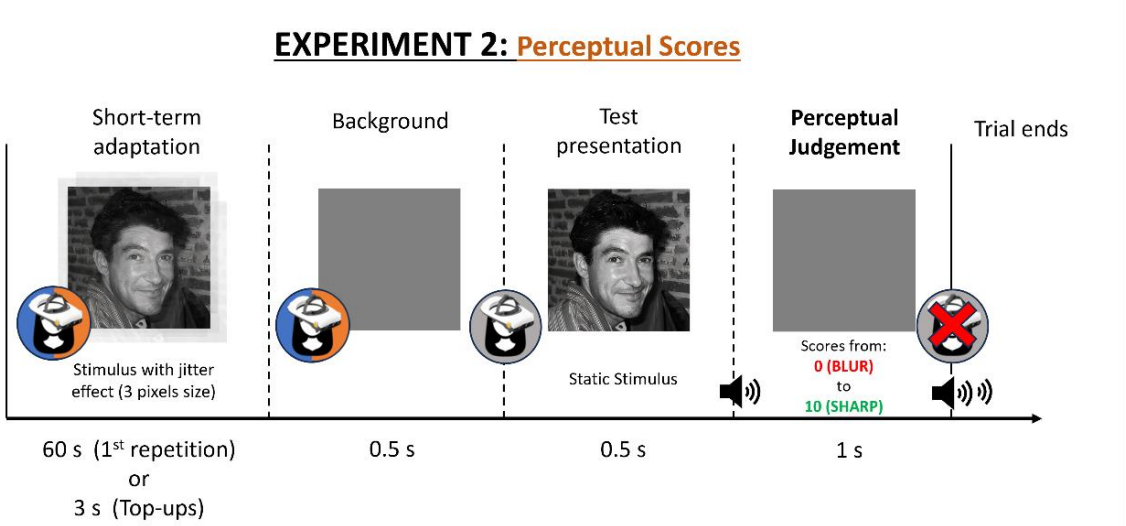

***Figure 8.4. Sequence for each QUEST trial in Experiment 2: Perceptual Scores (PS)**. Characteristics of stimulus and the type of simulation with SimVis Gekko (described by orange/blue and gray icons, representing pure bifocal lenses/commercial lenses and test corrections, respectively). The subject adapts for 60 s to a given lens, while looking at the (jittered) stimulus through the system simulating the lens. The stimulus is removed maintaining the simulated adaptation during 0.5 s. Then, the simulated test correction (gray icon) is introduced, and the static stimulus is presented for 0.5 s. The stimulus is removed, and the subject judges the perceived image from 0 (BLUR) to 10 (SHARP) in an interval of 1 s defined by sound signals. After that the test simulation ends.*

After 60 s of adaptation, with monofocal lens or with commercial multifocal lenses, the test presentation is shown for 0.5 s, and then the subject provides the perceptual score during a 1s interval. For each of the 5 adaptation conditions, there were 9 test conditions (3 additions and 3 energy balances) with 5 repetitions separated by 3 s readaptation periods (225 perceptual judgements in total).

The results of the adaptation to monofocal at all the evaluated test conditions were used as baseline for calculating the Shift in Perceptual Scores (Shift_PS) for the other adaptation conditions.

The entire process of both experiments was controlled by Psychtoolbox [182–184] in Matlab. This provided synchronization between SimVis Gekko simulations, stimuli presentation, and the collection of QUEST responses and Perceptual Scores.

8.2.5– Statistical analysis

Data from Experiments 1 and 2 were analyzed using IBM SPSS Statistics Version 28 (IBM Corp, USA). Descriptive statistics, including the mean SPDT and Shift_PS across subjects, standard deviations and 95% confidence intervals, were reported for the entire dataset, taking into account each adaptation and test condition for both experiments.

In our experiments, which involved repeated measurements, we employed a mixed-effects linear model [241] with SPDT and Shift_PS as the dependent variable for Experiment 1 and 2, respectively.

For Experiment 1, the model included fixed effects such as adaptation lens and near addition test. The random effect considered was 'Subject'. Additionally, we conducted pairwise comparisons, taking into account (1) near addition of test and comparing each adaptation lens and (2) adaptation lens comparing with each near addition test. These analyses allowed us to determine the significance and impact of the different conditions on adaptation aftereffects.

In Experiment 2, the model included as fixed effects the adaptation lens, far energy balance of test and the near addition test, with 'Subject' as the random effect. Furthermore, we conducted pairwise comparisons, considering the adaptation lens and comparing each near addition of test.

Throughout our analysis, we applied a significance level of $p<0.05$ to define statistical significance.

8.3– Results

8.3.1– Experiment 1

The QUEST algorithm followed in Experiment 1 provides the energy at far defining the PIQT between sharp and blur. Fig. 8.5A shows those thresholds for the baseline condition of adaptation - 60 seconds of adaptation to monofocal lens 100F/0N -, for the 5 near additions of the bifocal tests and the 6 subjects.

Figure 8.5B shows the corresponding PDT for Monofocal adaptation (the amount of near energy -or energy reduction- at far producing the threshold image degradation).

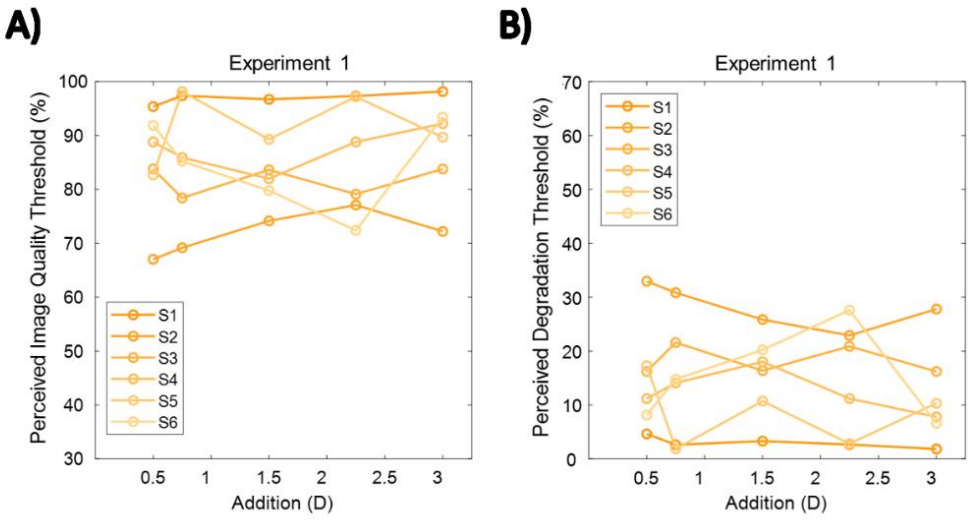

Figure 8.5. Results of Experiment 1 for monofocal lens adaptation (baseline) and the 5 near addition of the test for each subject: *(A) Perceived Image Quality Threshold (%) (PIQT) obtained by QUEST and (B) Perceived Degradation Threshold (%) (PDT) derived from results showed in A (100 – PIQT (%)).*

These results will serve as baseline for calculating the SPDT for other adaptation conditions, and each subject.

The results reveal a strong perceptual variability among subjects. The minimum PDT (Fig. 8.5 B) is observed in Subject 1 for the bifocal test with near addition of 3.00 D (1.83 %), while the maximum is found in Subject 2 for a bifocal test near addition of 0.5 D (32.96 %). The average PDT across near addition values and subjects was 14.30 ± 9.76 % for monofocal (100F/0N) adaptation.

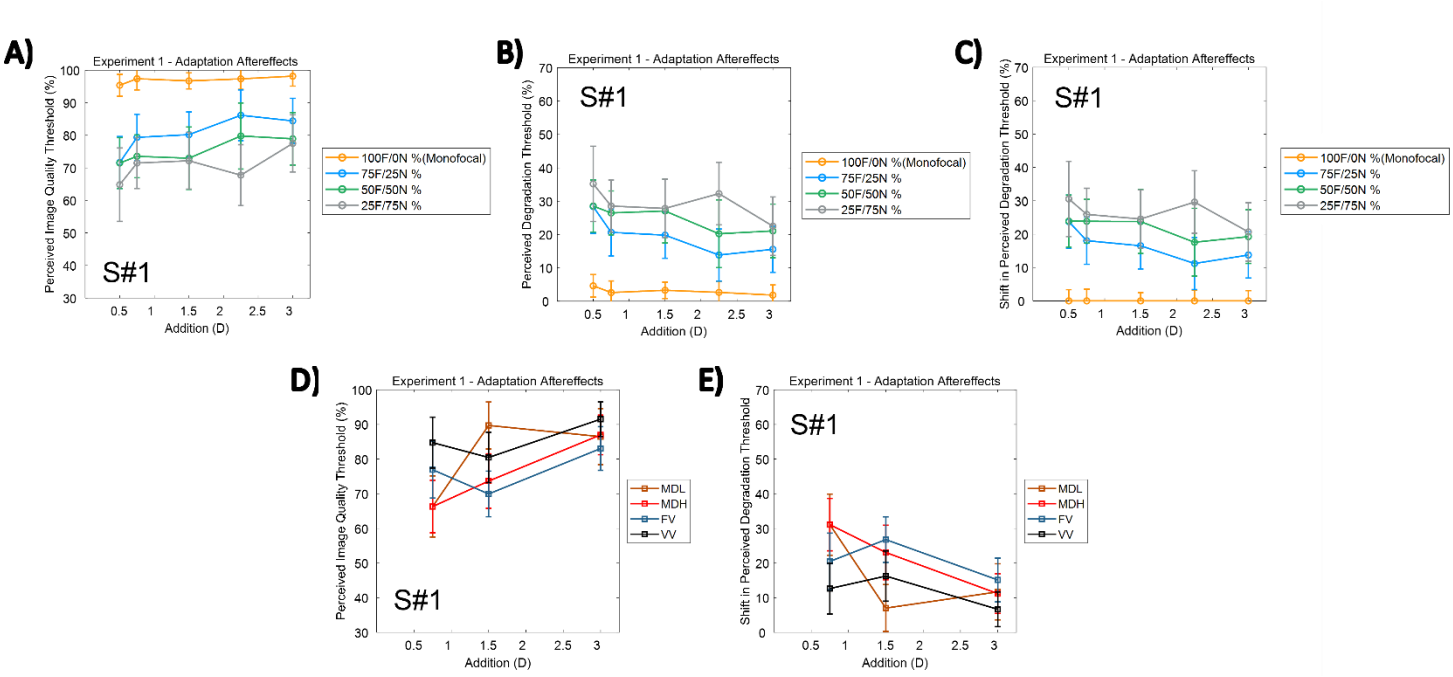

Figure 8.6. Results of Experiment 1 of one subject (S#1): *(A) Perceived Image Quality Threshold (%) (PIQT), (B) Perceived Degradation Threshold (%) (PDT) and (C) Shift in Perceived degradation Threshold (%) (SPDT; PIQT (%) – Monofocal Lens) for monofocal and generic bifocal adaptations, while (D) PIQT (%) and (E) SPDT (%) for commercial SV lenses adaptations. The error bars represent the estimated standard deviation provided by the QUEST algorithm for each condition.*

Figure 8.6 presents examples in one subject (S#1) of Experiment 1 results for all measured conditions. The error bars represent the estimated standard deviation provided by the QUEST for each combination of adaptation and test.

Panels A, B and C represent the results of using monofocal lens and pure bifocal lenses as adaptation conditions. Panel A shows the PIQT (%) obtained directly from Experiment 1 for each adaptation lens (represented by different color data series) and near addition test (different data points in x-axis). The PDT (%) are represented in panels B, and Panel C shows the SPDT (%) calculation (derived from PIQT and applying the monofocal lens as baseline,

respectively). The bottom row illustrates the results for adaptation to commercial lenses: PIQT (%) in panel D; and SPDT (%) in panel E.

Figure 8.7 summarizes the adaptation aftereffects (mean SPDT across subjects) for monofocal and bifocal lenses (A) and commercial SV lenses as adaptation (B). The bars represent the 95% confidence interval for each combined condition (adaptation + test).

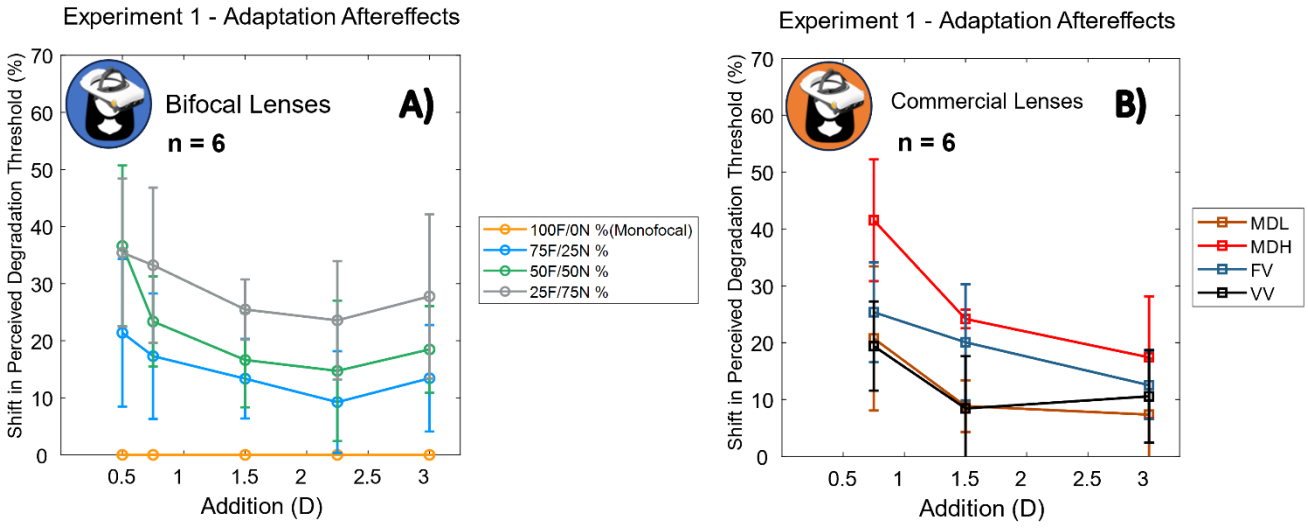

Figure 8.7. Adaptation aftereffects (SPDT) averaged across subjects in Experiment 1 for: *(A) generic bifocal lenses represented with circles (energy balances of 75F/25N, 50F/50N and 25F/75N %) and (B) commercial SV lenses (MDL, MDH, FV and VV) with squares. The near addition test was the same as adaptation for bifocal lenses (0.5, 0.75, 1,50, 2.25 and 3.00 D), while the near addition test for Commercial lenses was 0.75, 1.50 and 3.00 D. The error bars represent the 95% confidence interval for each condition.*

The largest SPDT aftereffects, in monofocal lens and bifocal lenses (panel A), were produced by the energy balance 25F/75N (29.09 ± 11.40 %; averaged across near addition of tests), the condition with more blur, and the near additions 0.5D (31.10 ± 13.90%; averaged across energy balance of adaptation), the lowest addition. The largest SPDT aftereffects produced by adaptation to commercial SV lenses (panel B), were found for lens MDH (27.71 ± 13.1 % averaged across near addition of tests; and the maximum value was obtained for 0.75 D, the lowest near addition test).

All the conditions produced adaptation aftereffects significantly different from zero ($p<0.05$). The adaptation lens and the near addition test were significant statistical factors influencing the aftereffects measured by SPDT ($F = 11.64$, $p < 0.01$ and $F = 11.38$, $p < 0.01$, respectively). The different adaptation lenses induced pairwise significant differences in adaptation aftereffects between 0.75 D and 1.50 D near additions ($p<0.01$; t-test). Pairwise comparisons between lenses for near addition 0.75 D revealed statistically significant

differences between MDH and both VV and 75F/25N % ($p < 0.05$). For 1.50D there were significant differences between MDL, and both MDH and 25F/75N % ($p < 0.01$).

On the other hand, the different near addition tests produced significantly different adaptation aftereffects for the adaptation lenses FV and MDH ($p<0.05$). Pairwise comparisons considering these adaptation lenses showed statistically significant differences between the near addition test of 0.75 D and 3.00 D ($p<0.05$) for FV and between the near addition test of 0.75 D with 1.50 D ($p<0.05$) and 3.00 D ($p<0.01$) for MDH, respectively.

8.3.2– Experiment 2

Figure 8.8 presents the results of adaptation aftereffects (mean Shift_PS across subjects), obtained in Experiment 2 from perceptual scores, vs energy balance of bifocal test. Each panel represents a different value of near add in the bifocal test: A) 0.75 D; B) 1.50 D; C) 3.00 D. Each data series (colored line) corresponds to an adaptation lens. The bars denote the 95% confidence interval for each condition (adaptation + test).

The maximum Shift_PS was observed for MDH adaptation with bifocal test condition of 50F/50N % and 1.50 D (4.13 ± 3.2 PS). Experiment 2 revealed significant Shift_PS for MDH (2.7 ± 2.2 PS) and FV (2.0 ± 1.2 PS) with 1.50 and 3.00 D near addition test conditions (averaged across energy balance of bifocal test).

The adaptation aftereffects, as determined by Shift_PS, indicated significant influence of the adaptation lens and energy balance of bifocal test ($F = 3.53$, $p<0.05$ and $F = 6.30$, $p < 0.01$) but not for near Addition test ($F = 1.06$, $p = 0.34$) A significant adaptation aftereffect was induced by different energy balances of the bifocal test for MDL when evaluated with near addition test of 3.00 D ($p = 0.02$). Pairwise comparisons considering these energy balances of the bifocal test revealed statistically significant differences between 25F/75N and 50F/50N % ($p<0.05$) for MDL adaptation and 3.00 D of near addition test.

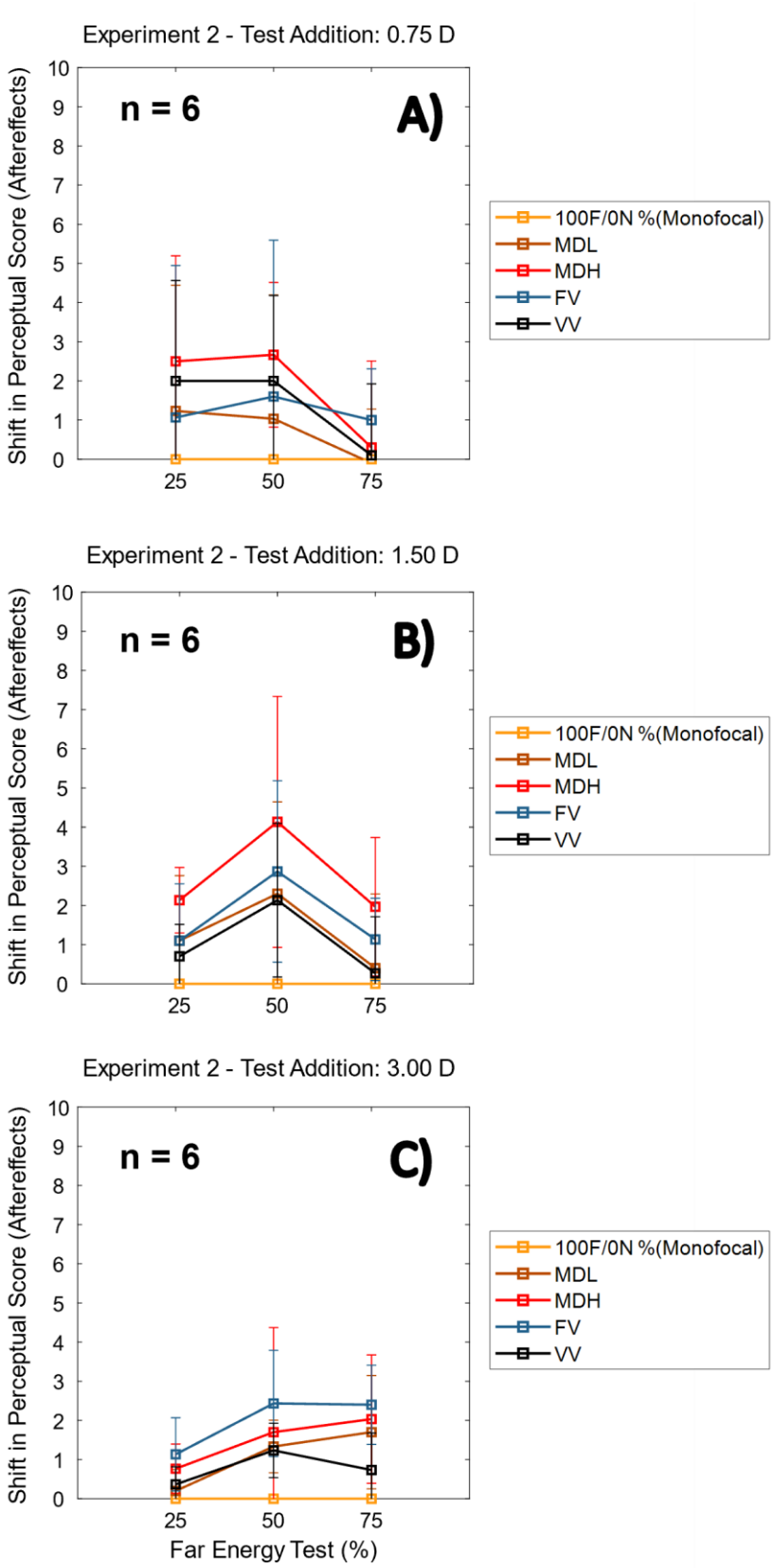

Figure ***8.8. Adaptation aftereffects (Shift_PS) averaged across subjects in Experiment 2 for commercial SV lenses (MDL, MDH, FV and VV) represented with squares****. Each graph represents different near addition test: (A) 0.75 D, (B) 1.50 D and (C) 3.00 D. Three different energy balances for bifocal test (25F/75N, 50F/50N and 75F/25N %) are represented for each near addition value. The error bars represent the 95% confident interval for each condition.*

8.4 – Discussion

In this study, two different psychophysical tasks were conducted to study the short-term adaptation aftereffects induced by both simulated generic bifocal lenses and commercial SV lenses using the clinical visual simulator SimVis Gekko. Experiment 1 employed an adaptive method based on energy balance (a key design parameter of bifocal lenses) and a simple 2AFC question (Sharp or blurred vision?) to find shifts in the neutral amount of blur after adaptation. Experiment 2 used perceptual scores after adapting to commercial SV lenses to find similar shifts but using bifocal test with different energy balances and near addition amounts.

The results of Experiment 1 revealed important differences across subjects in PIQT for monofocal lens adaptation (baseline adaptation condition), but there was a tendency to maintain similar values despite variations in the near addition of bifocal test images (Figure 8.5). In other words, the subjects exhibited differences on vertical offsets, suggesting a varying degree of blur tolerance, barely affected by addition. Although the subjects with the highest (S#2) and lowest (S#1) blur tolerance are highly myopic and hyperopic, respectively, there was no clear trend according to the refractive error as was seen in other studies with larger samples [257]. Personality effects have also been investigated to respond to the blur tolerance effect [258] and may play a role in this study.

Significant Adaptation aftereffects (SPDT) were observed for all generic and commercial SV lenses in Experiment 1 showing different levels of adaptation (Fig. 8.7). In our analysis of generic bifocal lenses (Fig. 8.7 A), we found that the energy balance in the adaptation correction was the attribute that most significantly influenced the adaptation process. Larger aftereffects shifts occurred when the energy balance had more percentage at near with a maximum of 29.09 ± 11.40 % for 25F/75N % across all near addition values.

Furthermore, a trend toward larger aftereffects shifts was observed for low near additions, reaching its maximum value for 0.5 D across different energy balance (31.10 ± 13.90 %). These results suggest a relationship between aftereffects and retinal image degradation. The visual degradation observed with low additions may be explained by the interaction between closely spaced foci, where a sharp image superimposes to a blurred, but still structured image, in comparison with higher adds that produce a lower contrast pedestal to the sharp image [103,244].

The data series for each energy balance in the adaptation, which varied with near add values, exhibited similar shapes but with vertical offsets. However, SPDT did not vary systematically with near adds. Notably, shifts between 50F/50N % and 25F/75N % were more pronounced than those between 75F/25N % and 50F/50N %. While our results aligned with Radhakrishnan et al.'s findings [103] regarding energy balance in the adaptation (highest aftereffects for 75F/25N % SV lenses), differences emerged in the SPDT variations with near adds values. Our findings show that SPDT is highest at 0.50 D, decreased for intermediate values and increased for high additions (3.00 D). In contrast, Radhakrishnan et al. observed

the greatest shift in NPF at 0.50 D, which remained constant for values up to the highest (1.50 D). These variations may be attributed to the variable used in the QUEST method. In the current study, we used bifocal lenses with different far/near energy balance, and same near add, while the prior study used pure blur varying magnitude of defocus. Other major methodological differences included simulated images produced by convolution in Radhakrishnan et al, as opposed to optically in a see-through configuration in the current study, monocular vs binocular and difference visual field, may have also played a role in the differences between the studies.

In Experiment 1, the adaptation to commercial SV lenses (Fig. 8.7 B) mirrored the behavior of generic SV lenses, considering a specific energy balance. However, the near addition of commercial lenses differed from that used in the bifocal test. The highest SPDT values were obtained for MDH and FV, while MDL and VV presented similar behavior among them, with more modest aftereffects. When compared to generic SV lenses, MDH, FV and MDL-VV presented a closer behavior to 25F/75N %, 50F/50N % and 75F/25N %, respectively. This comparison is expected when considering the lens designs: (1) MDH has a relatively high energy content at near, particularly for 4-mm pupils (described in Chapter 3), (2) FV has three foci with approximately the half of its energy at far and the remaining distributed between intermediate and near distances [259,260] (it varies according to pupil diameter), (3) MDL exhibits a smooth variation from +0.5 to -0.25 D for 4 mm (described in Chapter 3), and (4) VV has the its main peak at far with an enhanced range up to 2.50 D but with less energy percentage [261,262].

The pairwise comparisons of mixed linear models are consistent with these qualitative predictions. MDH (considered as 25F/75N %) showed statistically significant differences with VV and 75F/25N % for 0.75 D near addition, and MDL (considered as 75F/25N %) differed significantly from MDH and 25F/75N % for 1.50 D near addition.

Experiment 2 (Fig. 8.8) revealed aftereffects following adaptation to all commercial SV lens designs, with higher values observed for those that have more energy in the near focus or foci (MDH and FV). MDH and FV produced higher aftereffects when the series of bifocal test images had a near add close to the near focus of that of the adapting commercial lens. In other words, the shift in perceptual score was larger when evaluating a similar addition to the one to which subject was adapted to, suggesting a neural recoding for each adaptation lens.

Moreover, all commercial SV lenses presented the same trend with larger effects for a far energy balance of 25-50 % in the test correction and near add of 0.75 D, a far energy balance of 50 % in the test correction and near add of 1.50 D and a far energy balance of 50-75 % and near add of 3.00 D, in general terms.

In summary, we analyzed the adaptation aftereffects of generic bifocal and commercial SV lenses using SimVis, gaining a comprehensive understanding of how these adaptation aftereffects function. These aftereffects are primarily driven by conditions that produced a higher degradation for all lenses: an energy balance with a higher percentage at near and low

additions. However, a neural recoding appears to occur for each adaptation lens, as it seems to yield higher aftereffects when the test presents the same condition as the adaptation.

8.5 – Conclusion

In conclusion, the largest short-term adaptation aftereffects result from lenses with highest % energy at near and lower near addition and occurred also with commercial designs though the interaction between these parameters varied individually. Adaptation is most effective on test images with matching near addition magnitudes, highlighting the impact of lens design on both visual function and adaptation to optimize outcomes.

Chapter 9

Conclusions

This thesis was divided into three main sections: the first part described the process to obtain and validate MCLs simulations from in-vitro measurements and how to use SimVis Gekko to implement these simulations not only for replicating the current Fitting Guides of commercial MCLs, but to improve the lens selection (Chapters 3 and 4); the second part described the development of new functionalities of SimVis Gekko aiming at improving the evaluation of visual function tests through the synchronization of SimVis Gekko with MLA app and the implantation of astigmatism correction systems based on Stokes Lens principle (Chapter 5 and 6); and the third part described the perceptual effect that induces different adaptation conditions in the presentation of bifocal corrections and the short-term aftereffects produced by generic and commercial SV corrections (Chapters 7 and 8). The results of this thesis have an impact on contact lens practice for presbyopia, on the potential to improve the fitting process and the visual performance evaluation, and on understanding better the neural processes that play a role in the adaptation.

The main accomplishments of this thesis are:

1. The development of a computational and experimental method to calculate the TF-VS that makes possible the obtention of SimVis simulations of any MCL from *in-vitro* measurements of its power profile.

2. The implementation of these MCLs simulations as replication of the Fitting Guides enabling the evaluation of each combination of steps considering the near addition.

3. The development and evaluation of a novel 3D-VA metric aimed at improving the personalized selection of commercial MCLs, based on the measurement of visual acuity at different distances and on the subjects' visual lifestyle preferences.

4. The synchronization between SimVis Gekko and MLA App to speed up the evaluation in the clinical practice of different visual function tests, such as Visual Acuity and Contrast Sensitivity defocus curves, in an automated and efficient way using Adaptive Methods.

5. The development and calibration of an automated and motorized Stokes Lens System to be integrated into the SimVis Gekko modules, enabling to correct and induce different magnitudes and axis of astigmatism.

The specific conclusions of this thesis are:

1. The visual performance obtained with the MCL simulations of SimVis Gekko obtained using in-vitro measurements demonstrates good agreement compared to real MCLs across subjects for all designs, additions and refractive errors.

2. The implementation of all the Fitting Guides steps in SimVis Gekko using the 3D-VA metric would enable to improve the satisfaction on MCLs wearers from 72.92 % (only subjects that choose the FG step considering its addition) to a minimum of 91.67 % (including also subjects that choose other step prescribed by SimVis Gekko). This increment has the potential to enhance the adoption of MCLs among the presbyopic population.

3. The use of SimVis Gekko in conjunction with the MLA App is an effective method to perform defocus curves that reduces the exploration time of various visual tests, especially for Visual Acuity. This reduction could enable the evaluation of more combinations of multifocal designs in the same period than the traditional methods.

4. The Stokes Lens System characterization demonstrates the accuracy and reliability of this automatized and motorized approach under most of the conditions tested.

5. The calibration method of astigmatism axis, based on an image processing algorithm using the Optical Quality Bench located in the company, is comparable to the lensmeter calibration and it enables to calibrate the Stokes Lens System integrated in the SimVis Gekko modules in production processes.

6. The presentation of multifocal corrections after a BLUR adaptation state, using an ABRUPT transition lasting more than 5 s, enhances the acceptance of a wide range of corrections, particularly those with intermediate to high energy distribution in near vision.

7. This benefit can be matched through SMOOTH transitions of 5 and 30 s, serving as an alternative to quickly test different corrections regardless of the previously presented state.

8. The behavior of multifocal corrections can be described as a trade-off between benefit and cost that can help to better understand the visual performance provided by the different energy balances.

9. The more pronounced visual degradation occurs in corrections with low additions, but it does not offer significant benefits at near distances.

10. The most significant short-term adaptation aftereffects are observed with lenses that have the highest percentage of energy at near distances and lower near addition in generic lenses. This behavior occurred also with commercial lenses though the interaction between these parameters varied individually.

11. The adaptation aftereffects are most effective on test images with matching near addition magnitudes, highlighting the impact of lens design on both visual function and adaptation to optimize outcomes.

Scientific activities during this thesis

1. Scientific publications related to this thesis

1. E. Esteban-Ibañez, D. Montagud-Martinez, L. Sawides, A. Zaytouny, A. de Castro, I. Sisó-Fuertes, X. Barcala, D.P. Piñero, W.D. Furlan, C. Dorronsoro, E. Gambra. Simulation of daily soft multifocal contact lenses using SimVis Gekko: from in-vitro and computational characterization to clinical validation. *Sci Rep*, 8592 (2024). https://doi.org/10.1038/s41598-024-59178-1.

2. E. Esteban-Ibañez, Y. Marrakchi, L. Sawides, E. Gambra, C. Dorronsoro. Perceived image quality of natural video sequences through simulated bifocal corrections: effect of energy balance and adaptation state. *In preparation.*

3. E. Esteban-Ibañez, V. Rodríguez-López, E. Gambra, C. Dorronsoro, S. Marcos. Short-term adaptation aftereffects induced by simulated generic and commercial simultaneous vision corrections. *In preparation.*

4. E. Esteban-Ibañez, A. Molina-Martín, E. Martínez-Plaza, C. Dorronsoro, E. Gambra, D.P. Piñero. Improving replication of multifocal contact lenses fitting guides through SimVis Gekko in a clinical environment. *In preparation.*

2. Other scientific publications

1. V. Rodríguez-López, A.M. González-Ramos, E. Esteban-Ibañez, S. Marcos, E. Martinez-Enriquez. *In vivo* assessment of multifocal contact lens fitting based on anterior segment optical coherence tomography. *In preparation.*

3. Patents

1. WO2023/237691, E. Gambra, C. Dorronsoro, X Barcala, I Sisó-Fuertes, J.R. Alonso, M.P. Urizar, E. Esteban-Ibáñez, V. Rodríguez-López, S. Marcos. Binocular see-through vision device for far and near distances. June 8th, 2022. Ownership: 2EyesVision SL and CSIC. Status: PCT-extended.

4. Conferences

Personally presented

1. E. Esteban-Ibañez, V. Rodríguez-López, E. Gambra, C. Dorronsoro, S. Marcos. Short-term adaptation to simulated multifocal lenses. ARVO Annual Meeting 2024 Seattle (USA, 2024). *Poster contribution.*

2. E. Esteban-Ibañez, D. Montagud-Martinez, L. Sawides, A. Zaytouny, A. de Castro, I. Sisó-Fuertes, D.P. Piñero, W.D. Furlan, C. Dorronsoro, E. Gambra. Simulación de lentes de contacto multifocales blandas diarias: de la caracterización computacional basada en medidas *in-vitro* a la validación clínica. OPTOM 2024 (Spain, 2024). *Oral contribution.*

3. E. Esteban-Ibañez, A. Zaytouny, Y. Marrakchi, X. Barcala, I. Sisó-Fuertes, M. Rodríguez-Vallejo, J. Fernández, E. Gambra, C. Dorronsoro. Validación de la medida automática y optimizada de curvas de desenfoque de agudeza visual y sensibilidad al contraste. OPTOM 2024 (Spain, 2024). *Poster contribution.*

4. E. Esteban-Ibañez, C. Dorronsoro, E. Gambra. Simulation of daily soft multifocal contact lenses using SimVis Gekko: from in-vitro and computational characterization to clinical validation. Jornada de Doctorandos de Física UCM (Spain, 2023). *Oral contribution.*

5. E.Esteban-Ibañez, A. Zaytouny, Y. Marrakchi, X. Barcala, I. Sisó-Fuertes, M. Rodríguez-Vallejo, J. Fernández, E. Gambra, C. Dorronsoro.. Optimizing Visual Function Assessment: Synergy of SimVis Gekko and Multifocal Lens Analyzer App. PhDay CSIC (Spain, 2023). *Poster contribution.*

6. E. Esteban-Ibañez, D. Montagud-Martinez, L. Sawides, A. Zaytouny, A. de Castro, I. Sisó-Fuertes, X. Barcala, D.P. Piñero, W.D. Furlan, C. Dorronsoro, E. Gambra. Clinical validation of daily soft multifocal contact lens simulations using SimVis Gekko based on in-vitro measurements. Biophotonics for eye research summer school BER2023 (Spain, 2023). *Oral contribution.*

7. E. Esteban-Ibañez, E. Gambra, Y. Marrakchi, L. Sawides, C. Dorronsoro. Perceptual scores of image quality at far distance through optically simulated bifocal corrections: addition and energy balance implications. VI International Symposium of Young Optometrists (Online, 2022). *Oral contribution.*

8. E. Esteban-Ibañez, E. Gambra, Y. Marrakchi, L. Sawides, C. Dorronsoro. Perceived image quality of natural images through different bifocal corrections after adaptation to sharp or blur. Optica Fall Vision Meeting 2022 (United States, 2022). Poster *contribution.*

9. E. Esteban-Ibañez, E. Gambra, Y. Marrakchi, L. Sawides, C. Dorronsoro. Perceived image quality of natural images through bifocal corrections: effect of far/near energy balance and short-term neural adaptation. Visual and Physiological Optics (VPO) 2022 (United Kingdom, 2022). Oral *contribution.*

10. E. Esteban-Ibañez, D. Montagud-Martinez, L. Sawides, D.P. Piñero, W.D. Furlan, E. Gambra. *In vitro* and computational characterization of daily multifocal soft contact lenses for visual simulations using SimVis Gekko. Iberian Meeting of Optics Students IMOS 2022 (Portugal, 2022). *Oral contribution.*

Presented by collaborators

1. V. Rodríguez-López, Cristina Sánchez-García, E. Esteban-Ibañez, N. Arejita, C. Dorronsoro. Robustness of the Direct Subjective Refraction method. ARVO Annual Meeting 2023 (Online, 2023). *Oral contribution.*

2. V. Rodríguez-López, E. Esteban-Ibañez, C. Dorronsoro. Fast subjective estimation of astigmatism with the Direct Subjective Refraction. ARVO Annual Meeting 2021 (Online, 2021). *Poster contribution.*

5. Invited talks

1. Uso de simuladores visuales para la adaptación de lentes de contacto multifocales. I Jornadas internacionales de adaptación de lentes de contacto multifocales. Fundación ICAR (Online, 2023). *Oral talk.*

2. Perceived image quality of natural images through bifocal corrections: Experiment design. OPTICA Vision and Color Summer Data Blast (Online, 2022). *Oral talk.*

3. Simulador visual SimVis Gekko. Seminario de la asignatura Instrumentación Óptica Avanzada del Master Oficial de Optometría Avanzada y Ciencias de la Visión (MOACV). Universidad de Valencia (Valencia, 2022). *Oral talk.*

6. Research Stays

1. Marcos Lab, Center for Visual Science (CVS) – University of Rochester, Rochester (USA). From January to March (2023).

2. Diffractive Optics Group (DiOG) Lab, University of Valencia (España). 1 week (February 2022)

7. Grants

[2021-2024] Industrial PhD (IND2020/BMD- 17442) fellowship of the Madrid Regional Government, to develop this thesis project. Company advisor: Dr. Enrique Gambra. 2Eyes Vision. Academic Institution Advisor: Dr. Carlos Dorronsoro from the Visual Optics and Biophotonics Lab, Spanish National Research Council (CSIC).

[2024] ARVO International Travel Grant for ARVO Annual Meeting 2024, Seattle (USA).

[2023] Biophotonics for eye research summer school (BER2023) Travel Grant, Jaca (Spain).

[2023] Ayuda de Movilidad C (Estancia) de la convocatoria de ayudas para la participación en Congresos y Movilidad de los estudiantes de doctorado de la UCM, curso 2022-2023. Research Stay: Marcos Lab, Center for Visual Science – University of Rochester, Rochester (USA).

8. Awards

1. Comunicación oral seleccionada entre las 10 mejores del congreso (OPTOM 24): Simulación de lentes de contacto multifocales blandas diarias: de la caracterización computacional basada en medidas *in-vitro* a la validación clínica. Madrid, 12-14 abril 2024.

9. Other scientific activities

1. Member of the IO-CSIC OPTICA Student chapter, IOPTICA (formerly IOSA). Role of president in 2023 and treasurer in 2021. We organized internal seminars, talk as well as invited talks,

courses and participate in outreach activities in different Spanish cities collaborating with programs as Ciencia en el barrio, 11F, LGTBI+ in STEM, Scientifics seminars, Ciudad Ciencia.

2. The organizer of the 10th edition of the IOPTICA scientific seminars. Organized by IOPTICA (formerly IOSA) and held Institute of Optics of the Spanish National Research Council (CSIC) Madrid (Spain).

3. Committee member of Premios Fotón awards to recognize, motivate, and promote Scientific Communication (Fotón Emitido award) and Teaching (Fotón Absorbido award) in optics and photonics. Organized by the Institute of Optics of the Spanish National Research Council (CSIC) Madrid (Spain). Jury of the 2023 edition.

10. Other professional activities

1. On-site clinical demonstrations in national and international conferences: FacoElche (2024), OPTICA Fall Vision Meeting (2022), American Academy of Optometry (AAO) 2022.

2. Training in national and international hospitals, clinics and universities: Flaum Eye Institute (Rochester, USA), University of Alicante (Alicante, Spain) and CHU Morvan of Brest (France).

3. Clinical coordination of an international study conducted in the Flaum Eye Institute (University of Rochester): “Contact Lens Visual Simulation: Non-dispensing feasibility study”.

Bibliography

[1] Strenk SA, Strenk LM, Koretz JF. The mechanism of presbyopia. Prog Retin Eye Res 2005;24:379–93. https://doi.org/10.1016/j.preteyeres.2004.11.001.

[2] van Alphen GWHM, Graebel WP. Elasticity of tissues involved in accommodation. Vision Res 1991;31:1417–38. https://doi.org/10.1016/0042-6989(91)90061-9.

[3] Garner WH, Garner MH. Protein disulfide levels and lens elasticity modulation: Applications for presbyopia. Investig Ophthalmol Vis Sci 2016;57:2851–63. https://doi.org/10.1167/iovs.15-18413.

[4] Li S, Jie Y. Cataract surgery and lens implantation. Curr Opin Ophthalmol 2019;30:39–43. https://doi.org/10.1097/ICU.0000000000000547.

[5] Petrash JM. Aging and age-related diseases of the ocular lens and vitreous body. Investig Ophthalmol Vis Sci 2013;54:54–9. https://doi.org/10.1167/iovs.13-12940.

[6] Fricke TR, Tahhan N, Resnikoff S, Papas E, Burnett A, Ho SM, et al. Global Prevalence of Presbyopia and Vision Impairment from Uncorrected Presbyopia: Systematic Review, Meta-analysis, and Modelling. Ophthalmology 2018;125:1492–9. https://doi.org/10.1016/j.ophtha.2018.04.013.

[7] Berdahl J, Bala C, Dhariwal M, Lemp-Hull J, Thakker D, Jawla S. Patient and Economic Burden of Presbyopia: A Systematic Literature Review. Clin Ophthalmol 2020;Volume 14:3439–50. https://doi.org/10.2147/opth.s269597.

[8] Wolffsohn JS, Davies LN. Presbyopia: Effectiveness of correction strategies. Prog Retin Eye Res 2019;68:124–43. https://doi.org/10.1016/j.preteyeres.2018.09.004.

[9] Pointer JS. The presbyopic add. II. Age-related trend and a gender difference. Ophthalmic Physiol Opt 1995;15:241–8. https://doi.org/10.1016/0275-5408(94)00022-R.

[10] Rocha KM. Presbyopia on the Horizon. J Refract Surg 2021;37:S6–7. https://doi.org/10.3928/1081597X-20210408-01.

[11] Negishi K, Ayaki M, Kawashima M, Tsubota K. Sleep and subjective happiness between the ages 40 and 59 in relation to presbyopia and dry eye. PLoS One 2021;16:1–13. https://doi.org/10.1371/journal.pone.0250087.

[12] Wolffsohn JS, Leteneux-Pantais C, Chiva-Razavi S, Bentley S, Johnson C, Findley A, et al. Social media listening to understand the lived experience of presbyopia: Systematic search and content analysis study. J Med Internet Res 2020;22:1–10. https://doi.org/10.2196/18306.

[13] Pflugfelder SC, Stern ME. Biological functions of tear film. Exp Eye Res 2020;197. https://doi.org/10.1016/j.exer.2020.108115.

[14] Schein OD, Munuz B, Tielsch JM, Bandeen-Roche K, West S. Prevalence of dry eye among the elderly. Am J Ophthalmol 1997;124:723–8. https://doi.org/10.1016/S0002-9394(14)71688-5.

[15] Mai ELC, Lin C cheng, Lian I, Liao R, Chen M, Chang C. Population-based study on the epidemiology of dry eye disease and its association with presbyopia and other risk factors. Int Ophthalmol 2019;39:2731–9. https://doi.org/10.1007/s10792-019-01117-5.

[16] Obata H, Yamamoto S, Horiuchi H, Machinami R. Histopathologic Study of Human Lacrimal Gland: Statistical Analysis with Special Reference to Aging. Ophthalmology 1995;102:678–86. https://doi.org/10.1016/S0161-6420(95)30971-2.

[17] Lafosse E, Wolffsohn JS, Talens-Estarelles C, García-Lázaro S. Presbyopia and the aging eye: Existing refractive approaches and their potential impact on dry eye signs and symptoms. Contact Lens Anterior Eye 2020;43:103–14. https://doi.org/10.1016/j.clae.2019.08.005.

[18] Patel S, Boyd KE, Burns J. Age, stability of the precorneal tear film and the refractive index of tears. Contact Lens Anterior Eye 2000;23:44–7. https://doi.org/10.1016/S1367-0484(00)80024-7.

[19] van der Worp E, Bornman D, Ferreira DL, Faria-Ribeiro M, Garcia-Porta N, González-Meijome JM. Modern scleral contact lenses: A review. Contact Lens Anterior Eye 2014;37:240–50. https://doi.org/10.1016/j.clae.2014.02.002.

[20] Alipour F, Kheirkhah A, Jabarvand Behrouz M. Use of mini scleral contact lenses in moderate to severe dry eye. Contact Lens Anterior Eye 2012;35:272–6. https://doi.org/10.1016/j.clae.2012.07.006.

[21] Wolffsohn JS, Davies LN, Sheppard AL. New insights in presbyopia: impact of correction strategies. BMJ Open Ophthalmol 2023;8. https://doi.org/10.1136/bmjophth-2022-001122.

[22] Villegas EA, Artal P. Comparison of aberrations in different types of progressive power lenses. Ophthalmic Physiol Opt 2004;24:419–26. https://doi.org/10.1111/j.1475-1313.2004.00214.x.

[23] Jaschinski W, König M, Mekontso TM, Ohlendorf A, Welscher M. Comparison of progressive addition lenses for general purpose and for computer vision: An office field study. Clin Exp Optom 2015;98:234–43. https://doi.org/10.1111/cxo.12259.

[24] Sánchez-Brau M, Domenech-Amigot B, Brocal-Fernández F, Seguí-Crespo M. Computer vision syndrome in presbyopic digital device workers and progressive lens design. Ophthalmic Physiol Opt 2021;41:922–31. https://doi.org/10.1111/opo.12832.

[25] Sivardeen A, McAlinden C, Wolffsohn JS. Presbyopic correction use and its impact on quality of vision symptoms. J Optom 2020;13:29–34. https://doi.org/10.1016/j.optom.2018.12.004.

[26] Thite N, Desiato A, Shinde L, Wolffsohn JS, Naroo SA, Santodomingo-Rubido J, et al. Opportunities and threats to contact lens practice: A global survey perspective. Contact Lens Anterior Eye 2021;44. https://doi.org/10.1016/j.clae.2021.101496.

[27] Naroo SA, Nagra M, Retallic N. Exploring contact lens opportunities for patients above the age of 40 years. Contact Lens Anterior Eye 2022;45:101599. https://doi.org/10.1016/j.clae.2022.101599.

[28] Morgan PB, Efron N, Woods CA. An international survey of contact lens prescribing for presbyopia. Clin Exp Optom 2011;94:87–92. https://doi.org/10.1111/j.1444-0938.2010.00524.x.

[29] Vásquez Quintero A, Pérez-Merino P, De Smet H. Artificial iris performance for smart contact lens vision correction applications. Sci Rep 2020;10:1–12. https://doi.org/10.1038/s41598-020-71376-1.

[30] Orman B, Benozzi G. Pharmacological Treatments for Presbyopia. Drugs and Aging 2023;40:105–16. https://doi.org/10.1007/s40266-022-01002-4.

[31] Meghpara BB, Lee JK, Rapuano CJ, Mian SI, Ho AC. Pilocarpine 1.25% and the changing landscape of presbyopia treatment. Curr Opin Ophthalmol 2022;33.

[32] Price FW, Hom M, Moshirfar M, Evans D, Liu H, Penzner J, et al. Combinations of Pilocarpine and Oxymetazoline for the Pharmacological Treatment of Presbyopia: Two Randomized Phase 2 Studies. Ophthalmol Sci 2021;1:100065. https://doi.org/10.1016/j.xops.2021.100065.

[33] Vargas V, Vejarano F, Alió JL. Near Vision Improvement with the Use of a New Topical Compound for Presbyopia Correction: A Prospective, Consecutive Interventional Non-Comparative Clinical Study. Ophthalmol Ther 2019;8:31–9. https://doi.org/10.1007/s40123-018-0154-6.

[34] Waring GO, Price FW, Wirta D, McCabe C, Moshirfar M, Guo Q, et al. Safety and Efficacy of AGN-190584 in Individuals With Presbyopia: The GEMINI 1 Phase 3 Randomized Clinical Trial. JAMA Ophthalmol 2022;140:363–71. https://doi.org/10.1001/jamaophthalmol.2022.0059.

[35] Waring GO, Brujic M, McGee S, Micheletti JM, Zhao C, Schachter S, et al. Impact of presbyopia treatment pilocarpine hydrochloride 1.25% on night-driving performance. Clin Exp Optom 2023;00:1–8. https://doi.org/10.1080/08164622.2023.2279189.

[36] Korenfeld MS, Robertson SM, Stein JM, Evans DG, Rauchman SH, Sall KN, et al. Topical lipoic acid choline ester eye drop for improvement of near visual acuity in subjects with presbyopia: a safety and preliminary efficacy trial. Eye 2021;35:3292–301. https://doi.org/10.1038/s41433-020-01391-z.

[37] Wang W, Yan W, Müller A, He M. A global view on output and outcomes of cataract surgery with national indices of socioeconomic development. Investig Ophthalmol Vis Sci 2017;58:3669–76. https://doi.org/10.1167/iovs.17-21489.

[38] Lansingh VC, Carter MJ, Martens M. Global Cost-effectiveness of Cataract Surgery. Ophthalmology 2007;114:1670–8. https://doi.org/10.1016/j.ophtha.2006.12.013.

[39] Lundström M, Barry P, Henry Y, Rosen P, Stenevi U. Evidence-based guidelines for cataract surgery: Guidelines based on data in the European Registry of Quality Outcomes for Cataract and Refractive Surgery database. J Cataract Refract Surg 2012;38:1086–93. https://doi.org/10.1016/j.jcrs.2012.03.006.

[40] Carson D, Hill WE, Hong X, Karakelle M. Optical bench performance of AcrySof® IQ ReSTOR®, AT LISA® tri, and FineVision® intraocular lenses. Clin Ophthalmol 2014;8:2105–13. https://doi.org/10.2147/OPTH.S66760.

[41] Calladine D, Evans JR, Shah S, Leyland M. Multifocal versus monofocal intraocular lenses after cataract extraction. Cochrane Database Syst Rev 2012. https://doi.org/10.1590/1516-3180.20151331T2.

[42] Ruiz-Mesa R, Abengózar-Vela A, Ruiz-Santos M. A comparative study of the visual outcomes between a new trifocal and an extended depth of focus intraocular lens. Eur J Ophthalmol 2017;28:182–7. https://doi.org/10.5301/ejo.5001029.

[43] Cochener B, Group for the CS. Clinical outcomes of a new extended range of vision intraocular lens: International Multicenter Concerto Study. J Cataract Refract Surg 2016;42.

[44] Vounotrypidis E, Diener R, Wertheimer C, Kreutzer T, Wolf A, Priglinger S, et al. Bifocal nondiffractive intraocular lens for enhanced depth of focus in correcting presbyopia: Clinical evaluation. J Cataract Refract Surg 2017;43.

[45] Fernández J, Ribeiro F, Rocha-De-Lossada C, Rodríguez-Vallejo M. Functional Classification of Intraocular Lenses Based on Defocus Curves: A Scoping Review and Cluster Analysis. J Refract Surg 2024;40:e108–16. https://doi.org/10.3928/1081597X-20231212-01.

[46] Pieh S, Lackner B, Hanselmayer G, Zöhrer R, Sticker M, Weghaupt H, et al. Halo size under distance and near conditions in refractive multifocal intraocular lenses. Br J Ophthalmol 2001;85:816–21. https://doi.org/10.1136/bjo.85.7.816.

[47] Ortiz D, Alió JL, Bernabéu G, Pongo V. Optical performance of monofocal and multifocal intraocular lenses in the human eye. J Cataract Refract Surg 2008;34:755–62. https://doi.org/10.1016/j.jcrs.2007.12.038.

[48] Woodward MA, Randleman BJ, Stulting DR. Dissatisfaction after multifocal intraocular lens implantation. J Cataract Refract Surg 2009;35:992–7. https://doi.org/10.1016/j.jcrs.2009.01.031.

[49] Tchah H, Nam K, Yoo A. Predictive factors for photic phenomena after refractive, rotationally asymmetric, multifocal intraocular lens implantation. Int J Ophthalmol 2017;10:241–5. https://doi.org/10.18240/ijo.2017.02.10.

[50] Choi M, Im CY, Lee JK, Kim H, Park HS, Kim T. Visual Outcomes after Bilateral Implantation of an Extended Depth of Focus Intraocular Lens: A Multicenter Study. Korean J Ophthalmol 2020;34:439–45. https://doi.org/10.3341/kjo.2020.0042.

[51] Pandit RT. Monocular Clinical Outcomes and Range of Near Vision following Cataract Surgery with Implantation of an Extended Depth of Focus Intraocular Lens. J Ophthalmol 2018;2018. https://doi.org/https://doi.org/10.1155/2018/8205824.

[52] Jeon YJ, Yoon Y, Kim T, Koh K. Comparison Between an Intraocular Lens With Extended Depth of Focus (Tecnis Symfony ZXR00) and a New Monofocal Intraocular Lens With Enhanced Intermediate Vision (Tecnis Eyhance ICB00). Asia-Pacific Acad Ophthalmol 2021:0–6. https://doi.org/10.1097/APO.0000000000000439.

[53] Tañá-Sanz P, Rodríguez-Carrillo MD, Elvira-Giner B, Ruiz-Santos M, Montés-Micó R, Tañá-Rivero P. Enhanced Monofocal Extended Depth of Focus IOL With a Diffractive Surface Design. J Refract Surg 2021;37:595–600. https://doi.org/10.3928/1081597X-20210518-02.

[54] Wan KH, Au ACK, Kua WN, Ng ALK, Cheng GPM, Lam NM, et al. Enhanced Monofocal Versus Conventional Monofocal Intraocular Lens in Cataract Surgery: A Meta-analysis. J Refract Surg 2022;38:538–46. https://doi.org/10.3928/1081597X-20220707-01.

[55] American National Standards Institute. Ophthalmics Extended Depth of Focus Intraocular Lenses. ANSI; 2018. Available from: https://doi.org/10.1097/ICU.0000000000000490

[56] Mencucci R, Cennamo M, Venturi D, Vignapiano R, Favuzza E. Visual outcome, optical quality, and patient satisfaction with a new monofocal IOL, enhanced for intermediate vision: Preliminary results. J Cataract Refract Surg 2020;46:378–87. https://doi.org/10.1097/j.jcrs.0000000000000061.

[57] Fernández J, Rocha-de-Lossada C, Zamorano-Martín F, Rodríguez-Calvo-de-Mora M, Rodríguez-Vallejo M. Positioning of enhanced monofocal intraocular lenses between conventional monofocal and extended depth of focus lenses: a scoping review. BMC Ophthalmol 2023;23:101. https://doi.org/10.1186/s12886-023-02844-1.

[58] Rampat R, Gatinel D. Multifocal and Extended Depth-of-Focus Intraocular Lenses in 2020.

Ophthalmology 2021;128:e164–85. https://doi.org/10.1016/j.ophtha.2020.09.026.

[59] Ong H, Evans J, Allan B. Accommodative intraocular lens versus standard monofocal intraocular lens implantation in cataract surgery (Review). Cochrane Database Syst Rev 2014. https://doi.org/10.1002/14651858.CD009667.pub2.www.cochranelibrary.com.

[60] Schallhorn SC, Teenan D, Venter JA, Schallhorn JM, Hettinger KA, Hannan SJ, et al. Monovision LASIK versus presbyopia-correcting IOLs: Comparison of clinical and patient-reported outcomes. J Refract Surg 2017;33:749–52. https://doi.org/10.3928/1081597X-20170721-03.

[61] Reilly CD, Lee WB, Alvarenga L, Caspar J, Garcia-Ferrer F, Mannis MJ. Surgical Monovision and Monovision Reversal in LASIK. Cornea 2006;25.

[62] Kelava L, Barić H, Bušić M, Čima I, Trkulja V. Monovision Versus Multifocality for Presbyopia: Systematic Review and Meta-Analysis of Randomized Controlled Trials. Adv Ther 2017;34:1815–39. https://doi.org/10.1007/s12325-017-0579-7.

[63] Alió JL, Amparo F, Ortiz D, Moreno L. Corneal multifocality with excimer laser for presbyopia correction. Curr Opin Ophthalmol 2009;20:264–71. https://doi.org/10.1097/ICU.0b013e32832a7ded.

[64] Shetty R, Brar S, Sharma M, Dadachanji Z, Lalgudi V. PresbyLASIK: A review of PresbyMAX, Supracor, and laser blended vision: Principles, planning, and outcomes. Indian J Ophthalmol 2020;68:2723. https://doi.org/10.4103/ijo.IJO_32_20.

[65] Alió JL, Chaubard JJ, Caliz A, Sala E, Patel S. Correction of presbyopia by technovision central multifocal LASIK (PresbyLASIK). J Refract Surg 2006;22:453–60. https://doi.org/10.3928/1081-597x-20060501-06.

[66] Ang RET, Cruz EM, Pisig AU, Solis MLPC, Reyes RMM, Youssefi G. Safety and effectiveness of the SUPRACOR presbyopic LASIK algorithm on hyperopic patients. Eye Vis 2016;3:1–10. https://doi.org/10.1186/s40662-016-0062-6.

[67] Jackson WB, Tuan KA, Mintsioulis G. Aspheric Wavefront-guided LASIK to Treat Hyperopic Presbyopia: 12-Month Results With the VISX Platform. J Refract Surg 2011;27:519–29. https://doi.org/10.3928/1081597X-20101110-02.

[68] Epstein RL, Gurgos MA. Presbyopia treatment by monocular peripheral presbyLASIK. J Refract Surg 2009;25:516–23. https://doi.org/10.3928/1081597X-20090512-05.

[69] Vargas-Fragoso V, Alió JL. Corneal compensation of presbyopia: PresbyLASIK: an updated review. Eye Vis 2017;4:4–11. https://doi.org/10.1186/s40662-017-0075-9.

[70] Binder PS. Intracorneal Inlays for the Correction of Presbyopia. Eye Contact Lens Sci Clin Pract 2017;43:267–75. https://doi.org/10.1097/ICL.0000000000000381.

[71] Bouzoukis DI, Kymionis GD, Limnopoulou AN, Kounis GA, Pallikaris IG. Femtosecond Laser–assisted Corneal Pocket Creation Using a Mask for Inlay Implantation. J Refract Surg 2011;27:818–20. https://doi.org/10.3928/1081597X-20110706-01.

[72] Vukich JA, Durrie DS, Pepose JS, Thompson V, van de Pol C, Lin L. Evaluation of the small-aperture intracorneal inlay: Three-year results from the cohort of the U.S. Food and Drug Administration clinical trial. J Cataract Refract Surg 2018;44.

[73] Moshirfar M, Desautels JD, Wallace RT, Koen N, Hoopes PC. Comparison of FDA safety and efficacy data for KAMRA and raindrop corneal inlays. Int J Ophthalmol 2017;10:1446–51. https://doi.org/10.18240/ijo.2017.09.18.

[74] Sánchez-González JM, Borroni D, Rachwani-Anil R, Rocha-de-Lossada C. Refractive corneal inlay implantation outcomes: a preliminary systematic review. Int Ophthalmol 2022;42:713–22. https://doi.org/10.1007/s10792-021-02024-4.

[75] Malandrini A, Martone G, Menabuoni L, Catanese AM, Tosi GM, Balestrazzi A, et al. Bifocal refractive corneal inlay implantation to improve near vision in emmetropic presbyopic patients. J Cataract Refract Surg 2015;41.

[76] Waring GOI V, Klyce SD. Corneal Inlays for the Treatment of Presbyopia. Int Ophthalmol Clin 2011;51.

[77] Lindstrom RL, MacRae SM, Pepose JS, Hoopes PC. Corneal inlays for presbyopia correction. Curr Opin Ophthalmol 2013;24:281–7. https://doi.org/10.1097/ICU.0b013e328362293e.

[78] Beer SMC, Werner L, Nakano EM, Santos RT, Hirai F, Nitschke EJ, et al. A 3-year follow-up study of a new corneal inlay: Clinical results and outcomes. Br J Ophthalmol 2020;104:723–8. https://doi.org/10.1136/bjophthalmol-2019-314314.

[79] Kipp L, Skibowski M, Johnson RL, Berndt R, Adelung R, Harm S, et al. Sharper images by focusing soft X-rays with photon sieves. Nature 2001;414:184–8. https://doi.org/10.1038/35102526.

[80] Furlan WD, García-Delpech S, Udaondo P, Remón L, Ferrando V, Monsoriu JA. Diffractive corneal inlay for presbyopia. J Biophotonics 2017;10:1110–4. https://doi.org/10.1002/jbio.201600320.

[81] Furlan WD, Montagud-Martínez D, Ferrando V, García-Delpech S, Monsoriu JA. A new trifocal corneal inlay for presbyopia. Sci Rep 2021;11:2–9. https://doi.org/10.1038/s41598-021-86005-8.

[82] Montagud-Martínez D, Ferrando V, Monsoriu JA, Furlan WD. Optical Evaluation of New Designs of Multifocal Diffractive Corneal Inlays. J Ophthalmol 2019;2019. https://doi.org/10.1155/2019/9382467.

[83] Hipsley AM, Hall B, Rocha KM. Scleral surgery for the treatment of presbyopia: where are we today? Eye Vis 2018;5:1–11. https://doi.org/10.1186/s40662-018-0098-x.

[84] Schachar RA. Human accommodative ciliary muscle configuration changes are consistent with Schachar's mechanism of accommodation. Investig Ophthalmol Vis Sci 2015;56:6075. https://doi.org/10.1167/iovs.15-17452.

[85] Davidson RS, Dhaliwal D, Hamilton RD, Jackson M, Patterson L, Stonecipher K, et al. Surgical correction of presbyopia. J Cataract Refract Surg 2016;42.

[86] Hipsley AM, Ma DHK, Sun CC, Jackson MA, Goldberg D, Hall B. Visual outcomes 24 months after LaserACE. Eye Vis 2017;4:1–11. https://doi.org/10.1186/s40662-017-0081-y.

[87] Evans BJW. Monovision: A review. Ophthalmic Physiol Opt 2007;27:417–39. https://doi.org/10.1111/j.1475-1313.2007.00488.x.

[88] Handa T, Mukuno K, Uozato H, Niida T, Shoji N, Minei R, et al. Ocular dominance and patient

satisfaction after monovision induced by intraocular lens implantation. J Cataract Refract Surg 2004;30.

[89] Lopes-Ferreira D, Neves H, Queiros A, Faria-Ribeiro M, Peixoto-De-Matos SC, González-Méijome JM. Ocular dominance and visual function testing. Biomed Res Int 2013;2013. https://doi.org/10.1155/2013/238943.

[90] Pardhan S, Gilchristt J. The effect of monocular defocus on binocular contrast sensitivity. Ophthalmic Physiol Opt 1990;10:33–6. https://doi.org/10.1111/j.1475-1313.1990.tb01103.x.

[91] Johanndottir KR, and Stelmach LB. Monovision: a Review of the Scientific Literature. Optom Vis Sci 2001;78:646–51. https://doi.org/10.1097/00006324-200109000-00009.

[92] Smith CE, Allison RS, Wilkinson F, Wilcox LM. Monovision: Consequences for depth perception from large disparities. Exp Eye Res 2019;183:62–7. https://doi.org/https://doi.org/10.1016/j.exer.2018.09.005.

[93] Erickson P. Potential range of clear vision in monovision. J Am Optom Assoc 1988;59:203–5.

[94] Burge J, Rodriguez-Lopez V, Dorronsoro C. Monovision and the Misperception of Motion. Curr Biol 2019;29:2586-2592.e4. https://doi.org/10.1016/j.cub.2019.06.070.

[95] Read JCA. Visual Perception: Monovision Can Bias the Apparent Depth of Moving Objects. Curr Biol 2019;29:R738–40. https://doi.org/10.1016/j.cub.2019.06.035.

[96] Collins MJ, Goode A. Interocular blur suppression and monovision. Acta Ophthalmol 1994;72:376–80. https://doi.org/10.1111/j.1755-3768.1994.tb02777.x.

[97] Wolffsohn JS, Hunt OA, Basra AK. Simplified recording of soft contact lens fit. Contact Lens Anterior Eye 2009;32:37–42. https://doi.org/10.1016/j.clae.2008.12.004.

[98] Werner JS SB. Optics and Vision of the ageing eye. Bass M Ed Handb Opt Class Vis X-Ray Opt Mc Graw Hill, Pp 1323 8 2001.

[99] Gatinel D, Pagnoulle C, Houbrechts Y, Gobin L. Design and qualification of a diffractive trifocal optical profile for intraocular lenses. J Cataract Refract Surg 2011;37:2060–7. https://doi.org/10.1016/j.jcrs.2011.05.047.

[100] Rosa AM, Miranda ÂC, Patrício MM, McAlinden C, Silva FL, Castelo-Branco M, et al. Functional magnetic resonance imaging to assess neuroadaptation to multifocal intraocular lenses. J Cataract Refract Surg 2017;43:1287–96. https://doi.org/10.1016/j.jcrs.2017.07.031.

[101] Fernandes P, Ferreira C, Domingues J, Amorim-de-Sousa A, Faria-Ribeiro M, Queirós A, et al. Short-term delay in neural response with multifocal contact lens might start at the retinal level. Doc Ophthalmol 2022;145:37–51. https://doi.org/10.1007/s10633-022-09870-2.

[102] Fernandes PR, Neves HI, Lopes-Ferreira DP, Jorge JM, González-Méijome JM. Adaptation to Multifocal and Monovision Contact 2013;90:228–35.

[103] Radhakrishnan A, Dorronsoro C, Sawides L, Marcos S. Short-term neural adaptation to simultaneous bifocal images. PLoS One 2014;9. https://doi.org/10.1371/journal.pone.0093089.

[104] Goes FJ. Visual results following implantation of a refractive multifocal IOL in one eye and a diffractive multifocal IOL in the contralateral eye. J Refract Surg 2008;24:300–5. https://doi.org/10.3928/1081597x-20080301-13.

[105] Hayashi K, Yoshida M, Hirata A, Yoshimura K. Short-term outcomes of combined implantation of diffractive multifocal intraocular lenses with different addition power. Acta Ophthalmol 2015;93:e287–93. https://doi.org/10.1111/aos.12591.

[106] Parekh D, Asokan R, Purkait S, Iqbal A. Multifocal versus modified monovision corrections: A non-dispensing comparison of visual assessment in presbyopic neophytes. Indian J Ophthalmol 2023;71:1837–42. https://doi.org/10.4103/ijo.IJO_2027_22.

[107] Sanders E, Wagner H, Reich LN. Visual Acuity and "Balanced Progressive" Simultaneous Vision Multifocal Contact Lenses. Eye Contact Lens 2008;34.

[108] Freeman MH, Charman WN. An exploration of modified monovision with diffractive bifocal contact lenses. Contact Lens Anterior Eye 2007;30:189–96. https://doi.org/10.1016/j.clae.2006.12.006.

[109] Ganesh S, Brar S, Gautam M, Sriprakash K. Visual and Refractive Outcomes Following Laser Blended Vision Using Non-linear Aspheric Micro-monovision. J Refract Surg 2020;36:300–7. https://doi.org/10.3928/1081597X-20200407-02.

[110] Zheleznyak L, Sabesan R, Oh JS, MacRae S, Yoon G. Modified monovision with spherical aberration to improve presbyopic through-focus visual performance. Investig Ophthalmol Vis Sci 2013;54:3157–65. https://doi.org/10.1167/iovs.12-11050.

[111] Stapleton F, Keay L, Jalbert I, Cole N. The epidemiology of contact lens related infiltrates. Optom Vis Sci 2007;84:257–72. https://doi.org/10.1097/OPX.0b013e3180485d5f.

[112] López-de la Rosa A, Martín-Montañez V, López-Miguel A, Fernández I, Calonge M, González-Méijome JM, et al. Ocular response to environmental variations in contact lens wearers. Ophthalmic Physiol Opt 2017;37:60–70. https://doi.org/10.1111/opo.12338.

[113] González-Méijome JM, Jorge J, Almeida JB, Parafita MA. Contact lens fitting profile in Portugal in 2005: Strategies for first fits and refits. Eye Contact Lens 2007;33:81–8. https://doi.org/10.1097/01.icl.0000235271.64089.85.

[114] Efron N, Morgan PB, Nichols JJ, Walsh K, Willcox MD, Wolffsohn JS, et al. All soft contact lenses are not created equal. Contact Lens Anterior Eye 2022;45:101515. https://doi.org/10.1016/j.clae.2021.101515.

[115] Alvarez-Peregrina C, Sanchez-Tena MA, Martin M, Villa-Collar C, Povedano-Montero FJ. Multifocal contact lenses: A bibliometric study. J Optom 2020. https://doi.org/10.1016/j.optom.2020.07.007.

[116] Pérez-Prados R, Piñero DP, Pérez-Cambrodí RJ, Madrid-Costa D. Soft multifocal simultaneous image contact lenses: a review. Clin Exp Optom 2017;100:107–27. https://doi.org/10.1111/cxo.12488.

[117] Remón L, Pérez-Merino P, Macedo-de-Araújo RJ, Amorim-de-Sousa AI, González-Méijome JM. Bifocal and Multifocal Contact Lenses for Presbyopia and Myopia Control. J Ophthalmol 2020;2020:1–18. https://doi.org/10.1155/2020/8067657.

[118] Faria-Ribeiro M, González-Méijome JM. Multifocal contact lenses: towards customisation? Ophthalmic Physiol Opt 2019;39:37–45. https://doi.org/10.1111/opo.12597.

[119] Bakaraju RC, Tilia D, Sha J, Diec J, Chung J, Kho D, et al. Lentes de contacto de profundidad de foco extendido vs. dos lentes multifocales comerciales: Parte 2. Rendimiento visual tras una

semana de uso. J Optom 2018;11:21–32. https://doi.org/10.1016/j.optom.2017.04.001.

[120] Tilia D, Bakaraju RC, Chung J, Sha J, Delaney S, Munro A, et al. Short-term visual performance of novel extended depth-of-focus contact lenses. Optom Vis Sci 2016;93:435–44. https://doi.org/10.1097/OPX.0000000000000806.

[121] Corpus G, Piñero DP. Short-Term Effect of Wearing of Extended Depth-of-Focus Contact Lenses in Myopic Children: A Pilot Study. Appl Sci 2022;12:431. https://doi.org/10.3390/app12010431.

[122] Wolffsohn JS, Dumbleton K, Huntjens B, Kandel H, Koh S, Kunnen CME, et al. BCLA CLEAR - Evidence-based contact lens practice. Contact Lens Anterior Eye 2021;44:368–97. https://doi.org/10.1016/j.clae.2021.02.008.

[123] Rodríguez-Vallejo M, Montagud D, Monsoriu JA, Furlan WD. On the power profiles of contact lenses measured with NIMO TR1504. J Optom. 2017;10(4):265–6. https://doi.org/10.1016/j.optom.2016.10.002.

[124] Merchea M, Evans D, Kannarr S, Miller J, Kaplan M, Nixon L. Assessing a modified fitting approach for improved multifocal contact lens fitting. Contact Lens Anterior Eye 2019;42:540–5. https://doi.org/10.1016/j.clae.2019.06.006.

[125] Stapleton F, Bakkar M, Carnt N, Chalmers R, Vijay AK, Marasini S, et al. CLEAR - Contact lens complications. Contact Lens Anterior Eye 2021;44:330–67. https://doi.org/10.1016/j.clae.2021.02.010.

[126] Jalbert I, Golebiowski B, Stapleton F. Measuring Contact Lens Discomfort. Curr Ophthalmol Rep 2015;3:106–10. https://doi.org/10.1007/s40135-015-0070-z.

[127] Begley CG, Chalmers RL, Mitchell GL, Nichols KK, Caffery B, Simpson T, et al. Characterization of Ocular Surface Symptoms From Optometric Practices in North America. Cornea 2001;20.

[128] Chalmers RL, Begley CG, Moody K, Hickson-Curran SB. Contact Lens Dry Eye Questionnaire-8 (CLDEQ-8) and opinion of contact lens performance. Optom Vis Sci 2012;89:1435–42. https://doi.org/10.1097/OPX.0b013e318269c90d.

[129] Pesudovs K, Garamendi E, Elliott DB. The Contact Lens Impact on Quality of Life (CLIQ) questionnaire: Development and validation. Investig Ophthalmol Vis Sci 2006;47:2789–96. https://doi.org/10.1167/iovs.05-0933.

[130] Schiffman RM, Christianson MD, Jacobsen G, Hirsch JD, Reis BL. Reliability and validity of the ocular surface disease index. Arch Ophthalmol 2000;118:615–21. https://doi.org/10.1001/archopht.118.5.615.

[131] Buckhurst PJ, Wolffsohn JS, Gupta N, Naroo SA, Davies LN, Shah S. Development of a questionnaire to assess the relative subjective benefits of presbyopia correction. J Cataract Refract Surg 2012;38:74–9. https://doi.org/10.1016/j.jcrs.2011.07.032.

[132] McAlinden C, Pesudovs K, Moore JE. The development of an instrument to measure quality of vision: The quality of vision (QoV) questionnaire. Investig Ophthalmol Vis Sci 2010;51:5537–45. https://doi.org/10.1167/iovs.10-5341.

[133] García-Marqués JV, Macedo-De-Araújo RJ, Cerviño A, García-Lázaro S, McAlinden C, González-Méijome JM. Comparison of short-term light disturbance, optical and visual performance outcomes between a myopia control contact lens and a single-vision contact lens.

Ophthalmic Physiol Opt 2020;40:718–27. https://doi.org/10.1111/opo.12729.

[134] Madrid-Costa D, García-Lázaro S, Albarrán-Diego C, Ferrer-Blasco T, Montés-Micó R. Visual performance of two simultaneous vision multifocal contact lenses. Ophthalmic Physiol Opt 2013;33:51–6. https://doi.org/10.1111/opo.12008.

[135] Madrid-Costa D, Tomás E, Ferrer-Blasco T, García-Lázaro S, Montés-Micó R. Visual performance of a multifocal toric soft contact lens. Optom Vis Sci 2012;89:1627–35. https://doi.org/10.1097/OPX.0b013e31826b0934.

[136] Fernández J, Rodríguez-Vallejo M, Tauste A, Albarrán C, Basterra I, Piñero D. Fast Measure of Visual Acuity and Contrast Sensitivity Defocus Curves with an iPad Application. Open Ophthalmol J 2019;13:15–22. https://doi.org/10.2174/1874364101913010015.

[137] Ferrer-Blasco T, Madrid-Costa D. Stereoacuity with balanced presbyopic contact lenses. Clin Exp Optom 2011;94:76–81. https://doi.org/10.1111/j.1444-0938.2010.00530.x.

[138] Ferrer-Blasco T, Madrid-Costa D. Stereoacuity with simultaneous vision Multifocal contact lenses. Optom Vis Sci 2010;87:663–8. https://doi.org/10.1097/OPX.0b013e3181eb98b9.

[139] Sanchez I, Ortiz-Toquero S, Blanco M, Martin R. A new method to analyse the effect of multifocal contact lenses on visual function. Contact Lens Anterior Eye 2018;41:169–74. https://doi.org/10.1016/j.clae.2017.11.005.

[140] Fernandes P, Amorim-de-Sousa A, Queirós A, Escandón-Garcia S, McAlinden C, González-Méijome JM. Light disturbance with multifocal contact lens and monovision for presbyopia. Contact Lens Anterior Eye 2018;41:393–9. https://doi.org/10.1016/j.clae.2018.03.006.

[141] Katz MSJ, Jonna G. Adaptive Optics: Astronomy, Military Might, and Retinal Imaging. J Pediatr Ophthalmol Strabismus 2015;52:11–11. https://doi.org/10.3928/01913913-20141230-03.

[142] Davies R, Kasper M. Adaptive optics for astronomy. Annu Rev Astron Astrophys 2012;50:305–51. https://doi.org/10.1146/annurev-astro-081811-125447.

[143] Marcos S, Artal P, Atchison DA, Hampson K, Legras R, Lundström L, et al. Adaptive optics visual simulators: a review of recent optical designs and applications [Invited]. Biomed Opt Express 2022;13:6508. https://doi.org/10.1364/boe.473458.

[144] Sawides L, de Gracia P, Dorronsoro C, Webster M, Marcos S. Adapting to blur produced by ocular high-order aberrations. J Vis 2011;11:21. https://doi.org/10.1167/11.7.21.

[145] Sawides L. Correction and control of ocular aberrations with adaptive optics. Effects on Human Vision. In: Universidad de Valladolid, 2013.

[146] Liang J, Williams DR, Miller DT. Supernormal vision and high-resolution retinal imaging through adaptive optics. J Opt Soc Am A 1997;14:2884. https://doi.org/10.1364/josaa.14.002884.

[147] Vinas M, Benedi-Garcia C, Aissati S, Pascual D, Akondi V, Dorronsoro C, et al. Visual simulators replicate vision with multifocal lenses. Sci Rep 2019;9:1–11. https://doi.org/10.1038/s41598-019-38673-w.

[148] Benedi-Garcia C, Vinas M, Lago CM, Aissati S, de Castro A, Dorronsoro C, et al. Optical and visual quality of real intraocular lenses physically projected on the patient's eye. Biomed Opt Express 2021;12:6360. https://doi.org/10.1364/boe.432578.

[149] Wahl S, Song C, Ohlendorf A. Comparison of two devices to simulate vision with intraocular lenses. Clin Ophthalmol 2019;13:123–30. https://doi.org/10.2147/OPTH.S188890.

[150] Lundstrom L, Romashchenko D, van der Mooren M, Unsbo P, Börjeson C, Canovas C. Compact telescopic system for subjective evaluation of intraocular lens designs. Invest Ophthalmol Vis Sci 2022;63:1802 – F0418-1802 – F0418.

[151] Barcala Gosende X. Binocular Simultaneous Vision Simulator : validation and implementation of the Sim + Vis technology in the clinic. In: Universidad Complutense de Madrid, 2021.

[152] Lago López CM. Development of new applications of simultaneous vision simulator. In: Universidad Complutense de Madrid, 2023.

[153] Dorronsoro C, Radhakrishnan A, Alonso-Sanz JR, Pascual D, Velasco-Ocana M, Perez-Merino P, et al. Portable simultaneous vision device to simulate multifocal corrections. Optica 2016;3:918. https://doi.org/10.1364/OPTICA.3.000918.

[154] Sawides L, Castro A de, Lago CM, Barcala X, Zaytouny A, Marcos S, et al. SimVis simulations of multifocal IOL designs based on public-literature data. Proc.SPIE, vol. 11871, 2021, p. 118710O. https://doi.org/10.1117/12.2595035.

[155] Sisó-Fuertes, I. SimVis Simulation of LASIK Corneal Ablation Patterns For Presbyopia Correction, Computational, On-Bench and Clinical Validations. Poster contribution presented at the European Society of Cataract and Refractive Surgeons (Amsterdam 2022).

[156] Barcala X, Vinas M, Ruiz S, Hidalgo F, Nankivil D, Karkkainen T, et al. Multifocal contact lens vision simulated with a clinical binocular simulator. Contact Lens Anterior Eye 2022:101716. https://doi.org/10.1016/j.clae.2022.101716.

[157] Hervella L, Villegas EA, Robles C, Artal P. Spherical Aberration Customization to Extend the Depth of Focus With a Clinical Adaptive Optics Visual Simulator. J Refract Surg 2020;36:223–9. https://doi.org/10.3928/1081597X-20200212-02.

[158] Tabernero J, Otero C, Pardhan S. A comparison between refraction from an adaptive optics visual simulator and clinical refractions. Transl Vis Sci Technol 2020;9:1–9. https://doi.org/10.1167/tvst.9.7.23.

[159] Rodriguez-Lopez V, Geisler W, Dorronsoro C. Spatiotemporal defocus sensitivity function of the human visual system. Biomed Opt Express 2023;14:3654. https://doi.org/10.1364/boe.486242.

[160] Rodriguez-Lopez V, Hernandez-Poyatos A, Dorronsoro C. Defocus flicker of chromatic stimuli deactivates accommodation. Biomed Opt Express 2023;14:3671. https://doi.org/10.1364/boe.486466.

[161] Akondi V, Sawides L, Marrakchi Y, Gambra E, Marcos S, Dorronsoro C. Experimental validations of a tunable-lens-based visual demonstrator of multifocal corrections. Biomed Opt Express 2018;9:6302. https://doi.org/10.1364/BOE.9.006302.

[162] Dorronsoro C, Barcala X, Gambra E, Akondi V, Sawides L, Marrakchi Y, et al. Tunable lenses: dynamic characterization and fine-tuned control for high-speed applications. Opt Express 2019;27:2085. https://doi.org/10.1364/oe.27.002085.

[163] Lopez-de-Haro AG, Barcala X, Martinez-Ibarburu I, Marrakchi Y, Gambra E, Rodriguez-Lopez V, et al. Closed-loop experimental optimization of tunable lenses. Appl Opt 2022;61:8091–9.

https://doi.org/10.1364/AO.467848.

[164] Marrakchi Y, Barcala X, Gambra E, Martinez-Ibarburu I, Dorronsoro C, Sawides L. Experimental characterization, modelling and compensation of temperature effects in optotunable lenses. Sci Rep 2023;13:1575. https://doi.org/10.1038/s41598-023-28795-7.

[165] Self H. Optical tolerances for alignment and image differences for binocular helmet-mounted displays. Tech Rept from HARRY G ARMSTRONG Aerosp Med Res LAB WRIGHT-PATTERSON AFB OH 1986.

[166] Akondi V, Dorronsoro C, Gambra E, Marcos S. Temporal multiplexing to simulate multifocal intraocular lenses: theoretical considerations. Biomed Opt Express 2017;8:3410. https://doi.org/10.1364/BOE.8.003410.

[167] Vinas M, Aissati S, Gonzalez-Ramos AM, Romero M, Sawides L, Akondi V, et al. Optical and Visual Quality With Physical and Visually Simulated Presbyopic Multifocal Contact Lenses. Transl Vis Sci Technol 2020;9:20. https://doi.org/10.1167/tvst.9.10.20.

[168] Madrid-Costa D, Ruiz-Alcocer J, García-Lázaro S, Ferrer-Blasco T, Montés-Micó R. Optical power distribution of refractive and aspheric multifocal contact lenses: Effect of pupil size. Contact Lens Anterior Eye 2015;38:317–21. https://doi.org/10.1016/j.clae.2015.03.008.

[169] Domínguez-Vicent A, Marín-Franch I, Esteve-Taboada JJ, Madrid-Costa D, Montés-Micó R. Repeatability of in vitro power profile measurements for multifocal contact lenses. Contact Lens Anterior Eye 2015;38:168–72. https://doi.org/10.1016/j.clae.2015.01.013.

[170] Belda-Salmerón L, Madrid-Costa D, Ferrer-Blasco T, García-Lázaro S, Montés-Micó R. In vitro power profiles of daily disposable contact lenses. Contact Lens Anterior Eye 2013;36:247–52. https://doi.org/10.1016/j.clae.2013.03.007.

[171] Kim E, Bakaraju RC, Ehrmann K. Reliability of power profiles measured on NIMO TR1504 (Lambda-X) and effects of lens decentration for single vision, bifocal and multifocal contact lenses. J Optom 2016;9:126–36. https://doi.org/10.1016/j.optom.2015.10.005.

[172] Gómez-Pedrero JA, Albarrán-Diego C, García-Montero M, Garzón N, Gonzalez-Fernandez V. Influence of Instrumental Factors in the Measurement of Power Profiles of Intraocular Lenses with a Commercial Deflectometer. Appl Sci 2023;13:9882. https://doi.org/10.3390/app13179882.

[173] Joannes L, Hough T, Hutsebaut X, Dubois X, Ligot R, Saoul B, et al. The reproducibility of a new power mapping instrument based on the phase shifting schlieren method for the measurement of spherical and toric contact lenses. Contact Lens Anterior Eye 2010;33:3–8. https://doi.org/10.1016/j.clae.2009.11.001.

[174] Domínguez-Vicent A, Marín-Franch I, Esteve-Taboada JJ, Madrid-Costa D, Montés-Micó R. Repeatability of in vitro power profile measurements for multifocal contact lenses. Contact Lens Anterior Eye 2015;38:168–72. https://doi.org/10.1016/j.clae.2015.01.013.

[175] de Juan V, Sanchez I, Ortiz-Toquero S, Martin R. Advantages, limitations, and diagnostic accuracy of photoscreeners in early detection of Amblyopia: a review. Clin Ophthalmol 2016;Volume 10:1365–73. https://doi.org/10.2147/OPTH.S93714.

[176] Clavé L, Torrents A, Millán MS. Visual Acuity at Various Distances and Defocus Curve: A Good Match. Photonics 2022;9:85. https://doi.org/10.3390/photonics9020085.

[177] Leek MR. Origins of Adaptive Psychophysical Procedures. Percept Psychophys 2001;63:1279–92.

[178] Treutwein B, Strasburger H. Fitting the psychometric function. Percept Psychophys 1999;61:87–106. https://doi.org/10.3758/bf03211951.

[179] Watson AB, Pelli DG. Quest: A Bayesian adaptive psychometric method. Percept Psychophys 1983;33:113–20. https://doi.org/10.3758/BF03202828.

[180] Treutwein B. Adaptive psychophysical procedures. Vision Res 1995;35:2503–22.

[181] Radhakrishnan A, Pascual D, Marcos S, Dorronsoro C. Vision with different presbyopia corrections simulated with a portable binocular visual simulator. PLoS One 2019;14:1–13. https://doi.org/10.1371/journal.pone.0221144.

[182] Brainard DH. The Psychophysics Toolbox. Spat Vis 1997;10:433–6.

[183] Pelli DG. The VideoToolbox software for visual psychophysics: transforming numbers into movies. Spat Vis 1997;10:437–42.

[184] Kleiner M, Brainard DH, Pelli D, Ingling A, Murray R, Broussard C. What's new in Psychtoolbox-3. Perception 2007;36:1–16. https://doi.org/10.1068/v070821.

[185] Rodríguez-Vallejo M, Llorens-Quintana C, Furlan WD, Monsoriu JA. Visual acuity and contrast sensitivity screening with a new iPad application. Displays 2016;44:15–20. https://doi.org/10.1016/j.displa.2016.06.001.

[186] Martins C, Amorim-De-Sousa A, Faria-Ribeiro M, Pauné J, González-Méijome JM, Queirós A. Visual Performance and High-Order Aberrations with Different Contact Lens Prototypes with Potential for Myopia Control. Curr Eye Res 2020;45:24–30. https://doi.org/10.1080/02713683.2019.1645182.

[187] Vinas M, Aissati S, Romero M, Benedi-Garcia C, Garzon N, Poyales F, et al. Pre-operative simulation of post-operative multifocal vision. Biomed Opt Express 2019;10:5801. https://doi.org/10.1364/BOE.10.005801.

[188] Kim E, Bakaraju RC, Ehrmann K. Power Profiles of Commercial Multifocal Soft Contact Lenses. Optom Vis Sci 2017;94:183–96. https://doi.org/10.1097/OPX.0000000000000998.

[189] Nti AN, Ritchey ER, Berntsen DA. Power profiles of centre–distance multifocal soft contact lenses. Ophthalmic Physiol Opt 2021;41:393–400. https://doi.org/10.1111/opo.12770.

[190] Plainis S, Atchison DA, Charman WN. Power profiles of multifocal contact lenses and their interpretation. Optom Vis Sci 2013;90:1066–77. https://doi.org/10.1097/OPX.0000000000000030.

[191] Rutschilling R, Fogt JS. Wear Experience of a Water Surface Daily Disposable Contact Lens in Existing Silicone Hydrogel Planned Replacement Lens Wearers. Clin Optom 2022;Volume 14:27–34. https://doi.org/10.2147/OPTO.S353666.

[192] Marsack JD, Thibos LN, Applegate RA. Metrics of optical quality derived from wave aberrations predict visual performance. J Vis 2004;4:8. https://doi.org/10.1167/4.4.8.

[193] Iskander DR. Computational aspects of the visual Strehl ratio. Optom Vis Sci 2006;83:57–9. https://doi.org/10.1097/01.opx.0000195563.82891.3b.

[194] Dorronsoro C, Alonso JR, Marcos S. Miniature simultaneous vision simulator instrument. Patent WO2015/049402 A1 (2015). http://hdl.handle.net/10261/135952.

[195] Barcala X, Zaytouny A, Rego-Lorca D, Sanchez-Quiros J, Sanchez-Jean R, Martinez-de-la-Casa JM, et al. Visual simulations of presbyopic corrections through cataract opacification. J Cataract Refract Surg 2023;49:34–43. https://doi.org/10.1097/j.jcrs.0000000000001040.

[196] ISO 10938:2016. Ophthalmic optics. Chart displays for visual acuity measurement. Printed, projected and electronic (2016).

[197] Yi F, Robert Iskander D, Collins M. Depth of focus and visual acuity with primary and secondary spherical aberration. Vision Res 2011;51:1648–58. https://doi.org/10.1016/j.visres.2011.05.006.

[198] Cheng X, Bradley A, Thibos LN. Predicting subjective judgment of best focus with objective image quality metrics. J Vis 2004;4:7. https://doi.org/10.1167/4.4.7.

[199] Brown BL, Hendrix SB. Partial Correlation Coefficients. Wiley StatsRef Stat. Ref. Online, Wiley; 2014, p. 1–8. https://doi.org/10.1002/9781118445112.stat06488.

[200] Wagner S, Conrad F, Bakaraju RC, Fedtke C, Ehrmann K, Holden BA. Power profiles of single vision and multifocal soft contact lenses. Contact Lens Anterior Eye 2015;38:2–14. https://doi.org/10.1016/j.clae.2014.07.008.

[201] Bakaraju RC, Ehrmann K, Ho A, Papas E. Inherent Ocular Spherical Aberration and Multifocal Contact Lens Optical Performance. Optom Vis Sci 2010;87:1009–22. https://doi.org/10.1097/OPX.0b013e3181fbad60.

[202] Leinonen J, Laakkonen E, Laatikainen L. Random measurement error in visual acuity measurement in clinical settings. Acta Ophthalmol Scand 2005;83:328–32. https://doi.org/10.1111/j.1600-0420.2005.00469.x.

[203] Rosser DA, Murdoch IE, Cousens SN. The Effect of Optical Defocus on the Test–Retest Variability of Visual Acuity Measurements. Investig Opthalmology Vis Sci 2004;45:1076. https://doi.org/10.1167/iovs.03-1320.

[204] Cardona G, López S, Guillon M, Dumbleton K, Theodoratos P, Gobbe M, et al. Pupil diameter , working distance and illumination during habitual tasks . Implications for simultaneous vision contact lenses for presbyopia. J Optom 2016;93:78–84. https://doi.org/10.1016/j.optom.2015.06.005.

[205] Vedhakrishnan S, Vinas M, Benedi-Garcia C, Casado P, Marcos S. Visual performance with multifocal lenses in young adults and presbyopes. PLoS One 2022;17:1–21. https://doi.org/10.1371/journal.pone.0263659.

[206] Artigas JM, Menezo JL, Peris C, Felipe A, Díaz-Llopis M. Image quality with multifocal intraocular lenses and the effect of pupil size. Comparison of refractive and hybrid refractive-diffractive designs. J Cataract Refract Surg 2007;33:2111–7. https://doi.org/10.1016/j.jcrs.2007.07.035.

[207] Bennett CR, Bex PJ, Bauer CM, Merabet LB. The Assessment of Visual Function and Functional Vision. Semin Pediatr Neurol 2019;31:30–40. https://doi.org/10.1016/j.spen.2019.05.006.

[208] Stalin A, Dalton K. Relationship of contrast sensitivity measured using quick contrast sensitivity function with other visual functions in a low vision population. Investig Ophthalmol

Vis Sci 2020;61. https://doi.org/10.1167/IOVS.61.6.21.

[209] Sabel BA, Wang J, Cárdenas-Morales L, Faiq M, Heim C. Mental stress as consequence and cause of vision loss: the dawn of psychosomatic ophthalmology for preventive and personalized medicine. EPMA J 2018;9:133–60. https://doi.org/10.1007/s13167-018-0136-8.

[210] Gupta N, Wolffsohn JSW, Naroo SA. Optimizing measurement of subjective amplitude of accommodation with defocus curves. J Cataract Refract Surg 2008;34:1329–38. https://doi.org/10.1016/j.jcrs.2008.04.031.

[211] Wolffsohn JS, Jinabhai AN, Kingsnorth A, Sheppard AL, Naroo SA, Shah S, et al. Exploring the optimum step size for defocus curves. J Cataract Refract Surg 2013;39:873–80. https://doi.org/10.1016/j.jcrs.2013.01.031.

[212] Chung STL, Legge GE. Comparing the shape of contrast sensitivity functions for normal and low vision. Investig Ophthalmol Vis Sci 2016;57:198–207. https://doi.org/10.1167/iovs.15-18084.

[213] Kelly DH, Savoie RE. A study of sine-wave contrast sensitivity by two psychophysical methods. Percept Psychophys 1973;14:313–8. https://doi.org/10.3758/BF03212397.

[214] Bühren J, Terzi E, Bach Mi, Wesemann W, Kohnen T. Measuring Contrast Sensitivity Under Different Lighting Conditions: Comparison of Three Tests. Optom Vis Sci 2006;83:290–8. https://doi.org/10.1097/01.opx.0000216100.93302.2d.

[215] Rossato M, Nart A, Messina G, Favro F, Rossato V, Rrutja E, et al. The Refraction Assessment and the Electronic Trial Frame Measurement during Standing or Sitting Position Can Affect Postural Stability. Int J Environ Res Public Health 2022;19:1558. https://doi.org/10.3390/ijerph19031558.

[216] Dorronsoro C, Barcala X, Gambra E, Akondi V, Sawides L, Marrakchi Y, et al. Tunable lenses: dynamic characterization and fine-tuned control for high-speed applications. Opt Express 2019;27:2085. https://doi.org/10.1364/OE.27.002085.

[217] Carracedo G, Carpena-Torres C, Pastrana C, Privado-Aroco A, Serramito M, Espinosa-Vidal TM, et al. A Comparison between Automated Subjective Refraction and Traditional Subjective Refraction in Keratoconus Patients. Optom Vis Sci 2021;98:597–604. https://doi.org/10.1097/OPX.0000000000001710.

[218] Ohlendorf A, Leube A, Wahl S. Steps towards smarter solutions in optometry and ophthalmology—Inter-device agreement of subjective methods to assess the refractive errors of the eye. Healthc 2016;4. https://doi.org/10.3390/healthcare4030041.

[219] Sawides L, Marcos S, Ravikumar S, Thibos L, Bradley A, Webster M. Adaptation to astigmatic blur. J Vis 2010;10:22–22. https://doi.org/10.1167/10.12.22.

[220] Novis C. Astigmatism and toric intraocular lenses. Curr Opin Ophthalmol 2000;11:47–50. https://doi.org/10.1097/00055735-200002000-00007.

[221] Alvarez LW. Development of variable- focus lenses and a new refractor. J Am Optom Assoc 1978;49:24–9.

[222] Barbero S. The Alvarez and Lohmann refractive lenses revisited. Opt Express 2009;17:9376. https://doi.org/10.1364/oe.17.009376.

[223] Zapata A, Barbero S. Mechanical design of a power-adjustable spectacle lens frame. J Biomed Opt 2011;16:055001. https://doi.org/10.1117/1.3582160.

[224] Stokes GG. On a Mode of Measuring the Astigmatism of a Defective Eye. In: Stokes GG, editor. Math. Phys. Pap. vol.2, vol. 2, Cambridge: Cambridge University Press; 2009, p. 172–5. https://doi.org/10.1017/CBO9780511702259.011.

[225] Foley JP, Campbell C. An Optical Device with Variable Astigmatic Power. Optom Vis Sci 1999;76:664–7. https://doi.org/10.1097/00006324-199909000-00025.

[226] Ferrer-Altabás S, Micó V. Characterization of a compact low-cost Stokes lens for astigmatism compensation in optical instruments. Appl Opt 2020;59:3347. https://doi.org/10.1364/AO.386247.

[227] Arines J, Acosta E. Low-cost adaptive astigmatism compensator for improvement of eye fundus camera. Opt Lett 2011;36:4164. https://doi.org/10.1364/ol.36.004164.

[228] Ferrer-altabás S, Sanz-sabater M, Micó V. Vectofocimetry : Dioptric power measurement in manual focimeters using power vectors 2021;146. https://doi.org/10.1016/j.optlaseng.2021.106703.

[229] Albero-Moreno JR, Albarrán-Diego C, Micó V. Validation of a set of compact and low-cost Stokes lenses aimed at refractive astigmatism measurement for optometric practice. Opt Eng 2022;61:121803. https://doi.org/10.1117/1.OE.61.12.121803.

[230] Albero-Moreno JR, Micó V, Albarrán Diego C. Subjective refraction using power vectors by updating a conventional phoropter with a Stokes lens for continuous astigmatic power generation. Ophthalmic Physiol Opt 2023;43:1029–39. https://doi.org/10.1111/opo.13181.

[231] Ozgur E, Reetz D, Akhoundi F, O'Brien N, Wycoff J, Voorakaranam R, et al. Parametric dog-bone-shaped tunable cylindrical fluidic lens. Appl Opt 2021;60:4755. https://doi.org/10.1364/AO.424659.

[232] Wang D, Hu D, Zhou Y, Sun L. Design and fabrication of a focus-tunable liquid cylindrical lens based on electrowetting. Opt Express 2022;30:47430. https://doi.org/10.1364/oe.478130.

[233] Thibos LN, Wheeler W, Horner D. Power vectors: An application of fourier analysis to the description and statistical analysis of refractive error. Optom Vis Sci 1997;74:367–75. https://doi.org/10.1097/00006324-199706000-00019.

[234] Kwon M, Legge GE, Fang F, Cheong AMY, He S. Adaptive changes in visual cortex following prolonged contrast reduction. J Vis 2009;9:20. https://doi.org/10.1167/9.2.20.

[235] Sawides L, de Gracia P, Dorronsoro C, Webster M, Marcos S. Adapting to blur produced by ocular high-order aberrations. J Vis 2011;11:21–21. https://doi.org/10.1167/11.7.21.

[236] Sawides L, Gracia P De, Dorronsoro C, Webster MA, Marcos S. Vision Is Adapted to the Natural Level of Blur Present in the Retinal Image. PLoS One 2011;6:1–6. https://doi.org/10.1371/journal.pone.0027031.

[237] Barcala X, Vinas M, Romero M, Gambra E, Mendez-Gonzalez JL, Marcos S, et al. Multifocal acceptance score to evaluate vision: MAS-2EV. Sci Rep 2021;11:1–15. https://doi.org/10.1038/s41598-021-81059-0.

[238] Esteban-Ibañez E, Gambra E, Marrakchi Y, Sawides L, Dorronsoro C. Poster Session: Perceived

image quality of natural images through different bifocal corrections after adaptation to sharp or blur. J Vis 2023;23:49. https://doi.org/10.1167/jov.23.11.49.

[239] Esteban-Ibañez E, Montagud-Martínez D, Sawides L, Zaytouny A, de Castro A, Sisó-Fuertes I, et al. Simulation of daily soft multifocal contact lenses using SimVis Gekko: from in-vitro and computational characterization to clinical validation. Sci Rep 2024;14:8592. https://doi.org/10.1038/s41598-024-59178-1.

[240] Barcala X, Vinas M, Ruiz S, Hidalgo F, Nankivil D, Karkkainen T, et al. Multifocal contact lens vision simulated with a clinical binocular simulator. Contact Lens Anterior Eye 2022:101716. https://doi.org/https://doi.org/10.1016/j.clae.2022.101716.

[241] Breslow NE, Clayton DG. Approximate Inference in Generalized Linear Mixed Models. J Am Stat Assoc 1993;88:9–25. https://doi.org/10.1080/01621459.1993.10594284.

[242] Vinas M, Dorronsoro C, Gonzalez V, Cortes D, Radhakrishnan A, Marcos S. Testing vision with angular and radial multifocal designs using Adaptive Optics. Vision Res 2017;132:85–96. https://doi.org/10.1016/j.visres.2016.04.011.

[243] Dorronsoro C, Radhakrishnan A, de Gracia P, Sawides L, Marcos S. Perceived image quality with simulated segmented bifocal corrections. Biomed Opt Express 2016;7:4388. https://doi.org/10.1364/BOE.7.004388.

[244] de Gracia P, Dorronsoro C, Sánchez-González Á, Sawides L, Marcos S. Experimental Simulation of Simultaneous Vision. Investig Opthalmology Vis Sci 2013;54:415. https://doi.org/10.1167/iovs.12-11219.

[245] de Gracia P, Dorronsoro C, Marcos S. Multiple zone multifocal phase designs. Opt Lett 2013;38:3526. https://doi.org/10.1364/ol.38.003526.

[246] Mon-williams M, Tresilian JR, Strang NC, Kochhar P, Wann JP. Improving vision : neural compensation for optical defocus. Proceedings Biol Sci 1998.

[247] George S, Rosenfield M. Blur Adaptation and Myopia. Optom Vis Sci 2004;81.

[248] Webster MA, Georgeson MA, Webster SM. Neural adjustments to image blur. Nat Neurosci 2002;5:839–40. https://doi.org/10.1038/nn906.

[249] Webster MA. Adaptation and visual coding. J Vis 2011;11:3–3. https://doi.org/10.1167/11.5.3.

[250] Neitz J, Carroll J, Yamauchi Y, Neitz M, Williams DR. Color perception is mediated by a plastic neural mechanism that is adjustable in adults. Neuron 2002;35:783–92. https://doi.org/10.1016/S0896-6273(02)00818-8.

[251] Sawides L, Dorronsoro C, de Gracia P, Vinas M, Webster M, Marcos S. Dependence of subjective image focus on the magnitude and pattern of high order aberrations. J Vis 2012;12:4–4. https://doi.org/10.1167/12.8.4.

[252] Sawides L, Dorronsoro C, Haun AM, Peli E, Marcos S. Using Pattern Classification to Measure Adaptation to the Orientation of High Order Aberrations. PLoS One 2013;8:e70856. https://doi.org/10.1371/journal.pone.0070856.

[253] Applegate RA, Sarver EJ, Khemsara V. Are All Aberrations Equal? J Refract Surg 2002;18. https://doi.org/10.3928/1081-597X-20020901-12.

[254] Aissati S, Benedi-Garcia C, Vinas M, de Castro A, Marcos S. Matching convolved images to optically blurred images on the retina. J Vis 2022;22:1–14. https://doi.org/10.1167/jov.22.2.12.

[255] Marcos S, Barbero S, Jiménez-Alfaro I. Optical Quality and Depth-of-field of Eyes Implanted With Spherical and Aspheric Intraocular Lenses. J Refract Surg 2005;21:223–35. https://doi.org/10.3928/1081-597X-20050501-05.

[256] Kompaniez E, Abbey CK, Boone JM, Webster MA. Adaptation Aftereffects in the Perception of Radiological Images. PLoS One 2013;8:e76175. https://doi.org/10.1371/journal.pone.0076175.

[257] Cufflin MP, Mankowska A, Mallen EAH. Effect of blur adaptation on blur sensitivity and discrimination in emmetropes and myopes. Investig Ophthalmol Vis Sci 2007;48:2932–9. https://doi.org/10.1167/iovs.06-0836.

[258] Woods RL, Colvin CR, Vera-Diaz FA, Peli E. A relationship between tolerance of blur and personality. Investig Ophthalmol Vis Sci 2010;51:6077–82. https://doi.org/10.1167/iovs.09-5013.

[259] Zapata-Díaz JF, Rodríguez-Izquierdo MA, Ould-Amer N, Lajara-Blesa J, López-Gil N. Total Depth of Focus of Five Premium Multifocal Intraocular Lenses. J Refract Surg 2020;36:578–84. https://doi.org/10.3928/1081597X-20200720-01.

[260] Montés-Micó R, Madrid-Costa D, Ruiz-Alcocer J, Ferrer-Blasco T, Pons ÁM. In vitro optical quality differences between multifocal apodized diffractive intraocular lenses. J Cataract Refract Surg 2013;39:928–36. https://doi.org/10.1016/j.jcrs.2012.12.038.

[261] Azor JA, Vega F, Armengol J, Millan MS. Optical Assessment and Expected Visual Quality of Four Extended Range of Vision Intraocular Lenses. J Refract Surg 2022;38:688–97. https://doi.org/10.3928/1081597X-20220926-01.

[262] Lago CM, De Castro A, Marcos S. Computational simulation of the optical performance of an EDOF intraocular lens in post-LASIK eyes. J Cataract Refract Surg 2023;49:1153–9. https://doi.org/10.1097/j.jcrs.0000000000001260.